

1989

# Archaeomagnetic Directional Studies Of Large Fired Structures In Britain

Gentles, Dougall Stanley

<http://hdl.handle.net/10026.1/2326>

---

<http://dx.doi.org/10.24382/1309>

University of Plymouth

---

*All content in PEARL is protected by copyright law. Author manuscripts are made available in accordance with publisher policies. Please cite only the published version using the details provided on the item record or document. In the absence of an open licence (e.g. Creative Commons), permissions for further reuse of content should be sought from the publisher or author.*

Archaeomagnetic Directional Studies Of Large Fired  
Structures In Britain.

by

Dougall Stanley Gentles.

Submitted to the Council for National Academic Awards in  
Partial Fulfilment for the Degree of Doctor of  
Philosophy.

Sponsoring Establishment:  
Plymouth Polytechnic

Department of Geological Sciences.

January 1989.

# Archaeomagnetic Directional Studies of Large Fired Structures in Britain.

by

Dougall Stanley Gentles.

## Abstract

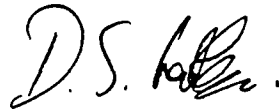
Archaeomagnetic directional dating of several Scottish sites has been undertaken by extensive sampling of large, physically stable vitrified exposures. Isothermal remanences and the demagnetisation patterns isolated using alternating magnetic fields and thermal methods, show that vitrification occurred under limited oxidation at temperatures  $>600^{\circ}\text{C}$  and that the vitrification was physically stable below  $600^{\circ}\text{C}$  at all but one of the sampled structures. Remanence directions were isolated by demagnetisation techniques and show that these sampled forts and duns collectively span a period from the late 3rd century B.C. to 5th century A.D. Calibration of mean magnetic directions shows general consistency with  $^{14}\text{C}$  dating but not with thermoluminescence dates. An archaeomagnetic curve of "best fit" incorporating all dating methods largely confirms the previous Iron Age secular variation curve. Field observations, systematic sampling and magnetic measurement of features of various archaeological ages, as well as an experimental kiln, has shown that there are both random and systematic directional deviations which do not precisely correlate with other magnetic properties. These deviations are thought to be due to more complex factors than that suggested by standard refraction corrections and appear to be attributable to not only magnetic distortions through already cooled magnetic materials but also complex localised magnetic interactions during cooling. Magnetic heterogeneity can contribute toward randomising such effects. Movement on cooling was insignificant in most cases whilst fabric anisotropy did not cause significant magnetic deflections. Systematic and preferential sampling of rapidly cooled areas gives the most consistent results, although mean magnetic directions from slowly cooled and magnetically heterogeneous structures can also give well defined magnetic directions.

Declaration.

This is to certify that the work submitted for the Degree of Doctor of Philosophy under the title "Archaeomagnetic directional studies of large fired structures in Britain" is the result of original work.

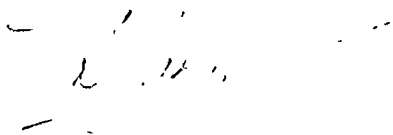
All authors and works consulted are fully acknowledged. No part of this work has been accepted in substance for any other degree and is not being concurrently submitted in candidature for any other degree.

Candidate



D.S. GENTLES.

Research supervisor



Prof. D.H.TARLING.



For Babs in gratitude.

Love,

A handwritten signature in cursive script, appearing to be 'D. J.', with a large initial 'D' and a flourish.

For Laura.

To my Father (in memoriam).

To my Mother (in thanks).

## Acknowledgements

I would like to thank the following :

Professors M.B. Hart and S.K. Runcorn in whose departments the work was carried out.

Professor D.H. Tarling for supervising the project in both the University of Newcastle upon Tyne and Plymouth Polytechnic.

Professor L. Alcock and Dr. I.B.M. Ralston for their cooperation and advice. Thanks also to Dr.E. Mackie, Ms. Harden, Ms. Nisbet and Mr. Robinson for help and discussions.

My colleagues and Staff of both departments particularly Dr. D.K. Potter for useful debates and Mrs. S. Leary for typing the first draft of the figures list and references. Thanks also to the technicians in both departments.

The Scottish Development Department, particularly Mr. P. Ashmore, for permission to sample the monuments.

The Science and Engineering Research Council for financial support.

## CONTENTS

Abstract.	i
Declaration.	ii
Dedications.	iii
Acknowledgements.	v
List of Figures.	ix
List of Tables.	xvii

### **Chapter One General Introduction**

1.1 Magnetisation and types of magnetic remanence.	1
1.2 Isothermal remanent magnetisation (I.R.M.)	4
1.3 Other laboratory induced remanences.	4
1.4 Field orientation/laboratory preparation of specimens.	5
1.5 Demagnetisation methods.	7
1.6 Statistical analysis.	9
1.6a The stability of remanence.	9
1.6b Precision.	11
1.7 Archaeodirectional determinations.	11
1.8 Low field susceptibility meters.	12
1.9 Causes of magnetic directional variation in large archaeological structures.	13
1.10 Physical movement.	15
1.11 Magnetic anisotropy.	16
1.12 Inhomogeneity.	18
1.13 Magnetic distortions on cooling.	18
1.14 Archaeological aims.	19

### **Chapter Two The Scottish Vitrified Forts, an introduction.**

2.1 Introduction.	20
2.2 Vitrification and its causes.	23
2.3 Constructive.	24
2.4 Destructive.	25
2.5 Discussion.	31
2.6 Summary.	35

### **Chapter Three The magnetic properties of a vitrified dun, Tor a'Chorcain, Langwell, Ross and Cromarty.**

3.1 Location and description.	37
3.2 Sampling strategy.	40

3.3	Field observations.	40
3.4	Demagnetisation behaviour.	44
3.5	Discussion.	55
3.6	Isothermal remanent magnetisation curves.	70
3.7	General.	72
3.8	Archaeological implications.	75
3.9	Summary.	79

#### Chapter Four

##### The vitrified structures sampled.

4.1	Introduction.	83
4.2	Craig Phadrig, Fort.	85
4.3	Dunnideer, Fort.	94
4.4	Dun Skeig, Fort and Dun.	101
4.5	Finavon, Fort.	108
4.6	Knock Farril, Fort.	119
4.7	Langwell, Fort and Dun.	130
4.8	Tap O'Noth, Fort.	131
4.9	Summary.	141

#### Chapter Five

##### Calibration of archaeomagnetic directional dating of the vitrified forts.

5.1	Archaeological methods.	143
5.2	Radiocarbon ( $^{14}\text{C}$ ).	145
5.3	Thermoluminescence (T.L.).	146
5.4	Archaeomagnetism (A.M.).	147
5.5	Comparison of dates.	148
5.6	The Iron Age secular variation curve.	154
5.7	Archaeomagnetic age assignments.	164
5.8	Summary.	165

#### Chapter Six

##### The magnetic properties of a triple flued experimental kiln from the Lunt Roman Fort, Baginton, Warwickshire.

6.1	Description.	171
6.2	Sampling method.	171
6.3	Laboratory observations.	178
6.4	Magnetic properties of the sub-specimens.	204
6.5	Magnetic distortions on cooling.	224
6.6	Spatial distribution/concentration of magnetic materials in the building materials.	232
6.7	Spatial variation in the type of magnetic mineral.	232

6.8	Demagnetisation methods.	233
6.9	Movement during cooling.	234
6.10	Magnetic anisotropy.	235
6.11	Summary.	236

## Chapter Seven

### Other Ancient Structures sampled.

7.1	Archaeomagnetic report on two clay hearths from the Neolithic site at Buxton, Derbyshire.	239
7.2	Archaeomagnetic report on two iron smelting furnaces from Crawcwellt, North Wales.	243
7.3	Archaeomagnetic report on a brick kiln from the Quayside, Newcastle upon Tyne.	250
7.4	Archaeomagnetic report on a tile kiln from the Roman Fort (Arbeia), South Shields.	256
7.5	Summary.	263

## Chapter Eight

### Conclusions.

8.1	Physical movement.	265
8.1a	Large scale.	265
8.1b	Small scale.	267
8.2	Magnetic anisotropy.	268
8.3	Weathering.	269
8.4	Inhomogeneity and magnetic interactions on cooling.	270
8.5	Demagnetisation methods.	278
8.6	Accuracy of archaeomagnetic dating.	278
8.7	Archaeological implications of the A.M. age assignments.	281
8.8	The vitrification process.	284
8.9	Future work.	285
	References.	289
	Papers and Abstracts.	A300

## Figures

- Figure 2.1      Distribution map of vitrified forts in Scotland showing relative fort sizes.
- Figure 3.1      Plan of Tor a'Chorcain. (After Nisbet, 1974).
- Figure 3.2      Section of Tor a'Chorcain. (After Nisbet, 1974).
- Figure 3.3      Demagnetisation behaviour of specimen directions using A.F. (Stereographic projection).
- Figure 3.4      Demagnetisation behaviour of specimen intensities using A.F.
- Figure 3.5      As/Zijderveld plot of LA1.
- Figure 3.6      As/Zijderveld plot of LB2.
- Figure 3.7      As/Zijderveld plot of LC1.
- Figure 3.8      As/Zijderveld plot of LD2.
- Figure 3.9      Demagnetisation behaviour of specimen intensities thermally treated.
- Figure 3.10     Demagnetisation behaviour of specimen directions thermally treated.
- Figure 3.11     As/Zijderveld plot of LB8.
- Figure 3.12     As/Zijderveld plot of LB9.
- Figure 3.13     As/Zijderveld plot of LB10.
- Figure 3.14     As/Zijderveld plot of LB11.
- Figure 3.15     Magnetic susceptibility changes during heating.

- Figure 3.16 Stereoplot of location mean magnetic directions, Langwell.
- Figure 3.17 Plot of specimen field orientations for location A.
- Figure 3.18 Plot of most stable field corrected magnetic directions for location A.
- Figure 3.19 Variation of magnetic properties through a vitrified wall section at location A (declination and inclination).
- Figure 3.20 Variation of magnetic properties through a vitrified wall section at location A (solid angle).
- Figure 3.21 Isothermal remanence curves. Location B.
- Figure 3.22 Stereoplot of individual specimen magnetic directions and overall mean, Langwell.
- Figure 3.23 Stereoplot of the site mean magnetic direction, Langwell.
- Figure 4.1a Distribution map of vitrified forts in Scotland indicating those sampled. (After Mackie, 1976).
- Figure 4.1b Plan of Craig Phadrig. (After Small and Cottam, 1972).
- Figure 4.2 As/Zijderveld plot of CP7a.
- Figure 4.3 As/Zijderveld plot of CP4b.
- Figure 4.4 Stereoplot of individual specimen directions, Craig Phadrig.
- Figure 4.5 Stereoplot of the site mean magnetic direction, Craig Phadrig.
- Figure 4.6 Plan of Dunnideer. (After Feachem, 1983).
- Figure 4.7 As/Zijderveld plot of DD6a.



- Figure 4.8 Stereoplot of individual specimen directions and overall mean, Dunnideer.
- Figure 4.9 Stereoplot of the site mean magnetic direction, Dunnideer.
- Figure 4.10 Plan of Dun Skeig. (After Feachem,1983).
- Figure 4.11 As/Zijderveld plot of DSK4.
- Figure 4.12 Stereoplot of individual specimen directions and overall mean, Dun Skeig.
- Figure 4.13 Stereoplot of the site mean magnetic direction, Dun Skeig.
- Figure 4.14 Plan of Finavon.(After Childe,1934).
- Figure 4.15 As/Zijderveld plot of FA1v.
- Figure 4.16 As/Zijderveld plot of FB15.
- Figure 4.17 Stereoplot of location mean directions, Finavon.
- Figure 4.18 Stereoplot of individual specimen directions and overall mean, Finavon.
- Figure 4.19 Stereoplot of the site mean magnetic direction, Finavon.
- Figure 4.20 Plan of Knock Farril. (After Ordnance Survey,1964).
- Figure 4.21 As/Zijderveld plot of KF1a.
- Figure 4.22 As/Zijderveld plot of KF2b.
- Figure 4.23 Stereoplot of location mean directions, Knock Farril.
- Figure 4.24 Stereoplot of individual specimen directions and overall mean, Knock Farril.

- Figure 4.25 Stereoplot of the site mean magnetic direction, Knock Farril.
- Figure 4.26(a) Sketch plan of Tap'o Noth.
- Figure 4.26(b) As/Zijderveld plot of TN2a.
- Figure 4.27 As/Zijderveld plot of TN6b.
- Figure 4.28 Stereoplot of location mean directions, Tap 'o Noth.
- Figure 4.29 Stereoplot of individual specimen directions and overall mean, Tap 'o Noth.
- Figure 4.30 Stereoplot of the site mean magnetic direction, Tap 'o Noth.
- Figure 5.1(a) Chart of absolute dates for Craig Phadrig.
- Figure 5.1(b) Chart of absolute dates for Finavon.
- Figure 5.1(c) Chart of absolute dates for Langwell.
- Figure 5.1(d) Archaeomagnetic curve based on T.L. dates.
- Figure 5.1(e) Archaeomagnetic curve based on  $^{14}\text{C}$  dates.
- Figure 5.1(f) Composite archaeomagnetic curve based on several dating methods.
- Figure 5.1(g) Archaeomagnetic curve based on lake sediments. (After Clark *et al* 1988).
- Figure 5.2 Secular variation curve with theoretical Iron Age section. (After Tarling, 1988).
- Figure 5.3 Stereoplot of observed site mean magnetic directions.
- Figure 5.4 Stereoplot of site mean magnetic directions and circles of 95% confidence.
- Figure 5.5 Chart of archaeomagnetic dates for all sampled forts.

- Figure 6.1      Plan of triple flued experimental kiln.
- Figure 6.2(a)   Temperature as a function of time.
- Figure 6.2(b)   Stereoplot of 1c.
- Figure 6.2(c)   As/Zijderveld plot of 1c.
- Figure 6.2(d)   Intensity as a function of A.F. (Specimen 1c).
- Figure 6.3      Declination as a function of azimuth (core specimens).
- Figure 6.4      Inclination as a function of azimuth (core specimens).
- Figure 6.5      Solid angle as a function of azimuth (core specimens).
- Figure 6.6      Intensity as a function of azimuth (core specimens).
- Figure 6.7      Susceptibility as a function of azimuth (core specimens).
- Figure 6.8      Declination as a function of floor diameter.
- Figure 6.9      Inclination as a function of floor diameter.
- Figure 6.10     Stereoplot of level A specimen magnetic directions.
- Figure 6.11     Stereoplot of level B specimen magnetic directions.
- Figure 6.12     Stereoplot of level C specimen magnetic directions.
- Figure 6.13     Stereoplot of floor core specimens.
- Figure 6.14     Mean of all level A core specimens.
- Figure 6.15     Mean of all level B core specimens.
- Figure 6.16     Mean of all level C core specimens.

- Figure 6.17 Overall mean of all core specimens.
- Figure 6.18 Mean of all core floor specimens.
- Figure 6.19 Overall mean of all kiln wall core specimens.
- Figure 6.20 Intensity as a function of depth into kiln wall (core specimens).
- Figure 6.21 Susceptibility as a function of depth into kiln wall (core specimens). East side.
- Figure 6.22 Susceptibility as a function of depth into kiln wall (core specimens). West side.
- Figure 6.23 Declination as a function of depth into kiln wall (core specimens). East side.
- Figure 6.24 Declination as a function of depth into kiln wall (core specimens). West side.
- Figure 6.25 Inclination as a function of depth into kiln wall (core specimens). East side.
- Figure 6.26 Inclination as a function of depth into kiln wall (core specimens). West side.
- Figure 6.27 Solid angle as a function of depth into kiln wall (core specimens).
- Figure 6.28 Declination as a function of azimuth (sub-specimens).
- Figure 6.29 Inclination as a function of azimuth (sub-specimens).
- Figure 6.30 Solid angle as a function of azimuth (sub-specimens).
- Figure 6.31 Intensity as a function of azimuth (sub-specimens).
- Figure 6.32 Stereoplot of 1cm depth specimen magnetic directions.

- Figure 6.33 Stereoplot of 2cm depth specimen magnetic directions.
- Figure 6.34 Stereoplot of 3cm depth specimen magnetic directions.
- Figure 6.35 Stereoplot of 4cm depth specimen magnetic directions.
- Figure 6.36 Stereoplot of 5cm depth specimen magnetic directions.
- Figure 6.37 Stereoplot of 6cm depth specimen magnetic directions.
- Figure 6.38 Mean of all level 1 sub-specimens.
- Figure 6.39 Mean of all level 2 sub-specimens.
- Figure 6.40 Mean of all level 3 sub-specimens.
- Figure 6.41 Mean of all level 4 sub-specimens.
- Figure 6.42 Mean of all level 5 sub-specimens.
- Figure 6.43 Mean of all level 6 sub-specimens.
- Figure 6.44 Overall mean of all sub-specimens.
- Figure 6.45 Intensity as a function of depth into kiln wall (sub-specimens).East side.
- Figure 6.46 Intensity as a function of depth into kiln wall (sub-specimens).West side.
- Figure 6.47 Declination as a function of depth into kiln wall (sub-specimens).East side.
- Figure 6.48 Declination as a function of depth into kiln wall (sub-specimens).West side.
- Figure 6.49 Inclination as a function of depth into kiln wall (sub-specimens).East side.

- Figure 6.50      Inclination as a function of depth into kiln wall (sub-specimens). West side.
- Figure 6.51      Solid angle as a function of depth into kiln wall (sub-specimens).
- Figure 7.1        As/Zijderveld plot of 0057/4.
- Figure 7.2a(i)   As/Zijderveld plot of F41/2.
- Figure 7.2a(ii) As/Zijderveld plot of F10/2a.
- Figure 7.2b      Mean magnetic direction of Crawcwellt Iron Smelting Furnace.
- Figure 7.3a      As/Zijderveld plot of 10F/1.
- Figure 7.3b      Mean magnetic direction of Quayside Brick Kiln.
- Figure 7.4a      As/Zijderveld plot of SH6.
- Figure 7.4b      Mean magnetic direction of South Shields Tile Kiln.

### List of Tables

- Table 3.1 Most stable specimen magnetic directions for Langwell, Dun.
- Table 4.1 Most stable specimen magnetic directions for Craig Phadrig, Fort.
- Table 4.2 Most stable specimen magnetic directions for Dunnideer, Fort.
- Table 4.3 Most stable specimen magnetic directions for Dun Skeig, Dun.
- Table 4.4 Most stable specimen magnetic directions for Finavon, Fort.
- Table 4.5 Most stable specimen magnetic directions for Knock Farril, Fort.
- Table 4.6 Most stable specimen magnetic directions for Tap O'Noth, Fort.
- Table 5.1 Summary of dates available for the sampled vitrified structures.
- Table 6.1 Most stable core specimen magnetic directions.
- Table 6.2 Sub-specimen magnetic directions defined by repeated measurement (ten times) at 50 mT.
- Table 7.1 Most stable specimen magnetic directions for Buxton Hearths.
- Table 7.2 Most stable specimen magnetic directions for Crawcwellt Iron Smelting Furnaces.
- Table 7.3 Most stable specimen magnetic directions for the Quayside Brick Kiln.
- Table 7.4 Most stable specimen magnetic directions for South Shields Tile Kiln.

## CHAPTER ONE

### General Introduction

#### 1.1. Magnetisation and types of magnetic remanence

In most heated archaeological materials the vast majority of the observed magnetic remanence was acquired during the final cooling. This thermo-remanence is usually accompanied by a time dependent low temperature (viscous) component, whilst a chemical remanence can also be present, particularly if the specimens are weathered.

The theory of thermo-remanent magnetisation (T.R.M.) acquisition is described in various publications (Neel, 1949; Nagata, 1961; Aitken, 1974; Tarling, 1983). A natural remanent magnetisation (in this case largely thermoremanent) measured at room temperature can be described as a summation of the remanences acquired as a result of cooling below the Curie point of the magnetic mineral(s) (Neel, 1949). The magnitude of magnetic intensity will depend on the magnetic mineral present, its composition, grain size, i.e. on the bulk susceptibility of the material, and on the rate of cooling (Fox and Aitken, 1980). Each of these factors is likely to be



variable even within the same ancient structure. All the vitrified structures sampled in this study are likely to have been heated to well above  $675^{\circ}\text{C}$ , the Curie point of haematite (Nisbet, 1975), but hearth structures may only possess a partial thermo-remanence as a result of incomplete heating of the magnetic particles in the material. Polyphase magnetisations are also possible where fired building materials have been re-used in later heated structures (Evans and Mareschal, 1986).

A Viscous remanent magnetisation (V.R.M.) can be acquired by all magnetic grains in a specimen as a result of exposure to the geomagnetic field over a period of time. The intensity of the V.R.M. acquired depends on the strength of the ambient field and on the relaxation time of the magnetic grains. Relaxation time is the time taken for the internal energy barriers of any magnetic grain to be exceeded by external physical factors, such as temperature and the geomagnetic field. The V.R.M. is normally removed during the initial stages of demagnetisation by thermal or alternating fields and is often detected by a marked non-linearity of the thermal or coercivity spectrum.

A high temperature viscous component (Tarling 1983)

may also result if a material is heated for some time at a constant temperature. If this is prolonged in an archaeological context this could cause particles with longer relaxation times to relax into the ambient field acting over the feature.

A chemical remanent magnetisation (C.R.M.) may be acquired as a result of the growth of magnetic crystals at a constant (usually room) temperature. Thus goethite ( $\alpha$ -FeOOH) and lepidocrocite ( $\gamma$ -FeOOH) may form as a result of weathering. Also weathering products may undergo further chemical changes with consequent changes in the original magnetisation as a result of firing e.g. goethite or lepidocrocite converting to haematite (Tarling, 1983).

When already magnetised particles are deposited in a sediment then a depositional (detrital) remanence (D.R.M.) can result as a consequence of the physical rotation of magnetic grains during the deposition process. D.R.M. acquisition is affected by the environment of deposition, the shape of the magnetic grains, and the subsequent history of the deposit (Tarling 1983; Clark *et al* 1988; Tarling, 1988). As this study was largely concerned with factors affecting the acquisition of T.R.M.'s, depositional remanences were not directly pertinent.

### 1.2. Isothermal remanent magnetisation (I.R.M.) curves

As the saturation magnetisation of haematite is <1% of magnetite, the net remanence acquired as a result of applying a strong magnetic field at a constant temperature is some two orders of magnitude greater for magnetite than haematite. Also the iron rich titanomagnetites (and maghaemite) saturate in fields of 0.01-0.1 T unlike haematite which mostly saturates at fields over 1-3 T (Tarling, 1983). Thus by inducing a d.c. component in incremental steps it is usually possible to estimate the type of magnetic mineral by the saturation moment and the field at which this occurs. However as I.R.M. curves can be dominated by only a small percentage of magnetite (Tarling, 1983), and the fact that coercivity is dependent on grain size, the results from this method were also taken in conjunction with the behaviour of specimen remanences on thermal demagnetisation, to determine the probable mineral type.

### 1.3. Other laboratory induced remanences

An anhysteretic remanent magnetisation (A.R.M.) may be acquired when a ferromagnetic particle is subjected

simultaneously to alternating and direct magnetic fields (Stephenson et al 1986). This effect was reduced by mu-metal shielding and the use of Helmholtz coils maintaining zero field over the specimen.

A rotational remanent magnetisation (R.R.M.) and/or a gyro-remanent magnetisation (G.R.M.) may also occur as a result of placing the specimen within an A.F. field (Wilson and Lomax, 1972; Stephenson et al, 1986). These two types of remanence are acquired along the axis of rotation of the specimens (Wilson and Lomax, 1972). However the primary remanences in A.F. demagnetised specimens showed high magnetic stability (Tarling and Symons, 1967), whilst the intensity of magnetisation generally decreased after each incremental demagnetisation step. Acquisition of a laboratory remanence would normally result in an increase of magnetic intensity.

#### 1.4. Field orientation/laboratory preparation of specimens

Specimens were orientated in the field using sun/magnetic compasses and an inclinometer. The orientation of a horizontal strike line, marked on a plastic disc glued to a fixed feature, was measured relative to true North. The maximum dip of the surface of

the disc was measured  $90^{\circ}$  from the horizontal strike line.

Specimens were removed in most cases by chipping small irregular shaped pieces of fired material from the structure. In general materials were chosen that were physically stable, appeared magnetically homogeneous and were apparently unweathered. (For the Lunt kiln however (Chapter Six), the specimens were pre-cut prior to firing and orientation but without incurring significant movement during the firing process).

In the laboratory some of the irregular sized specimens used in thermal demagnetisation and I.R.M. work from Langwell (Chapter Three) were cut into cores. The strike arrow was transferred from the disc onto the specimen. For the Lunt kiln the large pre-cut hand specimens with discs attached were drilled and then cut into 2cm cores. Again the disc strike line was transferred onto the specimens. This process introduced an additional possible error of  $\pm 1^{\circ}$  for the Langwell and Lunt specimens. The Lunt sub-specimens were cut, using a brass hacksaw, from the cores. All specimens were stored in random orientations so that any V.R.M. acquired should also be random relative to the variable fiducial mark orientations.

### 1.5. Demagnetisation methods

The application of an alternating field (A.F.) of strength greater than that of the coercivity of the domains in the specimen will result in the magnetisation of the domain flipping so that its easy direction lies with a component in the direction of the applied field (Tarling, 1983). However if the A.F. does not exceed the coercivity of the easy axes of magnetisation then the original remanence will remain unchanged. If the Earth's field is cancelled over the specimen then those remanence directions with coercivities less than the applied A.F. strength will be randomised, providing the specimen is magnetically isotropic. They will then remain randomised as the peak field intensity is gradually reduced. If the specimen is tumbled in an A.F. then magnetic grains with coercivities less than or equal to the applied field will have their magnetisations changed according to the angle between the easy axes and the A.F. A two axis tumbling system will result in a 95% presentation of the specimens directions to the applied field (Hutchings, 1967). Thus it is possible to dissect the remanence by incrementally increasing the A.F. over a tumbling specimen and by

cancelling the ambient field. Ideally the A.F. field should be pure as a d.c. component could result in the acquisition of an anhysteretic remanent magnetisation.

Although this method does not induce chemical changes in the specimens it often fails to completely demagnetise specimen remanences (see Chapters Three and Four). This may be due to laboratory remanences, but no archaeologically spurious magnetic directions were observed. Although magnetic intensities typically  $100 \times 10^{-8} \text{ Am}^2/\text{g}$  were observed, even after demagnetisation at fields of 100 mT, (Chapter Three), the magnetic directions mostly consisted of a single stable vector. Also nearly all specimen directions were defined at A.F.  $\sim 50 \text{ mT}$ , and so were less subject to increasing "noise" at fields  $>50 \text{ mT}$  (Tarling, 1983). Thus although laboratory remanences may have been present, these were not significant with respect to the magnetic directions observed.

With increased temperature the relaxation time of each magnetic particle will reduce exponentially. This enables the magnetisation of grains with lower relaxation times to flip into a direction along their easy axes. If these axes are randomly oriented then this essentially demagnetises the affected grains. On cooling in zero

magnetic field these directions will remain randomised assuming that each particles easy axis is randomly orientated. However those grains with longer relaxation times than the duration of the heating will retain their original magnetisation, and thus it is possible to determine the blocking temperature ( $T_b$ ) spectrum of any given specimen. ( $T_b$  can be defined as the temperature at which the remanence acquired during cooling becomes established within a magnetic domain for the duration of the experiment (Tarling, 1983)). Thermal demagnetisation in this study was carried out in a furnace with zero magnetic field maintained by Helmholtz coils and mu-metal shielding.

However this method can induce chemical changes and thus to monitor the chemical stability of the magnetic minerals the low field susceptibility was measured prior to each demagnetisation step.

## 1.6. Statistical analysis

### 1.6a The stability of remanence

Remanence stability has been determined objectively by the use of a Stability index (S.I.; Tarling and Symons, 1967), based on directional consistency over successive



( $\geq 3$ ) incremental demagnetisation steps, i.e. the lowest scatter over the widest range of demagnetising treatment.

Thus:

$$S.I. = \max (\text{range of treatment}^2 / \text{c.s.d.})$$

Where c.s.d. is the circular standard deviation (Fisher 1953). This compares with subjective estimations of stability of thermally and A.F. demagnetised specimens of:

S.I. <1 unstable; 1-2 metastable; 2-5 stable; >5 very stable

Although other indices exist and were occasionally used, these are more sensitive to changes in magnetic intensity than direction and thus could define a low stability remanence with high directional stability (Tarling, 1983). All the data were also plotted on equal angle stereographic projections and As/Zijderveld plots (As and Zijderveld, 1958; Dunlop, 1979), in order to determine the visual consistency of magnetic direction during partial demagnetisation. In addition linearity of magnetic components was occasionally estimated using the least squares fit along the demagnetisation path of any

one specimen, Kirschvink (1980).

#### 1.6b Precision

The errors in the mean magnetic directions in this study were expressed in terms of a 95% circle of confidence ( $\alpha_{95}$ ). This is derived from the deviation of individual specimen magnetic directions from the mean direction based on Fisher (1953) which requires at least 7 observations to be statistically meaningful. There is thus a 95% probability that the true mean magnetic direction lies within the circle of confidence around the observed mean. For large numbers of directions the precision of the mean is increasingly well defined, the smaller the value of  $\alpha_{95}$ , the greater the precision (Fisher, 1953).

#### 1.7 Archaeodirectional determinations

The magnetisation of a rotating specimen induces a current in a ring fluxgate, the amplitude of which depends on the intensity of magnetisation of the specimen in the plane perpendicular to the axis of rotation, and its direction in that plane is given by the phase angle (Molyneux, 1971). The noise level of the magnetometer used was  $0.24 \times 10^{-8} \text{ Am}^3$  measured with the specimen holder

empty. The specimen holder was modified to accept cylinders of 5.5cm high x 5.1cm diameter. Each specimen was measured in six different positions in order to average out the affects of inhomogeneity in the specimen. Calibration was undertaken using a 2cm x 2cm standard within a 5.5cm high x 5.1cm diameter cylindrical holder. The specimen remanences were then measured relative to the fiducial mark on the orientation disc, and a field correction was applied later. Most of the specimen magnetic moments in this study were ten times greater than the noise level of the magnetometer.

#### 1.8. Low field susceptibility meters

The low field susceptibility was measured in those specimens thermally treated in order to monitor whether chemical changes occurred during heating. Similar measurements were also made on other specimens to estimate the bulk magnetic content of the specimens, based on the susceptibility measured in three mutually perpendicular axes. As such it served as an indication of magnetic heterogeneity. The apparatus used was a susceptibility bridge (Collinson and Molyneux, 1967; Collinson, 1983). This instrument was checked for repeatability of

measurement and results indicated a standard deviation of 0.41 on the basis of nine repeat measurements on the same specimen. (Susceptibility measurements are presented in the Appendices).

#### 1.9. Causes of magnetic directional variation in large archaeological structures.

Previous workers noted the presence of apparent systematic variations of magnetic direction in kiln structures of varying ages (Harold, 1960; Weaver 1961, 1962; Aitken and Weaver, 1962; Aitken and Hawley, 1971; Dunlop and Zinn, 1980; Hoyer, 1982). The directional deviations, (in the case of azimuthally sampled structures), often took the form of a sinusoidal variation in declination around the kiln with steeper mean inclinations on the North side of the kiln as opposed to the South. Shallower mean inclinations were also found in the floors.

The observed magnetic deviations were usually accounted for by magnetic "refraction" whereby any secondary cooling portion of the structure would acquire a magnetisation proportional to the geomagnetic field strength and the magnetic field acquired in the primary

cooled area. Abrahamsen (1986) has described in detail the mechanism behind magnetic "refraction", whilst also pointing out that shape anisotropy is an integral part of such distortions. Thus for a horizontal plane Abrahamsen's correction is:

$$\Delta I = I_0 - I = \tan^{-1}((1 + 4\pi k_{app.SI}) \tan I) - I$$

Where  $\Delta$  = the refraction error,  $I$  = inclination and  $k_{app}$  = apparent susceptibility.

In fact Abrahamsen (op cit) calculates that for  $k_{app}$  of  $10^{-3}$ ,  $10^{-2}$  and  $5 \cdot 10^{-2}$  emu/cm<sup>3</sup> the refraction corrections may attain values up to ca.  $0.3^\circ$ ,  $3^\circ$ , and  $13^\circ$  respectively depending on the angle of incidence. Such "refraction" corrections assume a correlation between one magnetic property and another.

Other recent studies (Tarling et al, 1986), have shown that many kiln structures do not show a systematic pattern of magnetic distortion, but rather the greatest scatter was associated with the greatest large scale inhomogeneity. In particular there was no 1:1 correlation between magnetic intensities and the magnitude of directional scatter. "Refraction corrections" (e.g. Aitken

and Hawley, 1971), assume that there is a correlation, although these authors also pointed out the complex nature of such magnetic deviations.

Thus, given that in a number of instances non-systematic directional deviations were observed, as well as apparently systematic ones, these inconsistencies were investigated in large fired structures of different shape exhibiting differential cooling, inhomogeneity, and fabric anisotropies in order to isolate the cause(s) of such anomalies. The following is a description of potential causes of magnetic deviation.

#### 1.10. Physical movement

One of the basic assumptions in archaeomagnetic directional determinations is that the material sampled has not moved since the last firing. In kilns it is often the flue join to the walls which is most likely to move from its original position. Similarly kiln furniture may also be disturbed as a result of refuse dumping into the kiln, or collapse, like the walls due to the overburden of archaeological remains. Hearth materials are often disturbed by superposition of settlement which can cause differential subsidence and/or compaction often depending

on the hearth construction. Uniform movement, unless detected by excavation, can lead to totally misleading results, but large scale differential movement within a structure can be detected by comparison of the specimen magnetic directions as these should be similar. In order to provide a control on movement therefore the structures were sampled in various places and the specimen directions compared. Uniform movement over distances of  $\geq 12\text{m}$  was thought very unlikely in the case of the vitrified forts.

Diurnal and seasonal changes in temperature are a feature of even well sheltered archaeological environments (Gentles and Smithson, 1986), and thus physical stress to the specimen may occur as a result of expansion/contraction etc. Therefore direct exposure to the elements, as in the case of the Lunt kiln (Chapter Six), are likely to result in rehydration, frost shattering, and exfoliation effects, each of which may result in the physical loss of some of the original T.R.M..

#### 1.11. Magnetic anisotropy

Any alignment of magnetic mineral shapes or crystalline axes can give rise to a magnetic anisotropy

that may cause a deviant direction of remanence. In general shape anisotropy is dominant in magnetite whilst in haematite magnetocrystalline anisotropy is prevalent (Aitken, 1974).

Alignment of magnetic grains with uni-axial anisotropy could occur as a result of systematic pinching and smoothing of the clay e.g. in pottery manufacture. The anisotropy caused by this mechanism may therefore have a relationship with the position of the specimen on the fired feature. In addition the vitrified structures showed visual evidence of flowage of molten materials and in some cases retained the original geological fabrics. Such fabric anisotropies are discussed further in Chapters Three and Six.

The deflection of the thermal remanence from the ambient field direction can occur as a result of the magnitudes of the principal axes of the anisotropy ellipsoid as well its orientation, relative to the field location of the rock (Stephenson *et al*, 1986). As the intensity of magnetisation of magnetic grains is dependent on the rate of cooling and various other factors, the cooling history is likely to be integrally related to the degree of deflection. Recent work has also shown that



rocks with low anisotropy of susceptibility can have a much higher anisotropy of remanence (Potter and Stephenson, 1988).

#### 1.12. Inhomogeneity

Magnetic heterogeneity can occur at the microscopic (domain) level up to the gross magnetic differences in building materials. As gross differences in building materials of different geological histories are likely to result in distinct coercivity spectra, the remanence acquired through any one cooling may be variable depending on e.g. grain size and type of magnetic mineral. Furthermore the marked differences in  $T_b$  which may occur for example as a result of an igneous rock being incorporated as a repair in a clay built kiln, could lead to magnetic interactions at the border of the two different materials on cooling.

#### 1.13. Magnetic distortions on cooling

The systematic magnetic deviations noted by previous workers were not restricted to experimental kilns (Harold, 1960; Aitken and Hawley, 1971). Hoyer (1982) also showed that systematic magnetic differences were also present in

modern brick built kilns. As such this phenomena pervades a wide variety of kiln types. However, as mentioned, there are also a number of apparently similar structures which do not show systematic variations in magnetic direction (Tarling et al 1986), and some which show both (e.g. Weaver, 1962; Dunlop and Zinn, 1980). All of these studies have shown that restricted sampling would result in misleading magnetic results, whilst also showing that high magnetic intensities did not always correlate with the greatest directional scatter.

#### 1.14. Archaeological aims:

It was intended to delimit the probable time span of the sampled Scottish Vitrified Forts by magnetic means whilst also limiting some of the models for their vitrification. The features of these forts have been described by Mackie (1976) and Buchsenschutz and Ralston (1981). Few have been excavated using modern methods and their archaeological analysis is hampered by the lack of chronologically diagnostic artefacts.

## CHAPTER TWO.

---

### The Scottish Vitrified Forts, an introduction.

#### 2.1. Introduction

The mode of origin and chronological significance of the Scottish Vitrified Forts have been a source of controversy for hundreds of years (e.g. Anderson 1779; Tytler 1783; Pennant 1790 in Cotton 1954; Cotton 1954). The first recorded notice of a vitrified fort was by Pennant in 1769, but was not published until 1790. These structures have been fired in antiquity causing the component materials to partially melt thereby fusing the constituents of the core of their stone walls. The degree of vitrification at various excavated/unexcavated sites is variable as are the number of sites recognised as vitrified. For example Nisbet (1975) recognised 105 sites, whilst Mackie (1976) acknowledged 78 sites. Such lists have been available since the 19th century e.g. Christison (1898). However Mackie expressed reservations about 15 sites and Nisbet also had reservations about the number reported as vitrified. The later lists were often made up

of sites already listed in earlier publications with a few other sites based on the respective authors observations e.g. Cotton's (1954) list is probably derived largely from that of Christison (above) and Childe (1946). The likelihood is that many of the sites discovered by earlier field workers were automatically incorporated in the later lists. This suggests that the lists available are at least in part dependent on the vigilance of 19th century field workers.

The locations of the principal sites (Fig. 2.1) indicate a fairly widespread distribution with concentrations in the Inverness, Fort William, Great Glen, Argyll, N.E. and S.W. Scottish areas (after Mackie 1976). Notable is the lack of such forts in the main highland regions and their clustering on agricultural land. Attempts have been made to draw attention to the spatial distributions of the forts, the relationship of this to fort size (Mackie 1976), and the relationship of areal extent and altitude (Ralston 1983), but these parameters need not necessarily have chronological significance (Collis 1977). Nevertheless excavations, with associated radiocarbon dates have shown that the vitrified forts are not restricted to any one time period, and Dark Age sites (e.g. Dunsinnan, Mote of Mark, Green Castle at

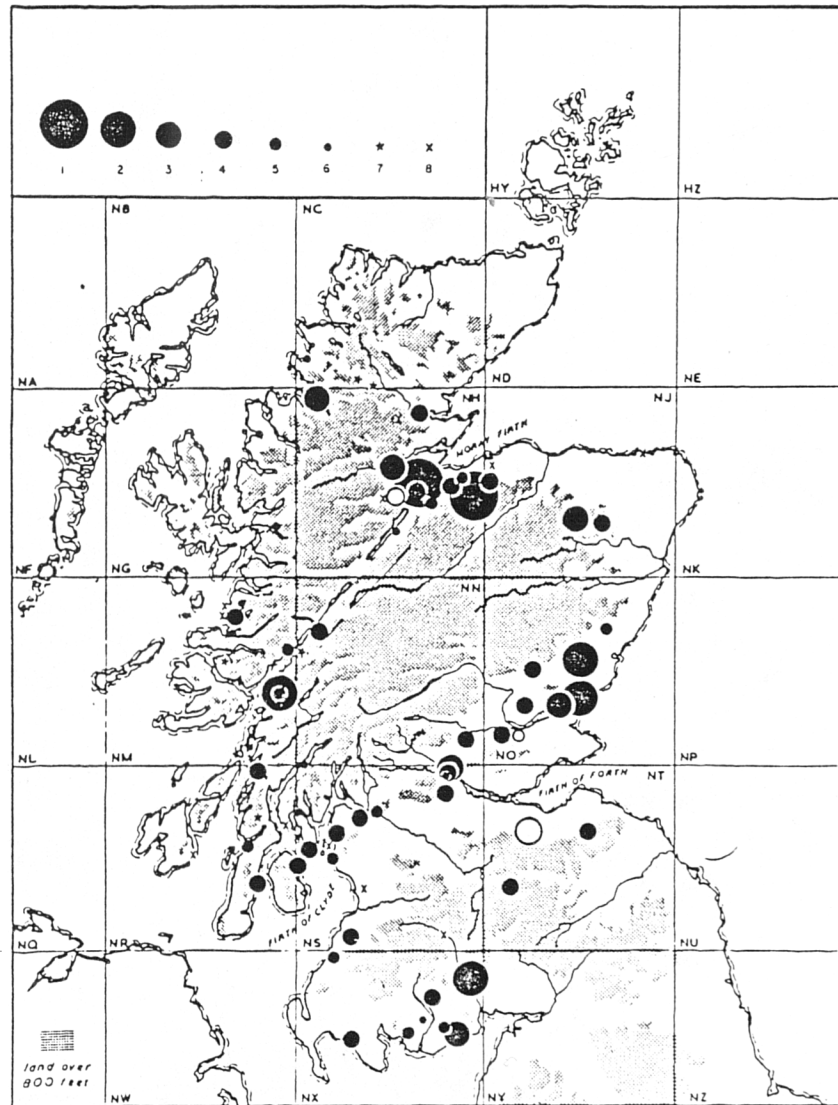


Figure 2.1 Distribution map of vitrified forts in Scotland showing relative fort sizes. (After Mackie 1976).

Portknockie), show vitrification as well as Iron Age ones (e.g. Finavon, Dun Lagaidh), (Alcock 1971; Mackie, 1976; Ralston, 1978; Laing, 1979; Alcock, 1985). This situation is complicated by the fact that many of the sites have multi-occupations e.g. Craig Phadrig, Langwell, Castle Point, Cullykhan (Greig, 1970; Greig, 1972; Small and Cottam, 1972; Nisbet, 1974).

As so few sites have been excavated by modern methods, with associated absolute dates, it is important to establish provisional *terminus ante quem* dates obtainable by measuring the remanent magnetism in exposed vitrified outcrops. These can be related to the radiocarbon dates derived from the internal stratigraphy of each site where possible.

For some, absolute dates were either already available or being obtained whilst this study was in progress. The chronological comparisons are discussed in Chapter Five.

## 2.2. Vitrification and its causes.

The following is a review of the major theories put forward to explain the varying degrees of vitrification observed. It is intended to provide a historical background against which the study of magnetic aspects of

the vitrified forts can be placed. In particular the study in Chapter Three was partially designed to determine how this dun was vitrified through understanding the factors affecting the acquisition of thermal remanences. Two basic causes have been proposed, constructive and destructive.

### 2.3. Constructive.

Williams (1777) believed that the forts were deliberately vitrified in order to bind and strengthen the walls. Anderson (1779) suggested the use of a vitreous iron ore and the mixing of stones with clay powder to aid the fusion of the core of the walls for constructive purposes. Christison (1898) also believed in the constructive argument, with the exception of those forts with limited vitrification which he classed as accidental. Macculloch (1824) believed in the constructive theory, pointing out that some forts were too low for use as beacons and he could not envisage how the firing of a dry stone wall, with timber, could produce vitrification. Stuart (1869) agreed with Jamieson (in Stuart 1869) that the vitrified forts were the result of constructive activity and extended this argument to the Bohemian vitrified forts mentioned by Keller (in Stuart op cit). Further Bartholemy (1846) (also in Stuart (1869)), when

talking of the fort at Peran, Brittany, suggested that the forts were designed to vitrify when set alight in order to strengthen the walls. Smith (1872) also noted vitrification at Perran. He adhered to the view of creative vitrification in order to stabilise the wall but with loose stones to top the wall, giving the opportunity "of throwing down pieces on an enemys head." Smith therefore felt that the walls were not intended to be vitrified to any great height.

#### 2.4. Destructive.

Tytler (1783) believed "... that the appearance of vitrification on some of those hills are the accidental effects of fire upon a structure composed of combustible and fusible materials, and by no means the consequence of an operation intended to produce that effect." He rejected the idea of volcanic action put forward by the Bishop of Derry (in Tytler) and suggested the use of wood, as well as stone, in the fabric of the original wall with a double row of palisades or stakes "warped across by boughs laid very closely together ... as to confine all the materials ... that were thrown in between them." Anderson (1883) (in Cotton, 1954) felt that there was insufficient evidence for constructive vitrification at that time.



M'Hardy (1906) undertook chemical analysis of vitrified samples from Finavon, Tap o'Noth and Eilean-nan-Gobhar and enquired into the method of construction. In order to limit the possibilities he decided to attempt reconstructions using a variety of combustible and non-combustible materials. He had previously noted that a large amount of slag was obtainable from burning grass or straw in stacks which had time to compact thus restricting the amount of air available for combustion e.g. Hay Mount Farm, Kelso. One of his constructions therefore involved slow burning (18 hours) using stone and brushwood, piled on alternatively to slow the rate of combustion as firing continued, and, by applying heat from below. By this method he achieved a small mass of vitrified material in the core of the fire and concluded that vitrification was possible by this method but that beacons (in terms of open blazing masses) would not cause vitrification similar to some of the vitrified forts unless fired over a prolonged period. M'Hardy argued against the constructive theory by saying that the vitrification was not continuous and that the slaggy mass often occurred where a strong wall was least needed, as at Dunagoil. Hibbert (1833) also rejected the idea that the vitrified forts were deliberately created

for defence but thought that the forts were the result of beacon fires. He noted that the beacon cairns of Elsness, Orkney, were composed of argillaceous schist and were variably vitrified, apparently by burning heath on stones since only fossil wood was available in Orkney. Hibbert thought that the ramparts of loose stones served the additional purpose of cairns on which fuel was placed. Hedges (1975) reported on the excavation of two Orcadian burnt mounds at Liddle and Beaquoy and suggested that they were the remains of domestic structures in which cooking activities led to the existence of large amounts of fire cracked stone, ash and carbon. He also noted the existence of vesicular material in association with these mounds which were analysed using the petrologic microscope and found to be fused silt or soil (Hedges 1975).

In 1935 Childe suggested that the vitrification was caused by a constructive technique, but, in 1937, his opinion changed following experiments where he tried to vitrify model timber laced drystone walls by piling brushwood against the sides of those at Plean Colliery, Stirlingshire, and at Rahoy, Argyll, (Childe and Thorneycroft, 1937a). He concluded that the firing of a timber laced wall could cause the core to be vitrified in a manner similar to the Vitrified Forts. However Childe

also noted the small scale of his experiments compared to the vitrification at, for example, Finavon. He made the point that whether the forts were deliberately vitrified was "an open question." Also notable was the fact that the Plean Colliery wall had an outer skin of fire bricks around the basalt core. The former may have had the effect of radiating heat back in to the core of the wall thus artificially increasing temperatures.

Similar results have since been achieved at Tullos Hill, Aberdeen, by Ralston (1980; 1986) using gabbro as the main building stone. Ralston noted that much effort was required to achieve limited vitrification and he concluded that vitrification was unlikely to result just during the course of battle, but a deliberate policy would be required to raze a fort. However a fire amongst thatched lean-to structures was also considered. He also concluded that the wind direction would be important. The difficulty in vitrifying timber laced walls led Ralston, (1986) to suggest that those walls showing evidence of ignition from the outer faces were more likely to indicate a controlled destruction after the cessation of hostilities. This hypothesis was supported by Dixon, (1976) in Ralston, (1986), who also attempted a wall firing. In addition Ralston (1986) concludes that it is

reasonable to assume that the irregular nature of many vitrified blocks on many sites cannot have provided a serviceable defence without supplementation. In this connection he notes that to his knowledge there are no instances of a later construction contemporary with the vitrification episode.

Fredriksson *et al.* (1983), using chemical analyses, noted that internal melting showed that vitrification was the result of *in situ* melting of stones in a timber laced wall. There was no evidence that fluxing agents had a significant role in the melting process and therefore the temperatures must have been in the range of those for natural basaltic and granitic systems i.e. 900-1100<sup>o</sup> C, or lower if substantial water pressures were sustained. However the authors noted anomalous enrichments of phosphorous suggesting that the walls contained organic materials. In addition the presence of metallic iron spherules suggested reducing conditions during vitrification, implying that the walls were densely packed and possibly covered with impervious materials e.g. sod.

The general conclusion was that the walls were built using sophisticated techniques. "Whether or not vitrification was intentional cannot be determined definitely at this time; however it does appear that the

Celts anticipated or planned for the fires." (Fredriksson *et al.* 1983). Brothwell *et al.* (1974) concluded that the analytical evidence did not support the idea of a bloomery but that the rock analyses supported the claim of *in situ* vitrification as put forward by Childe and Thorneycroft (1937a). They stated that, considering the high temperatures produced and the fact that c.60 vitrified forts are seen in a limited geographical area of Scotland, "we do not believe that this type of structure is the result of accidental fires. Careful planning and construction were needed."

Mackie (1976) was scathing of this conclusion and stated that all Brothwell and his colleagues could conclude, apart from distinguishing between vitrified rock and metal slag, was that the rock had melted and that the composition of the melt indicated the approximate temperature reached. Mackie believed that nearly all excavated evidence suggested that the vitrified forts were timber laced dry stone walls destroyed accidentally or deliberately by fire. In support of this he noted that the vitrification is incomplete at many sites e.g. Sleep Hill, whilst even at Rahoy and Inverpolly (severely vitrified structures) the fused mass was never more than 1.5-2m high and therefore inadequate as a defensive

wall. Mackie also noted that every excavation of a vitrified fort, except Rahoy, had shown that lumps of vitrification occurred over the ruins of a thick dry stone wall with vertical faces. In addition he stated that the stratification observed in every excavated vitrified fort showed that the burning occurred at the end of the use of the fort and that "... it did not occur at the beginning of the occupation of any site." Mackie has further persuasive points for Abernethy where beam holes indicated an unburnt timber laced wall with interior occupation. This argued that firing was destructive as it did not occur at the beginning of the use of this site. He also believed that the dry rubble core, containing thousands of air spaces, was responsible for the vitrification although he recognised the problems in explaining the degree of vitrification observed on some sites. Mackie concluded that huge quantities of brushwood, in a determined effort at arson, may have been required but that the evidence for destructive vitrification was overwhelming.

## 2.5. Discussion.

Clearly there is no general agreement as to why or how these structures were vitrified. The presence of beam

holes at unburnt sites but showing occupation horizons, e.g. Abernethy, and the traces of beam holes on those sites, vitrified with no immediate post-firing occupation, together with Childe's and Ralston's experimental evidence, argue that some vitrified forts are burned timber-laced forts. However this may not apply to all forts. Some are vitrified duns e.g. Rahoy and Langwell, whilst few if any beam holes noted extend right through the wall thickness at any site although at Langwell distorted beam holes were reported (Nisbet 1974). However at Castle Law, Abernethy, the inner wall was noted to have beam holes which extended to a depth of one full arm (Christison 1898).

Christison (1898) noted that the vitrification on the forts he examined was mostly located towards the top of the walls and only reached the bottom accidentally. In many sites this appears to be the case e.g. Finavon, Craig Phadrig and Carradale. In Ritchie and Ritchie, (1985) the authors suggested that there was reason to believe that the forts were only timber laced in the upper parts. If we accept that the presence of timber lacing is indicated by vitrification then timber lacing was likely to have been present in the upper parts of numerous forts in Scotland. Mackie (1976) further stated

that it was the inner wall faces that often exhibited beam slots although, as Childe (1934) noted, these were not detected at Finavon. At Castle Law, Abernethy, both the inner and outer walls have beam holes including the outer face of the outer wall, but not the inner face (Christison 1898). The outer face of the inner wall had two rows 60-105cm above the base, whilst the outer face of the outer wall of the fort had beam holes high above the base (142.8 cm) as well as evidence for longitudinal timbers (Christison 1898). At Castle Law, Forgandenny, the outer surface of the inner wall was pierced at irregular intervals by a row of square holes and slits running deep into the wall with associated charred wood. Both walls at this site had a rubble core with associated vitrification. However the existence of longitudinal beams was not proved because no section was dug. Therefore the excavation by Bell (in Cotton 1954) leaves the question open as to whether the wall was timber laced or not (Christison 1898; Cotton 1954). Also notable is the vitrification associated with gateways e.g. Langwell (Nisbet 1974), Craig Phadrig (Small and Cottam 1972). It would appear that there is sufficient evidence to suggest that in some cases only parts of the walls were timber-laced. Perhaps this is an explanation for the variable



amounts of vitreous material observed at different sites.

The presence of sand in association with burnt and vitrified timber laced walls may deserve more attention. Keller (in Stuart 1869) noted, with respect to the Bohemian vitrified forts, that at Hradischt, near Strakenitz, one of the forts had a base of large blocks of granite, the gaps being filled with sand. At Wladar, near Luditz, there were large blocks of basalt with the interstices filled with quartz dust "which make it susceptible of the influence of fire". Keller noted that between the single blocks such layers of quartz sand were found almost vitrified, but that the main vitrification was always in the central part of the wall. At Finavon Childe (1934) noted the presence of sand in the vicinity of the South wall. At Green Castle, Portknockie, no vitrified material was found from the rampart section nor the paved areas of the interior but the defence contained longitudinal and transverse oak timbers that had been burnt. The core of the rampart contained sand, small cobbles and larger blocks which had been heat cracked, but the temperatures appeared to have been insufficient to vitrify the wall (Ralston 1978). Also notable in this context is Fredrikkson *et al.* (1983) who noted that there were high concentrations of phosphorous in the samples

tested which suggested the presence of organic materials, although they could find no evidence for the addition of fluxes. Local plants and trees, particularly bracken, are known to have been used in the past for the manufacture of soda glass by mixing the ashes of them with the sand before heating the mixture to a molten state (Hunt, 1970). Alternatively, in coastal areas, seaweed was used. Bracken ash is known to be a fluxing agent (Linsley pers. comm.). Therefore the recorded situations in which sand and wood are found associated with vitrification or burning, plus the chemical evidence for organic materials, lends some support to the possibility that at least some of the timber laced walls may have had additional constituents which may have aided the vitrification of their wall cores. Longley in Ralston (1986) notes that pottassium rich wood (e.g. Quercus), may help lower the temperature of silica, although Ralston concludes this affect would be marginal.

## 2.6. Summary

It would appear that, bearing in mind the limitations of the evidence, the fort walls were at least partially timber laced with a rubble core; that there is evidence for internal ranges of wooden structures, e.g.

Finavon (Childe 1934), and Langwell (Nisbet 1974), and that both organic materials (possibly including fluxing agents) were in some instances in association with silica. The existence of turf and thatch as building materials are implied by the suggested reducing conditions and the presence of timber ranges.

### CHAPTER THREE.

---

The magnetic properties of a vitrified dun.

Tor a'Chorcain, Langwell, Strath Oykel, Ross and  
Cromarty, 57.9°N, 4.7°W.

#### 3.1. Location and description

The site is an elongated hillfort on a rocky knoll, 32m O.D., in a loop of the River Oykel. Surface features suggest that it was double walled and that an additional feature on the North and South flanks was an outer ditch or terrace (Nisbet 1974). At the highest point, superimposed on the debris of the earlier defences, is a more or less circular structure, heavily vitrified, and broken on the East by an entrance flanked by a guard cell. Beam holes containing charcoal provide direct evidence for horizontal transverse timber lacing, (Nisbet, 1974). The internal diameter is 15.5m with the remaining wall 5.0m thick and 2.0m in height from the interior (Figs 3.1 & 3.2). The wall has inner and outer faces of well coursed slabs and a central spine of exceedingly solid burnt and

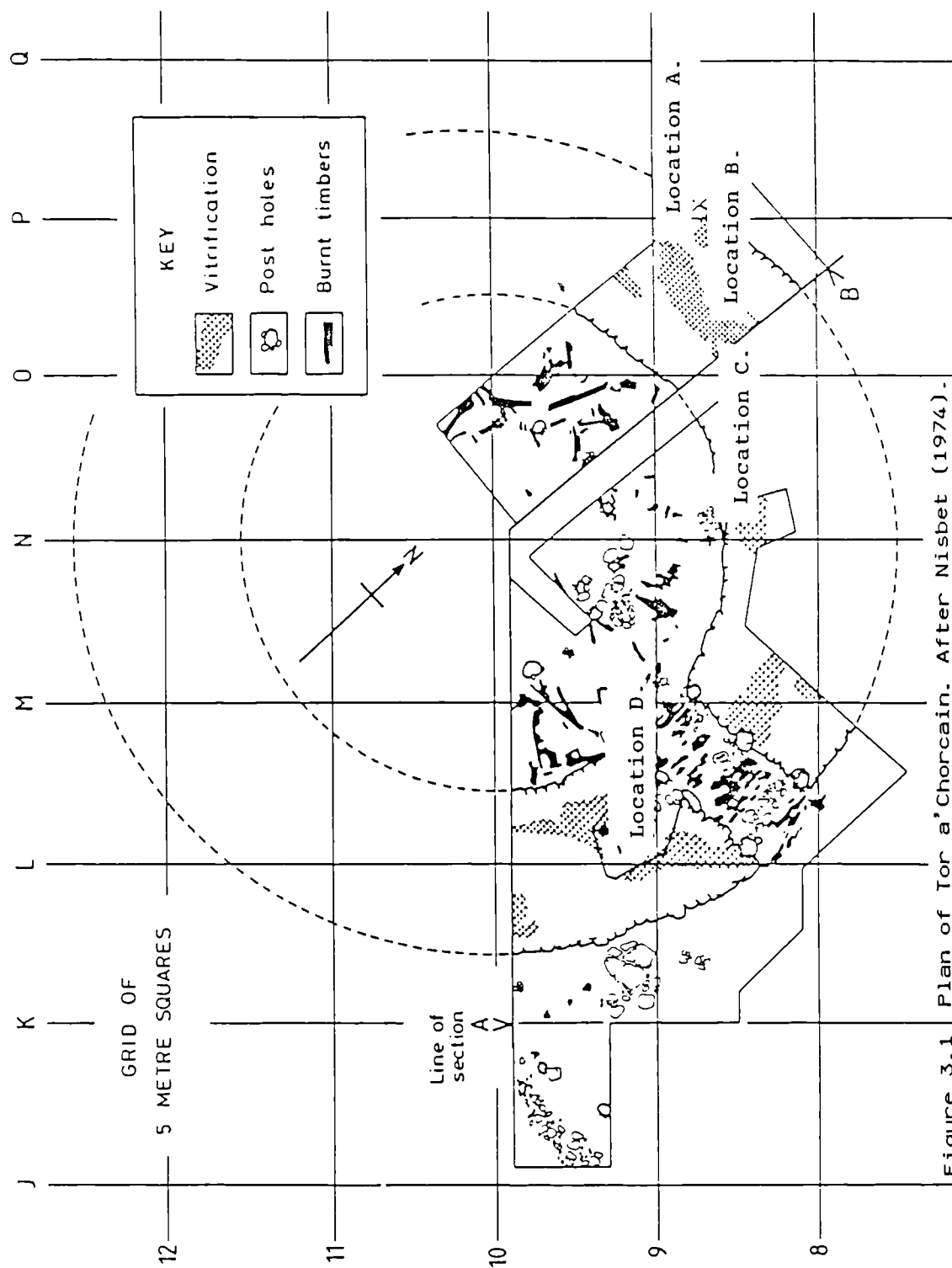


Figure 3.1 Plan of Tor a'Chorcain. After Nisbet (1974).

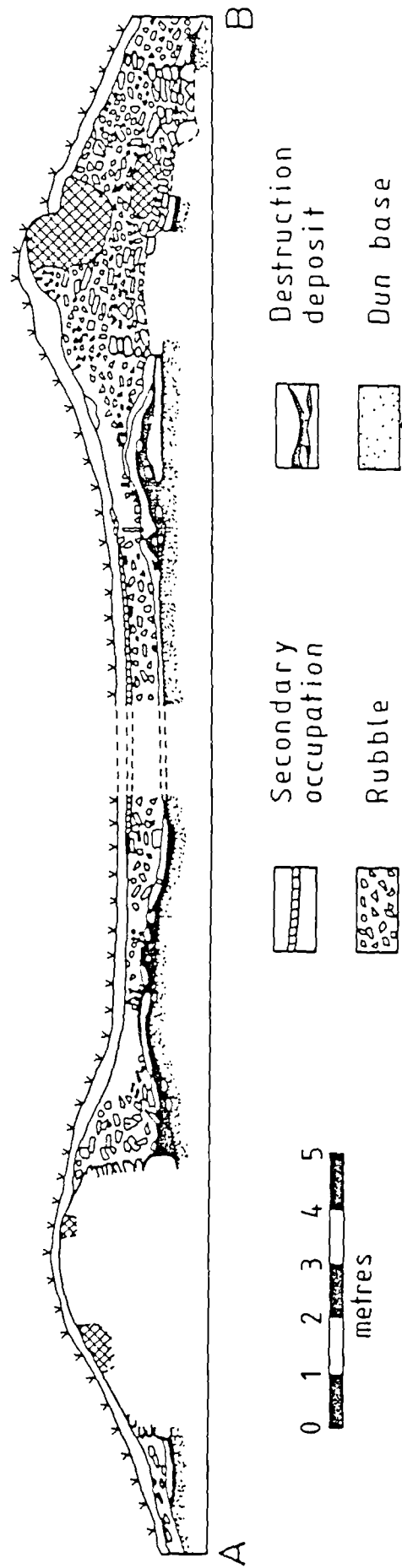


Figure 3.2 Section of Tor a'Chorrcain. After Nisbet (1974).

vitified stone. The dun was largely built of quartz schist with some quartz rich sandstone. Although there are no closely datable finds the timberwork of the dun has been radiocarbon dated (Nisbet 1974) and the vitrification has been dated using thermoluminescence (D.Sanderson pers.comm.).

### 3.2. Sampling strategy

Four locations on the dun wall were selected as sample areas (Fig 3.1) in order to (1) compare magnetic directional values from different parts of the vitrification, (2) provide a control on large scale differential movement, and (3) place controls on the contemporaneity of the burning.

### 3.3. Field observations

#### Locations A and B

A transverse section had been cut through the fused material in the North sector of the dun in 1973 for geological examination (Nisbet, 1974; Fig 3.1). In the centre of the wall was a fused mass of angular stones which extended North-South for 1.5m and appeared, from the limited exposures available, to be aligned longitudinally with the rest of the wall. The vitreous material was not

homogeneous but varied from a vesicular, black, low density cinder to a red glassy slag. These variations were taken to indicate either inhomogeneity in the building materials used and/or variations in the firing conditions. Weathering, indicated by superficial oxidation, appeared to be confined to the largely non-vitrified "shell" of the wall. Although considerable evidence of slumping was apparent in the dun, rubble immediately below and flanking the largest volume of vitrification at location B did not show evidence of major compaction which might have occurred had the fused mass slumped (Fig. 3.2). The vitrified core was exceedingly hard to hammer and structurally stable. This physical stability seemed to be confirmed in the section drawing (Fig. 3.2) which showed that the fused core was more durable than the outer faces and that some of the lower courses of the wall casing appeared to be still *in situ*. However the apparent displacement of some loose blocks in the upper parts of the wall might be consistent with localised movement, but not necessarily of the fused core during or after firing (Fig.3.2). On the West section (location A), sixteen specimens were taken at regular (c.10cm) intervals across the width of the vitrification, concentrating as far as possible on the most homogeneous material in order to test



for possible systematic deflections of remanent vectors through the wall. On the eastern section of the northern trench (location B), fourteen specimens were taken from a variety of vitrified types in order to compare their magnetic properties.

#### Location C

This was approximately halfway along the dun wall between locations A and D (Fig. 3.1). From the South the inner face included a "wedge" of fused stone flanked on both sides by inner facing blocks. The base of the wall was covered by rubble preventing a complete examination. The same inhomogeneity of materials was encountered, as in locations A and B, so sampling was restricted to apparently homogeneous materials.

A 7 cm diameter core had been removed from the centre of this fused mass for thermoluminescence dating. As the process of drilling might have created disturbance there was some doubt as to whether this wedge had remained *in situ* since the last firing.

It was therefore necessary to further assess the physical stability of this location. The inner facing blocks on the east side of the vitrification were displaced irregularly whilst the West ones were better

preserved. Neither side were perfectly horizontal. Another feature was a crack running through the eastern portion of the vitrification, possibly suggesting subsidence. However the vitrification extended northeastward for at least a metre and appeared, from the limited exposures available, to be aligned with the rest of wall in the upper, more northerly parts, suggesting no major wall movement. Much of the vitrification was brittle but the main body of the mass was hard and physically stable. On the West side the vitrification was fused with the core of the wall and partially with the inner facing stones, suggesting that it had been molten and then cooled in that position. Six specimens were removed from apparently *in situ* and homogeneous material.

#### Location D

The inner guardhouse wall was vitrified from c.0.5m to a maximum height of 1.8m above present ground level at location D. Angular small fragments were "welded" together by brown black glassy vesicular material. Below 0.5m coursed masonry was traced on all sides of the guard chamber (Fig. 3.1) and those courses supporting the vitrified mass were within 3-4° of horizontal. If they were originally flat then there was no major subsidence

after firing. The fused mass was solid and stable to hammering, and the vitrification was aligned with the rest of the wall exposed at this location suggesting no major post-firing displacement. Six specimens were removed, concentrating on apparently homogeneous materials.

The following sections describe how the most stable remanences were isolated, using both thermal and A.F. demagnetisation, whilst also considering, where relevant, the possible effects of anisotropy, magnetic distortion and inhomogeneity.

#### 3.4. Demagnetisation behaviour

Four specimens from location A (LA1,8,12,16) were demagnetised using alternating magnetic fields in 10 mT steps up to 70 mT and two from location D (LD5,6) up to 100 mT. Successive field corrected directions of remanence were plotted on a stereographic projection (Fig. 3.3). The remanence of specimens LA8, 12, and 16 from location A was found to be most stable (Tarling and Symons 1967) between 30 and 50mT (LA8, 12, 16), while LA1 was most stable between 50-70 mT, LD5 between 20-40 mT and LD6 between 60-100 mT. In all of these specimens an initial change in direction occurred as a low coercivity component was removed. Specimen LA1, like most others, did not show

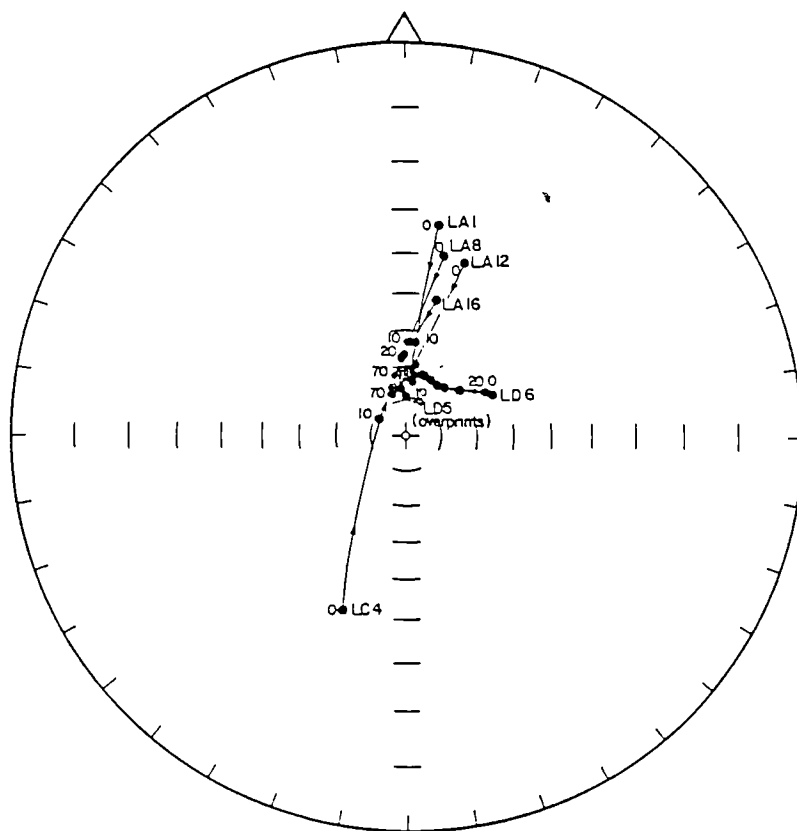


Figure 3.3  
Demagnetisation behaviour of specimen directions using A.F.  
(Equal angle stereographic polar projection).

a stable remanence below 30 mT. During A.F. demagnetisation most specimen inclinations moved from shallow, c.35°, to steep, c.70°, with a smaller westward movement in declination, although specimen LD6 showed a 25° westward movement in declination in erratic angular changes from 0 to 60 mT, with only a 12° increase in inclination (Fig. 3.3). Specimen LD5 showed little movement in declination or inclination during demagnetisation, but was consistent with the most stable A.F. cleaned directions defined between 20 and 50 mT in most specimens from the dun. Nevertheless many of the remanence directions were initially inconsistent with the present geomagnetic field (Fig. 3.3). Specimen intensities of magnetisations, plotted against applied A.F., showed a smooth decline with most magnetisation removed by 60 mT. All magnetic intensities at 70 mT were over  $100 \times 10^{-8} \text{ Am}^2/\text{g}$  whilst specimen LD5 had an intensity of  $85 \times 10^{-8} \text{ Am}^2/\text{g}$  at 100 mT (Fig.3.4), clearly demonstrating the importance of high coercivity components. Only one primary component of remanence was isolated in each of the specimens (e.g. Figs. 3.5, 3.6, 3.7, 3.8) from the four sampling locations.

The demagnetisation patterns of most specimens from locations A and B were similar to specimens LA1, LA8, LA12

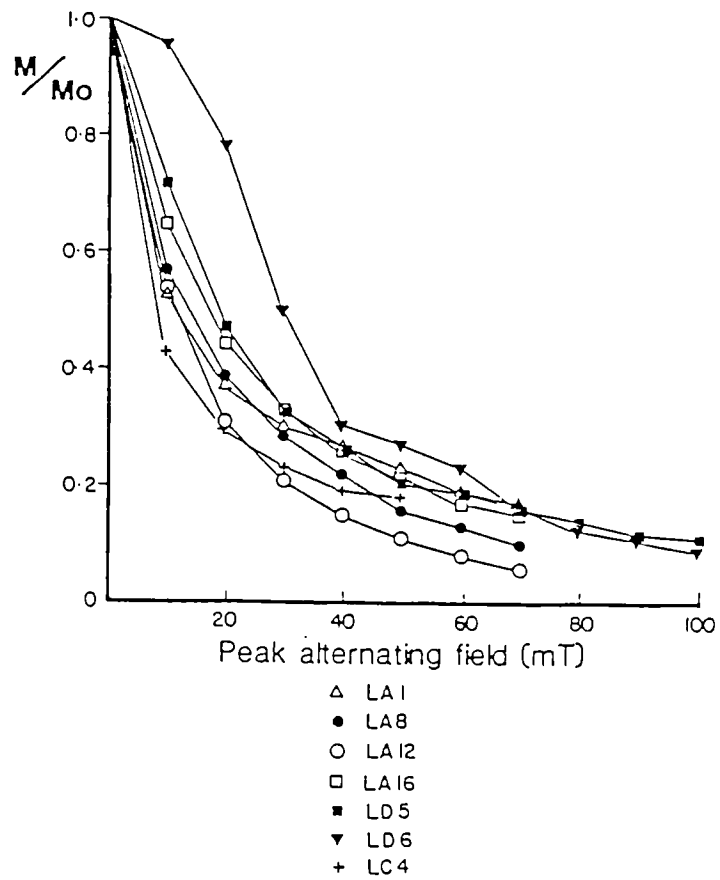


Figure 3.4

Demagnetisation behaviour of specimen intensities using A.F.

HOR. SCALE (\*~\*) = 181.000  
 VER. SCALE (X-X) = 192.000

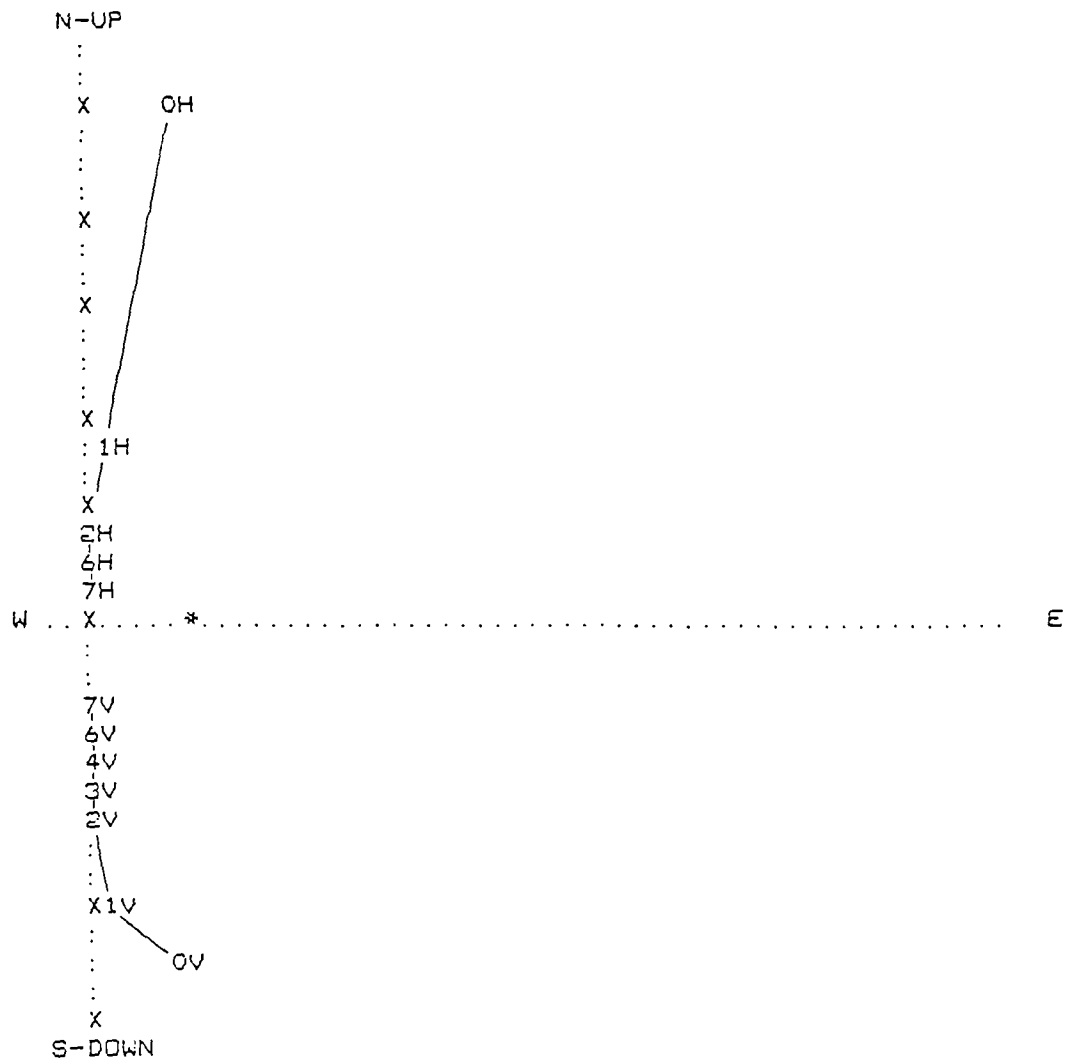


Figure 3.5 As/Zijderveld plot of LA1.  
 $\times 10^{-8} \text{ Am}^2/\text{g}.$

Figure 3.6 As/Zijdeveld plot of LB2.  
 $\times 10^{-8} \text{ Am}^2/\text{g}.$



HOR. SCALE (\*-\*) = 12029.000  
 VER. SCALE (X-X) = 12803.000

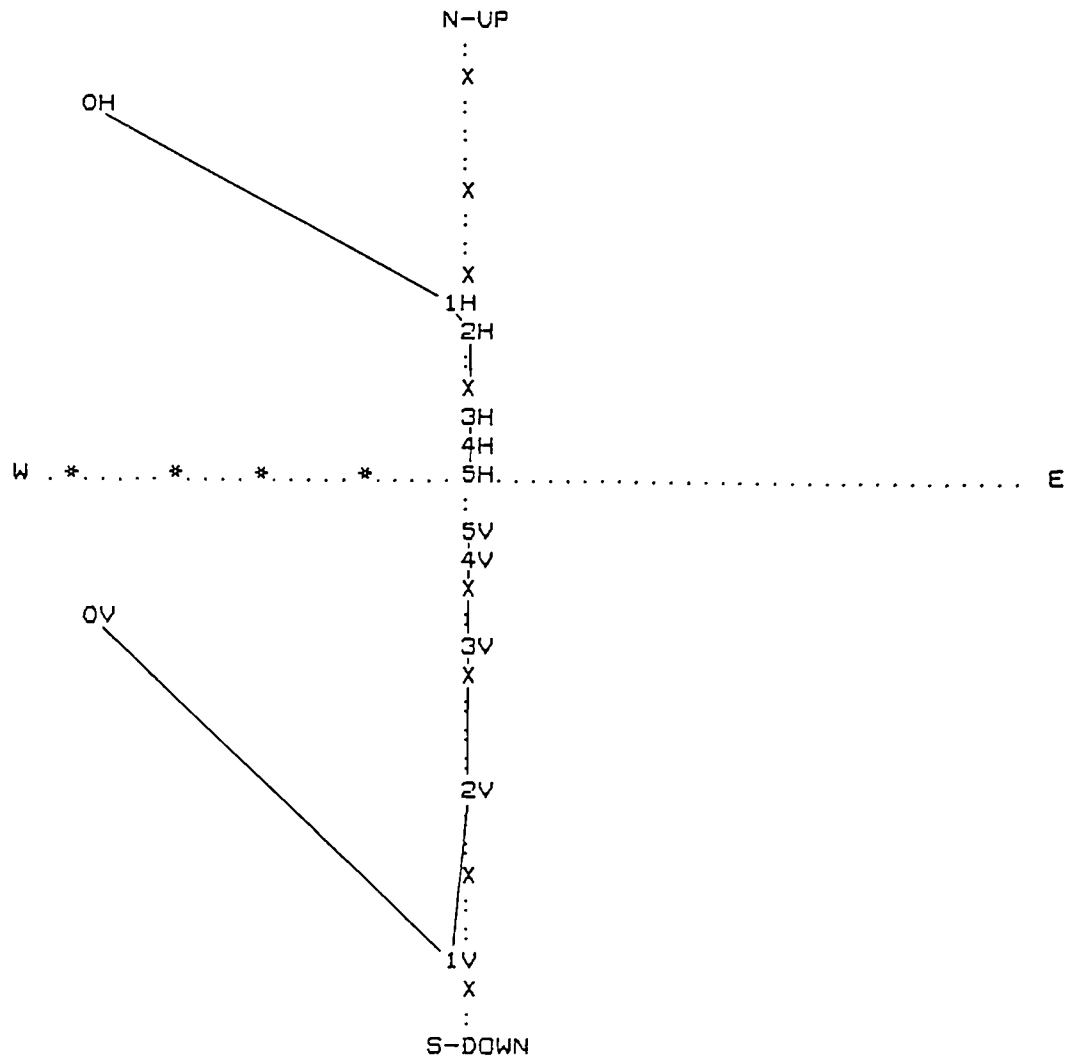
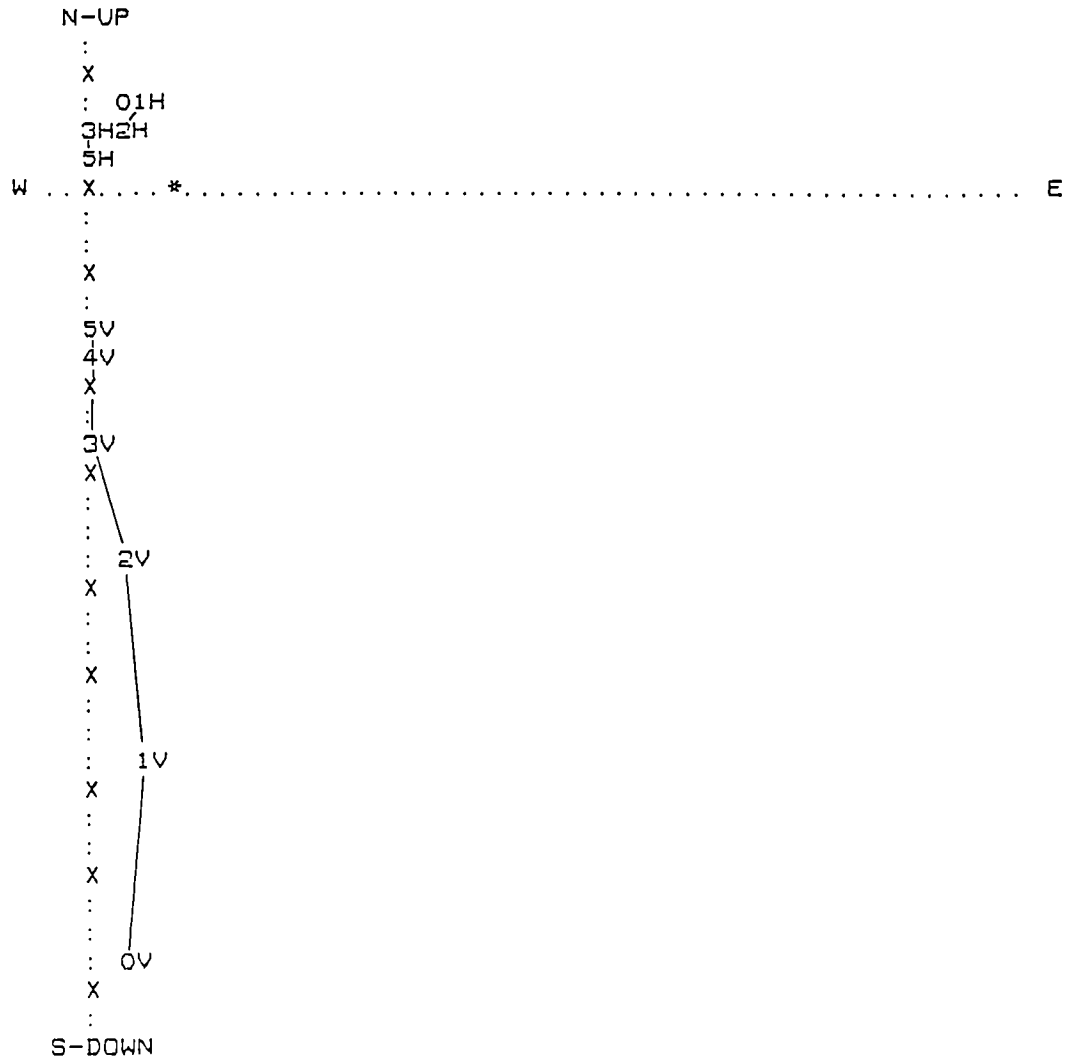


Figure 3.7 As/Zijderveld plot of LC1.  
 $\times 10^{-8} \text{ Am}^2/\text{g}$ .

HOR. SCALE (\*-\*) = 148.000  
 VER. SCALE (X-X) = 158.000



COMPONENT REMAINING

Figure 3.8 As/Zijderveld plot of LD2.  
 $\times 10^{-8} \text{ Am}^2/\text{g}.$

and LA16, with the exception of LA11 which showed a low coercivity component consistent with the Recent geomagnetic field direction. Specimen LC4 was typical of the vector movement observed in specimens from location C in that it showed a low coercivity component with an initial declination of  $201.3^{\circ}$  and inclination of  $38.8^{\circ}$  (Fig. 3.3) which is inconsistent with both the Recent geomagnetic field and the direction of the low coercivity components from locations A and B. Specimen LD5 showed little or no directional change, consistent with the directional demagnetisation patterns of most specimens from location D. However the low coercivity components from location D showed little consistency in declination and apart from LD2 and LD5 were in disagreement with the Recent geomagnetic field.

Four specimens from location B were demagnetised to  $700^{\circ}\text{C}$  in 50 and  $100^{\circ}\text{C}$  increments (Fig. 3.9 and 3.10). Angular changes in direction occurred at most steps, although the decrease in intensity was smooth. The magnetic directions moved towards the most stable directions defined by the A.F. method, but no consistent grouping was achieved (Fig. 3.10). Directional movement during demagnetisation showed a distinct curvature when plotted on an equal angle stereographic projection (Fig.

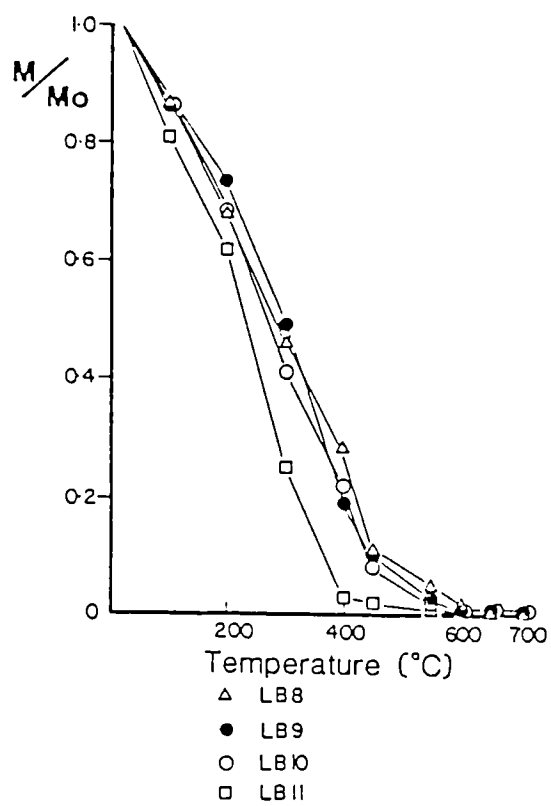


Figure 3.9

Demagnetisation behaviour of  
specimen intensities thermally  
treated.

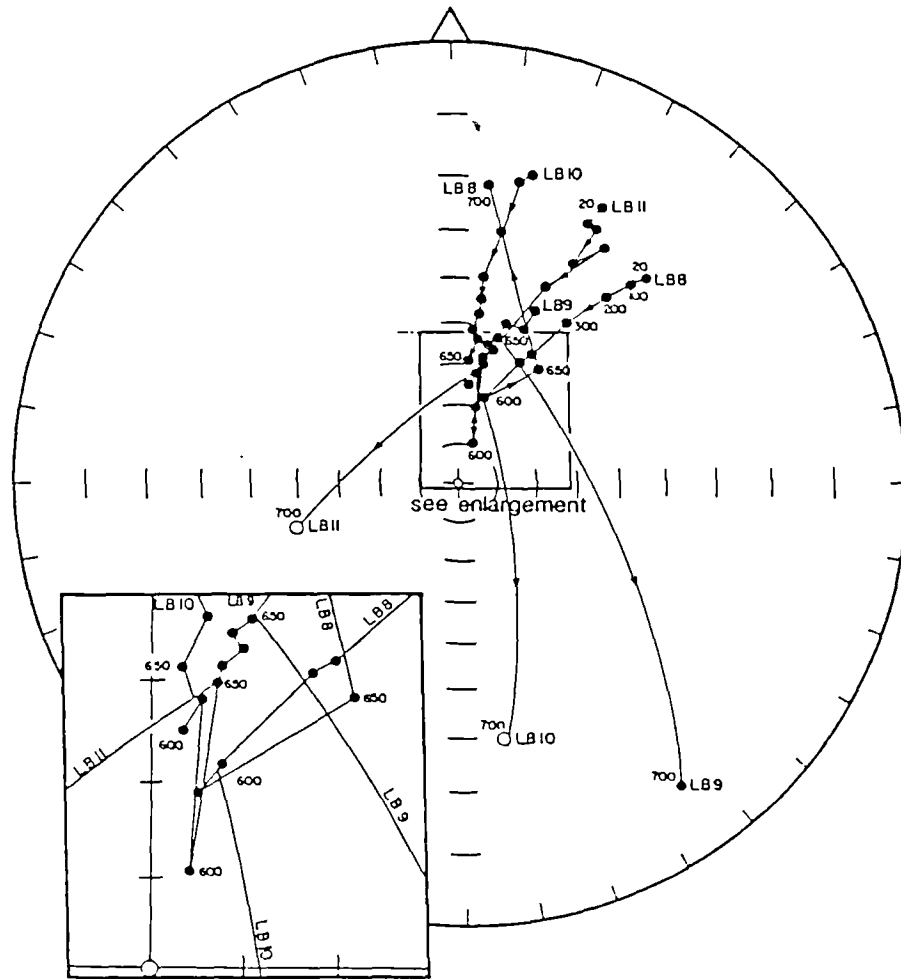


Figure 3.10

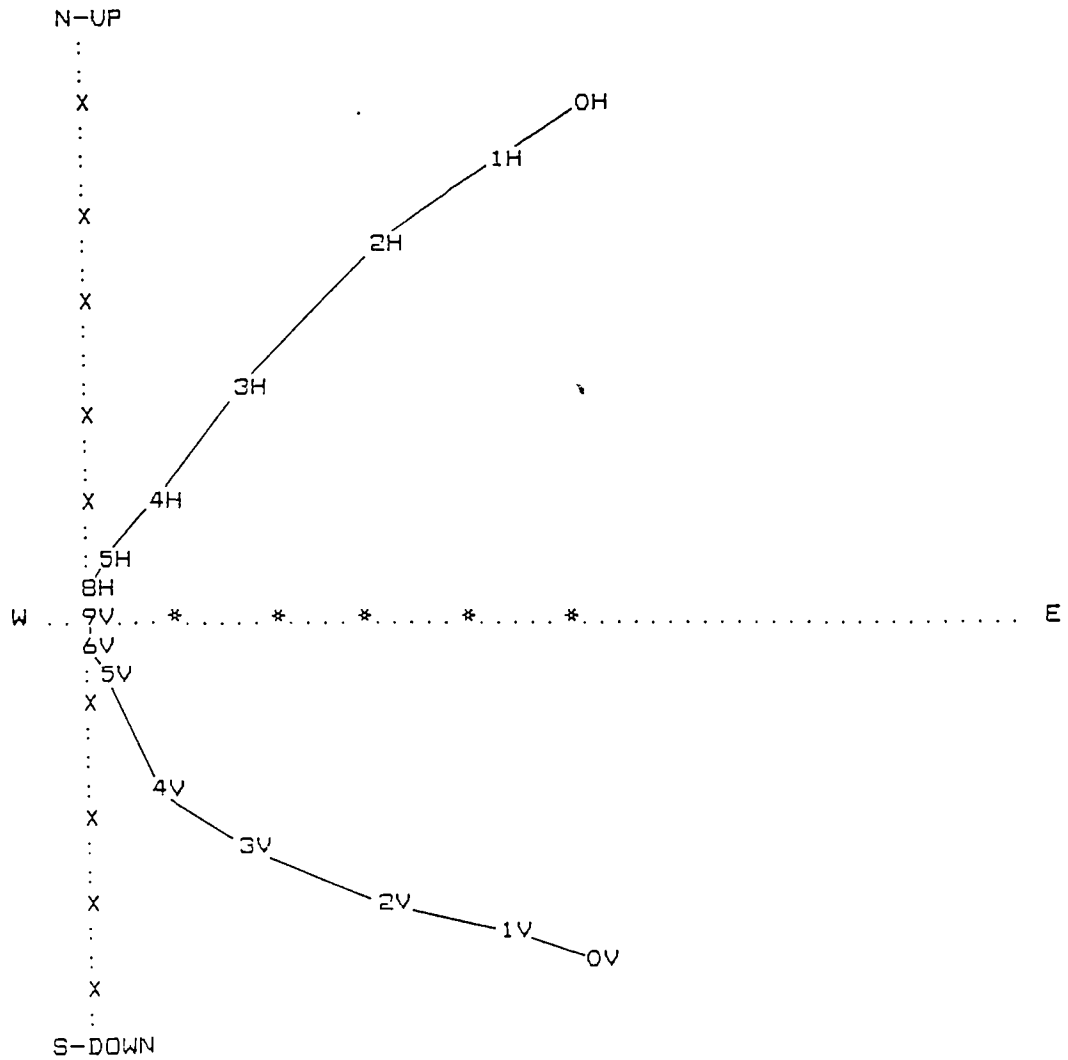
Demagnetisation behaviour of specimen directions thermally treated. Negative inclinations plot as hollow circles. (Equal angle stereographic polar projection).

3.10) whilst this curvature was also noted on Zijderveld diagrams of the same specimens (Figs. 3.11 to 3.14). Above 600°C the magnetic directions became increasingly scattered, whilst the intensity of magnetisation was weak and approached the noise level of measurement (Fig. 3.9). Like the A.F. demagnetised specimens the trend of directional movement during demagnetisation showed an initial component inconsistent with the present geomagnetic field direction. Specimens LB8, LB9, LB10 and LB11 showed some low field susceptibility change during heating (Fig. 3.15), possibly suggesting destruction of magnetic minerals, but there was little change in susceptibility for most specimens until temperatures at or above 550°C, suggesting that little or no chemical change occurred below that temperature (Fig. 3.15). Otherwise the magnetic behaviour of the specimens were consistent with each other in that the magnetic intensity diminished steadily, virtually to zero by 600°C.

### 3.5. Discussion

The vitreous material at this site appeared to be keyed in longitudinally and transversely with the walls at all four sample locations. This, and the stability of the walls to removal of specimens by hammering, suggested

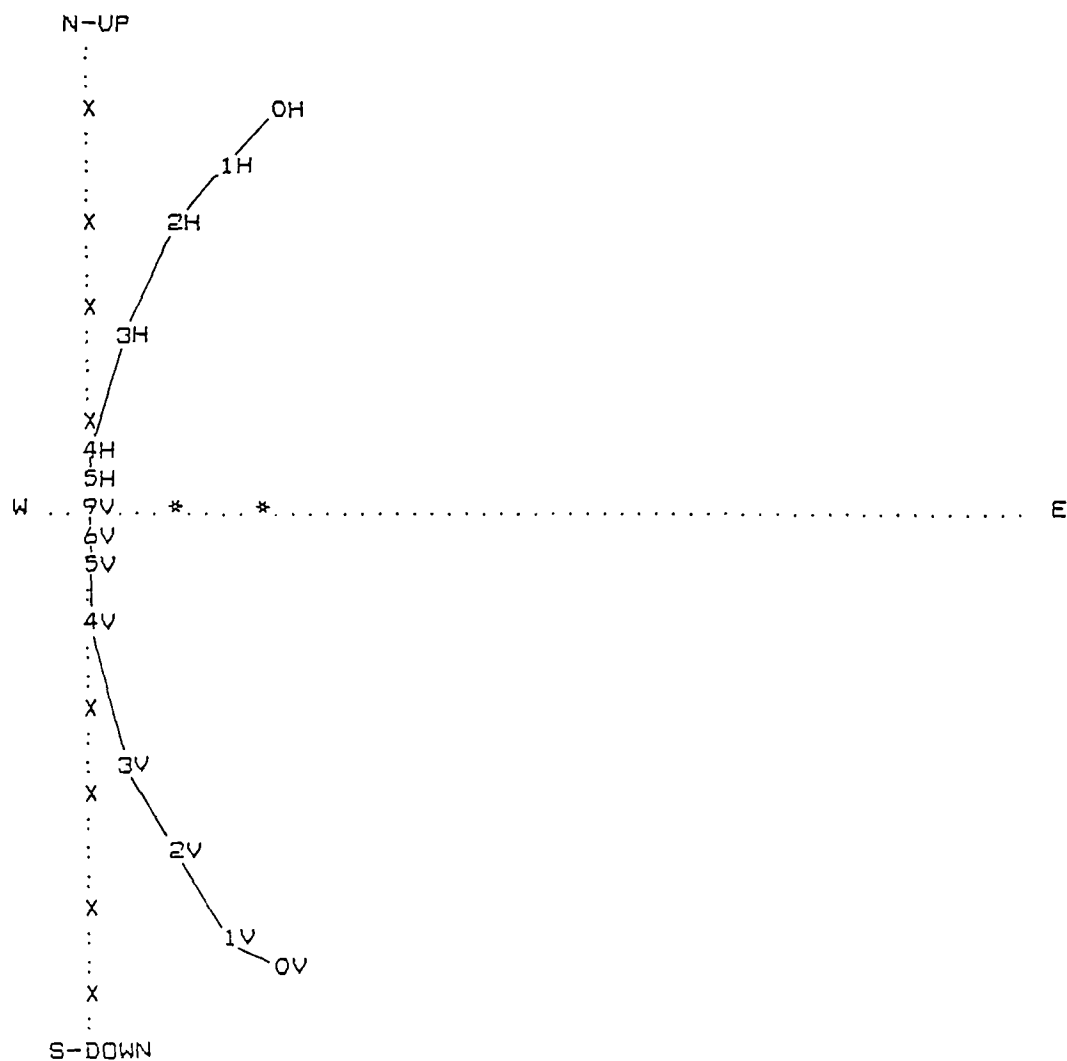
HOR. SCALE (\*-\*) = 104.000  
 VER. SCALE (X-X) = 111.000



COMPONENT REMAINING

Figure 3.11 As/Zijderveld plot of LB8.  
 $\times 10^{-8} \text{ Am}^2/\text{g}.$

HOR. SCALE (\*-\*) = 12.000  
 VER. SCALE (X-X) = 13.000



COMPONENT REMAINING

Figure 3.12 As/Zijderveld plot of LB9.  
 $\times 10^{-9} \text{ Am}^2/\text{g}$ .



HOR. SCALE (\*-\*) = 86.000  
 VER. SCALE (X-X) = 91.000

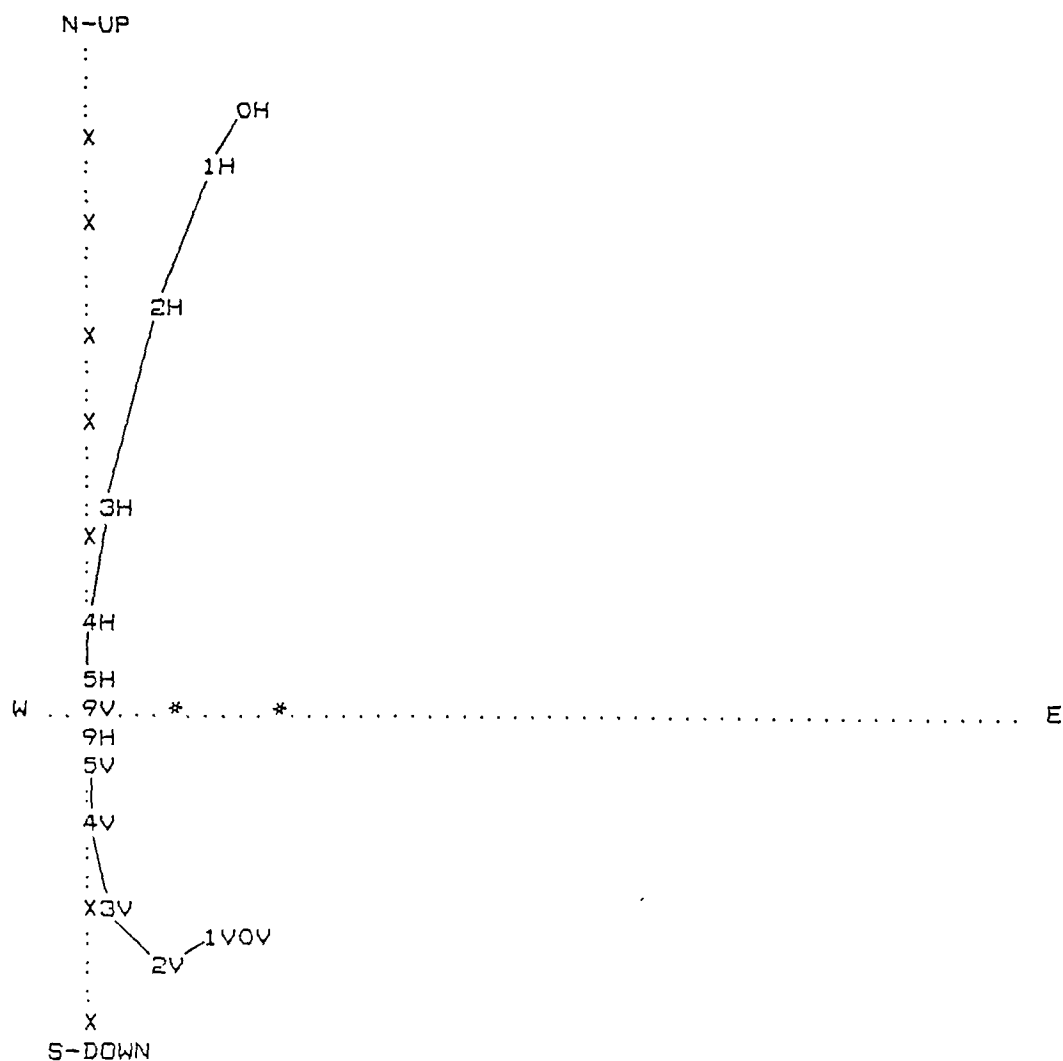
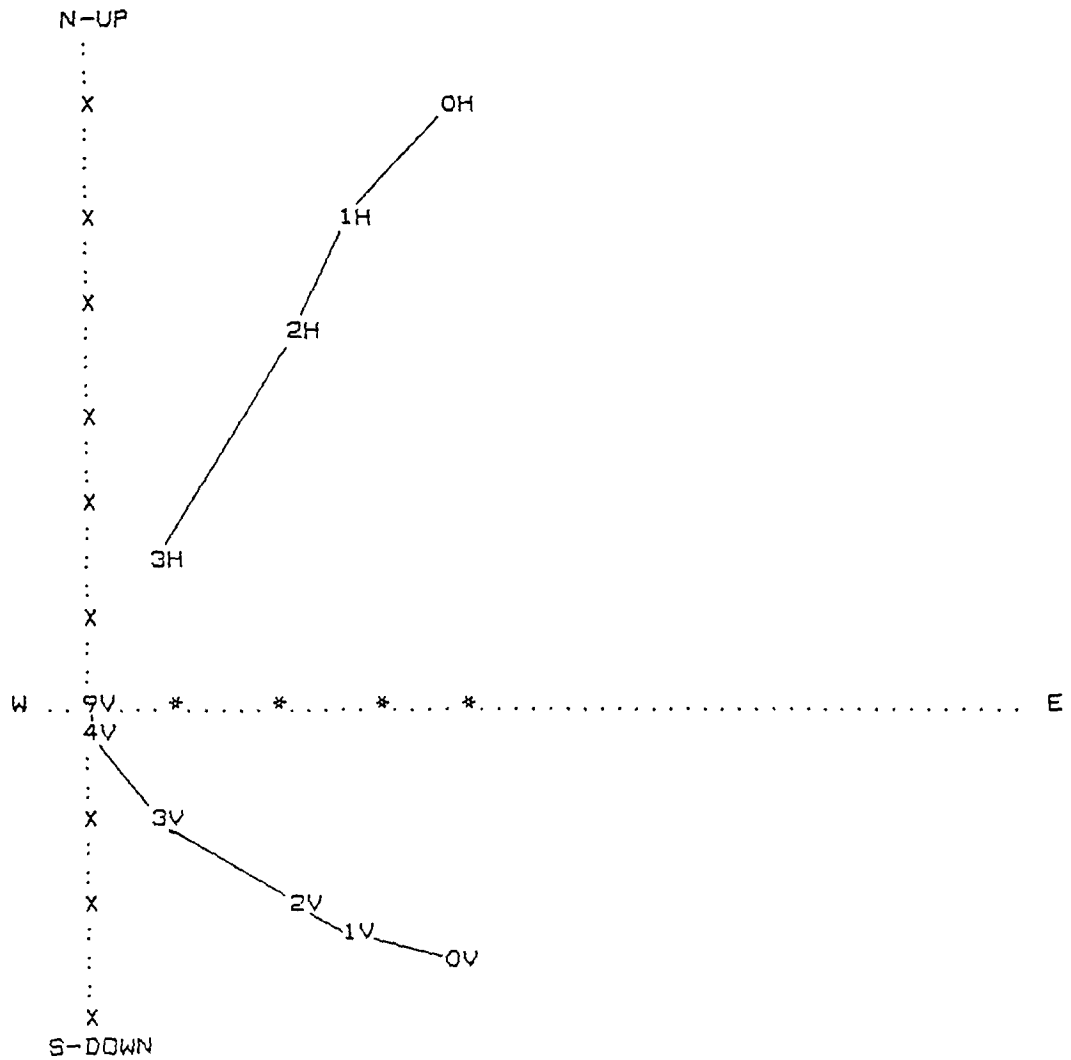


Figure 3.13 As/Zijderveld plot of LB10.  
 $\times 10^{-8} \text{ Am}^2/\text{g}$

HOR. SCALE (\*~\*) = 183.000  
 VER. SCALE (X~X) = 194.000



COMPONENT REMAINING

Figure 3.1 4 As/Zijderveld plot of LB11.  
 $\times 10^{-8} \text{ Am}^2/\text{g}.$

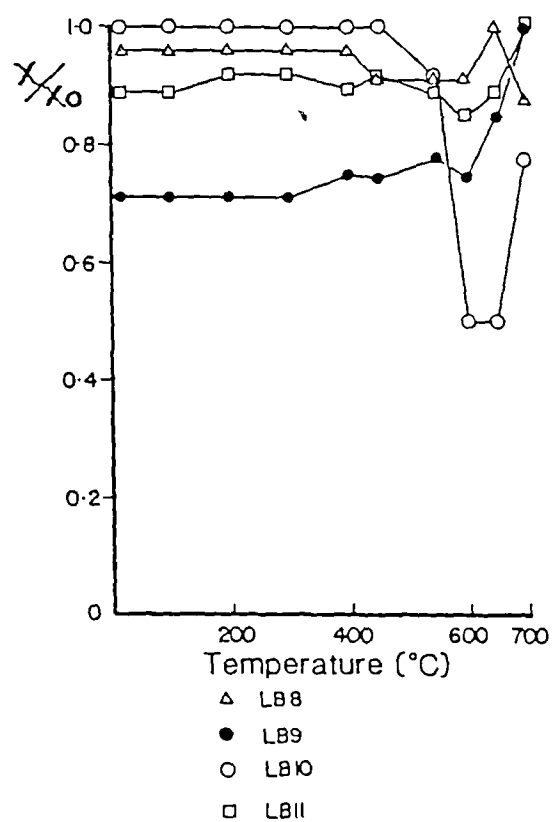


Figure 3.15

Magnetic susceptibility changes  
during heating.

that the vitrified material had not moved significantly since it was last fired. This inference was supported by the consistency between the mean magnetic directions and their circles of 95% confidence for three of the four locations, (Fig 3.16) excluding specimen directions (LB1 and LB5) which deviated by  $>20^{\circ}$  from all other specimens and those thermally demagnetised specimens which, as already mentioned, did not have magnetically stable end points. Although six specimens were taken from location D only LD2, LD5 and LD6 had archaeomagnetically meaningful directions after A.F. demagnetisation so there were insufficient specimen directions for a reliable mean direction for this locality i.e.  $N < 6$  (see Tarling 1983). However all the individual specimen inclination values from location D, were similar, except for LD3 falling between  $65^{\circ}$  and  $80^{\circ}$ . The similarity of the observed location mean directions, could be taken to indicate an upper limit to differential movement between the areas sampled. However there is a 95% probability that the true mean directions lay somewhere within the overlapping confidence circles and therefore there was no statistical difference between the observed mean magnetic directions from each location. This indicates that the mean magnetic directions are from the same population, strongly

# LANGWELL, FORT AND DUN.

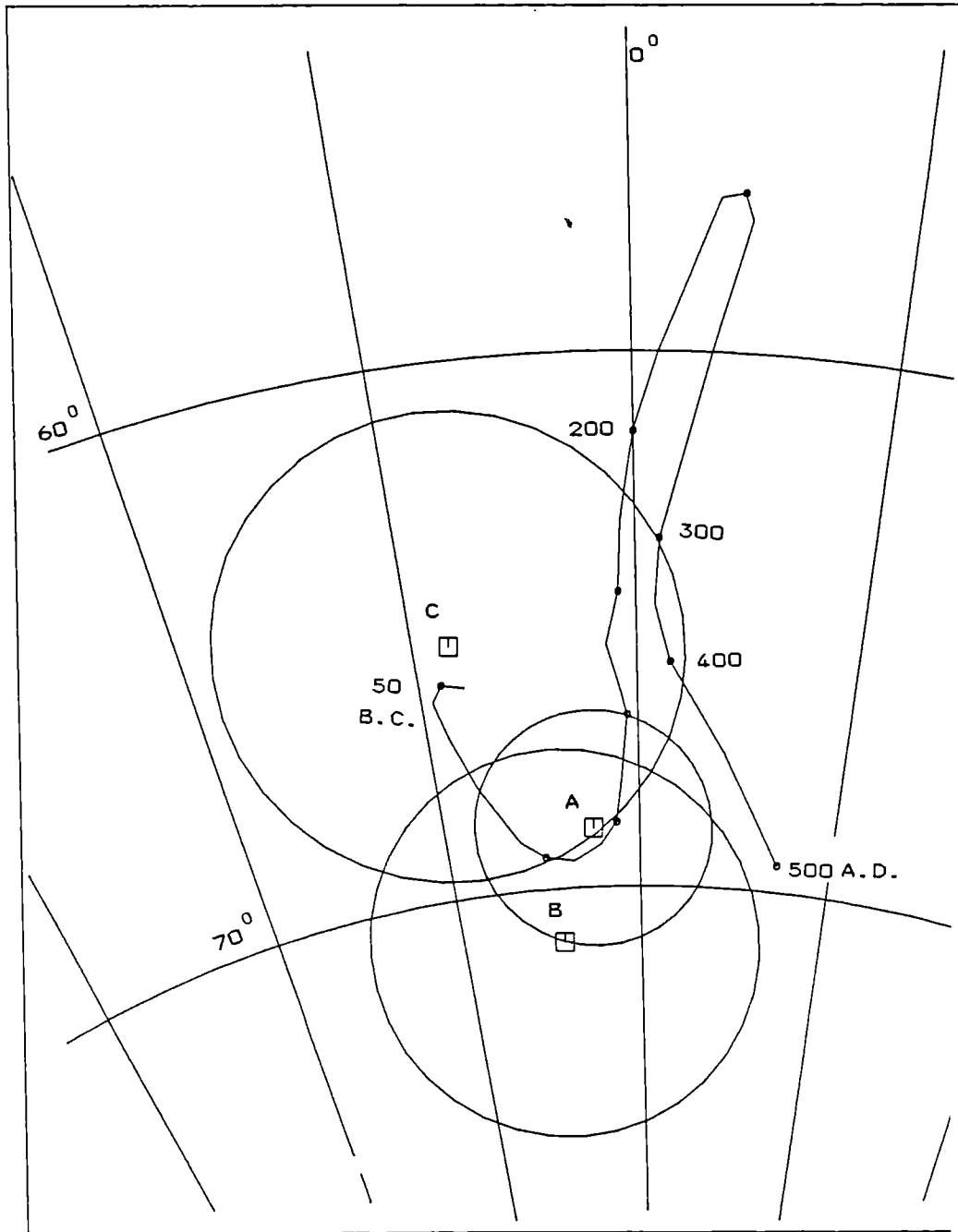


Figure 3.16 Stereoplot of location mean magnetic directions.

suggesting that the locations sampled had very similar cooling histories. (See "archaeological implications" for discussion of directional ambiguity). Further evidence of this is the overall mean direction of all specimens, an overall mean direction derived from the means A, B, and C, plus a mean of directionally consistent specimens from Location D. These have circles of 95% confidence of 1.6 and 3.9<sup>0</sup> respectively. The level of precision in the definition of these mean directions, based in the second case on only four observations, indicates inter-locational statistical compatibility at the 95% confidence level.

Although some individual specimens were visually anisotropic, with cleavage planes associated with oriented micas, the specimens were positioned randomly within the wall and so were irregularly oriented relative to the surrounding stones and to the ambient geomagnetic field. However some alignment of crystallised minerals may have occurred due to the flowage of molten matter but individual specimen magnetic directions from vitreous material were similar to those from non-vitreous and the mean magnetic directions from this vitreous type (mean of location B), were statistically identical with unvitified material (Fig. 3.16). As a further test the field

orientations of specimens taken from location A were plotted and compared with the most stable magnetic directions isolated using A.F. No obvious consistent systematic relationship could be observed between the position of the specimens in the field and the magnetic directions acquired (Figs 3.17 and 3.18).

Magnetic directions and intensities mostly defined after demagnetisation at 50 mT, (and magnetic susceptibilities measured after demagnetisation at 50 mT), were plotted against depth into the wall for location A to check for systematic correlations between changes in direction and other magnetic properties (Fig. 3.19; Table 3.1). Magnetic intensity values varied between  $38 \times 10^{-8} \text{ Am}^2/\text{g}$  and  $5090 \times 10^{-8} \text{ Am}^2/\text{g}$  prior to demagnetisation, and between 12 and  $783 \times 10^{-8} \text{ Am}^2/\text{g}$  after demagnetisation, whilst the intensities showed no clear systematic relationship with magnetic susceptibilities. Low magnetic susceptibilities were related to both high and low magnetic intensities. Irregular and erratic changes in both declination and inclination occurred through the wall, although greater variation was apparent in declination. (This would be expected with steep inclinations). Taking specimen LA1 as a reference the solid angular difference between it and other specimen

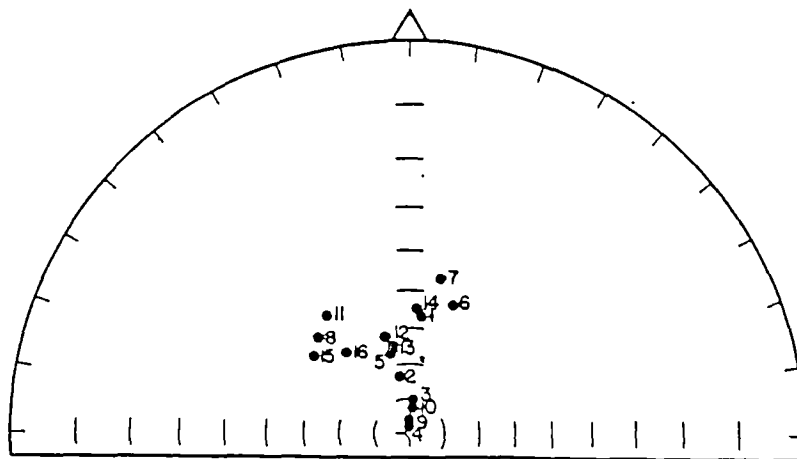


Figure 3.17

Plot of specimen field orientations for location A. (Equal angle stereographic polar projection).

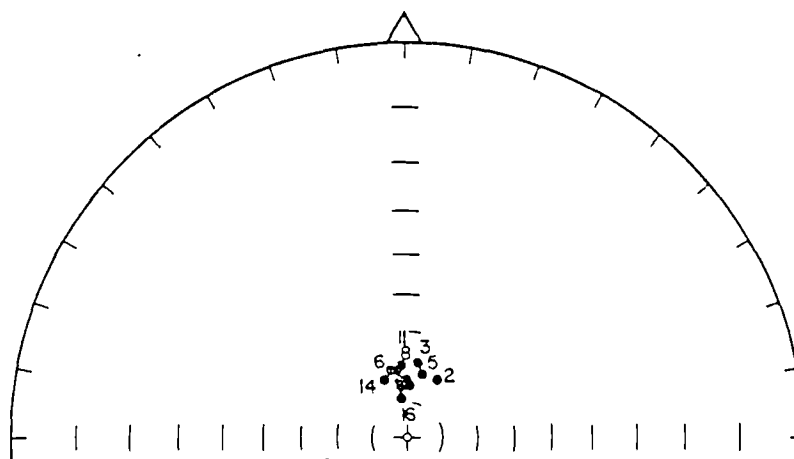


Figure 3.18

Plot of most stable field corrected magnetic directions for location A. (Equal angle stereographic polar projection).



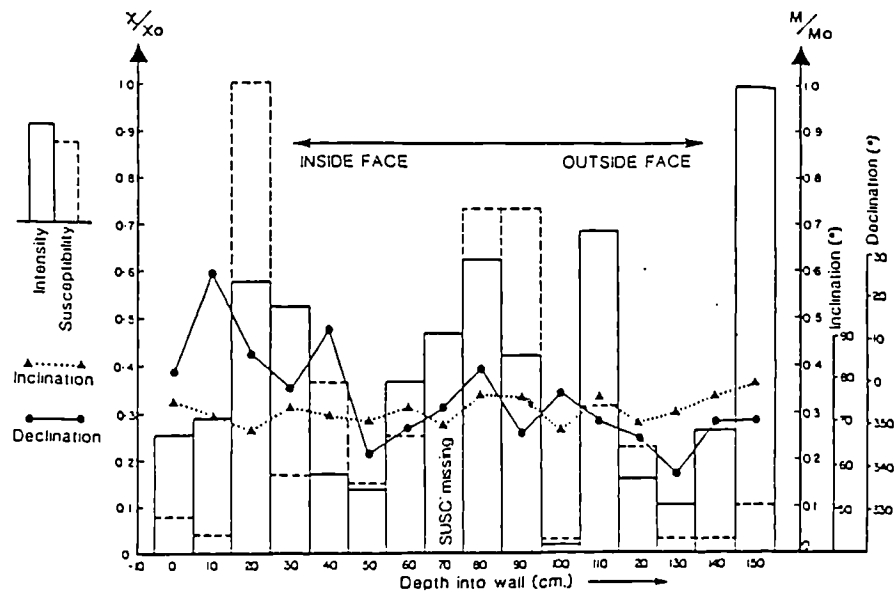


Figure 3.19

variation of magnetic properties through a  
vitrified wall section at location A  
(declination and inclination).

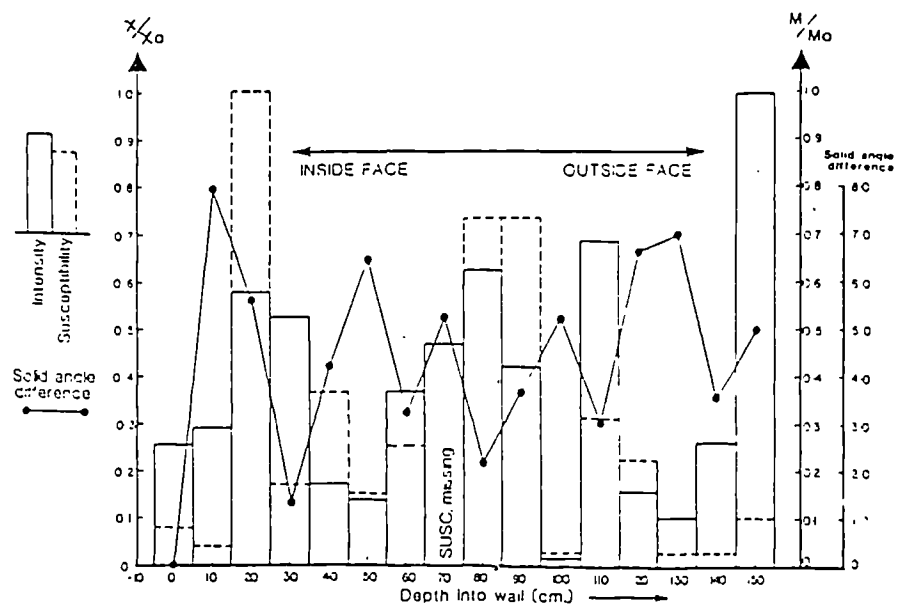


Figure 3.20

Variation of magnetic properties through a  
vitrified wall section at location A  
(solid angle).

**Table 3.1**

**Most stable specimen directions.**

Specimen.	Dec.	Inc.	Int.	$\alpha_{95}$	S.I.	Range.
			$\times 10^{-8} \text{ Am}^2/\text{g}$			mT
LA1	2.6	73.7	202.1	1.5	14.1	50-70
LA2	26.9	70.6	234.0	0.5	41.3	20-40
LA3	7.1	68.3	449.1	1.0	20.8	30-50
LA4	358.6	73.0	414.4	0.8	27.2	30-50
LA5	11.8	70.6	138.7	1.4	15.2	30-50
LA6	345.6	69.9	111.0	2.4	9.1	30-50
LA7	351.2	73.5	295.8	1.3	16.5	30-50
LA8	355.7	68.9	373.6	0.5	43.4	30-50
LA9	4.2	75.8	489.3	0.7	30.5	30-50
LA10	349.5	74.7	336.2	1.1	18.1	20-50
LA11	358.0	68.7	12.0	1.7	12.4	20-40
LA12	352.5	75.3	541.4	1.0	21.4	30-50
LA13	347.3	69.2	136.0	0.7	29.7	20-50
LA14	339.1	72.2	88.3	1.2	16.4	20-50
LA15	351.3	75.6	209.6	1.5	14.1	20-40
LA16	351.0	77.8	783.3	0.9	23.2	30-50
LB1	30.1	59.3	43.7	3.1	7.0	20-40
LB2	3.3	74.2	1902.5	0.3	74.6	30-50

LB3	351.6	77.2	80.1	1.0	20.9	30-50
LB4	353.0	75.4	93.0	1.1	18.0	20-50
LB5	32.7	73.8	207.0	0.9	23.0	30-50
LB6	357.9	76.9	86.7	1.0	22.5	30-50
LB7	351.1	69.2	60.8	1.5	14.1	30-50

<sup>13</sup>C

LB8	42.0	29.0	600.3	6.3	3.3	20-200
LB9	14.6	55.2	8.9	2.6	7.0	300-450
LB10	7.8	47.1	14.2	5.5	3.4	400-550
LB11	28.7	21.4	906.0	3.9	5.2	20-200

mT

LC1	358.3	68.1	7248.4	1.9	9.9	10-50
LC4	350.4	75.7	5.3	1.6	13.9	30-50
LC5	356.4	68.8	91.2	2.6	7.7	20-50
LC6	345.9	64.0	91.1	2.2	8.8	20-50
LC7	339.6	70.1	4.5	0.9	24.1	30-50
LC8	344.1	69.4	25.6	1.2	18.1	30-50
LD1	329.2	70.9	42.5	1.4	15.3	30-50
LD2	14.8	78.4	242.7	1.8	12.1	30-50
LD3	50.6	61.5	332.2	1.5	12.7	0-40
LD4	328.3	71.9	197.5	1.6	12.2	10-50
LD5	358.4	71.7	198.8	0.4	48.2	20-40
LD6	12.5	72.8	213.5	2.3	8.2	50-100

.

**Mean Meriden corrected direction for all specimens:**

Dec = 359.1	Inc = 68.7
N = 35	R = 34.702
$\alpha_{95} = 2.2$	K = 114.1

**Mean Meriden corrected direction for location A:**

Dec = 357.6	Inc = 68.9
N = 16	R = 15.944
$\alpha_{95} = 2.2$	K = 266.7

**Mean Meriden corrected direction for location B:**

Dec = 355.6	Inc = 71.0
N = 5	R = 4.991
$\alpha_{95} = 3.6$	K = 444.2

**Mean Meriden corrected direction for location C:**

Dec = 351.6	Inc = 65.3
N = 6	R = 5.978
$\alpha_{95} = 4.4$	K = 231.4

directions was calculated to determine the solid angular differences between the magnetic directions of specimens. The latter was plotted against the low field magnetic susceptibility and magnetic intensity measurements, with depth through the wall at location A. The smallest solid angular difference was between LA1 and LA4, but no consistent correlation between the angular separation of specimen magnetic directions and other magnetic properties was observed (Fig. 3.20).

### 3.6. Isothermal remanent magnetisation curves.

Three specimens from location B (LB12, LB13, LB14) were demagnetised at 100 mT, measured and isothermal remanences applied in incremental steps to a maximum applied field of 325 mT. When the magnetisation acquired was plotted against applied d.c. field it was found that the intensities of magnetisations of LB12 and LB13 became similar at applied fields above 100 mT, whilst the remanence of specimen LB14 continued to increase and did not saturate even after applying fields of 325 mT (Fig. 3.21).

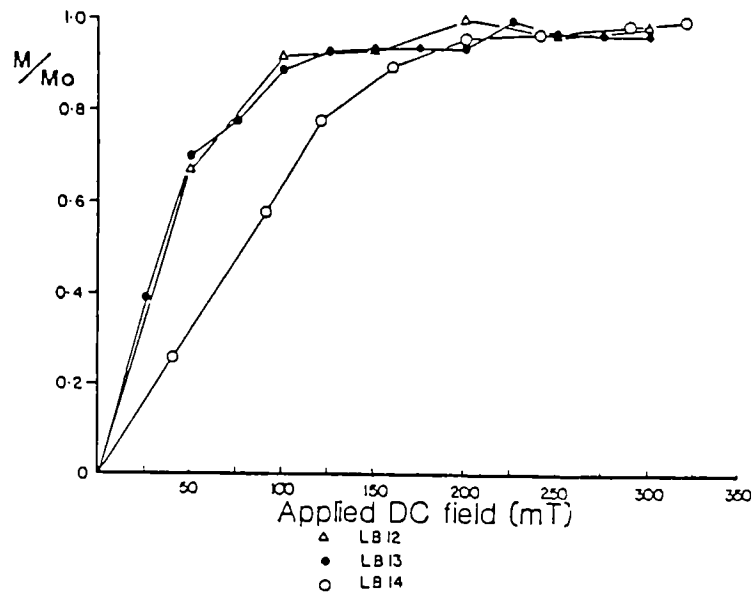


Figure 3.21  
Isothermal remanence curves.  
Location B.

### 3.7. General

The low temperature components isolated in both A.F. and thermally demagnetised specimens from location A were similar to each other but collectively different from the present geomagnetic field direction. This is puzzling as the specimens were stored in random orientation so any laboratory viscous remanence acquired would have been random relative to the variable fiducial mark orientations. The low temperature remanence would be expected to be associated with the geomagnetic field of the last c. 2000 years.

The distinct curvature of the thermally treated specimen directions during demagnetisation could conceivably have been caused by movement during cooling, but not all specimens show the same magnetic pattern, notably LD5 showing an extremely stable remanence between 0 and 100 mT with minimal directional movement. This direction was consistent with the end point directions from the thermally treated specimens and the most stable directions defined in most specimens between 20 and 50 mT. Further the degree of directional consistency between isolated areas on the dun, provides a control on any large scale differential movement either during cooling below 600 °C or after the last firing for those areas sampled.

The observed curvature could also be explained by overlapping blocking temperatures associated with a secondary firing but although some directions, isolated at 10-20 mT or less were consistent with magnetic directions in the Roman period, the majority of these directions were not repeatable over more than one demagnetisation step (Fig. 3.3). Further most magnetic directions prior to demagnetisation were inconsistent with the geomagnetic field values during the last 2.5k years.

Another possibility is that of lightning strikes which would result in an isothermal remanent magnetisation (I.R.M.), plus an anhysteretic remanent magnetisation (A.R.M.), although magnetisations produced in this way can be expected to be much more complex (Cox, 1961; Tarling, 1983).

The anomalous low coercivity component could also be a result of magnetic distortion affects occurring during cooling. Any secondary cooling portion of the structure, whether on a micro or macroscopic scale, would acquire a remanence in the ambient geomagnetic field, plus the field of the remanence acquired in the primarily cooled areas. In this case this could cause a shallowing of the vectors recorded in grains with a lower blocking temperature. Thus those specimens with higher magnetic intensities would be



expected to show the greatest scatter. It also follows that the directions defined at the highest temperature level, i.e. with the highest blocking temperatures, are likely to be the most consistent since, on cooling, they will have acquired their magnetisations first (Dunlop and Zinn, 1980). The thermally cleaned specimens do show the greatest consistency at high demagnetisation levels, as do those A.F. demagnetised. (Such consistency after thermal and A.F. cleaning is encouraging for archaeomagnetic directional dating by either technique).

The specimens demagnetised to  $700^{\circ}\text{C}$  indicated that the vitreous and non-vitreous fabric had been heated over the Curie point of magnetite, destroying all previous remanences. Therefore the differences in magnetic properties between specimens from location A were not related to low temperature differential heating. However the large differences in magnetic susceptibility over small and large distances across the wall at location A indicated magnetic inhomogeneity, possibly concomitant with varying oxidation states. (This variation could also be due to differences in the concentration and/or composition of the magnetic minerals present). Similarly differences in magnetic intensity could also be due to a number of factors including the magnetic mineralogy, the

duration of cooling, grain size, and the concentration of magnetic particles (Fox & Aitken, 1980; Walton, 1980; Thomas, 1981; McIlleland-Brown, 1984; Tarling, 1988). The variable fabrics of the wall core may have contributed toward random magnetic distortions on cooling.

Therefore, given the magnetic inhomogeneity, it is likely that localised magnetic interactions and larger scale magnetic distortions occurred during the cooling of this structure but these would not necessarily give rise to consistent systematic variation or correlation between magnetic directions, intensities and magnetic susceptibilities.

### 3.8. Archaeological implications

The similarity of the observed directions from separate locations on the dun suggests contemporaneity of burning. (However the 95% confidence circles calculated for the means of locations B and C were based on 6 specimens or less and were thus less reliable). The 95% circle of confidence calculated for location A on the other hand, based on 16 specimens agreed well with the circle of confidence calculated on the basis of all 30 specimens, (Figs 3.16 and 3.23). Therefore the similarity of the observed means (at the 95% confidence level), the similarity of individual specimen magnetic directions from

different parts of the dun and the fact that there appeared to be only one destruction deposit (Fig.3.2), it seems very likely that the burning of different parts of the dun were contemporary. Comparison of the mean magnetic direction based on all specimens with the archaeomagnetic secular variation curve (Clark *et al*, 1988), suggests that this firing occurred at some time between the late first century B.C. and the late first century A.D.. However a similar geomagnetic direction may have existed in the early part of the first millenium B.C. but evidence currently suggests it to have been c.30° East of the directions isolated for Langwell (Thompson and Turner, 1982; Clark *et al*, 1988). The fact that A.F. did not distinguish any secondary heating might suggest that the vitrification process was not an exercise of successive heatings, but if the last firing was at a temperature over the Curie point of the magnetic carrier then all earlier firings would be magnetically undetectable.

The thermal demagnetisation curves (directions and intensities) suggest that the specimens thermally treated had been originally heated to 600°C or above. The directional consistency at high temperature demagnetisation steps supports the conclusion that the wall at Location B was physically stable on cooling at or

below 600°C. The similarity of the magnetic components isolated using A.F. (see physical stability of the wall core), and thermal methods implies the same physical stability at the other sampling locations. The demagnetisation plots of intensity and direction showed that the magnetic mineral present in most thermally treated specimens was probably magnetite. The I.R.M. curves obtained from specimens LB12 and LB13 also indicated that magnetite was the dominant remanence carrier in these specimens, as magnetite saturates in fields of 1 T (Tarling, 1983). However the I.R.M. curve for specimen LB14 indicated the presence of haematite as the latter does not saturate until fields of over 1-3 T (Tarling, 1983), although magnetite was also present (Fig. 3.21). Magnetite is suggestive of an enclosed environment during firing as the magnetite would otherwise have oxidised to haematite.

The curvature shown by the vectors during thermal demagnetisation seemed best explained as being due to magnetic interactions during a slow cooling. Those areas fast cooled would be expected to show fewer magnetic deflections. If we accept this then those specimens with directions most consistent with the original geomagnetic field should be those which have cooled first and fast.

Conversely those specimens showing vector movement during demagnetisation and anomalous low coercivity/temperature components should be slowly cooled. Furthermore magnetic deflections are most likely to occur in materials of high magnetic intensity which in turn may distort the ambient geomagnetic field recorded in surrounding rocks (e.g. Tarling, 1988). Although there were exceptions where relatively low intensities correlated with anomalous components (LB9, LC5), it was interesting to note that nearly all specimens with high magnetic intensities had anomalous low coercivity/temperature components.

There were no closely dateable finds recovered during excavation, although stratigraphically the site appeared to have been occupied and re-occupied over a considerable time span (Nisbet, 1974). Most of the radiocarbon dates and associated standard deviations obtained for the timberwork of the dun varied between the fifth century B.C. to first century A.D. (H.Nisbet, pers. comm.), whilst Dun Lagaidh and other comparable vitrified structures seem to be concentrated in the seventh to sixth centuries B.C. for primary phases (Mackie, 1969).

The overall mean magnetic direction from Langwell, excluding individual magnetic directions clearly deviant from the closely agreeing majority, plotted adjacent to

that part of the archaeomagnetic secular variation curve consistent with an early first century A.D. date, whilst the 95% circle of confidence incorporated that part of the curve consistent with a Late First Century B.C. to Late First Century A.D. date (Fig. 3.23).

### 3.9. Summary

All specimens had stable to extremely stable remanences (Tarling and Symons, 1967). Thus although the magnetic directions showed a variation greater than that expected from orientation and measurement errors ( $>2^\circ$ ; Fig. 3.22), the mean magnetic directions from different parts of the dun were statistically consistent with each other at the 95% confidence level. The correlation between mean magnetic directions from vesicular and non-vesicular materials also suggested that fabric anisotropies did not cause systematic deviations.

The most stable directions were isolated at high temperature or high A.F. demagnetisation, and the most stable specimen primary remanences were probably acquired first on cooling. The likelihood of differential cooling between different areas on the dun was high, as was the likelihood of localised magnetic interactions on cooling. Random magnetic deflections are feasible and seem to have

LANGWELL, FORT AND DUN.

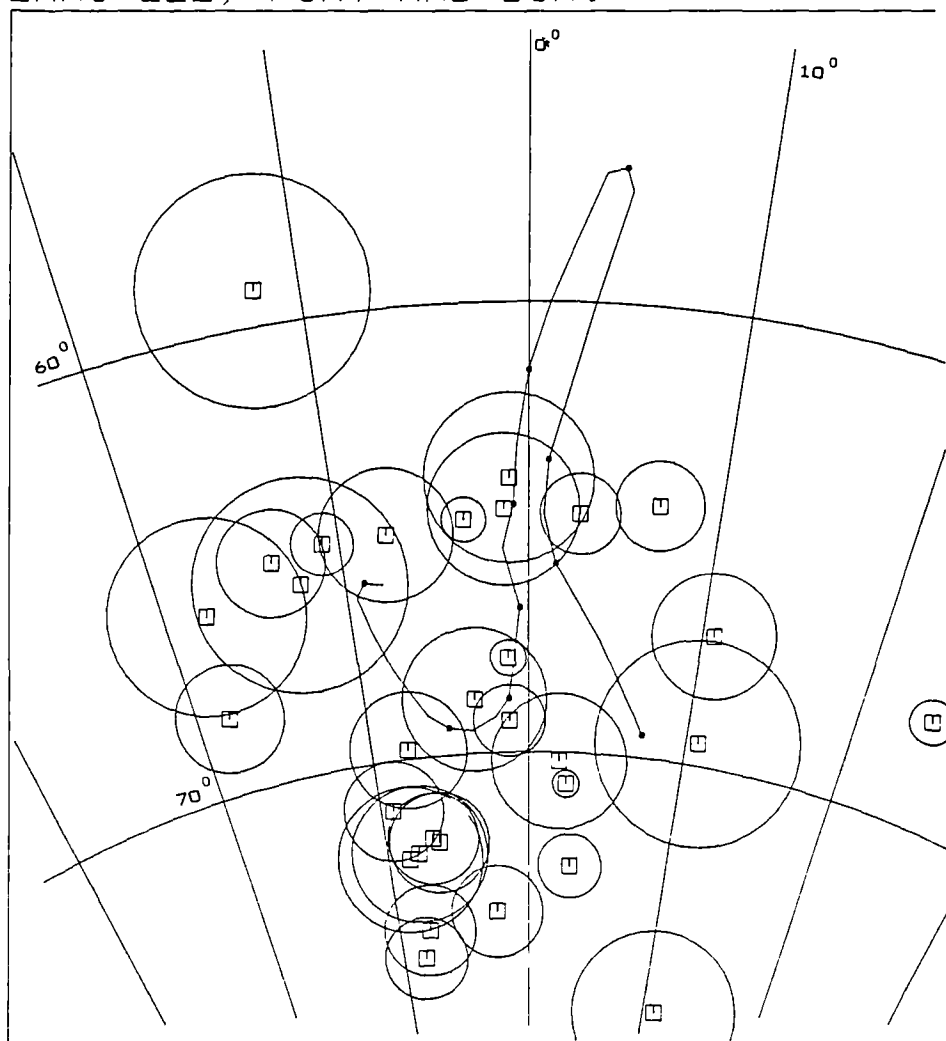


Figure 3.22 Stereoplot of individual specimen magnetic directions and overall mean.

# LANGWELL, FORT AND DUN.

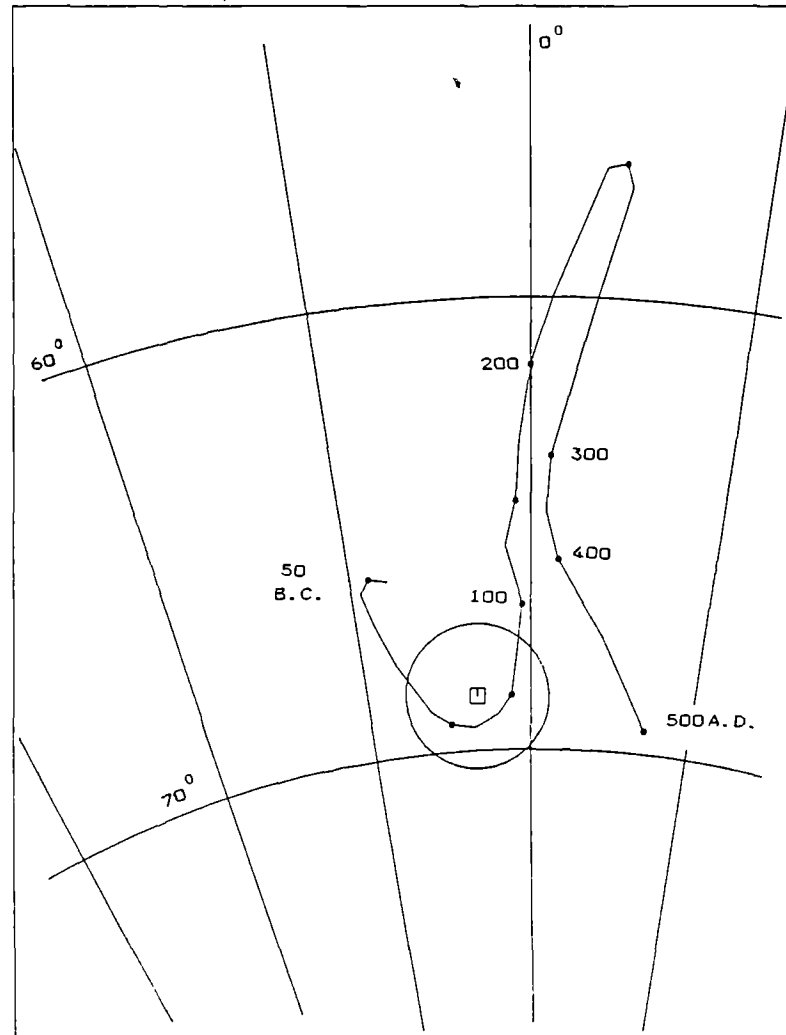


Figure 3.23 Stereoplot of the site  
mean magnetic direction.



been indicated by the demagnetisation pattern in high magnetic intensity specimens. Nevertheless systematic magnetic distortions do not preclude archaeomagnetic directional dating since they were not observed throughout the site. In fact there was no consistent systematic correlation between mean magnetic directions and other magnetic properties, nor between intensity and susceptibility. Inhomogeneity of magnetisation seems to have provided the conditions under which magnetic distortions occurred.

The presence of magnetite as the dominant remanence carrier in most specimens also showed that much of the vitrification occurred under conditions of limited oxidation and, by implication, in an enclosed environment. The vector movement pattern on thermal demagnetisation seems to indicate slow cooling in the core of the wall at location B and, by implication, elsewhere on the dun except at specific points at locations A and D where LA11 and LD5 seem to indicate localised faster cooling. The directional consistency between A.F. demagnetised specimens from several locations suggests (at the 95% confidence level) that the majority of the core of the wall had not moved significantly during cooling below 600<sup>0</sup>C or subsequent to the last firing.

## CHAPTER FOUR.

---

### The vitrified structures sampled.

#### 4.1. Introduction

This chapter is a record of the magnetic properties measured in selected vitrified structures in Scotland. Each site was chosen on some or all of the following criteria:

- a). Size of exposures and physical stability of the wall.
- b). Wall alignment.
- c). Amount of excavation.
- d). Degree of weathering.
- e). Availability of absolute dating methods.

In practise a best fit approach was applied as not all sites were ideal, whilst some were inaccessible or required extensive excavation for sampling to be practicable. The sites chosen are indicated in Fig. 4.1a. Most of the sites sampled are oblong in form and have been classified by Ralston (1983). These arguably show a cultural affinity on the basis of several architectural features, although this need not necessarily indicate

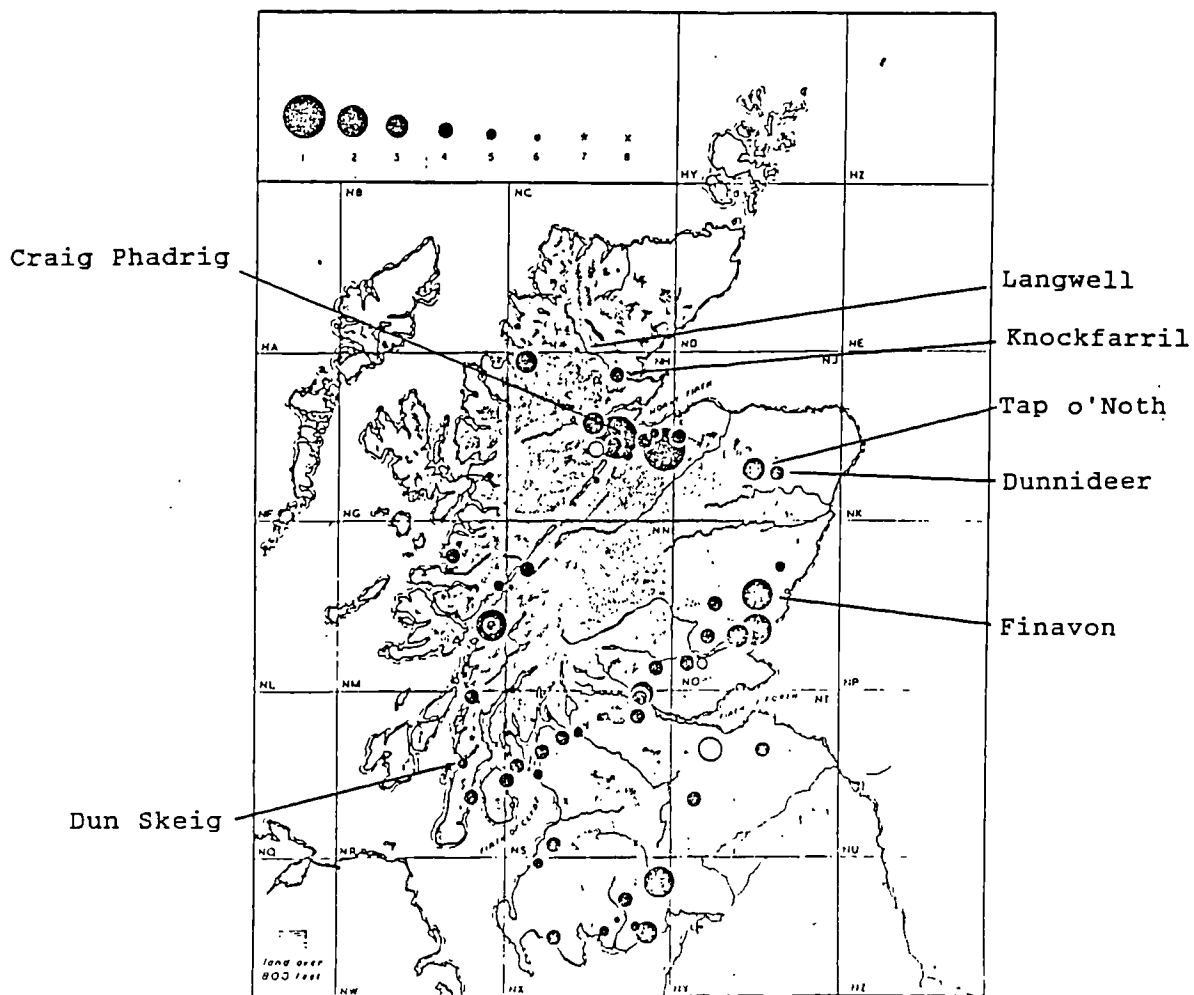


Figure 4.1a Distribution map of vitrified forts in Scotland indicating those sampled. (After Mackie 1976).

chronological similarity.

4.2. Craig Phadrig, Fort ( $57.5^{\circ}$  N.  $4.25^{\circ}$  W.),  
Invernesshire.

This Fort is one of the oblong series defined by Ralston (1983), situated strategically on the South shore of the Beauly Firth and consists of an inner vitrified wall (73.5 x 22.5m) and an outer one also vitrified (Feachem, 1983). The substratum is composed of middle Old Red Sandstone conglomerate whilst the structure is granite and sandstone (Nisbet 1975). The fort has a record of excavation and survey from the 18th century onwards (e.g. Williams 1777; Telford and Mackenzie in Cotton 1954; Small and Cottam 1972). Radiocarbon dates from the latter excavations revealed that the two walls date from c. 500 B.C., whilst these excavations also revealed later domestic occupation (hanging bowl and Dark Age E ware) (Feachem 1983). Thermoluminescence measurements derived from the inner wall centered on the second century B.C. (Strickertson *et al* 1988).

Little of the vitrified masses are exposed at the present time and small scale excavations were necessary at two locations, A and B (Fig. 4.1b), although

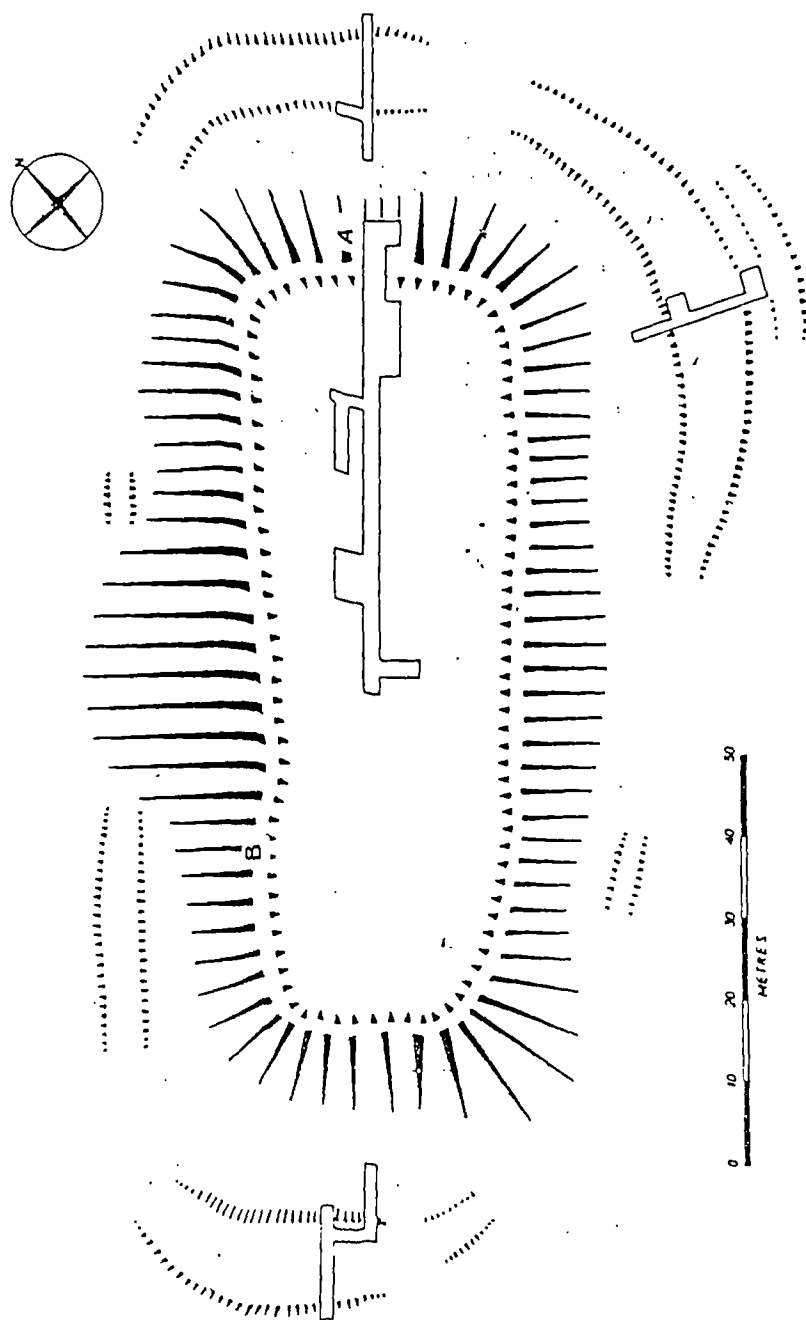


Figure 4.1b Plan of Craig Phadrig. (After Small and Cottam 1972).

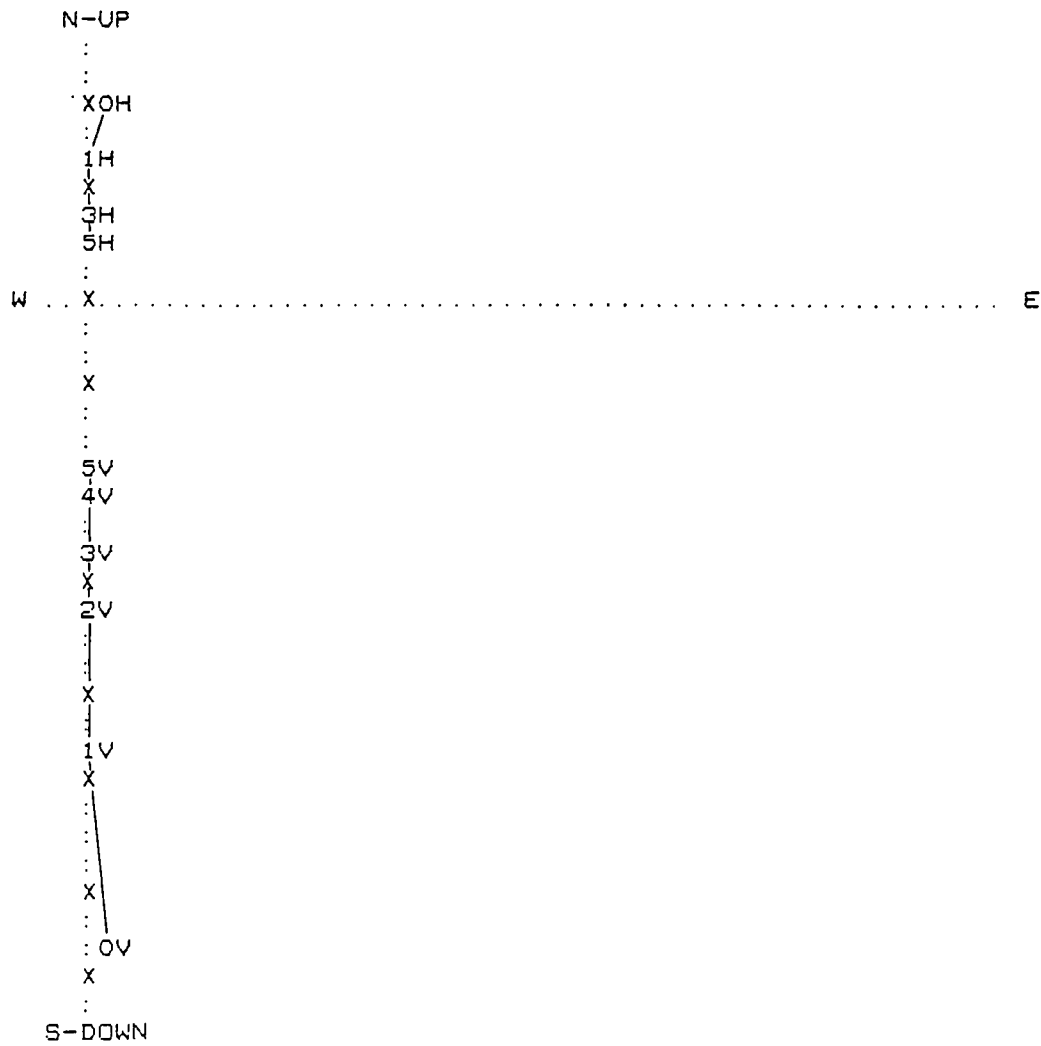
care was needed as section digging had the affect of destabilising the wall. Examination of the section at location A showed that tree roots could have caused movement subsequent to the last firing. However, despite a crack in the vitrification, it appeared to be keyed in to the core of the wall and was physically stable when hammered. Vitrification was noted to be mostly in the upper parts of the wall with burnt but not vitrified rubble lower down the section. The wall constituents appeared to be variably oxidised. A thermoluminescence core had been removed adjacent to this sampling location. Location B was exposed to a lesser extent by removal of turf from the top of the vitrified inner wall (c. 0.5m x 0.5m) and appeared, from the limited exposures available, to be *in situ*. A thermoluminescence core had also been taken adjacent to this location.

Three specimens were removed from location A and six from location B in order to provide a control on differential movement and contemporaneity of burning whilst also concentrating on apparently unweathered materials. Orientation was by magnetic compass due to cloud cover although the magnetism of the structure did not appear to affect the compass bearings. (No further opportunity to orientate specimens using a

suncompass was possible as access was restricted to one weekend by the Forestry Commission and manual help was only available for one day).

Nine specimens, mostly showing strong magnetisations ( $>101 \times 10^{-8} \text{ Am}^2/\text{g}$ ), were demagnetised at 10 mT intervals up to a peak alternating field of 50 mT. Most specimens were stable to very stable to demagnetisation using this method. Only one component was distinguished in each of the specimens (e.g. Figs. 4.2 and 4.3) suggesting only the final firing was recorded. The most stable specimen directions from each location were plotted on an equal angle stereographic projection and showed similar distributions, but one of the specimens from location A (8a) plotted eastward of location B specimen directions (Fig. 4.4). No mean was calculated for location A because of the small number of specimens. However given the general directional similarity between individual specimen directions it was thought unlikely that large scale differential movement between the two locations had occurred since the last firing. The overall mean magnetic direction was calculated on the basis of all specimens (Table 4.1). The magnetic directions from locations A and B should give a *terminus ante quem* date for the Iron Age occupation of the site (Small and Cottam 1972). On the

AS/ZIJDERVELD DIAGRAM  
 HOR. SCALE (\*-\*) = 528.000  
 VER. SCALE (X-X) = 562.000

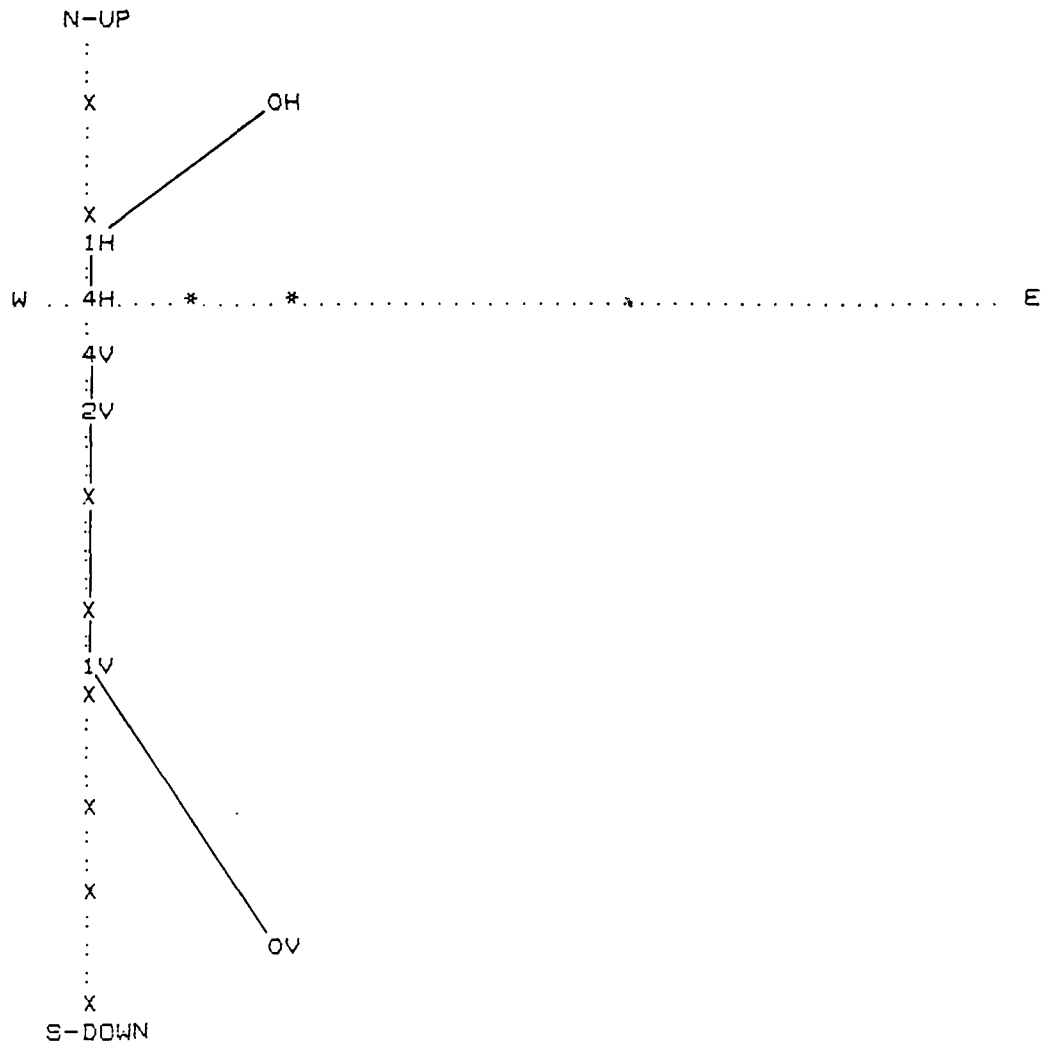


COMPONENT REMAINING

Figure 4.2 As/Zijderfeld plot of CP7a.  
 $\times 10^{-8} \text{ Am}^2/\text{g.}$



AS/ZIJDERVELD DIAGRAM  
 HOR. SCALE (\*-\*) = 6760.000  
 VER. SCALE (X-X) = 7195.000



COMPONENT REMAINING

Figure 4.3 As/Zijderveld plot of CP4b.  
 $\times 10^{-8} \text{ Am}^2/\text{g}$ .

# CRAIG PHADRIG, FORT.

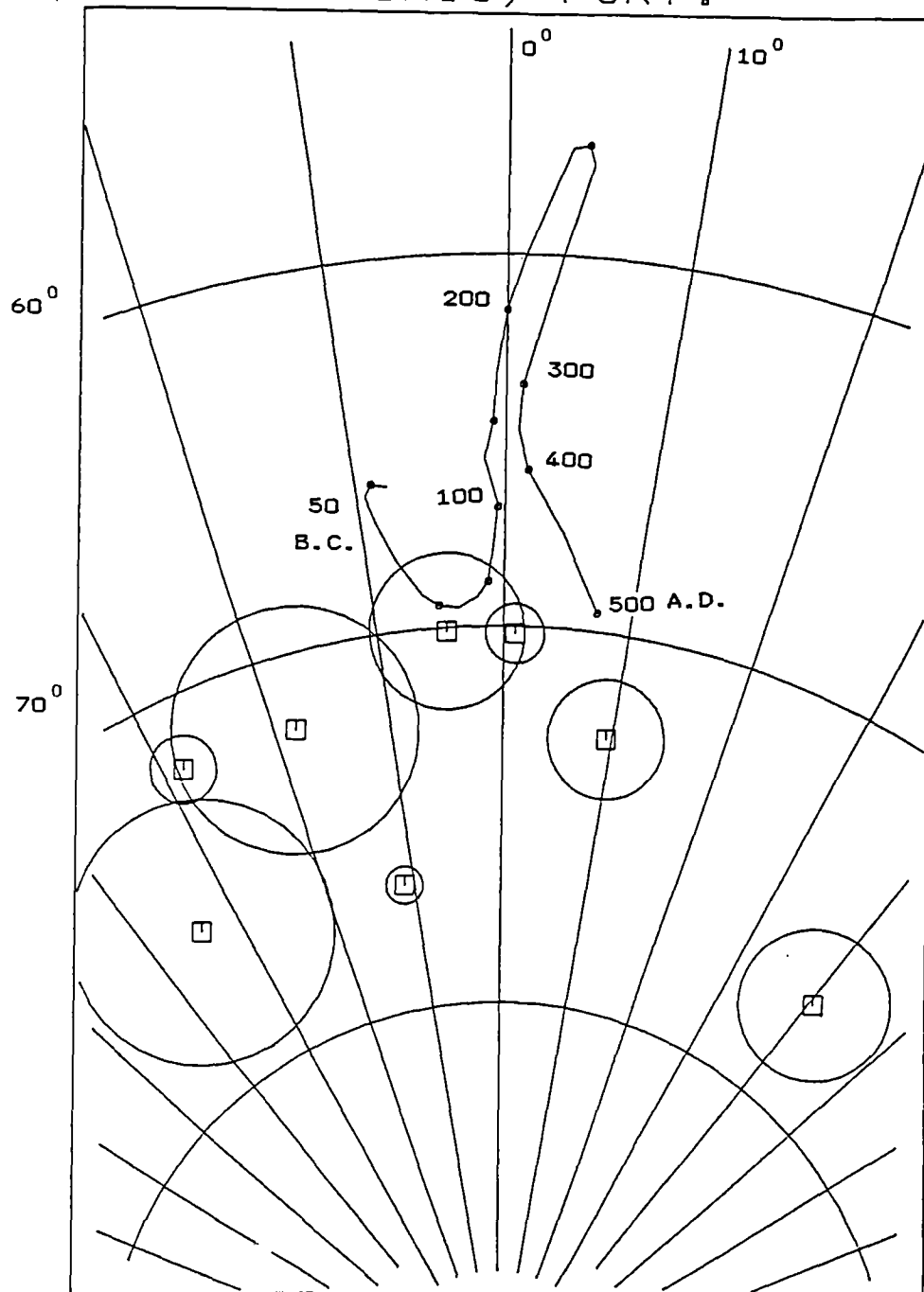


Figure 4.4  
Stereoplot of individual specimen directions.

# CRAIG PHADRIG, FORT.

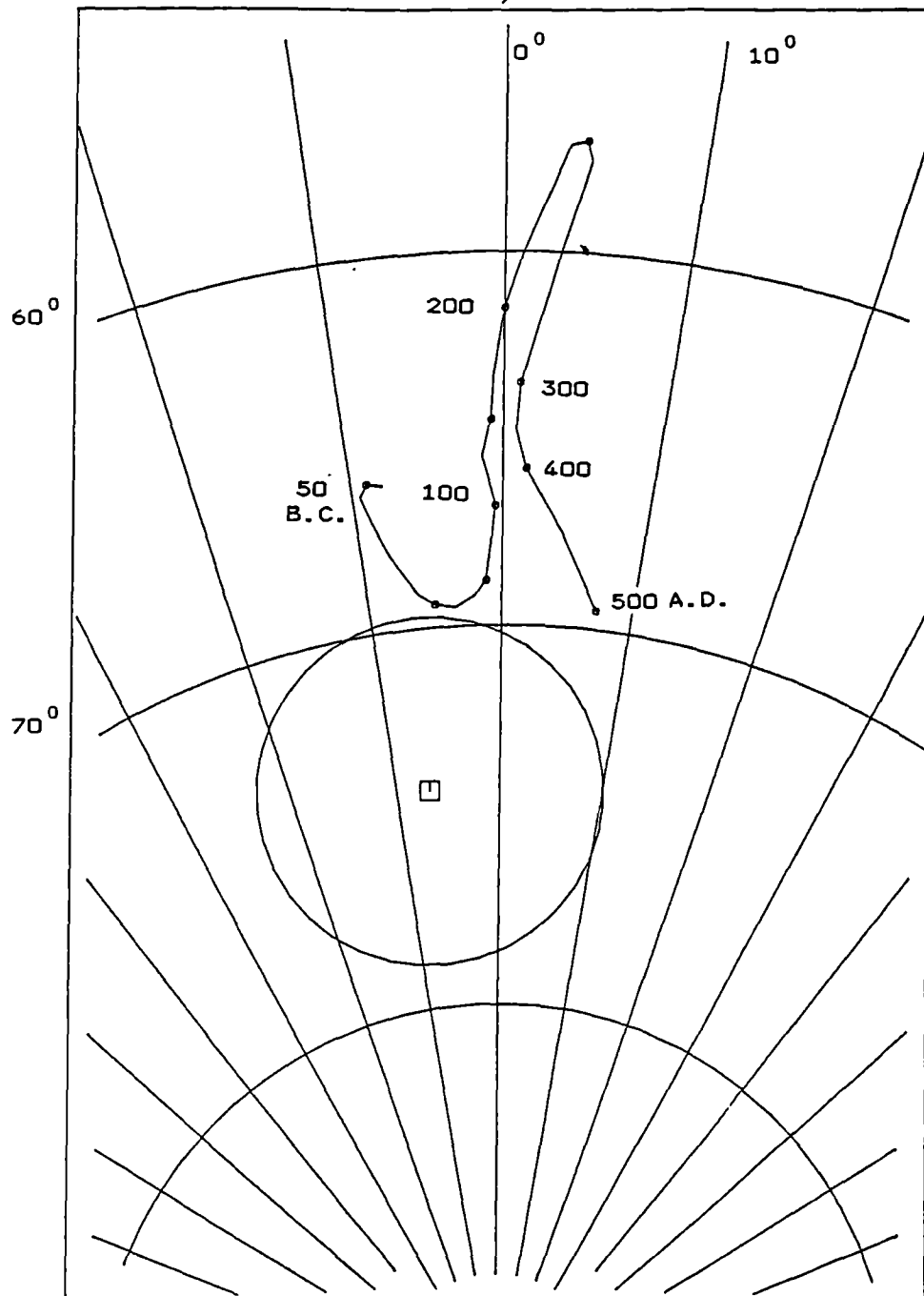


Figure 4.5

Stereoplot of the site mean magnetic direction.

basis of the present secular variation curve therefore, the overall mean magnetic direction, and the 95% circle of confidence, a date prior to 50 B.C. has been assigned to the last firing of the inner wall at locations A and B (Fig. 4.5).

**Table 4.1**  
**Most stable specimen directions.**

Specimen	Dec	Inc	Int	$\alpha_{95}$	S.I.	Range
			$\times 10^{-8} \text{ Am}^2/\text{g}$			mT
2a	11.7	75.7	160.2	1.6	12.6	20-50
7a	1.3	73.5	960.1	0.8	24.9	10-50
8a	49.3	78.6	1077.3	2.0	10.0	20-50
1b	339.1	75.3	40.8	3.3	5.7	10-50
2b	319.4	78.8	37.8	3.5	6.1	30-50
4b	347.7	79.7	4050.6	0.5	46.6	10-30
5b	327.3	75.1	327.4	0.9	24.9	10-30
6b	*5.1	74.7	8.6	13.6	1.6	0-20
7b	355.0	73.5	615.5	2.1	10.4	30-50

Unstable specimen directions\*

Mean Meriden corrected direction for all specimens  
excluding those magnetically unstable:

Dec = 353.2

Inc = 74.3

N = 8

R = 7.952

$\alpha_{95}$  = 4.6

K = 144.7

#### 4.3. Dunnideer, Fort ( $57.3^{\circ}$ N $2.5^{\circ}$ W), Aberdeenshire.

This Fort is one of the unfinished works noted by Feachem (1983) and one of the oblong series defined by Ralston (1983). It is unexcavated, situated on the Hill of Dunnideer and on the highest ground for kilometres around. The top of the hill is dominated by a medieval tower (Simpson, 1935), built partly from vitrified material from the oblong fort surrounding the tower. The fort measures 66 x 27 m internally with a depression near the West end probably representing the site of a well (Feachem 1983). Traces of outer works are present particularly on the North and East, whilst lower down the hill lie two incomplete ramparts. The remains have been interpreted as representing at least two main structural

phases, but the primary phase has not been identified (Feachem 1983).

Examination of the site revealed two main outcrops of vitreous and fused stone on the North and South sides of the Fort. The northern outcrop was aligned longitudinally with the apparent line of the wall (Fig. 4.6) and was traceable transversely for a distance of 2m. It was also exceedingly hard to hammer. The southern outcrop, although well fused on the whole, had a crack running through the centre and gave the appearance that it was two blocks leaning on one another. It was therefore concluded that there was evidence of movement since the last firing as the two pieces did not appear to be fused together. As the medieval tower incorporated vitrified blocks it was thought likely that these had been quarried from the vitrified fort. This may be shown by the overhanging vitrification with lower burnt/unfused rubble on the North side. Sampling was restricted to location A (Fig. 4.6) where six specimens were orientated using a suncompass and removed from apparently unweathered vitreous and non-vitreous materials.

All six specimens showed moderate to strong magnetic intensities before demagnetisation ( $>6.1 \times$

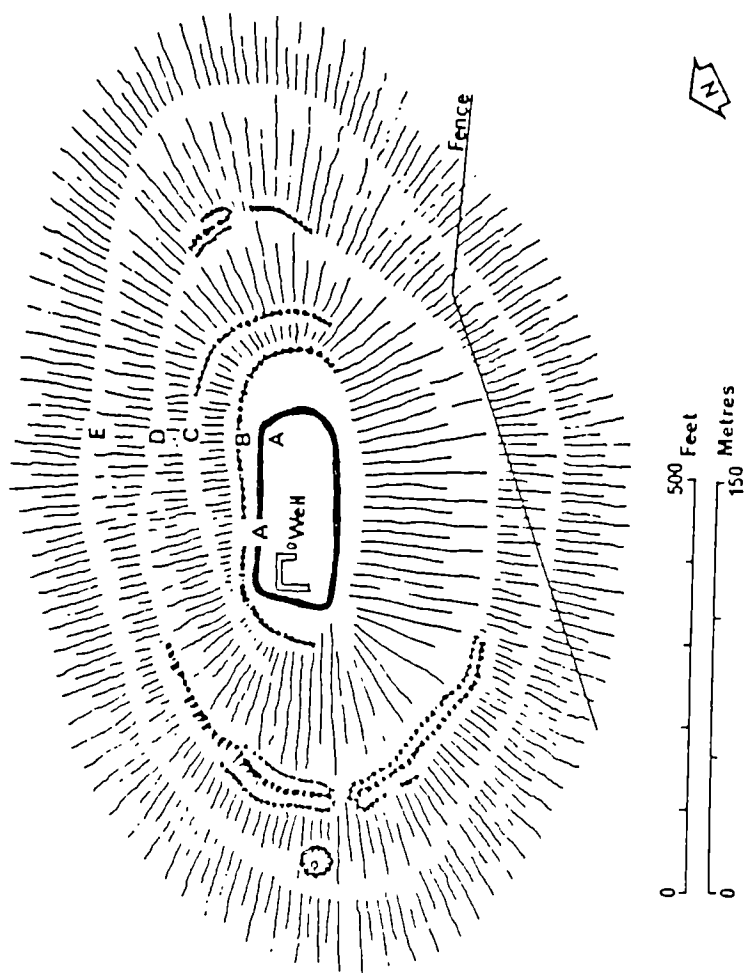


Figure 4.6 Plan of Durnideer. (After Feachem 1983).

$10^{-8} \text{ Am}^2/\text{g}$  ). They were demagnetised at 5 and 10 mT intervals up to a maximum peak alternating field of 50 mT depending on the measurable magnetic remanence (Table 4.2). All specimens after A.F. cleaning were stable to extremely stable to demagnetisation in alternating fields, only one component was distinguished in each of the specimens suggesting only the final firing was recorded (e.g. Fig. 4.7). Nevertheless the magnetic directions, although statistically well defined, showed considerable scatter when plotted on an equal angle stereographic projection (Fig. 4.8). As a result the overall mean and 95% circle of confidence, calculated on the basis of all specimens, was thought unreliable as an age determinant (Fig. 4.9).

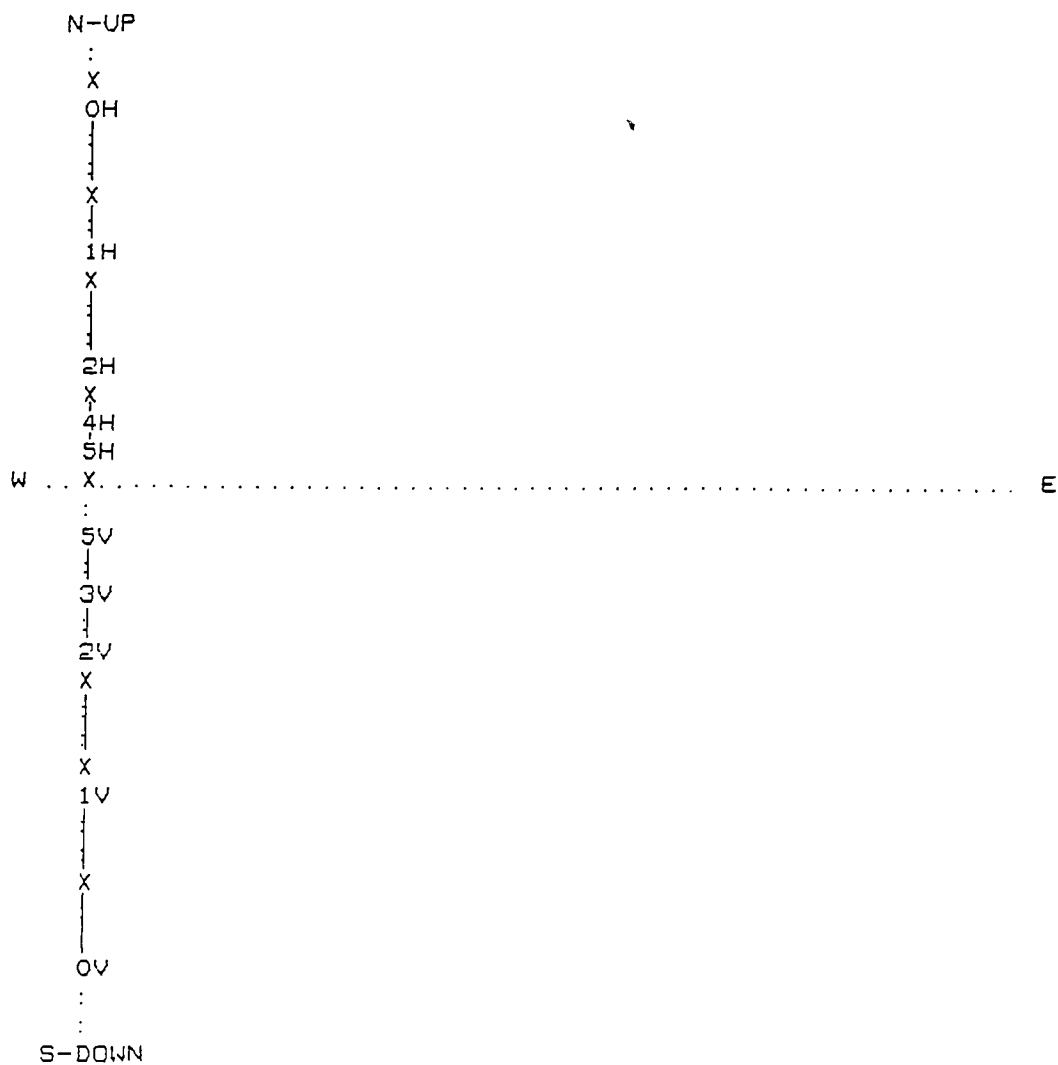
**Table 4.2**

**Most stable specimen directions.**

Specimen	Dec	Inc	Int	$\alpha_{95}$	S.I.	Range
			$\times 10^{-8} \text{ Am}^2/\text{g}$			mT
1	348.0	56.2	1.7	1.2	14.9	10-35
2	336.2	51.1	21.4	0.9	23.6	20-40
4	324.1	61.2	2.2	1.0	14.5	15-25



AS/ZIJDERVELD DIAGRAM  
 HOR. SCALE (\*-\*) = 15.000  
 VER. SCALE (X-X) = 16.000



COMPONENT REMAINING

Figure 4.7 As/Zijderveld plot of DD6a.  
 $\times 10^{-8} \text{ A m}^2/\text{g.}$

DUNNIDEER, FORT.

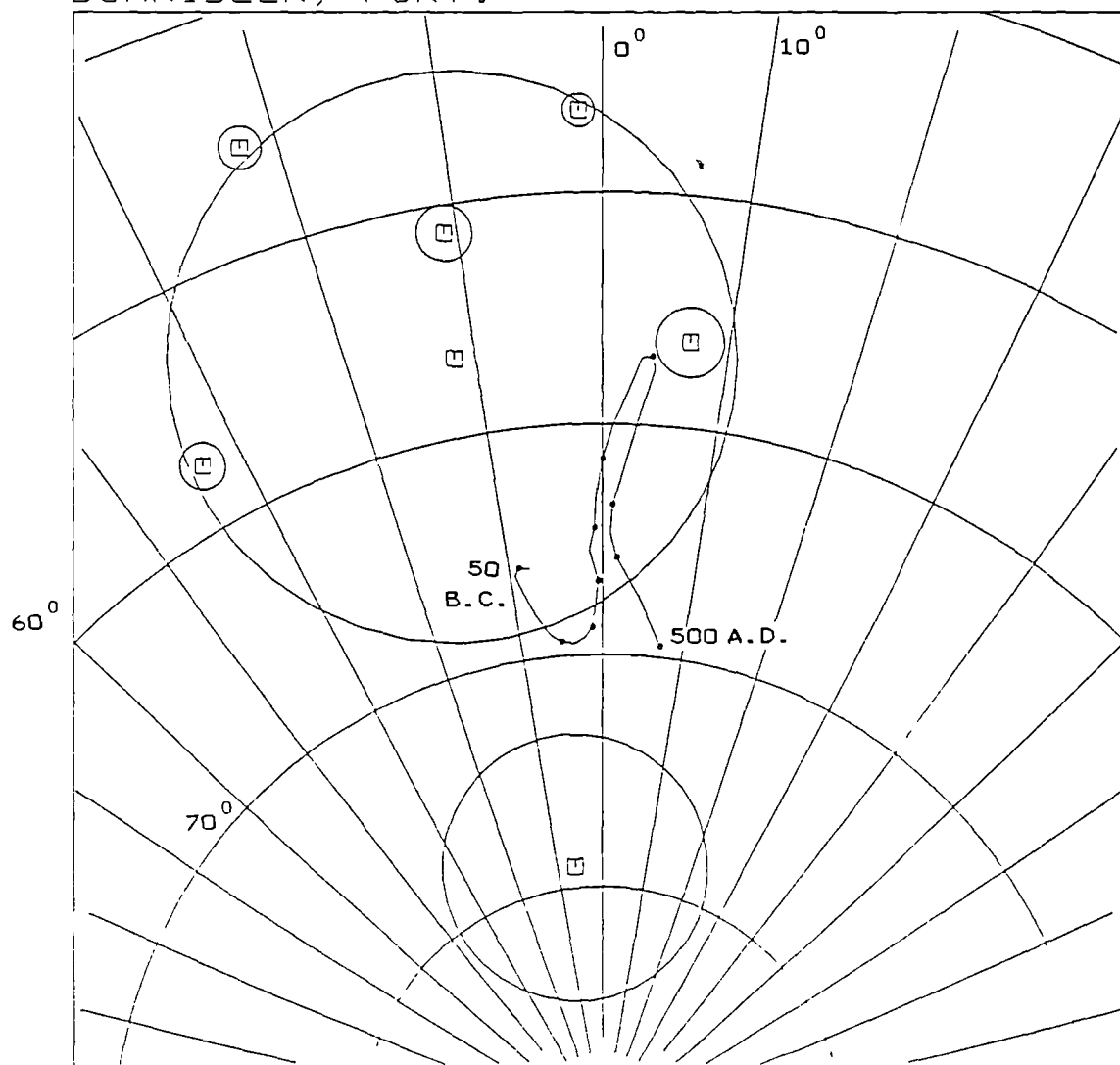


Figure 4.8  
Stereoplot of individual specimen directions  
and overall mean.

DUNNIDEER, FORT.

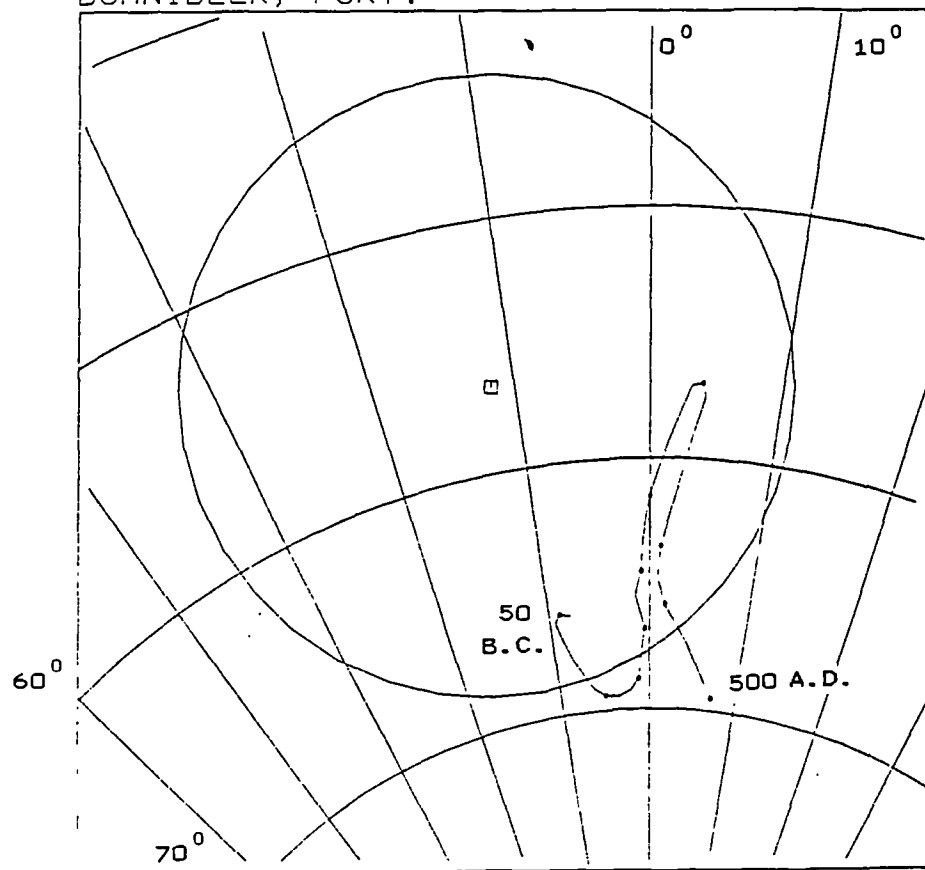


Figure 4.9  
Stereoplot of the site mean magnetic direction.

6	357.9	52.1	10.0	0.7	25.5	10-50
8	353.0	81.8	969.7	5.7	3.5	20-50
9	7.1	60.7	24.0	1.5	14.6	10-30

Mean Meriden corrected direction for all specimens:

Dec = 348.3                      Inc = 56.6

N = 6                              R = 5.835

$\alpha_{95} = 12.3$                       K = 30.4

#### 4.4. Dun Skeig, Fort and Dun (55.7° N 5.7° W) Argyll.

In plan the fort is rectilinear (113 x 36m) within a stone wall on a hill (156.3m O.D.) in a visually commanding position. At the South end is a large oval dun enclosing an area 26 x 18.8m which is vitrified. The secondary drystone dun situated 45m North East of the fort, measures about 13.5m in diameter within a wall c. 3.9m thick (Feachem 1983). The substratum is composed of Dalradian mica-schist with bands of schistose grit, whilst the structure of the vitrified dun is also of schist (Nisbet 1975). Although the site is unexcavated it is clearly a multi-occupation site from which dating of the vitrification

phase could provide a *terminus post quem* for the later dun which was built using vitrified material, and potentially a *terminus ante quem* for the fort as the vitrified dun partially overlay it (Ritchie and Ritchie 1985).

Due to the limited exposures on this site ten specimens were taken from a relatively large outcrop on the North wall of the vitrified dun (Fig. 4.10) covering as much of this as possible to ascertain whether differential movement was prevalent. Orientation was by magnetic compass because of inclement weather, but the magnetism of the dun did not appear to affect the magnetic bearings.

Nevertheless ten specimens with high magnetic intensities ( $>1608 \times 10^{-8} \text{ Am}^2/\text{g}$ ) were measured and demagnetised at 10 mT intervals up to a peak field of 50 mT (Table 4.3). All specimens were stable to extremely stable to demagnetisation in alternating fields and only one component of magnetisation was distinguished in each of the specimens (e.g. Fig. 4.11) suggesting that only the final firing was recorded. Most of the individual magnetic directions from the dun were reasonably consistent with each other, (Fig. 4.12), suggesting no large scale differential movement. The

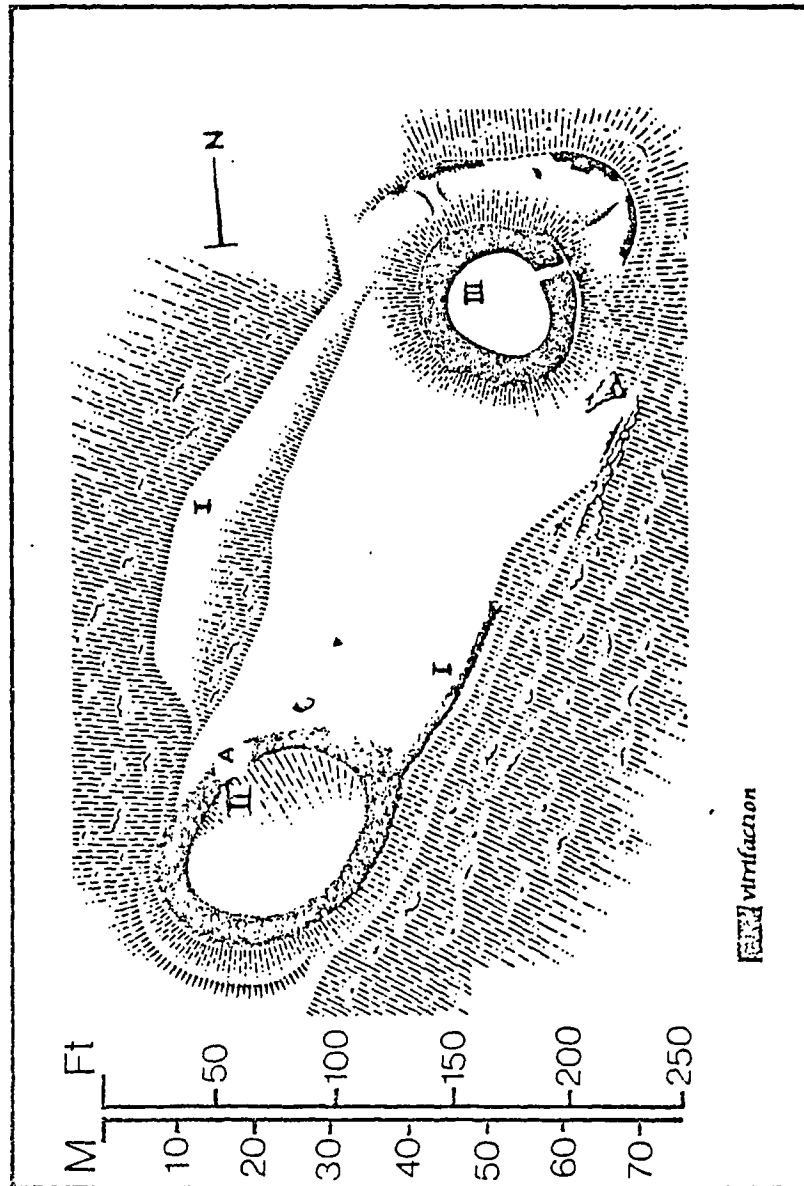
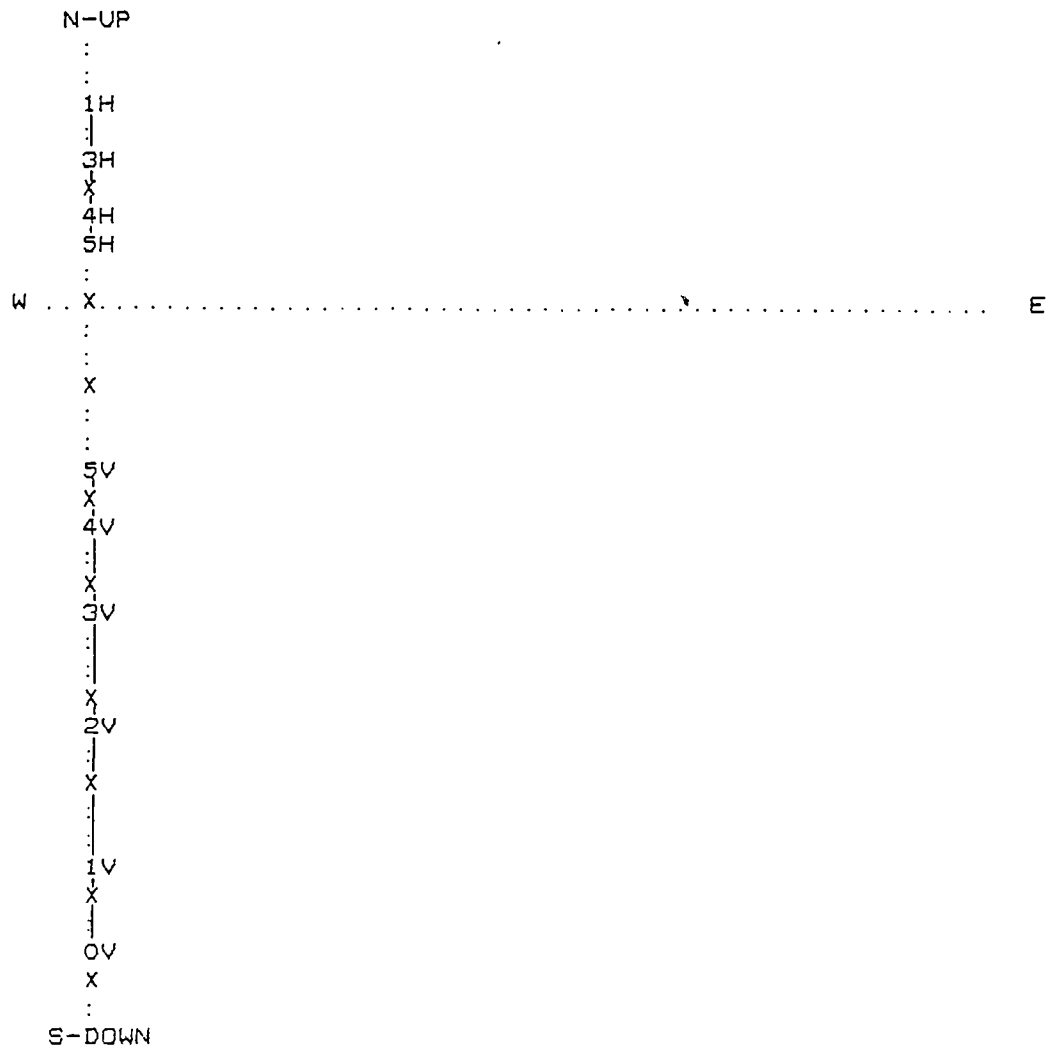


Figure 4.10 Plan of Dun Skeig. (After Feachem 1983).

AS/ZIJDERVELD DIAGRAM  
 HOR. SCALE (\*-\*) = 669.000  
 VER. SCALE (X-X) = 712.000



COMPONENT REMAINING

Figure 4.11 As/Zijderveld plot of DSK4.  
 $\times 10^{-8} \text{ Am}^2/\text{g}$

# DUN SKEIG, FORT AND DUN.

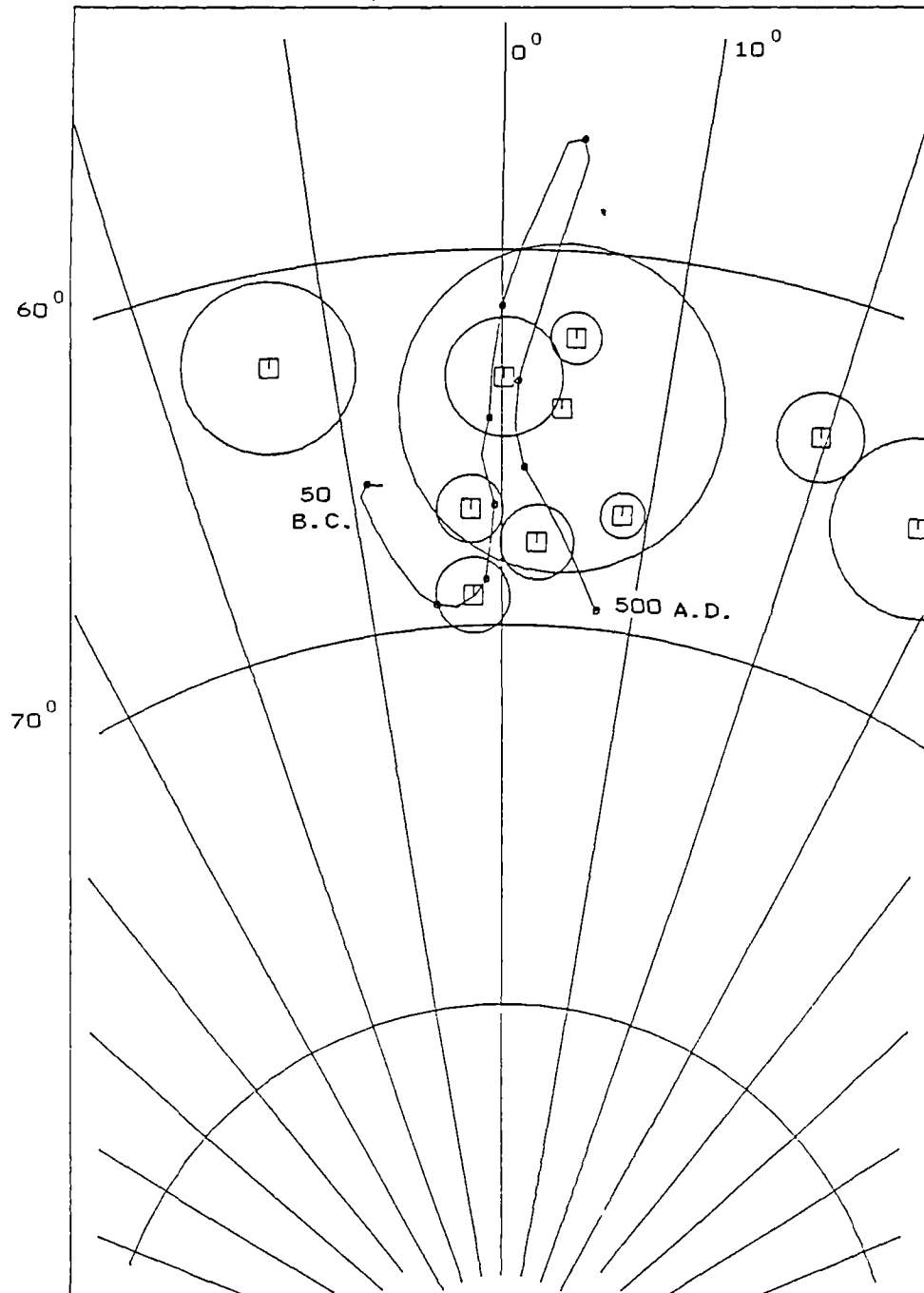


Figure 4.12  
Stereoplot of individual specimen directions  
and overall mean.



# DUN SKEIG, FORT AND DUN.

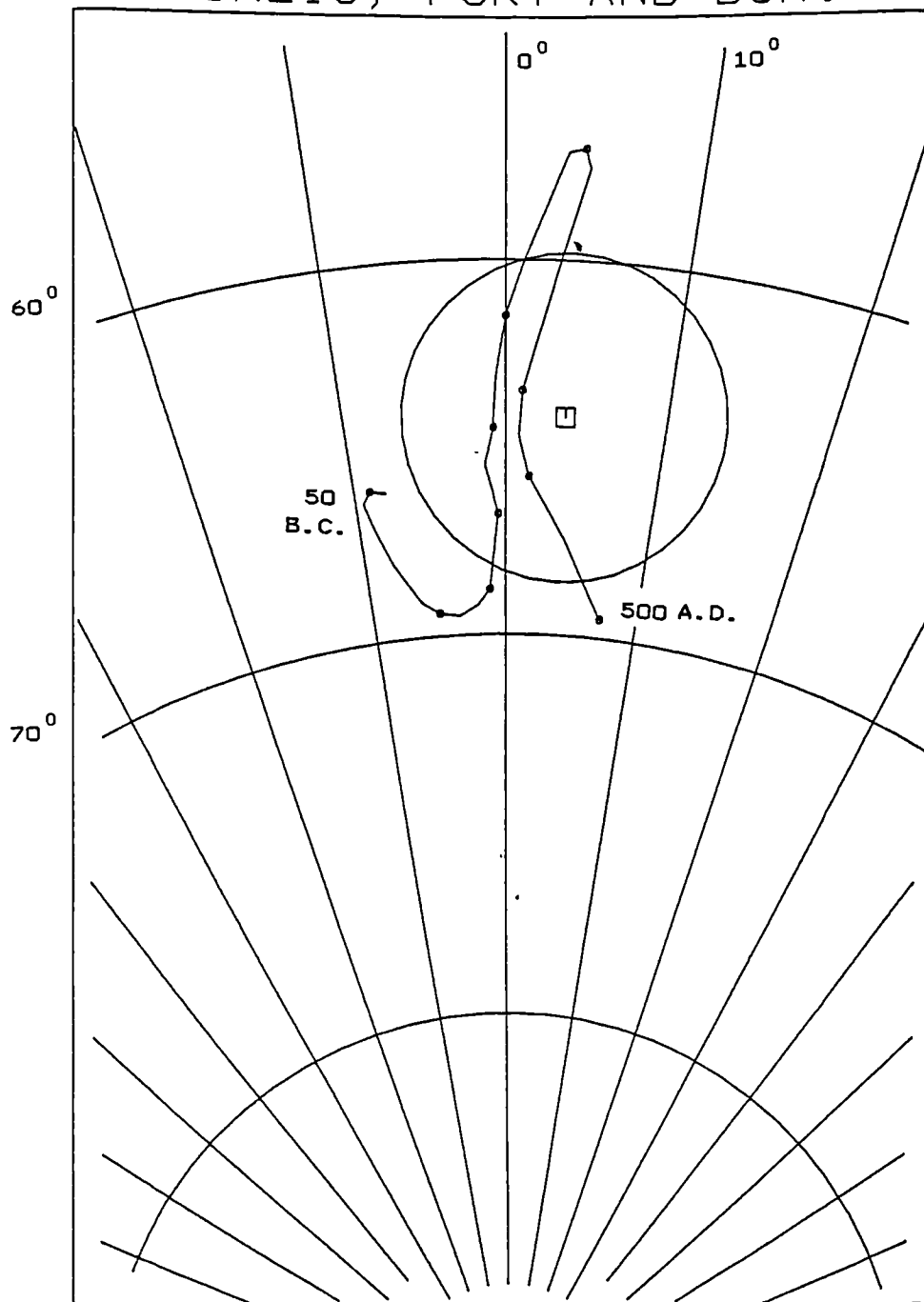


Figure 4.13

Stereoplot of the site mean magnetic direction.

observed mean lay adjacent to that part of the curve consistent with an age assignment in the fourth century A.D. However the 95% circle of confidence incorporated that part of the curve consistent with a late first to late fifth century A.D. date (Fig. 4.13). This suggested, along with the observable site sequence, that the secondary dun was built during or after the first to fifth century timespan A.D., whilst the original fort was built before or during the time interval defined by the 95% circle of confidence. The vitrified dun appears to have been last fired during the late first to late fifth century A.D. period.

**Table 4.3**

**Most stable specimen directions.**

Specimen	Dec	Inc	Int	$\alpha_{95}$	S.I.	Range
			$\times 10^{-8} \text{ Am}^2/\text{g}$			mT
1	359.4	66.0	1054.1	1.6	11.9	0-30
2	8.6	69.0	16530.6	0.6	37.9	0-20
3	28.1	66.4	4781.8	2.4	9.0	0-20
4	357.6	71.5	3169.4	1.0	22.6	0-20

5	2.5	70.0	828.9	1.0	18.1	0-40
8	19.9	65.5	1657.1	1.2	15.6	0-50
9	355.4	54.0	3536.4	1.7	12.6	20-40
10	357.2	69.3	784.0	0.9	20.7	10-50
11	3.7	64.8	880.6	0.7	26.8	20-50
12	344.6	65.5	1716.8	2.3	9.5	30-50

Mean Meriden corrected direction for all specimens:

Dec = 3.7

Inc = 64.2

N = 10

R = 9.925

$\alpha_{95}$  = 4.4

K = 120.3

#### 4.5. Finavon, Fort (56.7° N 3.0° W), Angus.

This fort is of oblong type as defined by Childe (1934) and Ralston (1983). Its dimensions are 150m x max. 36m internally (Feachem 1983), whilst the walls were c.6.0m thick and 3.6m high internally and 4.8m externally (Childe 1934). Excavation by Mackie established a date of 8th to 6th centuries B.C. for timbers found near the walls based on radiocarbon

(Mackie 1969). The site has the added characteristic of a hornwork on its eastern end, whilst the walls themselves were built on a course laid out regardless of the variation in the contours of the hill.

Examination of the site showed that there were few extensive outcrops of vitrification. Thus for location A (Fig. 4.14), a small scale excavation was undertaken to expose half the wall thickness and a trench dug at the foot of the wall to a depth of 1m. In this way it was possible to see that the wall core was aligned longitudinally and transversely, whilst also revealing that much of the lower unvitricified portions of the wall had fallen away leaving a hollow beneath the solid vitrified stone above. This further supported the conclusion that the vitrification was *in situ*, although Childe did record wall collapse at Finavon (Childe 1934). Location B (Fig. 4.14) was situated on the South wall toward the East where an area (2m x 1m) of vitrified stone was exposed and sampled. This material was situated on the apex of the apparent wall alignment and appeared to be consistently fused. Six specimens were removed from apparently unweathered vesicular and non-vesicular materials at locations A and B respectively. The fused material at both locations was

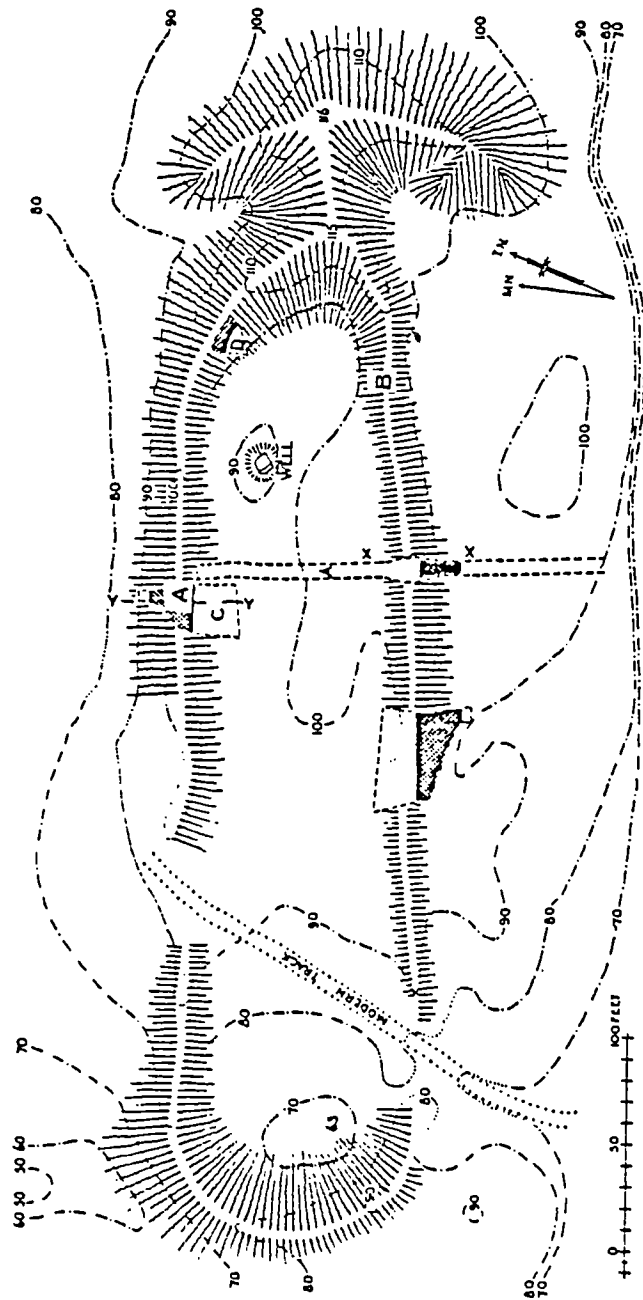


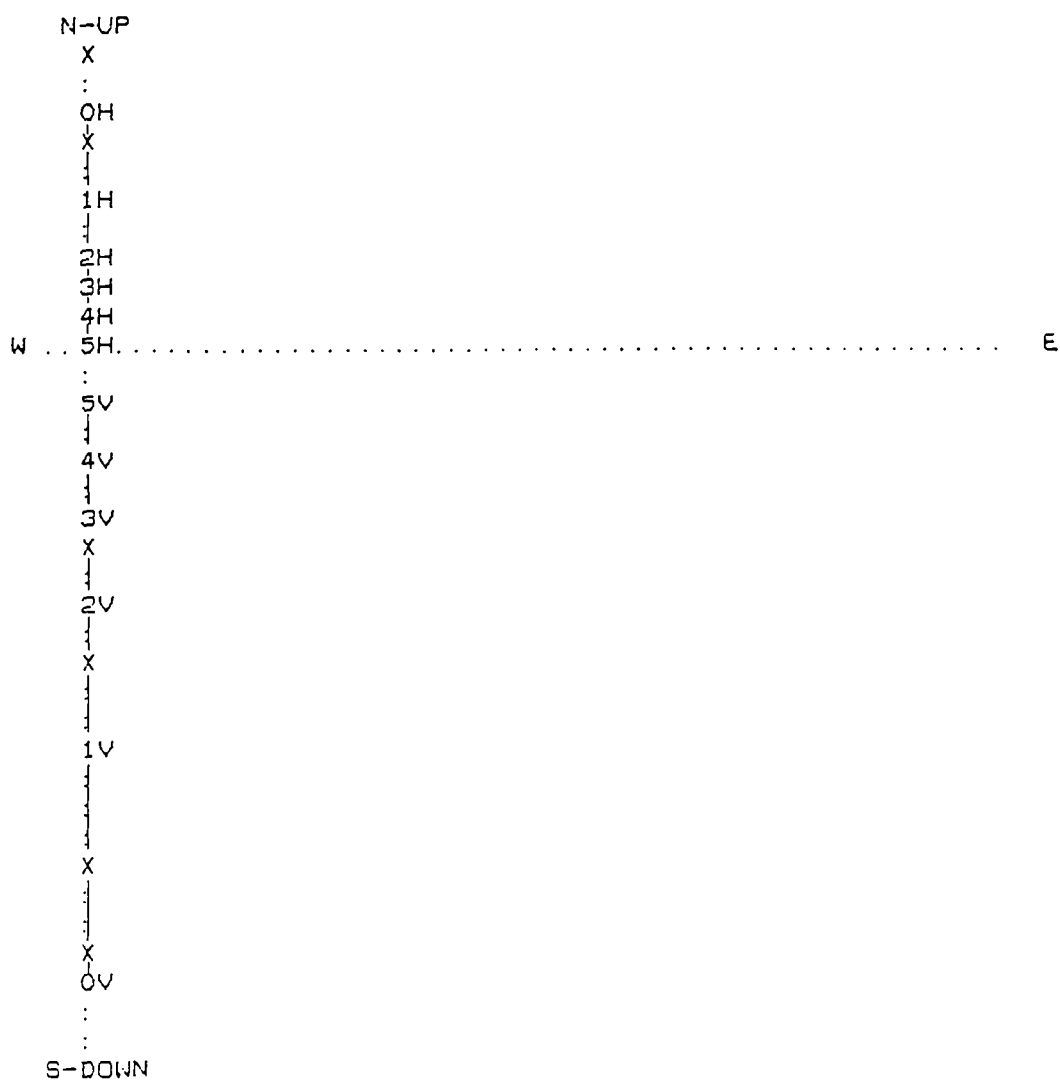
Figure 4.14 Plan of Finavon. (After Childe 1934).

resistant to hammering.

Twelve specimens with magnetisations  $>75 \times 10^{-8} \text{ Am}^2/\text{g}$  were demagnetised to 50 mT at 10 mT intervals (Table 4.4). All specimens were stable to extremely stable to demagnetisation using this method and only one component was distinguished in each of the specimens (e.g. Fig. 4.15 and 4.16), suggesting only the final firing was recorded. The specimen directions, from locations A and B were mostly consistent with each other when plotted (Fig. 4.18). The mean most stable directions from each location were plotted on an equal angle stereographic projection (Fig. 4.17) and it was found that both observed means lay close together whilst the circles of 95% confidence overlapped. This strongly suggested that no large scale differential movement had occurred since the last firing. Confirmation of statistical compatibility of both locations was provided by the F test (Tarling 1983) which showed that there was a >99% probability that the two means were from the same population.

The overall mean direction and 95% circle of confidence was calculated on the basis of all specimens and plotted on the present archaeomagnetic secular variation curve for Britain (Fig. 4.19). The

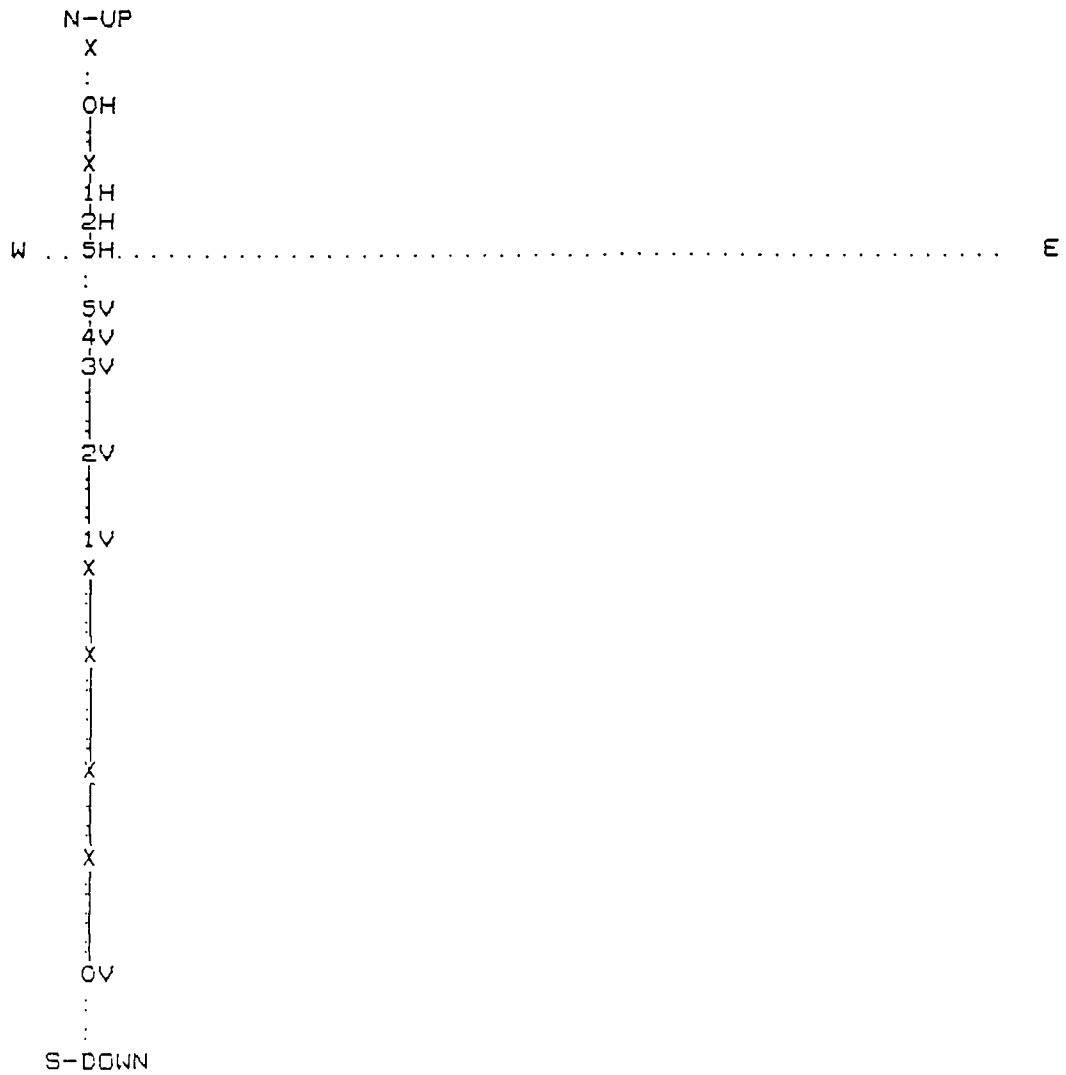
AS/ZIJDERVERELD DIAGRAM  
 HOR. SCALE (\*-\*) = 2249.000  
 VER. SCALE (X-X) = 2394.000



COMPONENT REMAINING

Figure 4.15 As/Zijderveld plot of FA1v.  
 $\times 10^{-8} \text{ Am}^2/\text{g}.$

AS/ZIJDERVELD DIAGRAM  
 HOR. SCALE (\*-\*) = 1387.000  
 VER. SCALE (X-X) = 1476.000



COMPONENT REMAINING

Figure 4.16 As/Zijderveld plot of FB15.

$\times 10^{-8} \text{ Am}^2/\text{g}$



# FINAVON, FORT.

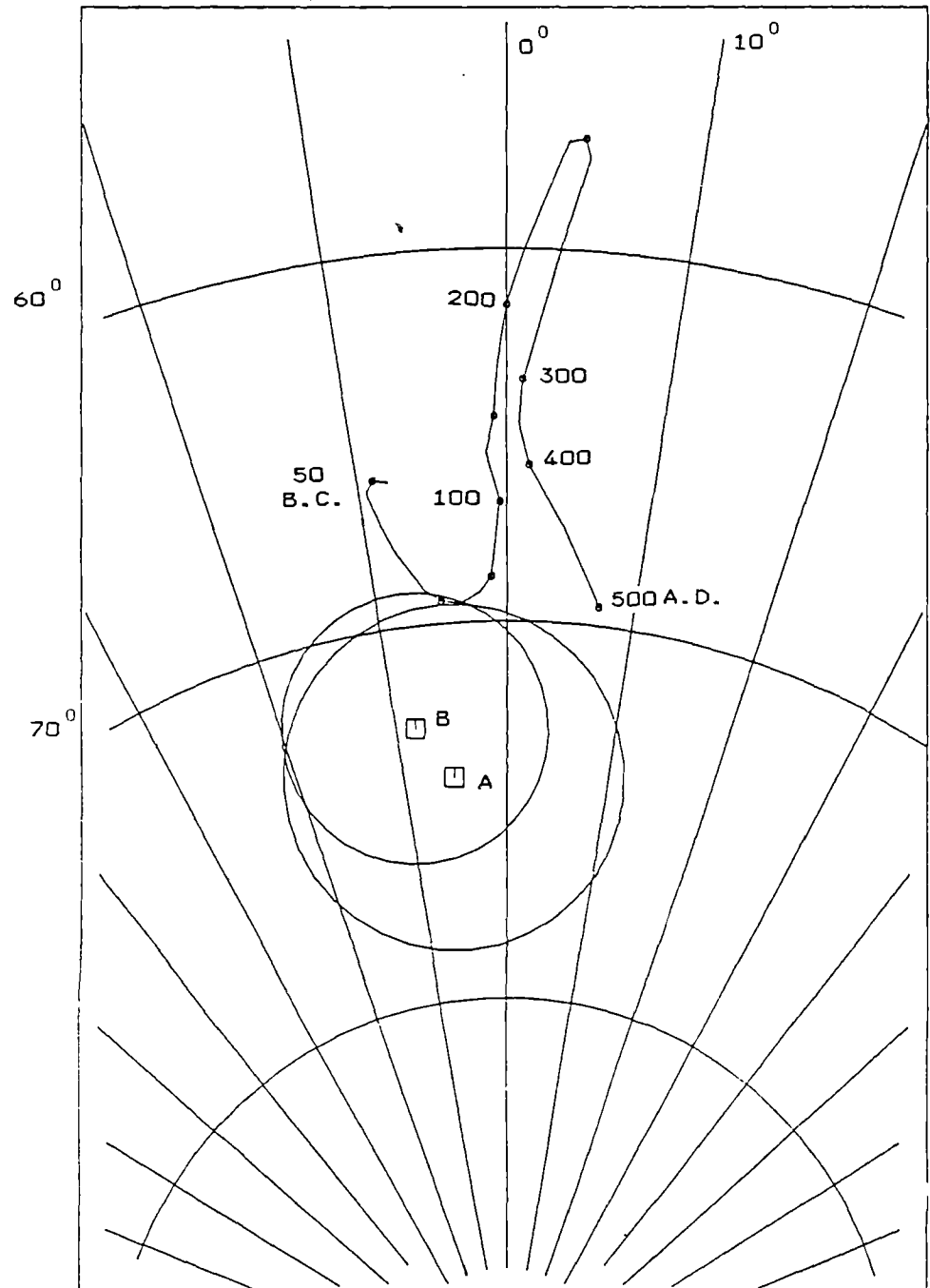


Figure 4.17  
Stereoplot of location mean directions.

# FINAVON, FORT.

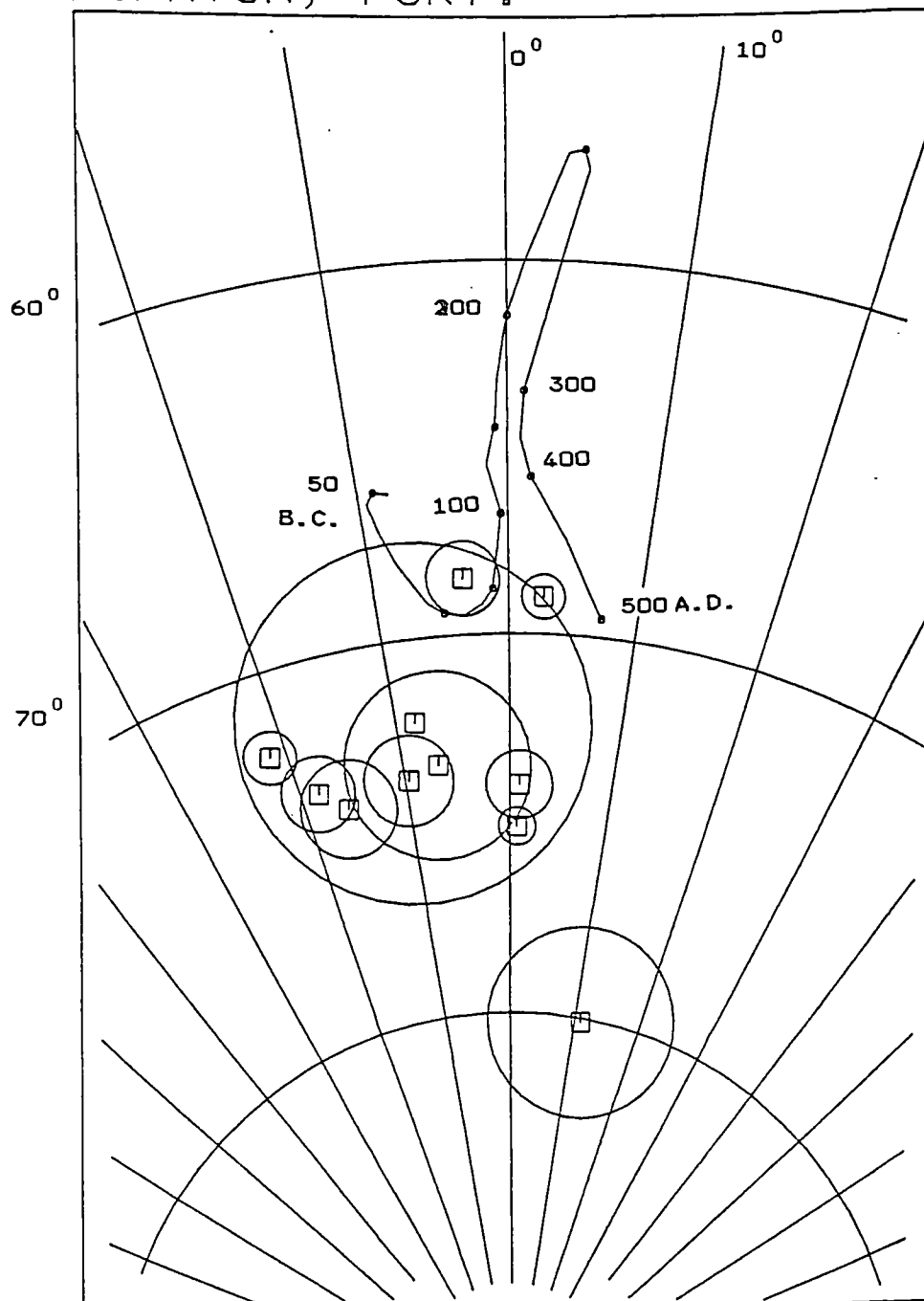


Figure 4.18  
Stereoplot of individual specimen directions  
and overall mean.

# FINAVON, FORT.

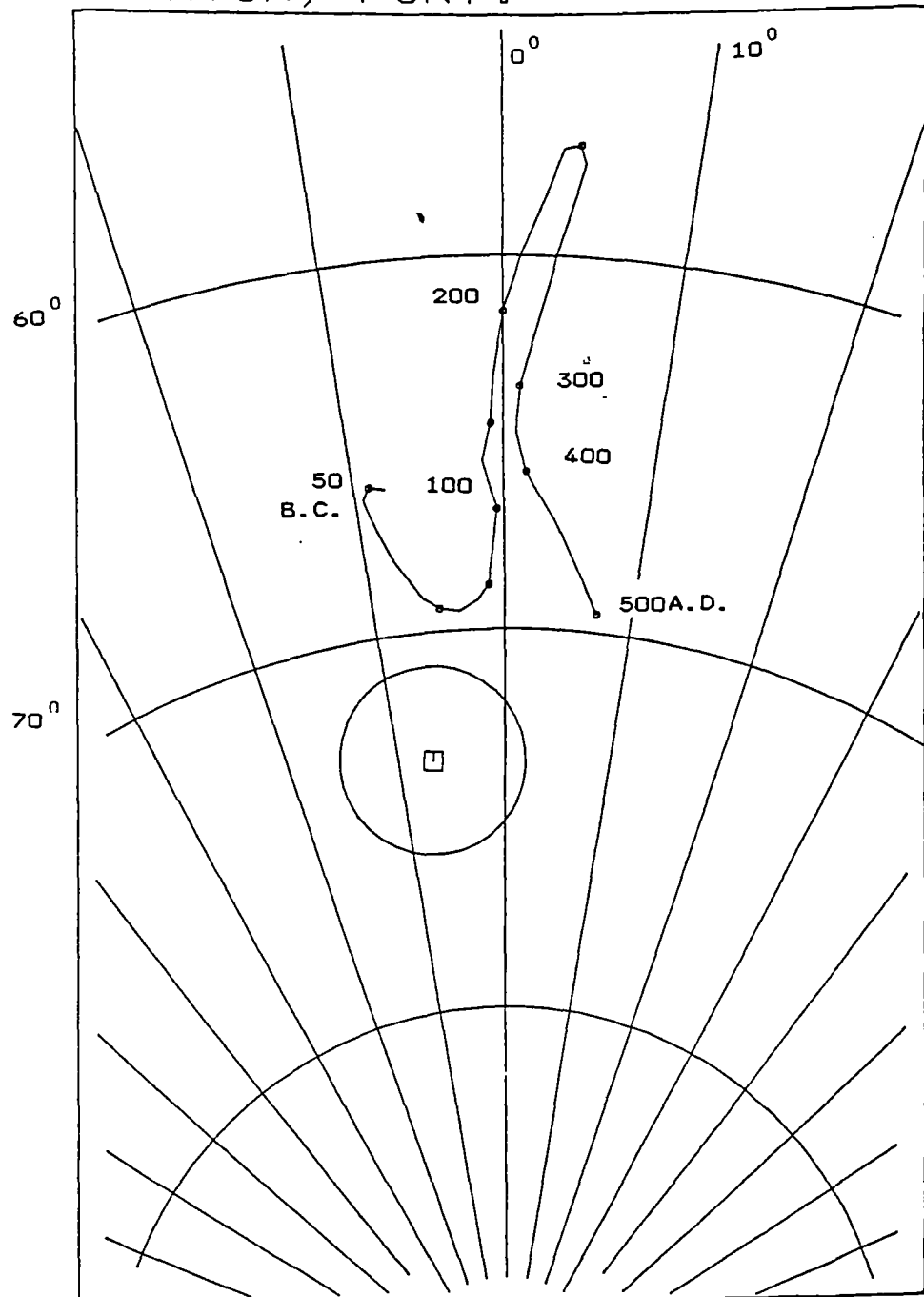


Figure 4.19  
Stereoplot of the site mean magnetic direction.

observed mean lay off the present curve but was consistent with a date prior to 50 B.C., whilst the 95% circle of confidence was consistent with a late first millenium B.C. date.

**Table 4.4**  
**Most stable specimen directions.**

Specimen	Dec	Inc	Int $\times 10^{-8} \text{ Am}^2/\text{g}$	$\alpha_{95}$	S.I.	Range mT
1a	231.7	67.2	2092.4	0.6	35.4	0-30
11a	1.5	76.6	669.2	0.9	21.5	20-50
12a	339.3	76.1	1695.9	1.0	20.9	10-30
1av	356.2	71.5	1486.8	1.0	21.1	30-50
2av	349.2	76.4	1054.9	1.2	15.2	10-50
3av	15.6	82.3	223.9	2.5	8.6	30-50
5b	283.8	76.1	430.3	1.2	17.7	30-50
6b	3.0	71.9	1177.9	0.6	31.3	10-40
7b	350.7	74.9	50.4	4.8	3.9	0-50
8b	335.9	74.9	1375.9	0.7	28.7	10-30

12b                    342.0   76.7       151.5   1.3       17.0       20-40

15b                    1.4   77.6       1683.3   0.5       47.4       10-30

Mean Meriden corrected direction for all specimens:

Dec = 353.2

Inc = 73.4

N     =   10

R     =   9.975

$\alpha_{95}$  =   2.5

K     =   356.1

Mean Meriden corrected direction for location A:

Dec = 354.9

Inc   =   74.1

N     =   5

R     =   4.985

$\alpha_{95}$  =   4.6

K     =   267.7

Mean Meriden corrected direction for location B:

Dec = 351.7

Inc   =   72.7

N     =   5

R     =   4.991

$\alpha_{95}$  =   3.6

K     =   431.0

#### 4.6. Knock Farril, Fort ( $57.5^{\circ}$ N $4.4^{\circ}$ W) , Ross and Cromarty.

This fort is situated on the summit of a narrow North East to South West oriented ridge with a very steep drop to the North, overlooking Loch Ussie to the South and the Cromarty Firth to the East. The source geology is middle Old Red Sandstone conglomerate, whilst the structure is composed of mixed gneiss, schist, quartzite and sandstone (Nisbet 1975). The fort is sub-rectangular/oval and is one of the oblong forts defined by Ralston (1983). In the South West part of the fort is the remains of a cistern c.5 m in diameter. In addition to the main enclosure there are hornworks at the East and West ends. There are in addition large unidentified outlines and features especially protruding vitrified walls to the East and West. Much of the structure is heavily vitrified. The dimensions of the main enclosure are 409 x 109 m maximum. Williams 1777 (in Cotton 1954) dug a trench transversely across the site and suggested that some of the northern wall had fallen outward.

Two locations were selected for sampling (locations A and B; Fig. 4.20), from which six specimens were respectively removed in order to provide a control on large scale differential movement concentrating on

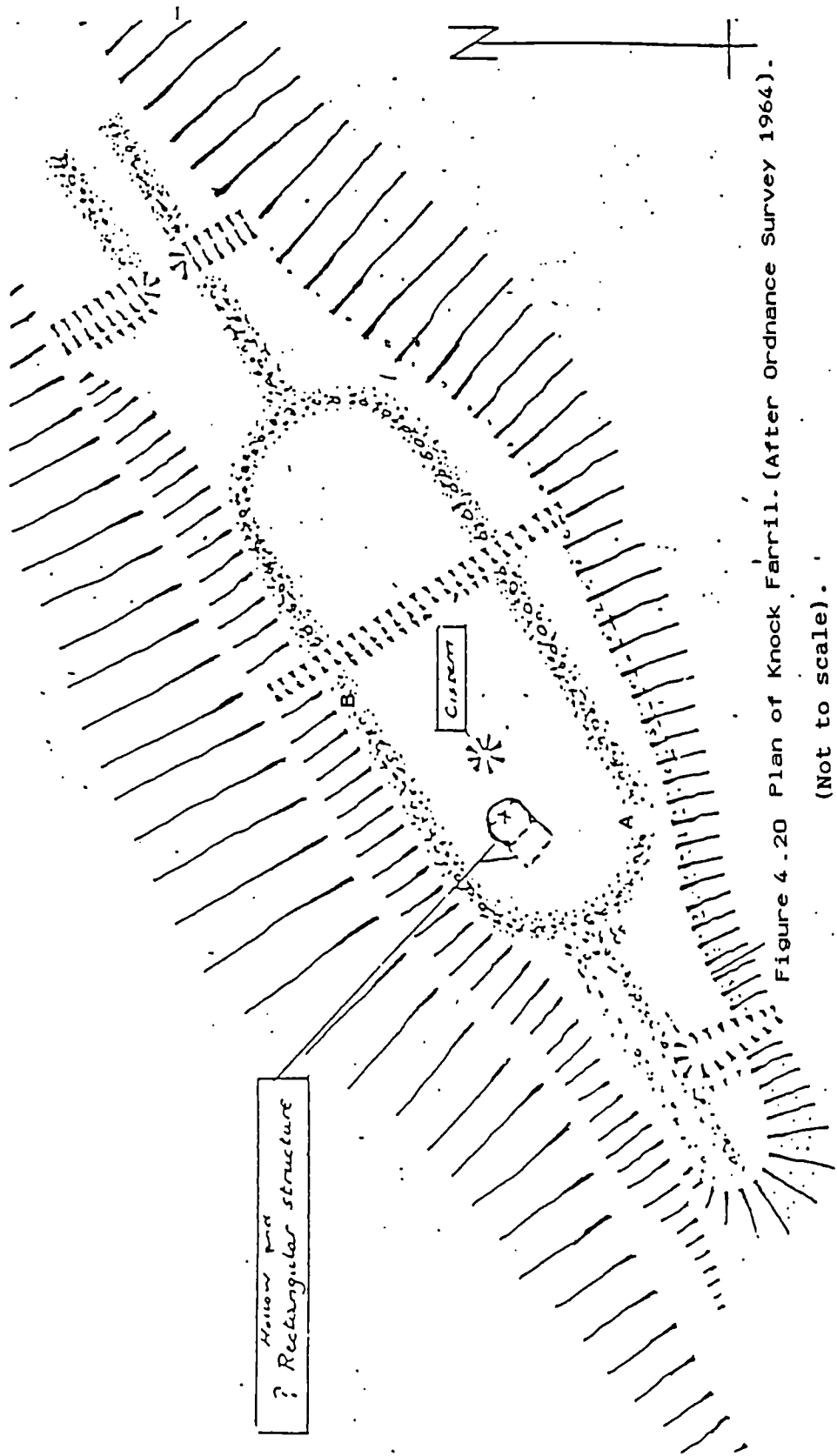


Figure 4.20 Plan of Knock Farril. (After Ordnance Survey 1964).

(Not to scale).

apparently unweathered material. Orientation was by sun compass and inclinometer. Both sampling locations coincided with thermoluminescence bore holes and were from large ( $>2\text{m}^2$ ) outcrops of vitrification. Both locations appeared to be aligned longitudinally and transversely with the wall remains. The vitrification showed differences in colour possibly due to different oxidation states, and in texture e.g. vesicular/low density cinder. Vitrification appeared from surface features to be internal with wall base outer faces preserved but much overgrown. Traces of vitrification can be found virtually round the whole perimeter. The rectilinear enclosure does not follow the contours of the hill but does align itself along the trend of the ridge.

Twelve specimens with magnetic intensities  $>181 \times 10^{-8} \text{ Am}^2/\text{g}$  were demagnetised at 10 mT intervals up to a peak alternating field of 50 mT. All specimens were stable to extremely stable to demagnetisation using this method, only one component was distinguished in each of the specimens (e.g. Figs. 4.21 and 4.22) suggesting only the final firing was recorded. When corrected to Meriden, the individual specimen magnetic directions from the two locations showed a similar grouping when plotted on an equal angle stereographic projection (Fig. 4.24). The



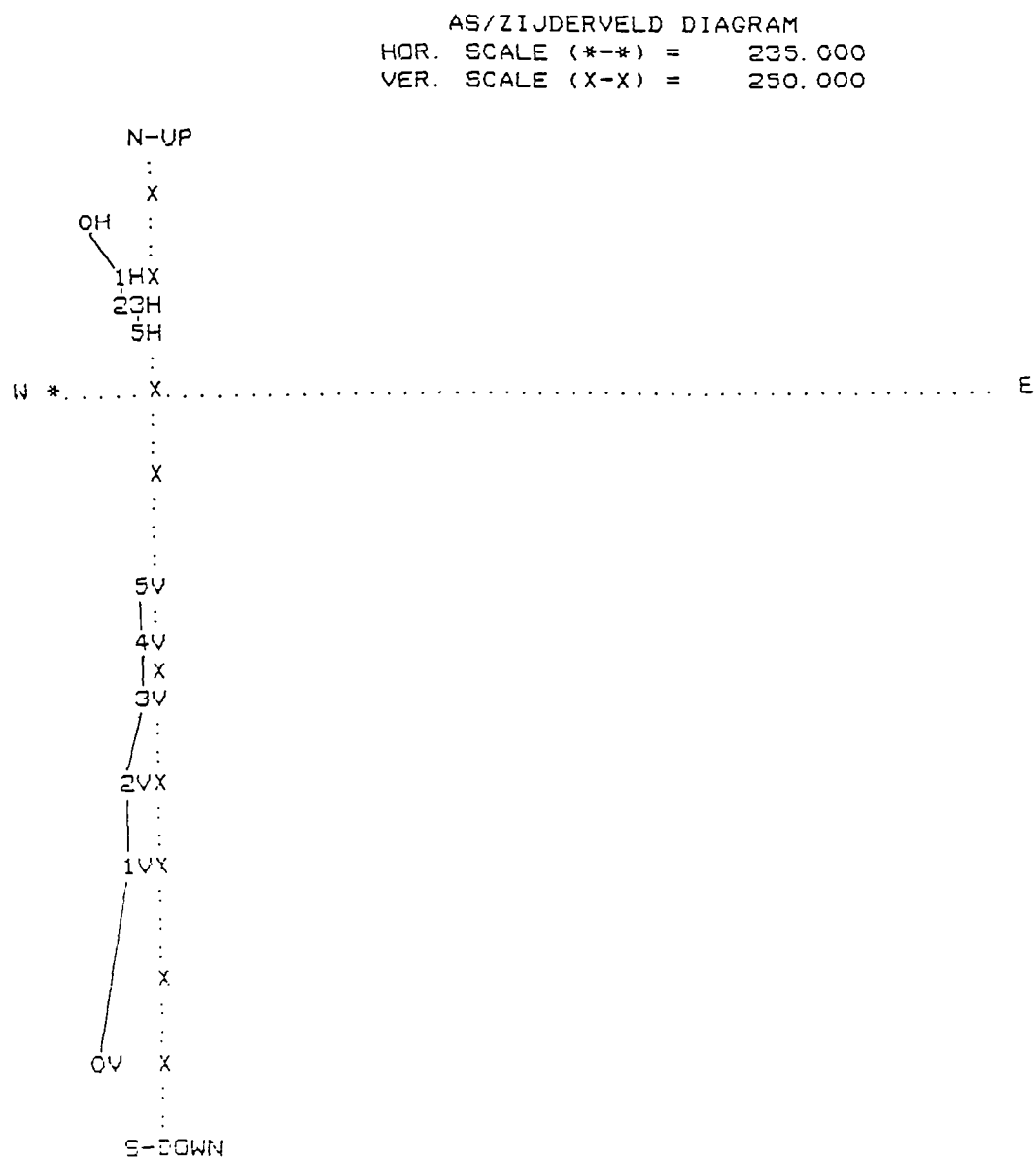
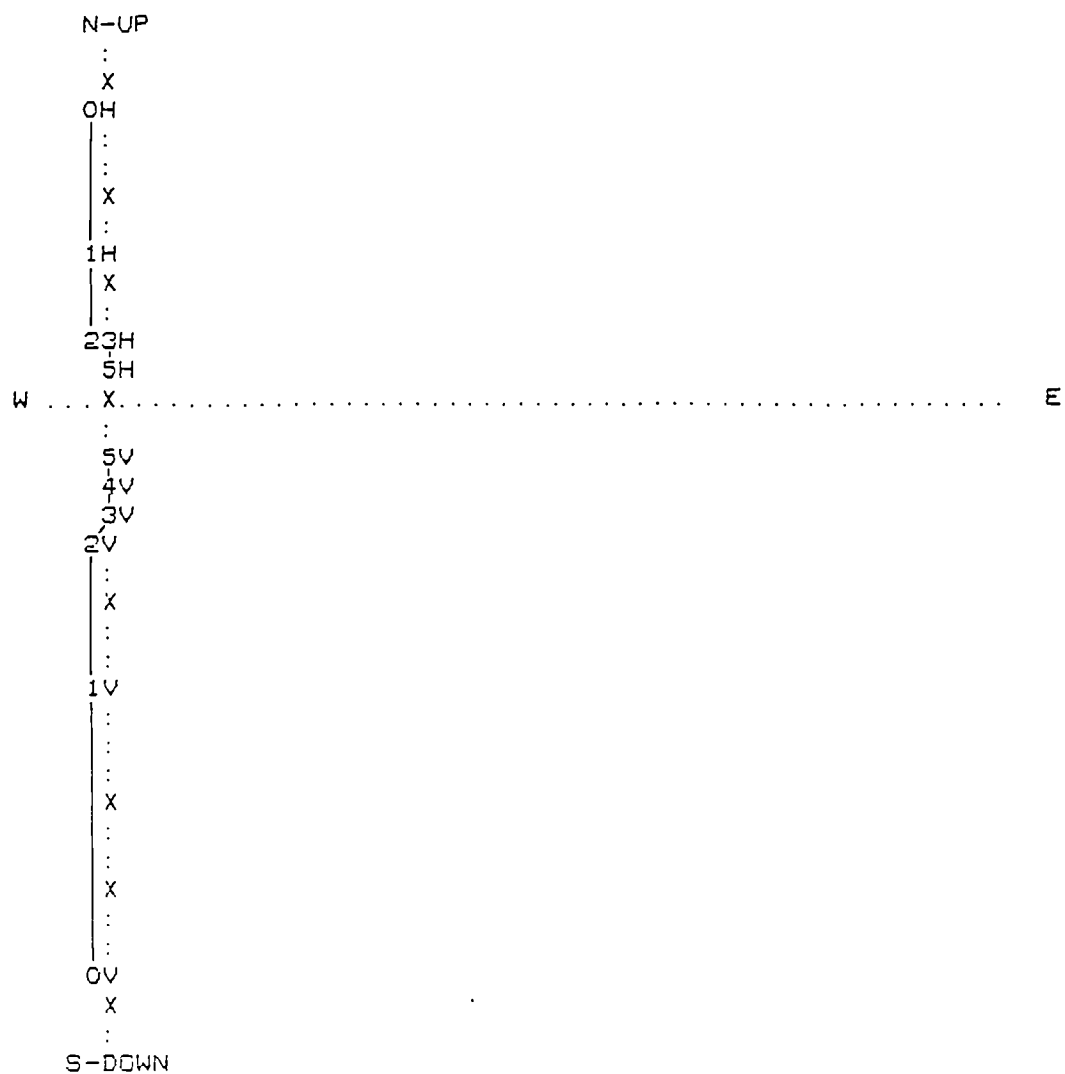


Figure 4.21 As/Zijderveld plot of KF1a.  
 $\times 10^{-8} \text{ Am}^2/\text{g}.$

AS/ZIJDERVELD DIAGRAM  
 HOR. SCALE (\*-\*) = 796.000  
 VER. SCALE (X-X) = 848.000



COMPONENT REMAINING

Figure 4.22 As/Zijderveld plot of KF2b.  
 $\times 10^{-8} \text{ Am}^2/\text{g}$ .

# KNOCKFARRIL, FORT.

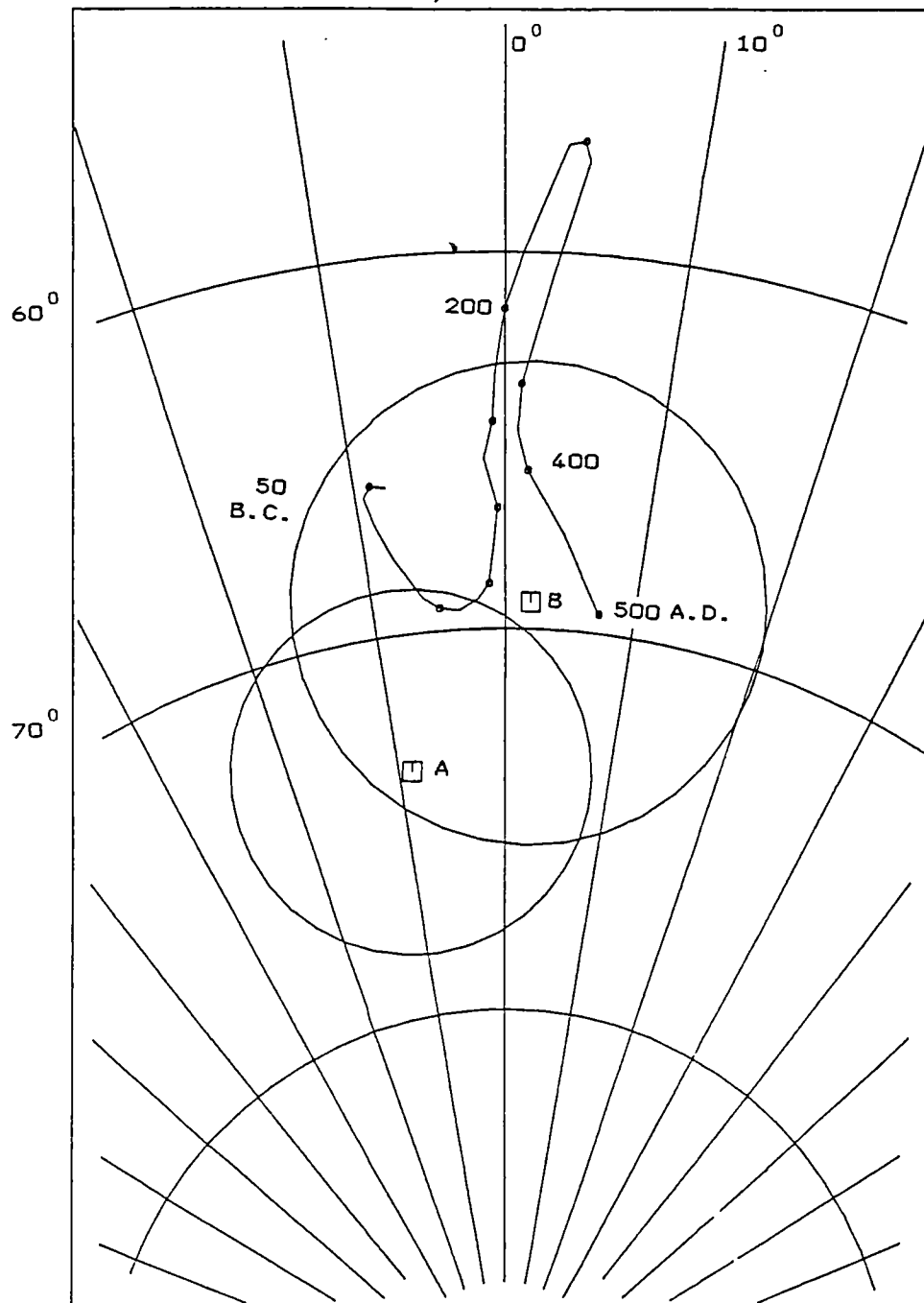


Figure 4.23  
Stereoplot of location mean directions.

# KNOCK FARRIL, FORT.

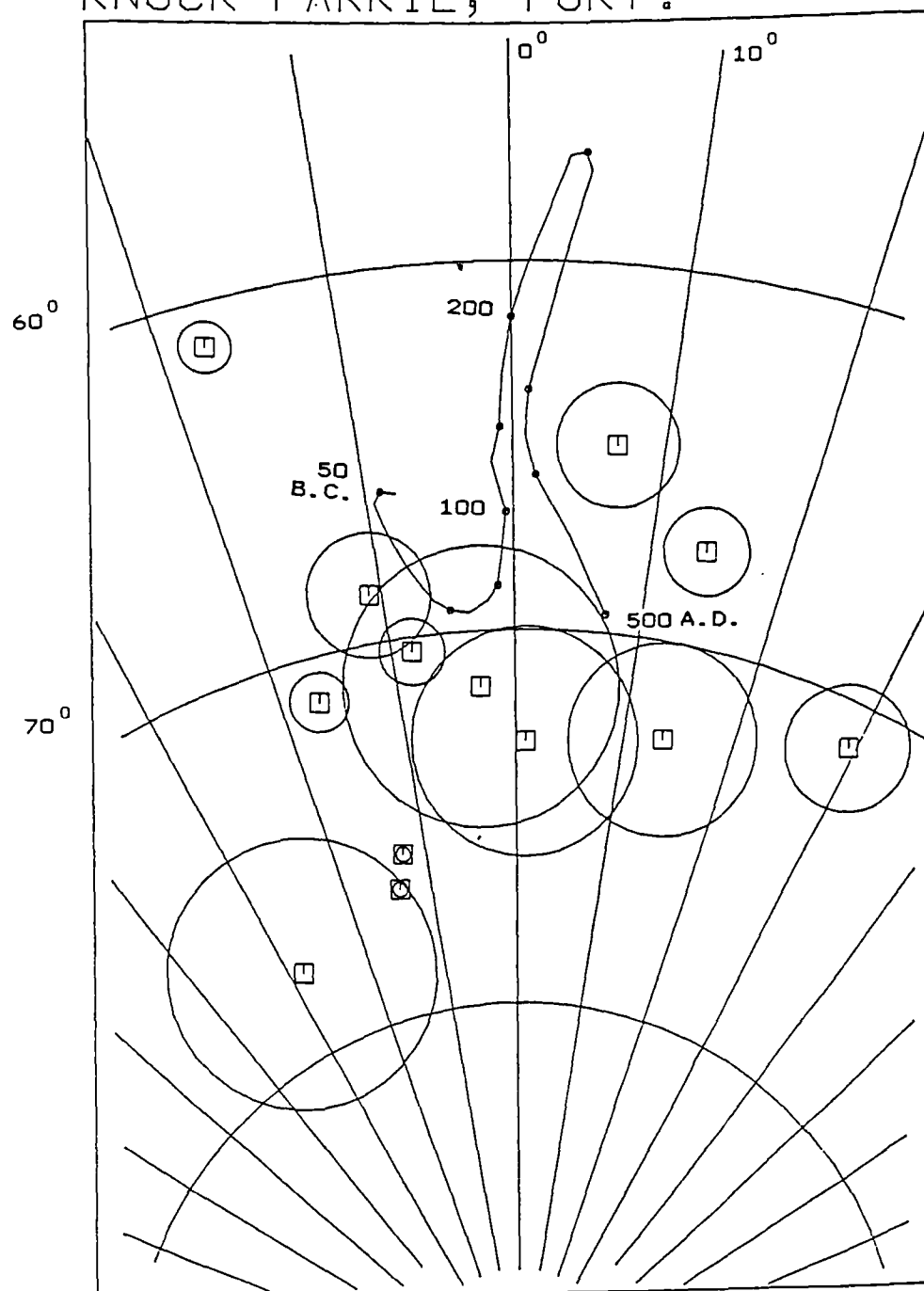


Figure 4.24

Stereoplot of individual specimen directions  
and overall mean.

mean directions with their circles of 95% confidence, suggested the magnetic directions from each location were statistically the same, strongly suggesting there had been no large scale differential movement since the last firing (Fig. 4.23). This was confirmed by the F test (Tarling 1983), which showed a >99% probability that the two location means were from the same population.

The overall observed mean based on all specimen directions plotted off the archaeomagnetic curve but consistent with a date in the late first millenium B.C.. The 95% circle of confidence also included that part of the curve consistent with a late first century B.C. to early first century A.D. date (Fig. 4.25).

# KNOCK FARRIL, FORT.

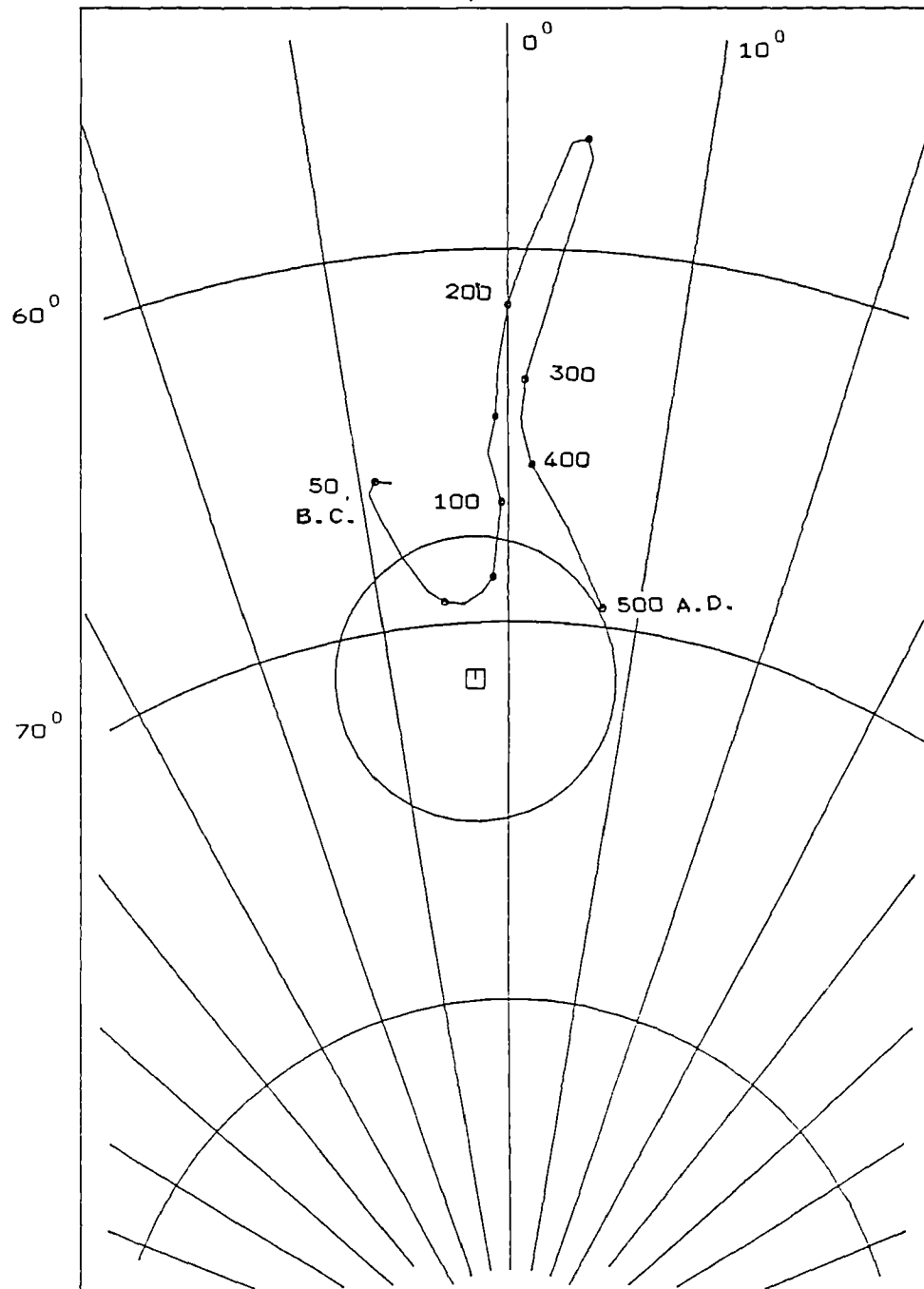


Figure 4.25

Stereoplot of the site mean magnetic direction.

**Table 4.5****Most stable specimen directions.**

Specimen	Dec	Inc	Int	$\alpha_{95}$	S.I.	Range
			$\times 10^{-8} \text{ Am}^2/\text{g}$			mT
1a	346.0	78.8	557.9	0.2	99.2	30-50
3a	326.1	80.7	56.6	3.6	5.1	0-50
4a	350.5	73.8	184.6	0.9	21.7	20-50
6a	15.5	70.6	741.1	1.2	16.7	10-40
7a	344.6	79.6	1626.9	0.2	113.1	10-50
8a	340.8	74.6	625.9	0.8	26.9	20-40
1b	1.8	76.1	181.5	3.1	6.0	0-50
2b	347.4	72.3	721.1	1.7	12.4	30-50
3b	340.0	65.5	977.2	0.7	30.1	0-30
4b	16.4	75.4	1088.9	2.6	7.7	0-30
5b	33.5	73.5	547.7	1.7	12.4	20-40
6b	7.3	68.5	749.1	1.7	11.7	0-30

Mean Meriden corrected direction for all specimens:

Dec = 357.1

Inc = 71.5

N = 12

R = 11.914

$\alpha_{95} = 3.8$

K = 128.6

,

Mean Meriden corrected direction for location A:

Dec = 351.2

Inc = 73.6

N = 6

R = 5.974

$\alpha_{95} = 4.8$

K = 190.9

Mean Meriden corrected direction for location B:

Dec = 1.9

Inc = 69.3

N = 6

R = 5.954

$\alpha_{95} = 6.4$

K = 109.0



4.7. Langwell ( $57.9^{\circ}$  N  $4.6^{\circ}$  W), Fort and Dun, Ross and Cromarty.

The site is situated on a West to East oriented ridge overlooking the River Oykel. Traces of an elongated hillfort can be seen just below the main summit, but the main feature is that of a near circular vitrified dun situated on the highest point of the ridge which has been partially excavated by Nisbet (1974). Geologically the structure is composed of a psammitic schist. Its internal diameter is 15 m, with walls 5m thick and 2m in height from the interior. The dun is heavily vitrified with numerous exposures for sampling, whilst a trench was cut through the vitrified core of the northern wall by Nisbet (1974) and a thermoluminescence core has been removed from location C (see Chapter Three). In all, four locations were sampled and oriented using suncompass, magnetic compass and inclinometer, the detailed results of which are presented in Chapter Three.

In brief the mean most stable magnetic directions from three of the four locations agreed statistically strongly suggesting that no large scale differential movement had occurred since the last firing. The

overall mean and circle of 95% confidence was consistent with a date centered on the first century A.D. but statistically incorporating late first century B.C. and late first century A.D. directions.

#### 4.8. Tap o' Noth, Fort ( $57.3^{\circ}$ N $2.8^{\circ}$ W), Aberdeenshire.

The Hill of Noth rises to a height of 555 m above sea level and is visible from the sea 50 kilometres to the East. This fort, the second highest in Scotland, is of oblong type as defined by Ralston (1983) and has wall remains c. 6.6m thick (Feachem 1983). The fort is heavily vitrified, measuring c. 100.5m x 31.5m, with a depression towards the South end of the fort which probably represents the site of a well. On the North and East flanks of the hill a second wall, mainly a row of detached boulders, is present whilst to the South of the fort and down slope there are platforms which may be for houses and/or quarry scoops (Feachem 1983; Ralston 1983).

On the North side of the fort there are large exposures ( $>3m^2$ ) of fused and vitrified material, and so two locations were selected from this area (A and B). Unfortunately no scaled plan for this site was available, but a sketch plan is incorporated (Fig. 4.26a).

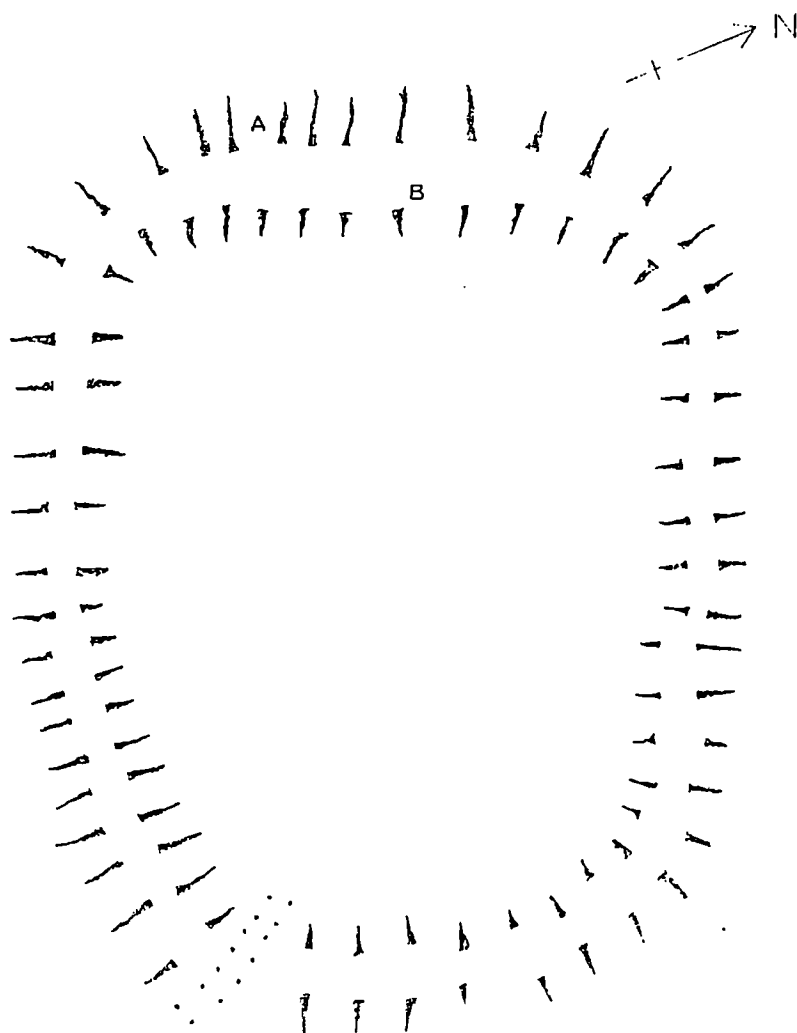
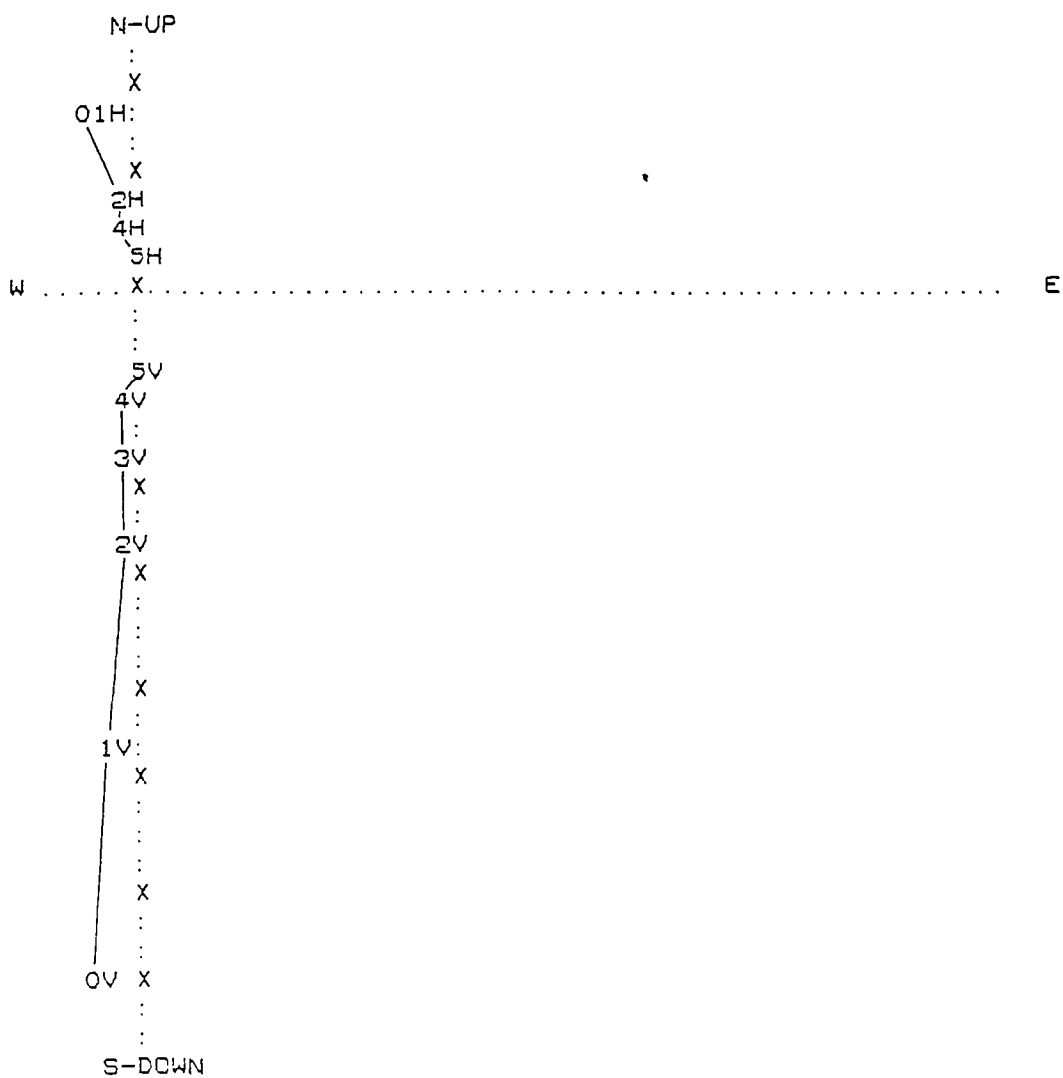


Figure 4.26 (a) Sketch plan of Tap o'Noth (Not to scale).

Elsewhere the majority of the site had smaller exposures emerging from the large quantities of rubble that overlay much of the walls. In some areas lower oxidised material had fallen away (or quarried), leaving hollows. This indicated that many of the upper vitrified masses were physically stable as they had not collapsed, although superficially the upper surfaces of the walls were fragile in places. Cracks appear at most points on the site, but it was clear from the large loose debris that much of the cracking was due to heat expansion and contraction during firing. Five specimens were removed from apparently unweathered material at location A and six from location B. All specimens were orientated using a suncompass and inclinometer.

All eleven specimens showing initial magnetisations  $>157 \times 10^{-8} \text{ Am}^2/\text{g}$  were demagnetised at 10 mT intervals. The maximum peak alternating field used was 90 mT (Table 4.6). The specimens were all stable to extremely stable to demagnetisation using this method whilst only one component of magnetisation was distinguished in each of the specimens (e.g Figs. 4.26b and 4.27). Most of the individual specimen directions showed a similar grouping from both locations when plotted, after correction to Meriden (Fig. 4.29) with the exception of 11b. Mean

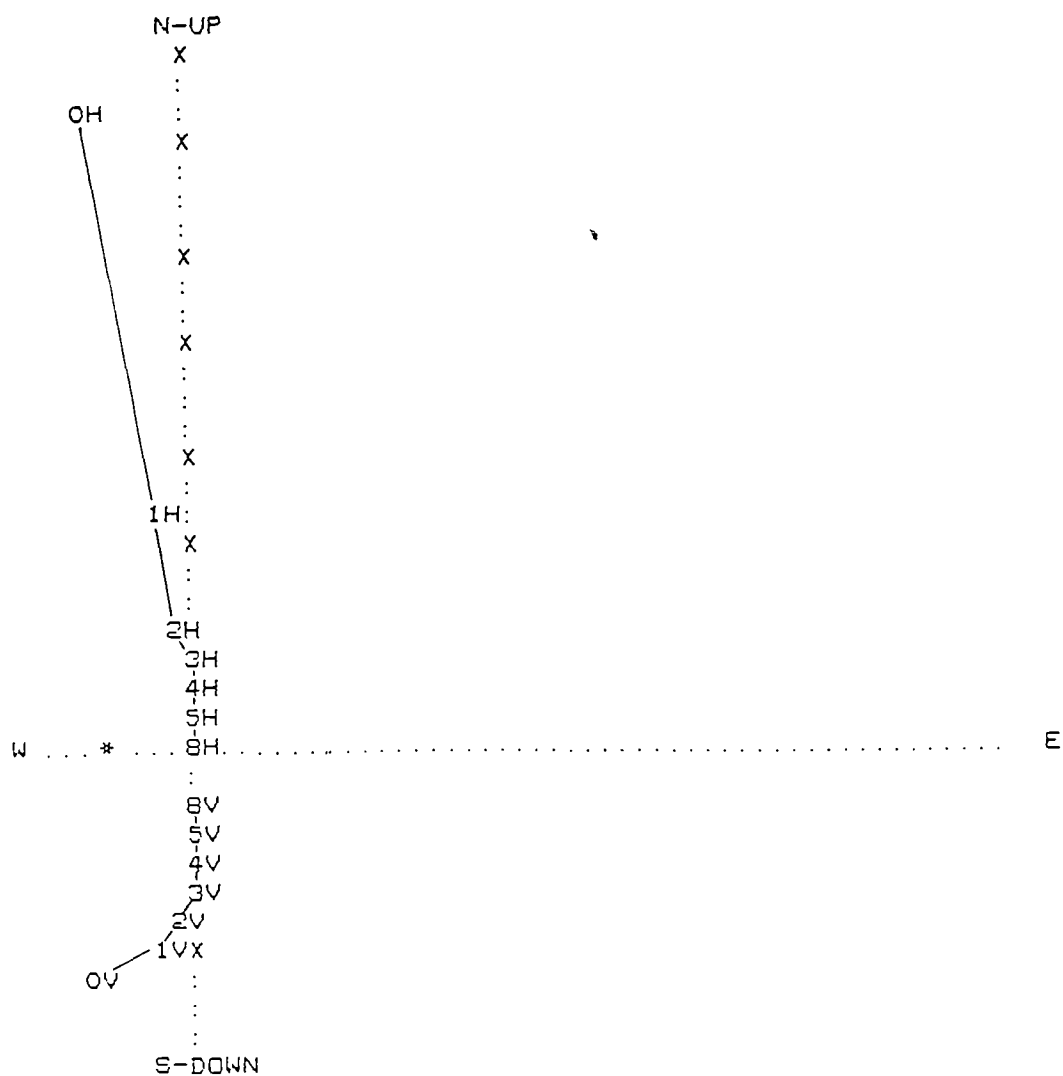
AS/ZIJDERVELD DIAGRAM  
 HOR. SCALE (\*-\*) = 1123.000  
 VER. SCALE (X-X) = 1195.000



COMPONENT REMAINING

Figure 4.26 As/Zijderveld plot of TN2a.  
 $\times 10^{-8} \text{ Am}^2/\text{g}$

VER. SCALE (X-X) = 2562.000



COMPONENT REMAINING

Figure 4.27 As/Zijderveld plot of TN6b.  
 $\times 10^{-8} \text{ A m}^2/\text{g}$ .

TAP 0° NORTH, FORT.

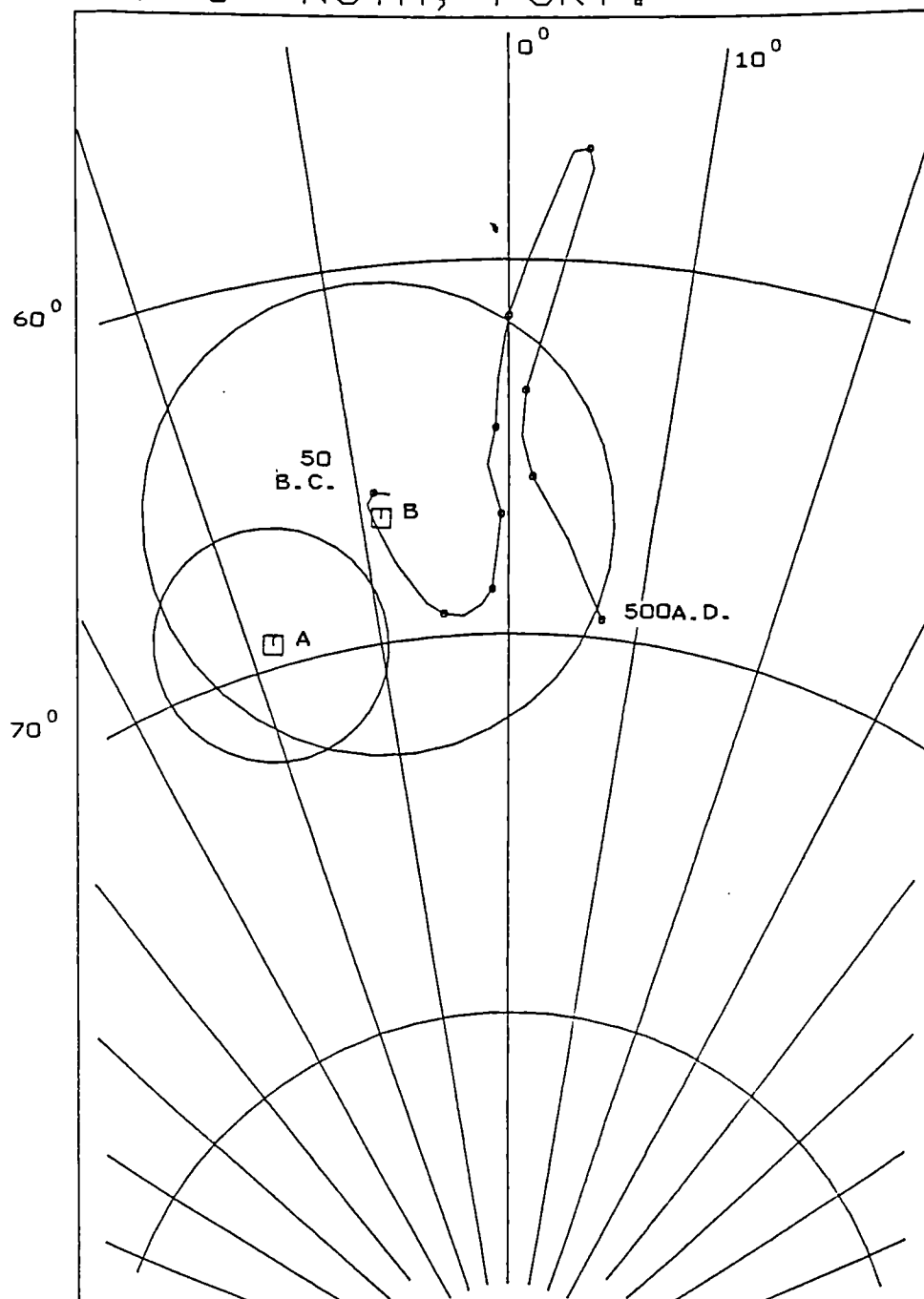


Figure 4.28

Stereoplot of location mean directions.

TAP 0° NORTH, FORT.

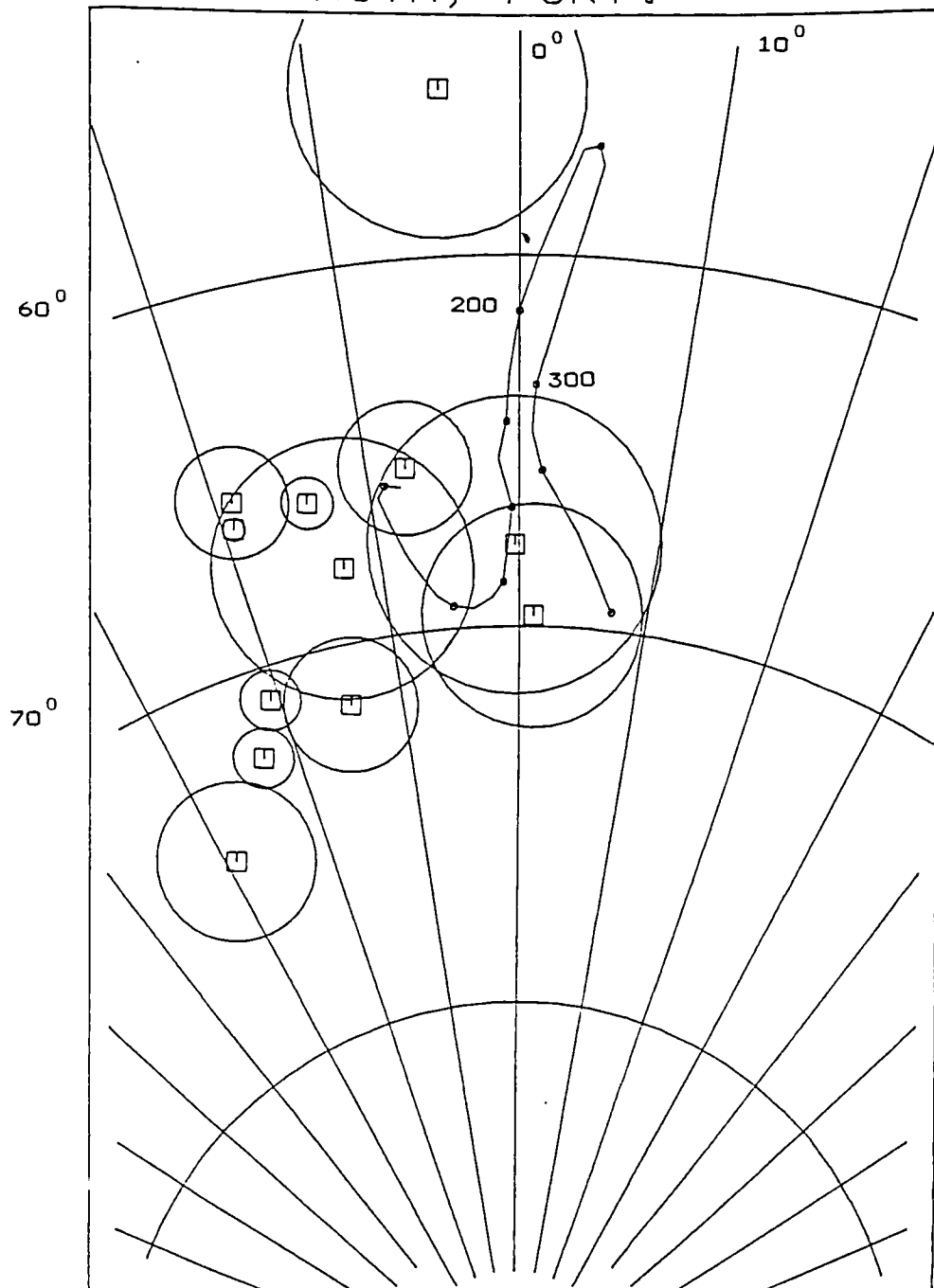


Figure 4.29  
Stereoplot of individual specimen directions  
and overall mean.



magnetic directions from each location were similar whilst the 95% circles of confidence showed that statistically the directions were the same (Fig. 4.28). Further evidence of this was provided by the F test (Tarling 1983) which showed there was a >99% probability that the two means were from the same population. This suggested that there had been no large scale differential movement since the last firing.

The overall observed mean magnetic direction based on all specimens plotted adjacent to that part of the archaeomagnetic secular variation curve consistent with a date in the first century B.C., whilst the 95 % circle of confidence encompassed that part of the curve relating to magnetic directions in the first century B.C. but with a slight overlap with an early first century A.D. direction (Fig. 4.30).

TAP 0° NORTH, FORT.

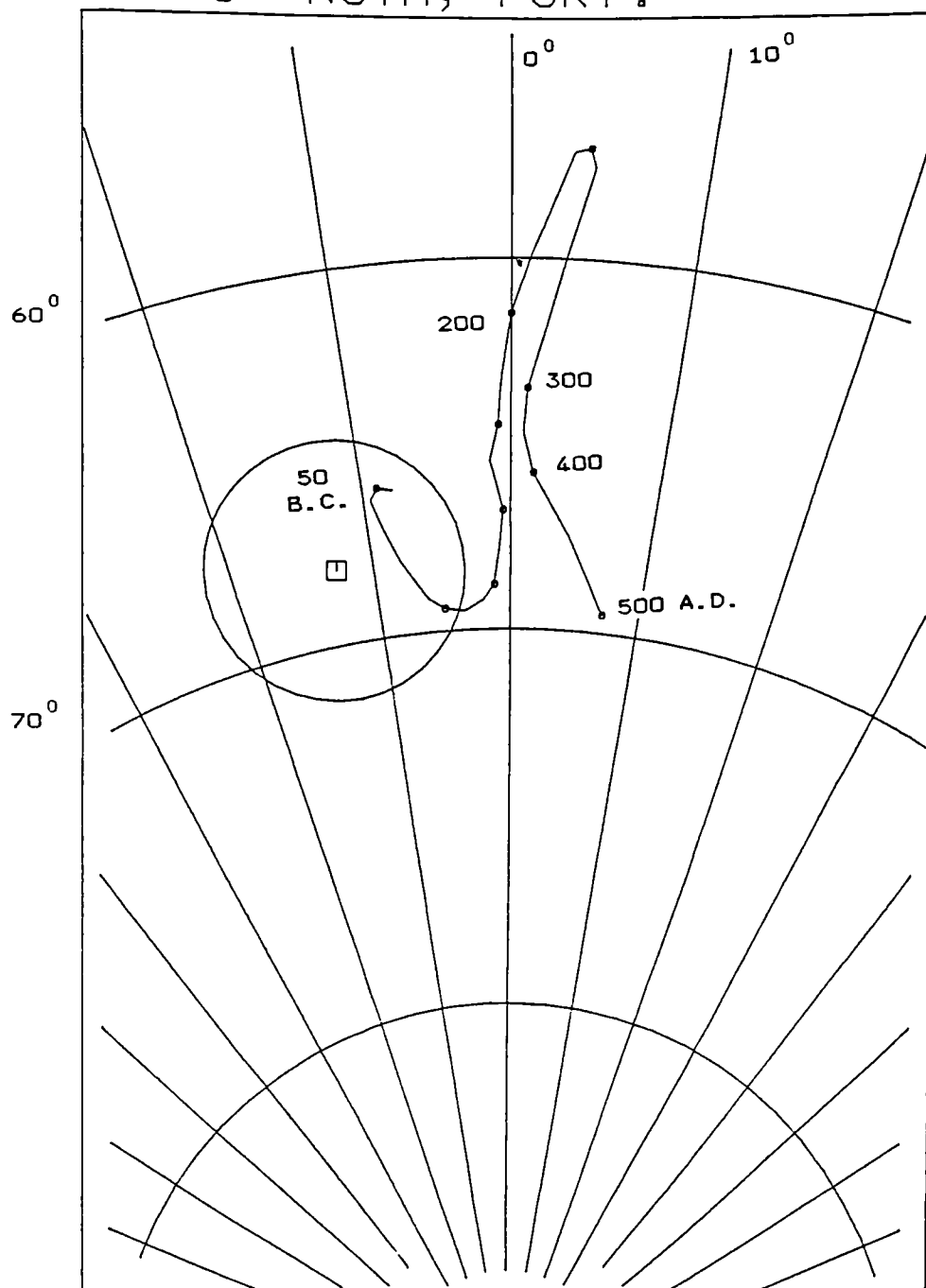


Figure 4.30  
Stereoplot of the site mean magnetic direction.

**Table 4.6**

**Most stable specimen directions.**

Specimen	Dec	Inc	Int $\times 10^{-8} \text{ Am}^2/\text{g}$	$\alpha_{95}$	S.I.	Range mT
1a	336.4	74.0	1673.0	0.8	28.0	30-50
2a	344.0	69.6	1266.4	0.6	33.2	30-50
3a	343.5	74.7	362.8	1.8	11.2	10-40
5a	333.6	75.3	371.6	0.8	27.6	20-40
6a	338.4	69.8	3054.5	0.3	69.8	10-40
2b	1.3	72.9	2882.2	3.0	7.3	40-60
3b	338.8	69.1	2137.0	1.5	13.1	60-90
4b	325.9	77.2	72.4	2.1	10.0	70-90
6b	359.5	71.2	1469.3	4.0	5.3	60-80
8b	351.5	69.2	22109.5	1.8	11.9	10-30
11b	355.3	60.1	1102.5	4.0	4.9	40-70

**Mean Meriden corrected direction for all specimens:**

**Dec = 347.3**

**Inc = 68.0**

N	=	11.0	R	=	10.941
$\alpha_{95}$	=	3.5	K	=	170.5

Mean Meriden corrected direction for location A:

Dec	=	341.8	Inc	=	69.4
N	=	5	R	=	4.993
$\alpha_{95}$	=	3.1	K	=	609.3

Mean Meriden corrected direction for location B:

Dec	=	351.3	Inc	=	66.7
N	=	6	R	=	5.956
$\alpha_{95}$	=	6.3	K	=	114.1

#### 4.9. Summary

Most specimens had stable to extremely stable remanences (Tarling and Symons 1967). Only one component of remanence was isolated in each of the specimens demagnetised using A.F. Most specimen magnetic intensities were strong to very strong prior to treatment whilst the magnetisation remaining at 50 mT was in most cases well above the noise level of the magnetometer.

When plotted on equal angle stereographic projections the specimen magnetic directions showed a variation greater than that expected from measurement and

orientation errors ( $>2^\circ$ ). This is most likely due to the large scale inhomogeneity encountered (Tarling 1986). In one particular instance however (Dunnideer), the directional scatter was so large as to preclude an archaeomagnetic age assignment. This seemed best explained as being due to large scale differential movement subsequent to the last firing. The latter emphasises that the single biggest cause of error in archaeomagnetic directional studies is physical disturbance of the sampling locality after firing.

## CHAPTER FIVE.

---

### Calibration of archaeomagnetic directional dating of the Vitrified Forts

#### 5.1. Archaeological methods

A detailed chronology based on artifactual evidence is in most instances, impossible due either to the paucity of finds on most excavated vitrified and timber laced sites or the "excavation" history of the monuments. The presence of exotic metalwork (e.g. fibulae) can be used in some instances (e.g. Castle Law, Abernethy; Rahoy, Morvern) to date use of individual sites to, for example, the La Tene period (Mackie 1976; Ritchie and Ritchie 1985). However the stratigraphical controls over the position of the artefacts, and therefore their chronological significance, are of varying quality. Therefore it is important to bear in mind that the vitrification may not be contemporary with the artefact discovered. A further complicating factor is that many of the forts are multi-occupation sites. The presence of Dark Age E ware at Craig Phadrig, for instance, showed that this fort had also been occupied in the Dark Ages

(Small and Cottam 1972). Although the site has been archaeologically explored (Small and Cottam, 1972) this was not exhaustive. Therefore it remains archaeologically possible that certain sections of the inner wall were burnt during the first millenium A.D. or later. Evidence from the Green Castle, Portknockie (Ralston, 1980) also showed that timber laced walls can belong equally to periods in the first millenium A.D. as well as B.C. (Alcock, 1971, Ritchie and Ritchie, 1985). As Mackie (1976) states, the vitrification phase on most excavated sites occurs at the end of the use of the site, with re-occupation occurring normally after a lapse in time. Thus artifacts beneath the layer associated with vitrification will date a period before the vitrification episode, providing there has been no later disturbance of the site. This should give a *terminus post quem* for the vitrification phase. However even if there has been a datable re-occupation this may be long after the burning of the walls. As such there may be no precise archaeological chronological control over the vitrification episode.

## 5.2. Radiocarbon ( $^{14}\text{C}$ ).

The principles and techniques of this dating method are described in various publications (e.g. Aitken 1974; Fleming 1976; Greene 1983). Uncorrected dates were obtained from Megaw and Simpson, (1984). Calibration using dendrochronology to obtain calendar years has been undertaken using Stuiver and Pearson (1986) and Pearson and Stuiver (1986). Where necessary radiocarbon years, calculated on the 5568 half life, have been converted to the 5730 half life (by multiplying by 1.029, Champion 1980). In calibrating, the tabulated conversions were used, quoted at 20 year intervals. In some instances there was no difference between the sample and tabulated observed means e.g. all the Langwell radiocarbon dates, whilst there was only one instance where a >9 year disparity existed between the tabulated and sample radiocarbon dates (N 1124) for the other sites. If the standard deviation fell between two tabulated standard deviations the greater number was quoted, thus overestimating the errors involved in preference to underestimating them. The ranges quoted take into account both the curve and sample standard deviations, giving the maximum estimate of the errors involved (Figs 5.1a-5.1c). In some cases the dendrochronological calibration resulted



in more than one equivalent age. Nearly all of these are plotted with the exception of one anomalously old age (N-1124; Craig Phadrig) which was excluded in order to preserve diagram clarity, but a summary of all ages are tabulated in Table 5.1. The nomenclature CAL B.P. from 1950 A.D. has been adopted.

### 5.3. Thermoluminescence.(T.L.).

The principles and techniques of this dating method are described in various publications (e.g. Goodyear 1971; Aitken 1974; Fleming 1976; Greene 1983). This method should date the last firing since temperatures of c.500°C are necessary for the release of energy from the crystal lattice (Greene 1983). The amount of energy released in the laboratory from any given sample should be directly proportional to the number of years elapsed since the last firing. However plateau testing was found to be a necessary requirement for the vitrified forts (Sanderson *et al* 1985; Strickertsson *et al* 1988) whilst dosimetry and differential crystal sensitivity to radiation are also potential problems in estimating age (Sanderson *et al* 1985). The T.L. dates are presented as age ranges (the overall error is used) at the 95% confidence level (Figs 5.1a-5.1c). The nomenclature CAL B.P. has been adopted.

#### 5.4. Archaeomagnetism (A.M.)

In quoting an archaeomagnetic date it is important to realise the field limitations such an age assignment has for the vitrified forts in Scotland. If we accept that the vitrification occurs at the end of the use of most sites then the dating of the vitrification episode should give a *terminus ante quem* for the pre vitrification phase (Mackie 1976). However the vitrification may not necessarily be of one phase or date. Thus sampling was, where possible, in at least two places to check for contemporaneity of the vitrification. It is also possible that the date of the last firing may not relate to the actual vitrification phase as strong re-heating could result in the destruction of all previous remanences. Nevertheless if the latter were the case the last firing would have to be in conditions of limited oxidation in order to retain the characteristic grey colour of the wall cores and prevent the oxidation of the magnetite. If we assume vitrification causes wall destruction, then it is likely that the magnetic remanence present relates to the original vitrification episode. If wall collapse did not occur as a result of initial vitrification the magnetic remanence may relate to a high temperature secondary firing. However

experimental firings of timber laced walls (e.g. Childe 1934; Buscenschutz et Ralston 1981), have shown that wall collapse occurs, and therefore it is reasonable to assume, on the available evidence, that the magnetic remanence relates to the original vitrification.

The archaeomagnetic dates are presented at the 95% level of confidence (Figs 5.1a-5.1c; Fig 5.5). The age range represents the precision with which the mean specimen directions have been defined. The nomenclature B.C. has been adopted, although to permit comparison of dates the archaeomagnetic age ranges are presented in years B.P. in the diagrams.

#### 5.5. Comparison of dates

It was not usually possible, using radiocarbon, to define a short time span characteristic of any context. In particular there is a flat area of the calibration curve between 800 and 400 B.C. which makes precise dating for the Early Iron Age very difficult (Pearson and Stuiver 1986).

Sample dates from contexts consistent with the destruction of each site did, in some cases, show age ranges later in date than from other often primary contexts. For example sample Gx 3274, associated with

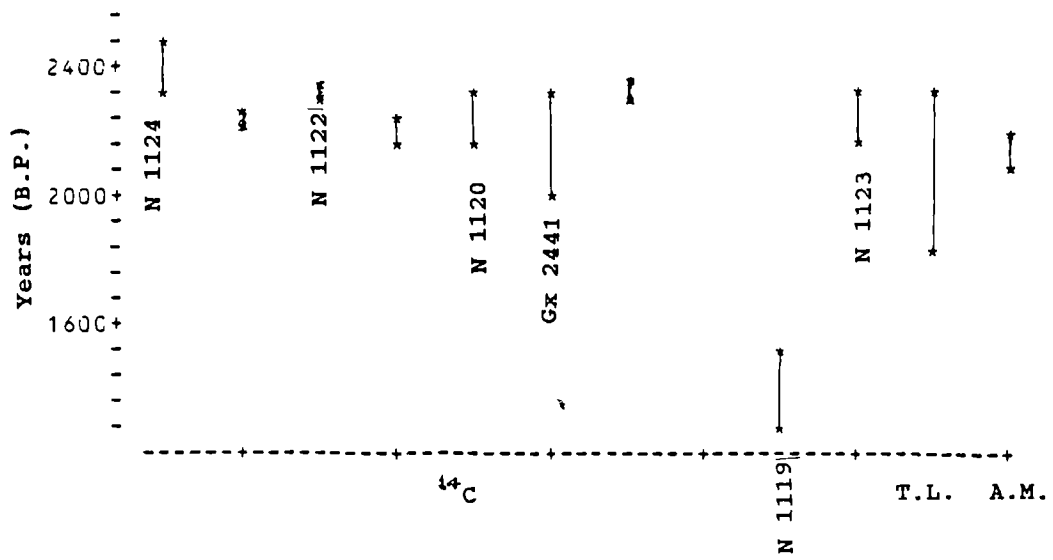


Figure 5.1 (a). Chart of absolute dates for Craig Phadrig.

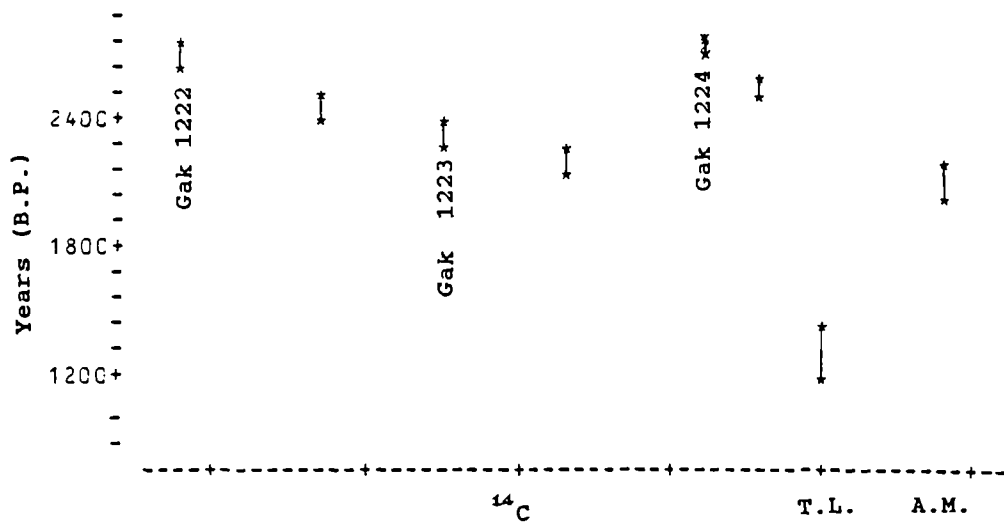


Figure 5.1(b). Chart of absolute dates for Finavon.

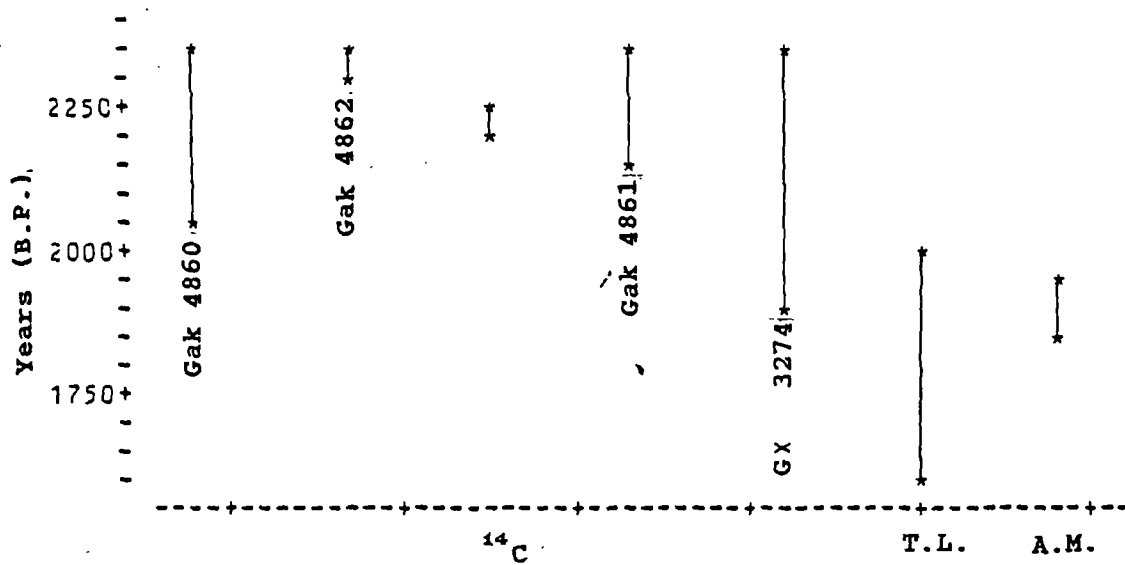


Figure 5. 1(c). Chart of absolute dates for Langwell.

Table 5.1

Summary of dates available for the sampled vitrified structures

Site	A.M.	T.L. *	$^{14}\text{C}$ #	Arch.
Craig Phadrig	c.180- c.90 B.C.	2.1 $\pm$ 0.2	1990-2704	Iron Age
Dun Skeig	c.70 A.D. -c.480 A.D.			Iron Age
Finavon	c.180- c.90 B.C.	1.3 $\pm$ 0.1	2150-2704	Iron Age
Knockfarril	c.200- c.100 B.C.	3.1 $\pm$ 0.3		Iron Age
Langwell	c.10 B.C.- c.80 A.D.	1.8 $\pm$ 0.2	1880-2357	Iron Age
Tap O'Noth	c.180 B.C.- c.10 A.D.	4.1 $\pm$ 0.4		Iron Age

\* = ka B.P. All T.L. dates after Strickertsson *et al* (1988)

# = Range of all Iron Age dates. All  $^{14}\text{C}$  dates calibrated after Pearson and Stuiver (1986)/Stuiver and Pearson (1986)

charcoal from a fallen roof timber at Langwell, showed an age range which overlapped with both the T.L. and A.M. age ranges (Fig. 5.1c). There is thus some evidence to support a correlation between the latest age ranges derived from radiocarbon and individual contexts consistent with fort wall destruction. However some of the radiocarbon dates are from primary contexts or re-occupations after the walls were burnt and thus the dating of the vitrification episode by radiocarbon can be very imprecise.

Other radiocarbon dates from Langwell suggest a primary occupation centered on 2341 CAL B.P. (Gak 4862-charcoal from the foundation course). T.L. and A.M. age ranges overlap, but collectively span the late first century B.C. to the fourth century A.D. (Fig. 5.1c). However the observed means of these age ranges differ considerably. This disparity could be due to miscalculations of radiation dose or the sensitivity of the crystalline materials used. The magnetic directions for the first century B.C. are apparently well dated (Clark *et al* 1988) whilst systematic magnetic distortion effects and large scale differential movement have been discounted for this site. Therefore there is no overwhelming reason to alter the configuration of the curve at this point particularly as, despite the

differences in observed means, all three dating methods (A.M., T.L. and some  $^{14}\text{C}$  dates) show overlapping age ranges for this site.

For Craig Phadrig sample Gx 2441 (charcoal from below rampart) showed an age range which overlapped with the T.L. age range (Fig. 5.1a), defining a Late Iron Age date with T.L. centered on 2100 B.P. The magnetic direction for Craig Phadrig lay off the 50 B.C. to present curve, although consistent with the theoretical curve for the Late Iron Age (Tarling 1988) and a date also centered on the second century B.C.

A Late Iron Age date (Gak 1223) was defined by radiocarbon at Finavon centering on 2337 CAL B.P. for charcoal from the occupation layer. However the T.L. date was much later in time (centered on 1300 B.P.). None of the radiocarbon dates were consistent with the T.L. date from this site (Fig. 5.1b).

Given the fact that the magnetic direction defined at Finavon was statistically identical with that from Craig Phadrig (at the 95% confidence level), it seems very likely that the magnetic direction from Finavon should also be assigned to the second century B.C. on the basis of the T.L. results from Craig Phadrig and the secular variation curve (Tarling 1988). However the T.L. result



(centered on 1300 B.P.) from Finavon remains disturbing. Similarly at Knockfarril and Tap o'Noth apparent Late Iron Age directions were associated with T.L. dates much earlier in date (Table 5.1). No radiocarbon dates are available for these sites. The observed mean magnetic directions were broadly similar with other Late Iron Age site directions (Craig Phadrig and Finavon).

#### 5.6. The Iron Age secular variation curve

The pattern of observed mean directions from Craig Phadrig, Finavon, Knockfarril and Tap O'Noth, can be assigned to different ages depending if the  $^{14}\text{C}$  or T.L. dates are taken in isolation for each site. As there was only a limited number of dated magnetic directions from this study, no attempt was made to define the trend of the curve by statistical methods.

If the T.L. dates from these sites are used to date the mean magnetic directions, then Tap o'Noth and Knockfarril define a Bronze Age part of the curve with westerly declinations. These magnetic directions would then move toward a steeper inclination in the Late Iron Age (L.I.A.), (Craig Phadrig), with a similar declination to the aforementioned forts. A Late Iron Age/Early Roman direction is defined by T.L. for Langwell

with a shallower inclination than many of the other sites, but with a similar declination. There is then a directional overlap in the mid first millenium A.D. (Finavon), with a mean direction dated to the Late Iron Age (Craig Phadrig; Fig. 5.1d). The dates stated on the curve represent the observed means only, so that for each date on the curve there is a statistical error (Table 5.1). Further the mean magnetic direction from Dun Skeig has been included in this curve, although undated by T.L., to preserve clarity in the diagram. It is presented in a bracketed form (Fig. 5.1d).

If radiocarbon determinations are used to calibrate then we find that there are statistically consistent L.I.A. dates for both Craig Phadrig and Finavon and a  $^{14}\text{C}$  date for Langwell consistent with wall destruction (Gx 3274; Fig. 5.1e). The age assignments stated on the curve are based on age ranges most consistent with wall destruction for each site. However equating the radiocarbon activity of the sample with actual date of vitrification remains a problem. As the other sites sampled do not have radiocarbon dates further comparision cannot be made.

As most of the sites sampled have no local long term field working tradition and a record of excavation both

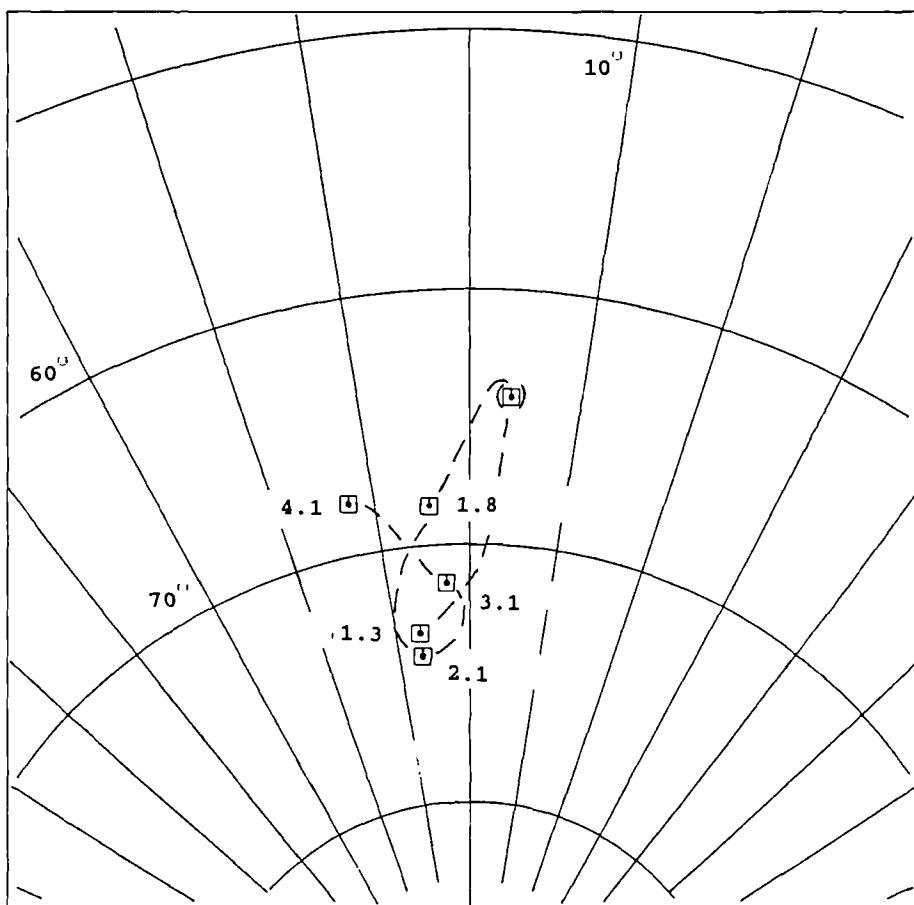


Figure 5.1(d) Archaeomagnetic curve based on T.L. dates (ka B.P.)

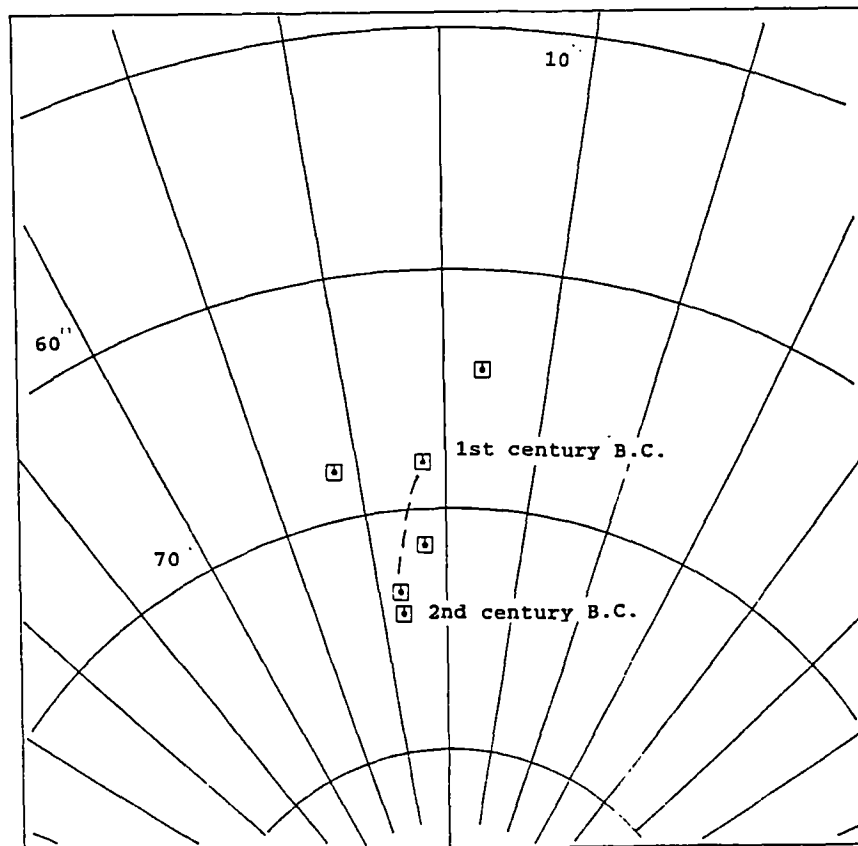


Figure 5.1a) Archaeomagnetic curve based on  $^{14}\text{C}$  dates

small scale, irregular and intermittent, with artefacts of limited chronological value (Ralston et al 1983; Ritchie and Ritchie 1985), no curve has been attempted on the basis of archaeological evidence. The dun at Langwell was half excavated, but provided artefacts of limited chronological significance. Architectural considerations of this dun, as well as for the rectilinear forts are not necessarily of chronological significance, and it is possible to argue that variations in building tradition are a response to different topographies, different functions, or social/political organisation, (Macsween, 1985), although typological evolution through time has been argued for some structures (Simpson, 1954b, Hamilton, 1962 in Macsween, 1985; Mackie, 1965c).

The dated mean magnetic directions for the Dark Ages, already available, show directions concentrated further East than the mean magnetic direction for Finavon. This fact does not support the T.L date for this site. The presence however of a fragmentary rotary quern at Finavon, because it represents a technological advance from saddle querns commonly used in the Iron Age, may indicate a late use of the site (Childe 1934). Nevertheless reference to the archaeomagnetic data base shows that archaeo-features assigned Bronze Age and Early Iron Age dates on

available archaeological evidence show mostly easterly declinations. Therefore the archaeomagnetic data base does not support the T.L. dating of the mean magnetic directions from Knockfarril and Tap O'Noth. As there are a reasonable number of magnetic observations (based on thermoremanences), for sites dated to this period it is probable that the easterly trend of Early Iron Age directions is a real one. If we also refer to the lake sediment curve based on a three point running mean from the combined lake sediment data, and some archaeological data, (Turner and Thompson, 1982; Clark et al 1988), then this also shows an easterly trend although with shallower inclinations than those from some of the forts, (Fig. 5.1g). Notable is the declination at 1000 B.C. (calibrated on the basis of radiocarbon - Clark et al 1988), which is c.35° East. Much evidence therefore is inconsistent with the T.L. dating of the mean magnetic directions from Knockfarril and Tap o'Noth.

It is thus possible to state that nearly all the evidence other than T.L. (i.e. <sup>14</sup>C, archaeologically dated thermo and depositional remanences), supports the assignment of the rectilinear forts to different periods during the Late Iron Age, and not to the Dark Ages or the Late Bronze Age. (With the exception of the T.L.

determination for Craig Phadrig which is statistically the same as some of the radiocarbon dates from the site and the expected archaeomagnetic age). Similarly there is agreement between all three dating methods for the dun at Langwell.

The fact however that some T.L. dates are so obviously inconsistent with the other evidence for date may merit cautionary treatment of the T.L. results. However as the problems associated with individual dates are not available in detail within the literature, it is not possible to be definitive about the reliability of these determinations.

Whilst it is realised that each dating method has its inherent problems, and that these are not always available for analysis within the literature, nevertheless with the numbers of magnetic observations now available, the general trend of the archaeomagnetic curve seems to be well defined in some areas, whilst the precision of this will increase as more magnetic results are obtained. Interestingly a best fit curve, based on the most mutually consistent age assignments (Fig. 5.1f), can be seen to be consistent with the theoretical Iron Age curve (Fig. 5.2) postulated by Tarling (1988).

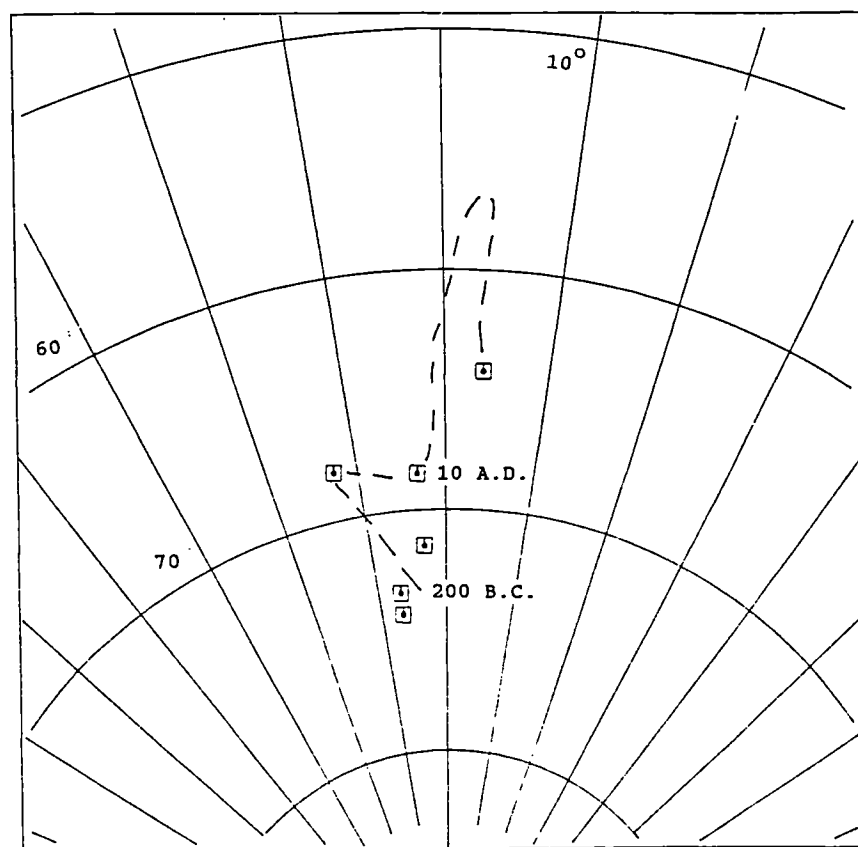


Figure 5.1(f) Composite archaeomagnetic curve based on several dating methods



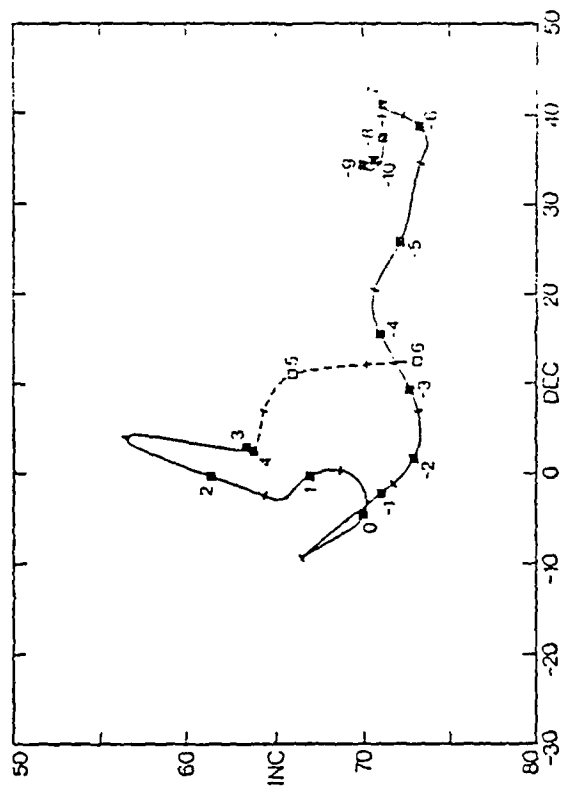


Figure 5.1b) Archaeomagnetic curve based on lake sediments. (After Clark et al 1988).

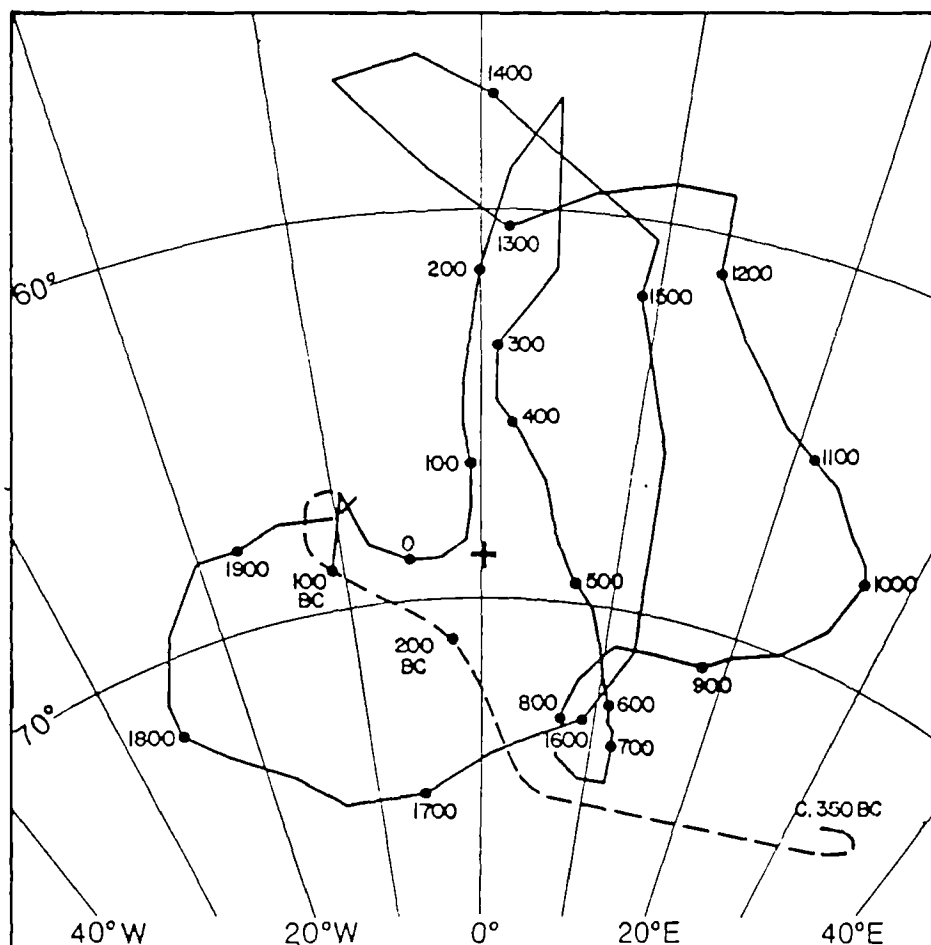


Figure 5.2 Secular variation curve with theoretical Iron Age section. (After Tarling 1988).

### 5.7. Archaeomagnetic age assignments

The statistically identical mean magnetic directions from Finavon and Craig Phadrig do not lie on any part of the secular variation curve from 50 B.C. to the present (Clark *et al* 1988). As such these directions must pre-date 50 B.C. Correlation with the lake sediment curve (Turner and Thompson 1982; Clark *et al* 1988), shows that Late Bronze Age magnetic directions are situated c.30° East whilst Early Iron Age directions also appear to be East of North, (Fig. 5.1g). The magnetic results from Finavon and Craig Phadrig therefore seem most likely to define the general trend of the Late Iron Age curve and agree well with the theoretical curve postulated for the Iron Age by Tarling (1988) also using thermoremanences. On the basis of the latter curve mean magnetic directions from Finavon and Craig Phadrig are consistent with a second century B.C. date for their last firings although their circles of 95% confidence incorporate a late third century B.C. date.

At Knockfarril the observed mean magnetic direction was similar with other Late Iron Age site directions (see Craig Phadrig and Finavon), confirmed by the theoretical secular variation curve for the Iron Age (Tarling 1988; Fig. 5.2). However Knockfarril had a 95% confidence circle

which overlapped with an Early Roman date although its observed mean was more consistent with a second century B.C. age. Tap O' Noth had a mean magnetic direction consistent with a late first century B.C. date (Fig. 5.3) and thus appears to be the most recently burnt rectilinear fort. (Its circle of 95% confidence just incorporates a very early first century A.D. date whilst crossing but not incorporating the observed mean from Langwell, Fig 5.4).

The mean magnetic direction for Langwell suggests that its walls were last fired between the late first century B.C. and the late first century A.D., whilst Dun Skeig was last fired between the first and fifth centuries A.D. (Fig. 5.4). Unfortunately the mean direction for this dun lies on an ambiguous part of the secular variation curve (Roman period), hence the large age range. A summary of archaeomagnetic dates is presented in Figure 5.5.

#### 5.8. Summary

Both Craig Phadrig and Finavon have similar observed means and statistically identical magnetic directions to Knockfarril (Figs. 5.3 and 5.4). This suggests contemporaneity of firing. Tap o'Noth appears to show the most recent firing within the rectilinear forts group. Interestingly those forts in estuarine settings were fired

## SITE COMPARISON.

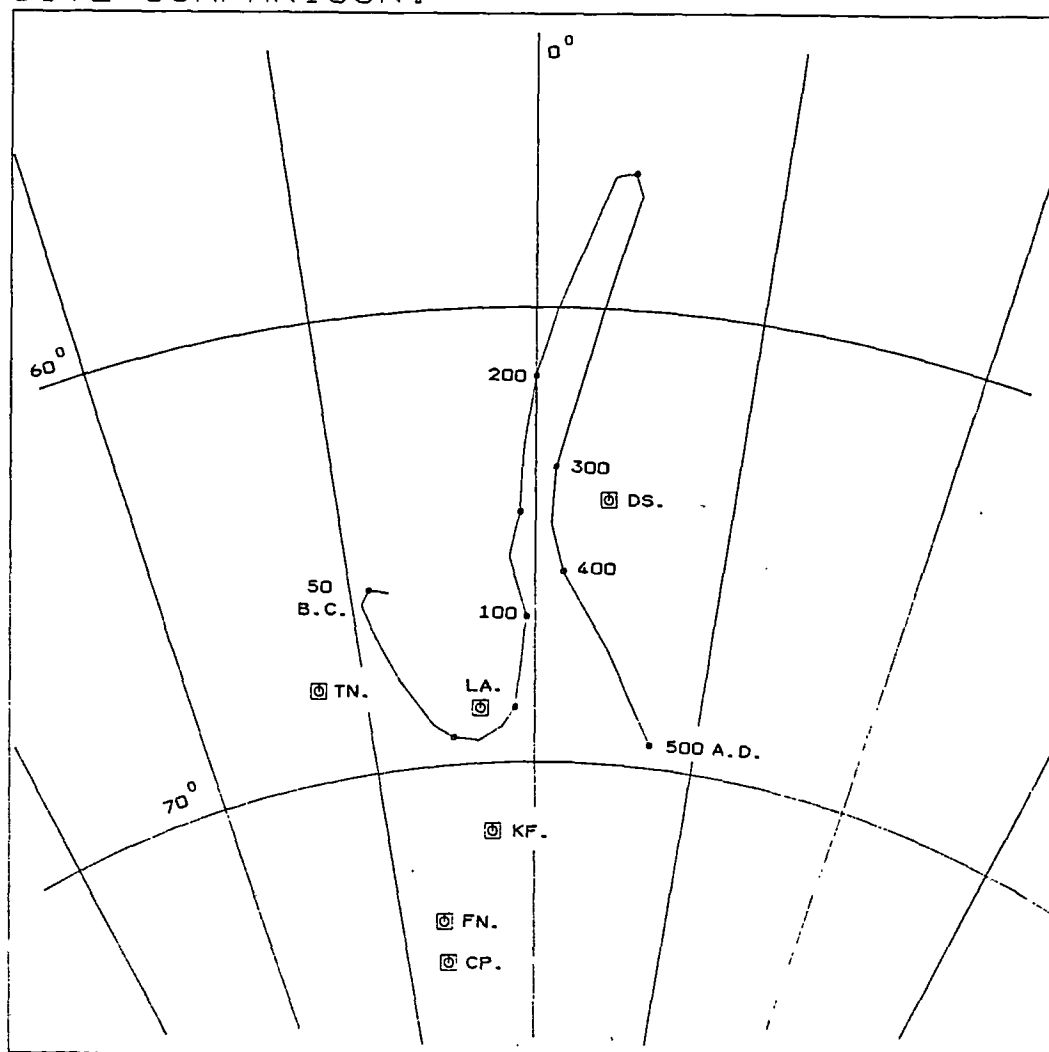


Figure 5.3 Stereoplot of observed site mean magnetic directions.

- ~ KF. = Knockfarril, Fort.
- ✓ TN. = Tap o' Noth, Fort.
- LA. = Langwell, Fort and Dun.
- CP. = Craig Phadrig, Fort.
- DS. = Dun Skeig, Fort and Dun.
- FN. = Finavon, Fort.

## SITE COMPARISON.

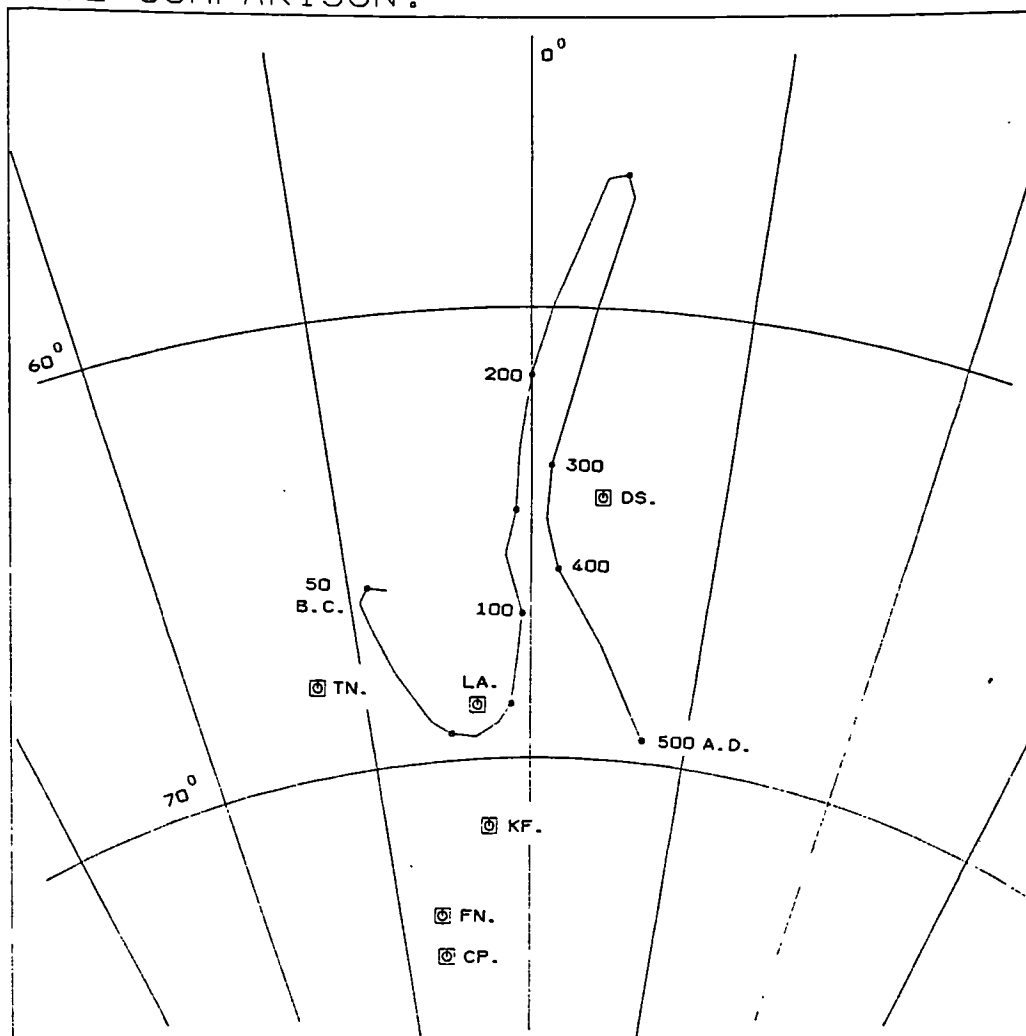


Figure 5.3 Stereoplot of observed site mean magnetic directions.

KF. = Knockfarril, Fort.

TN. = Tap o' Noth, Fort.

LA. = Langwell, Fort and Dun.

CP. = Craig Phadrig, Fort.

DS. = Dun Skeig, Fort and Dun.

FN. = Finavon, Fort.

# SITE COMPARISON.

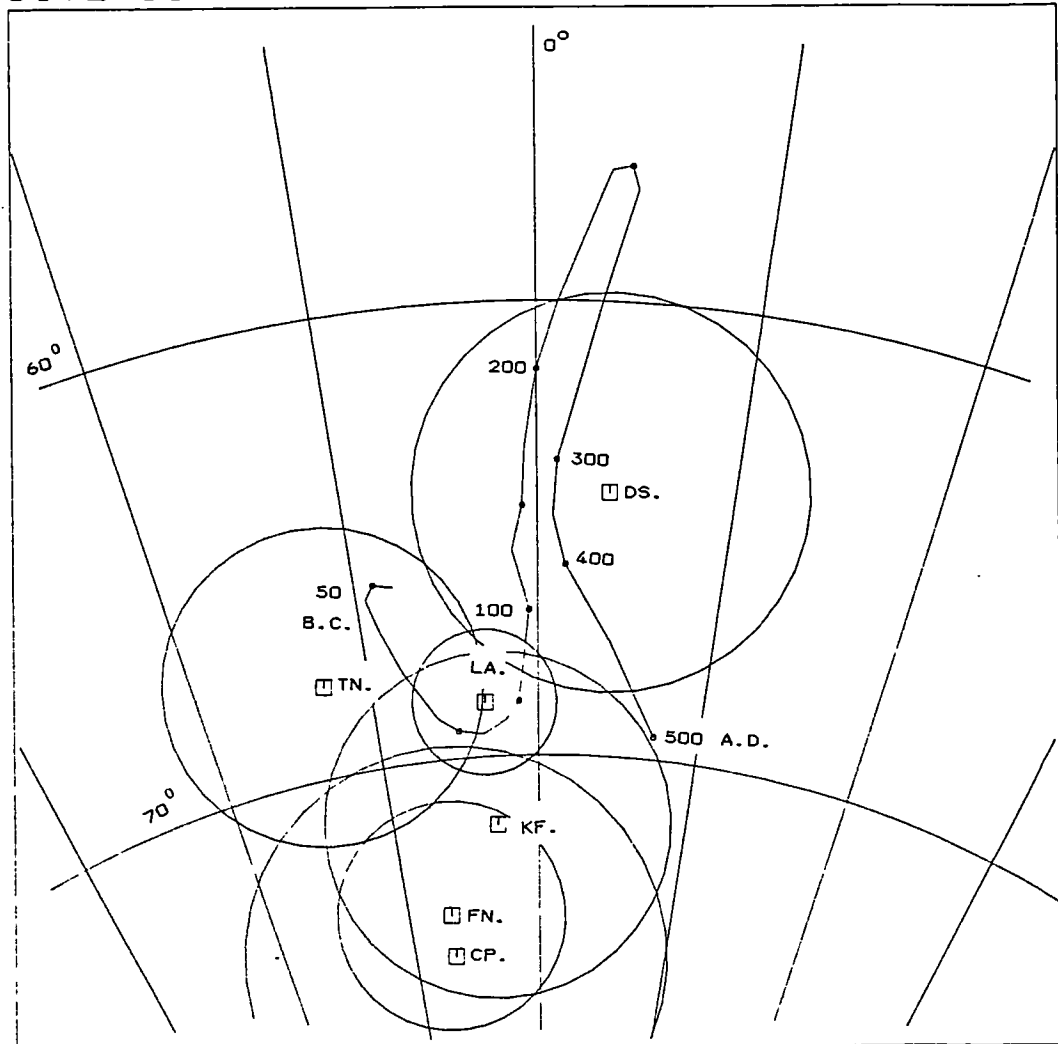


Figure 5.4 Stereoplot of site mean magnetic directions and circles of 95% confidence.

# SITE COMPARISON.

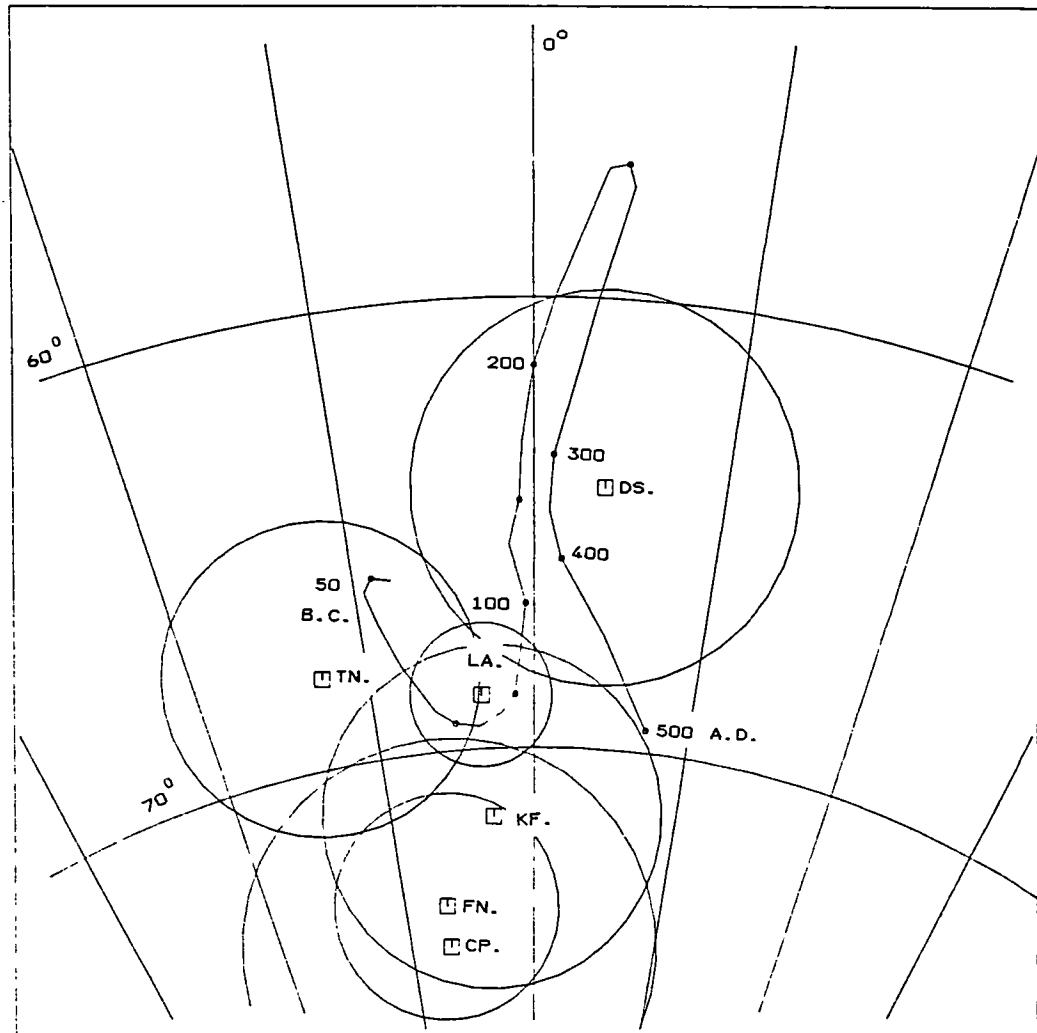


Figure 5.4 Stereoplot of site mean magnetic directions and circles of 95% confidence.



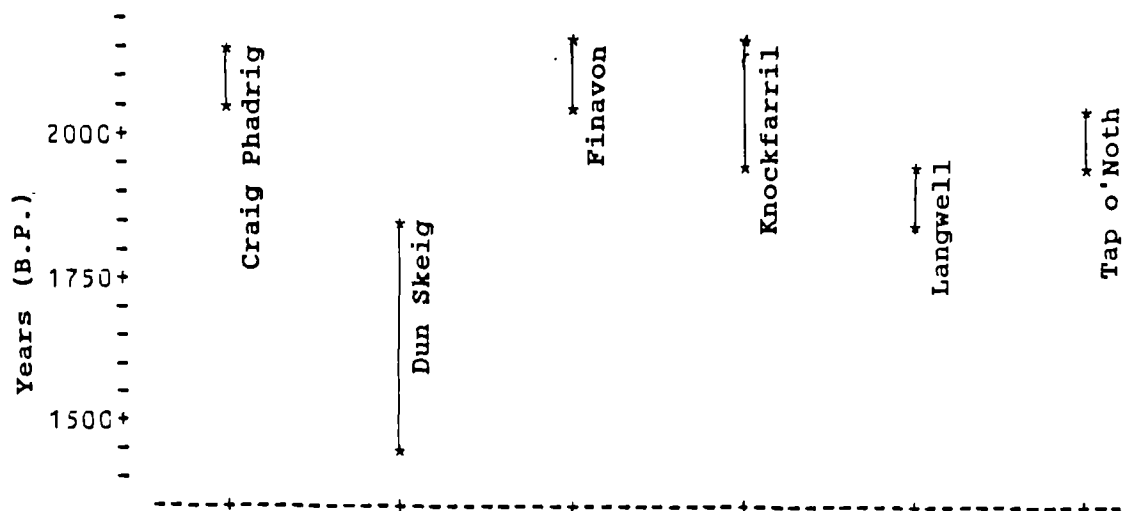


Figure 5.5 Chart of archaeomagnetic dates for all sampled forts.

first whilst Tap o' Noth further inland was burnt at a later date.

The duns (Dun Skeig and Langwell) appear from their mean directions to be later in date than the rectilinear forts (Fig. 5.4). Dun Skeig is unexcavated but the site sequence from visible remains shows that the drystone dun was built after the firing of the timber laced one (Feachem 1983; Ritchie and Ritchie 1985). As such it is likely that the dry stone dun post dates the late fifth century A.D., (Fig 5.4). This points to longevity in the use of dun structures.

The results from the rectilinear forts appear to define the general trend of the Late Iron Age curve, correlating broadly with that proposed by Tarling (1988), (Fig 5.2 and 5.4), whilst magnetic age assignments from all the vitrified structures sampled range from the late third century B.C. to late fifth century A.D. (On the basis of available magnetic information). However further definition of Late Bronze Age/Early Iron Age magnetic directions using thermoremanences would serve to further define the magnetic curve, hopefully permitting greater resolution of magnetic directional change over the Iron Age as a whole.

The agreement between magnetic directions and

absolute dating methods is good in certain instances e.g. Craig Phadrig and Langwell. The anomalous T.L. dates for other forts such as Finavon and Knockfarrell is disturbing. It is interesting to note that for all those forts sampled with  $^{14}\text{C}$  dates there is at least partial agreement with the magnetic results (Fig. 5.1a-c), although problems of equating the  $^{14}\text{C}$  activity of the sample with actual date still remain. The fact however that magnetic directions can be assigned to the Late Iron Age and later times on the basis of already dated magnetic results enables a measure of independence from the age assignments obtained by other methods for these forts.

## CHAPTER SIX

---

The magnetic properties of a triple flued experimental kiln from the Lunt Roman Fort, Baginton, 52.3° N, 1.7° W, Warwickshire.

### 6.1. Description.

The kiln was of updraught type, (Fig. 6.1), fired in 1985, and composed of one type of local clay which was well prepared and mixed. No sherds or other intrusive magnetic materials were used in the structure, which had three flues with no false floor. The pottery stack was placed directly on the base of the kiln. The structure was coal fired and internal air temperatures were monitored throughout the firing (Fig. 6.2a). The degree of expansion and contraction of the clay walls was monitored by direct measurement of the cracks in the walls and of the gap around the kiln circumference.

### 6.2. Sampling method.

As the superstructure of this kiln was a dome there was restricted sunlight to the inner parts of the kiln. Hence the discs were attached to the outer parts of the

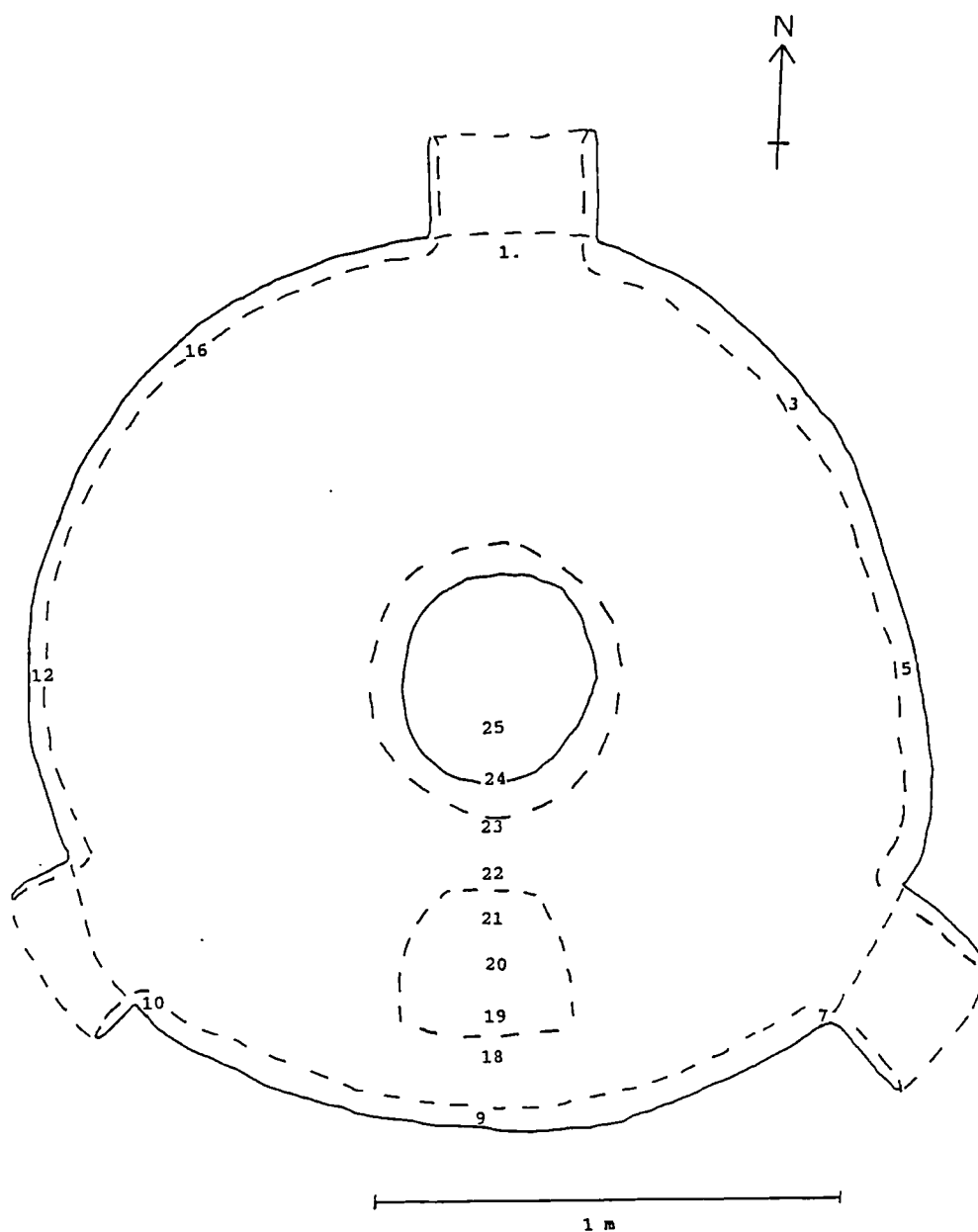


Figure 6.1 Plan of triple flued experimental kiln

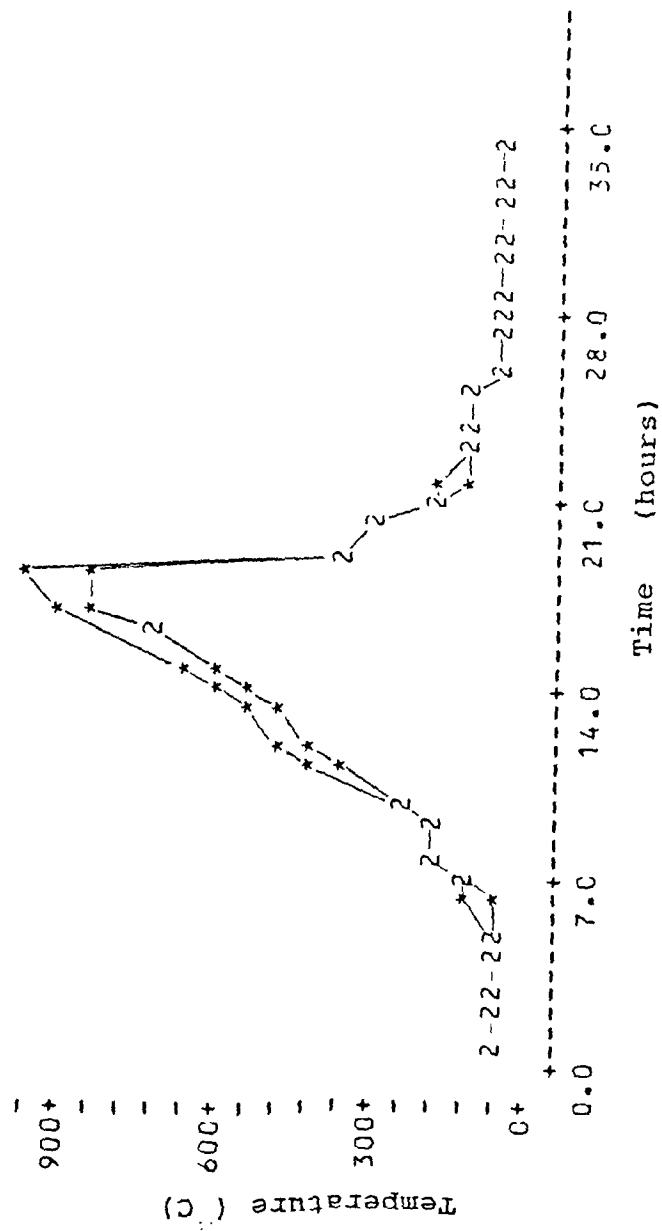


Figure 6.2 a Temperature as a function of time.

kiln wall according to azimuth to enable orientation by sun compass. (They were also at the same height as the two thermocouples). In order to facilitate sampling the kiln wall was cut prior to firing whilst the clay was still malleable. After firing oriented specimens could be removed that were representative of the whole cross section of the kiln wall. This enabled the study of the magnetic properties with depth through the wall as well as with azimuth. These large specimens were cut into smaller ones (c. 2cmx2cm cores) in the laboratory using a brass hacksaw prior to measurement. Where possible each individual sampling location had three cylinders cut from the main pre-cut specimen. These were allocated a number and letter. The number increased with distance round the kiln in a clockwise direction, whilst specimens with the letter A were from the outside shell of the kiln wall, those with the letter C from the inside skin of the kiln wall, whilst those with a letter B were situated in the centre of the wall (Table 6.1). Further specimens were taken from the floor of the kiln at 10cm intervals on a North-South transect (Table 6.1). As no direct sunlight reached the floor of the kiln strike measurements were made using a magnetic compass. The magnetism of the structure did not appear to affect this compass.

Table 6.1

Most stable core specimen magnetic directions.

Specimen.	Dec.	Inc.	Int.	$\alpha_{95}$	S.I.	Range
			$\times 10^{-8} \text{ Am}^2/\text{g}$			mT
Wall specimens:						
1A	355.8	65.5	10.6	1.4	9.8	0-50
1B	352.1	69.3	33.1	0.5	40.0	30-50
1C	3.4	60.7	2032.6	0.2	46.7	5-15
3A	352.1	59.7	8.1	1.5	10.6	7.5-50
3B	338.9	73.3	29.3	1.1	19.4	30-50
3C	339.3	67.6	202.4	0.6	35.4	30-50
5A	3.4	68.5	5.0	2.1	8.0	10-50
5B	336.6	65.7	10.8	1.6	9.3	0-50
5C	341.7	60.3	26.2	0.7	21.6	5-50
7A	9.9	66.3	9.6	1.7	7.7	0-20
7B	347.2	65.5	28.9	1.0	17.8	15-30
7C	13.6	60.9	303.0	0.5	42.1	20-50
9C	347.3	64.6	61.6	0.2	80.9	20-50
10A	18.3	69.7	4.4	1.2	17.5	30-50
10B	24.6	69.6	45.1	0.6	30.9	15-50
12A	354.3	69.3	10.9	2.6	8.1	20-40
12B	346.5	69.7	40.3	1.2	14.2	15-50



16A	359.6	66.8	6.5	2.5	6.8	0-40
16B	24.7	76.7	17.0	0.6	22.0	0-15
16C	358.1	74.8	47.4	0.6	26.4	0-10

Floor specimens:

18	8.2	68.3	10.4	1.3	11.8	0-50
19	349.2	65.7	7.9	2.9	5.1	0-40
20	343.7	67.3	16.6	1.6	9.8	0-10
21	356.4	62.5	10.7	1.3	11.7	5-40
22	5.3	63.8	12.2	0.8	20.1	0-50
23	4.8	61.1	5.0	1.0	13.8	0-20
24	353.7	69.4	6.7	1.0	18.4	15-40
25	4.8	67.3	27.6	0.3	53.9	0-10

Mean magnetic direction for all specimens:

Dec = 357.2	Inc = 67.2
N = 28	R = 27.825
$\alpha_{95} = 2.2$	K = 154.2

Mean magnetic direction for wall specimens:

Dec = 356.6	Inc = 67.8
N = 20	R = 19.851
$\alpha_{95} = 2.8$	K = 127.9

Mean magnetic direction for floor specimens:

Dec = 358.4	Inc = 65.8
N = 8	R = 7.977
$\alpha_{95} = 3.1$	K = 305.3

Mean magnetic direction for A specimens:

Dec = 1.2	Inc = 66.7
N = 7	R = 6.977
$\alpha_{95} = 3.7$	K = 262.0

Mean magnetic direction for B specimens:

Dec = 353.7	Inc = 70.8
N = 7	R = 6.947
$\alpha_{95} = 5.7$	K = 112.6

Mean magnetic direction for C specimens:

Dec = 354.2	Inc = 65.3
N = 6	R = 5.949
$\alpha_{95} = 6.7$	K = 98.9

### 6.3. Laboratory observations.

Twenty eight specimens were demagnetised at 10mT intervals up to a peak alternating field of 50 mT. Only one component of remanence was defined in each of the specimens confirming that only the last firing was recorded (e.g. Fig. 6.2c). Successive field corrected directions of remanence showed little variation after each incremental demagnetisation step (e.g. Fig. 6.2b). The most stable magnetic directions were defined, using a stability index (Tarling and Symons 1967). There did not appear to be any consistent correlation between the A.F. field at which the most stable directions were defined and the position of the specimens in the wall (Table 6.1), although there was a higher incidence of most stable directions defined between 20-50 mT and 30-50 mT in the level C specimens than in the level A. This suggested that the most stable remanence acquired in some of the specimens from the inner wall had a higher coercivity than some of the outer wall specimen remanences isolated over more incremental steps e.g. 0-50 mT (1A), Table 6.1.

Specimen intensities of magnetisations were higher for the inner wall than the outer at any one azimuthal location (Table 6.1), and generally showed a smooth

HDR. SCALE (H-K) = 601.000  
 VER. SCALE (V-V) = 617.000

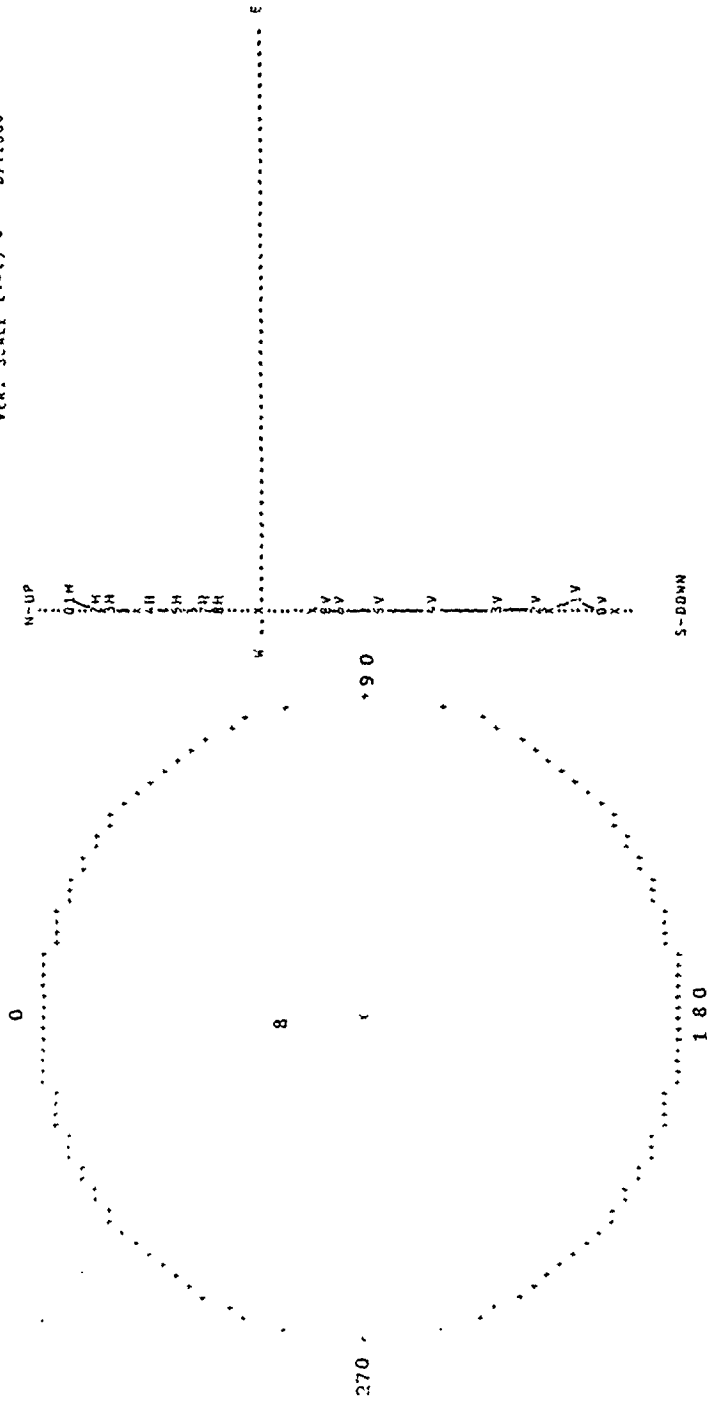


Figure 6.2b Stereoplot of 1c

Figure 6.2c As/Zijderveld plot of 1c  
 $\times 10^{-8} \text{ Am}^2/\text{g}$

decline after each demagnetisation step (e.g. Fig 6.2d). All specimen intensities varied between 2032.6 and  $4.4 \times 10^{-8} \text{ Am}^2/\text{g}$  after demagnetisation to 50 mT.

Specimens taken from the kiln wall were plotted as a function of azimuth (Figs. 6.3, 6.4). It was found that declination showed some sinusoidal dependence on azimuth for levels B and C. Most specimen declinations on the East side of the kiln plotted westward, some of those on the West side plotted eastward, but this was not the case for all specimens e.g. specimen 12B, (Table 6.1). Specimen declinations at azimuthal positions  $0^\circ$  and  $180^\circ$  were more consistent with each other and with the present Earth's magnetic field. Inclinations generally showed little variation with azimuth, whilst comparison of inclinations from the North and South sides showed that they were not consistently different.

Declinations from the outer surface (level A) however showed no clear pattern and less directional variation with azimuth, notably declinations trending East on the East side unlike other depths. Specimen inclinations for this level were largely consistent with each other and with the present Earth's Magnetic Field (Fig 6.4). Taking specimen 1B as a reference the angular separation (solid angle) of it from the other level B specimens was

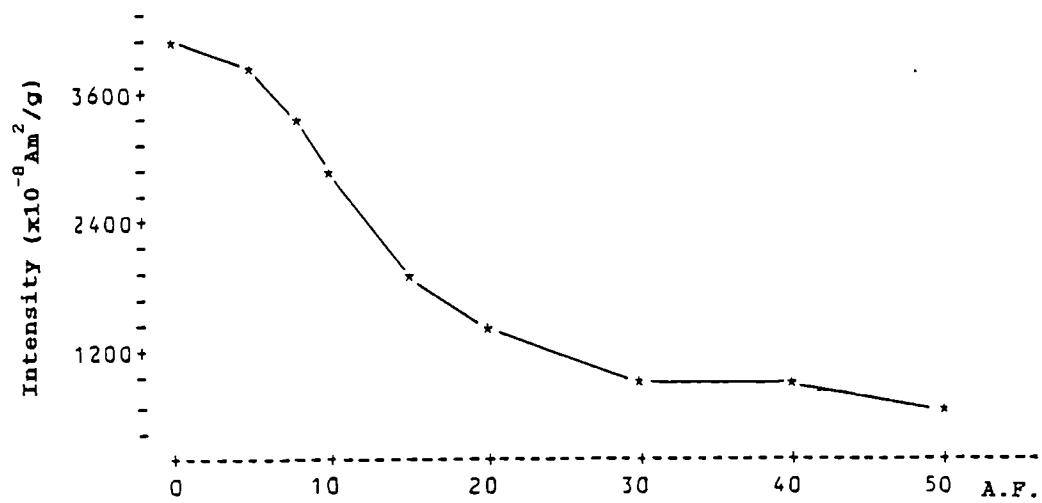


Figure 6.2d Intensity as a function of A.F. (Specimen 1c).

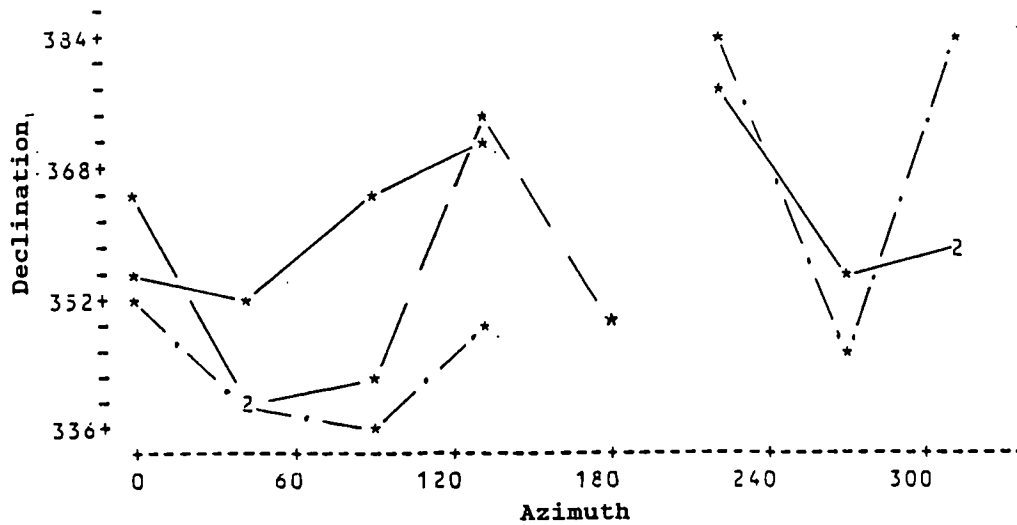


Figure 6.3 Declination as a function of azimuth  
(core specimens).

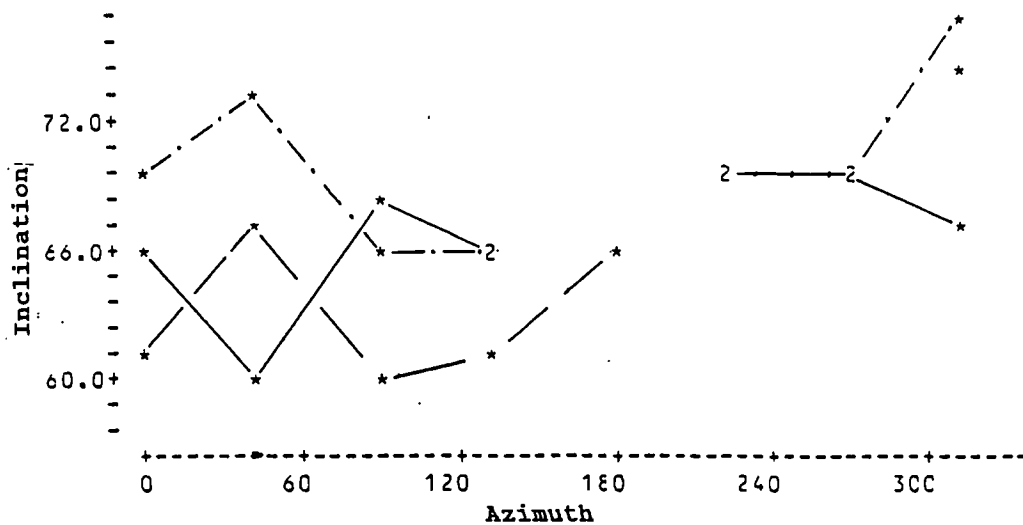


Figure 6.4 Inclination as a function of azimuth  
(core specimens).

Key for core specimen magnetic properties as a function of azimuth:

A = \_\_\_\_\_

B = -.-.-.-.-

C = -----

calculated and plotted against azimuth (Fig. 6.5). Unfortunately specimen 9b was damaged during cutting, but there was only a  $4^{\circ}$  angular separation between specimens at  $0^{\circ}$  and  $135^{\circ}$ . However the angular separation of  $0^{\circ}$  and  $180^{\circ}$  sub-specimens, mentioned later, was only  $3^{\circ}$  (specimens 1.2 and 9.2).

Magnetic intensities and initial susceptibilities showed the greatest variation for level C (Figs. 6.6, 6.7). There appeared to be a relationship between higher magnetic intensities for level C and the presence of stokeholes ( $0^{\circ}$ ,  $140^{\circ}$ , though not at  $230^{\circ}$ ). Levels B and A respectively showed greater similarity in magnetic intensities although the magnetic intensity of level B was normally higher than A for any one azimuthal location. This can be best seen by reference to Table 6.1. There did not appear to be any obvious systematic relationship between azimuth, intensity, and / or susceptibility, apart from level C.

Floor specimen declinations and inclinations were plotted against their location along the floor diameter (Figs 6.8, 6.9). Declinations were found to show an oscillating pattern across the floor, whilst inclinations showed less variation. Comparison of mean inclinations from the floor with the wall showed a  $1.6^{\circ}$  difference,



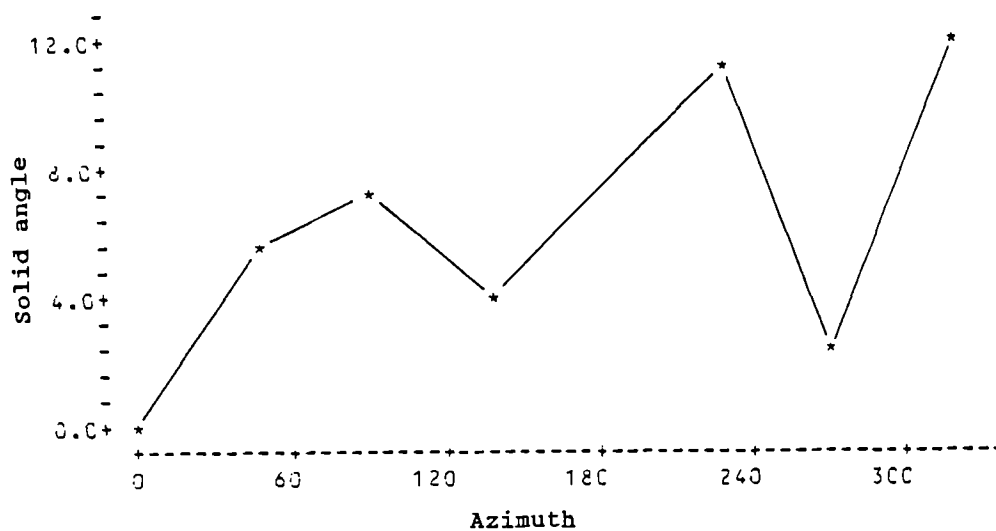


Figure 6.5 Solid angle as a function of azimuth (core specimens). Specimen b

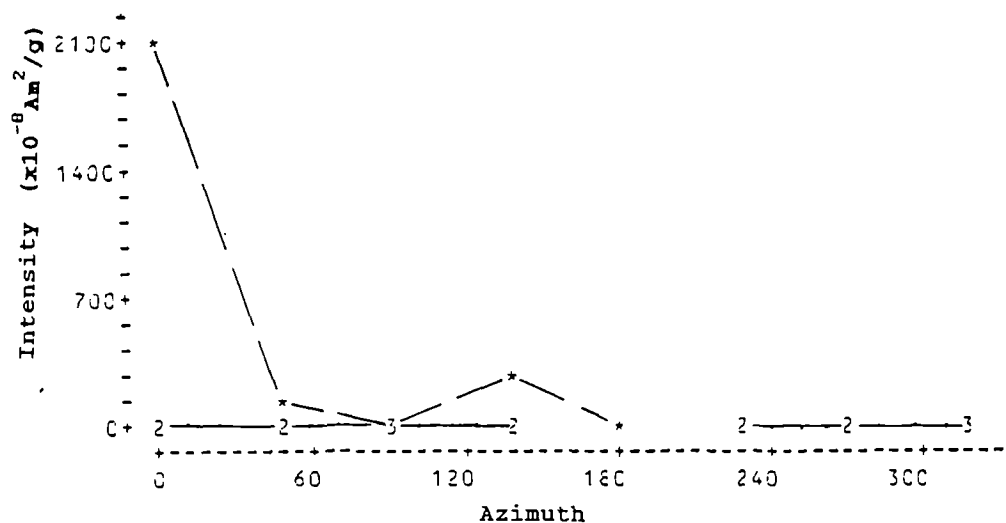


Figure 6.6 Intensity as a function of azimuth (core specimens).

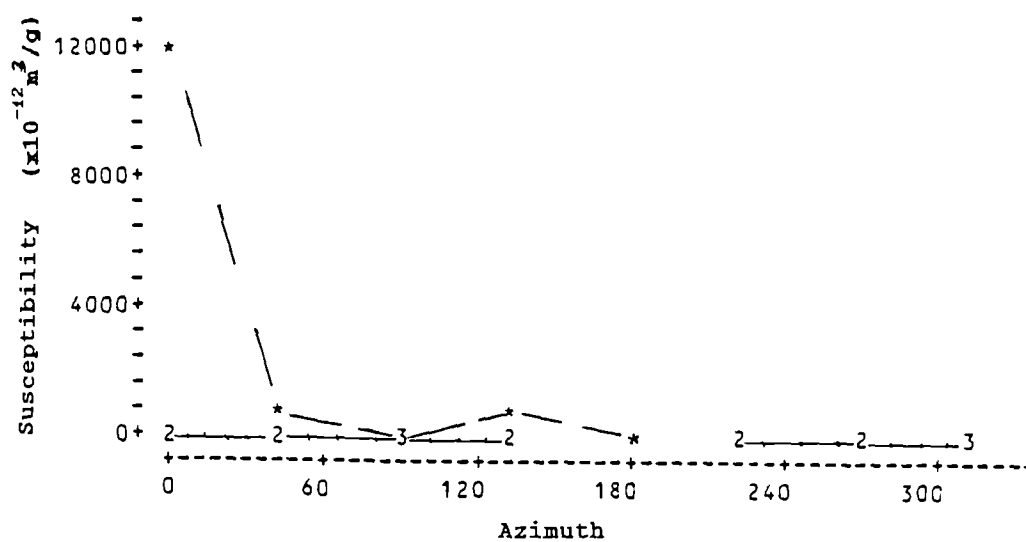


Figure 6.7 Susceptibility as a function of azimuth (core specimens).

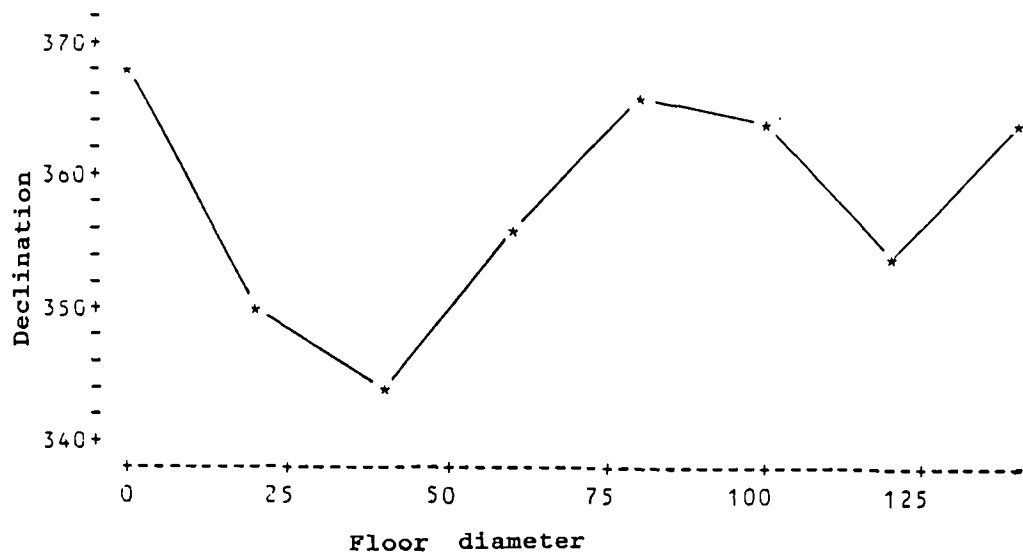


Figure 6.8 Declination as a function of floor diameter.

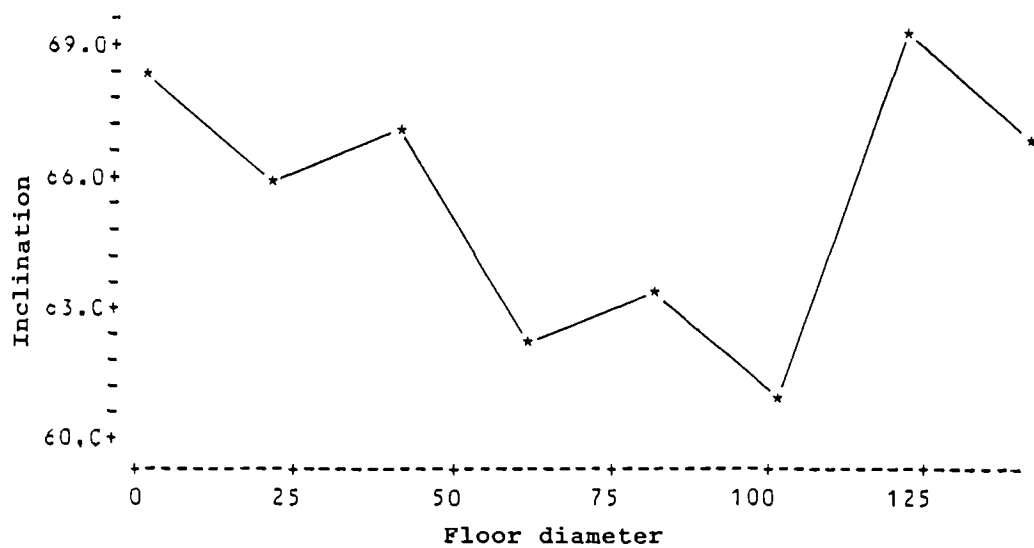


Figure 6.9 Inclination as a function of floor diameter.

those of the floor being slightly shallower than those from the wall.

When the most stable magnetic directions for each layer were plotted separately on a stereographic projection it was found that the outer surface specimen magnetic directions, although individually less well defined than for other layers, showed similar magnetic directions consistent with the present Earths Magnetic Field (Fig 6.10). The magnetic directions for the inner part of the wall were individually well defined, but showed a greater degree of directional scatter than for the outer surface (Figs 6.11). The magnetic directions for the inner surface were also well defined statistically but showed an even greater degree of directional scatter than B (Fig 6.12). The magnetic directions for the floor however showed minimal scatter (Fig. 6.13). Mean magnetic directions were calculated for all floor specimens, and for levels A, B and C respectively. These were plotted on equal angle stereographic projections showing the secular variation curve (Figs 6.14, 6.15, 6.16 and 6.18). Correction of specimen directions to a central location was unnecessary as the site lay within 20 km of Meriden. Level A was the statistically best defined of the wall specimens and consistent with the present Earths

# LUNT KILN, CORE SPECIMENS.

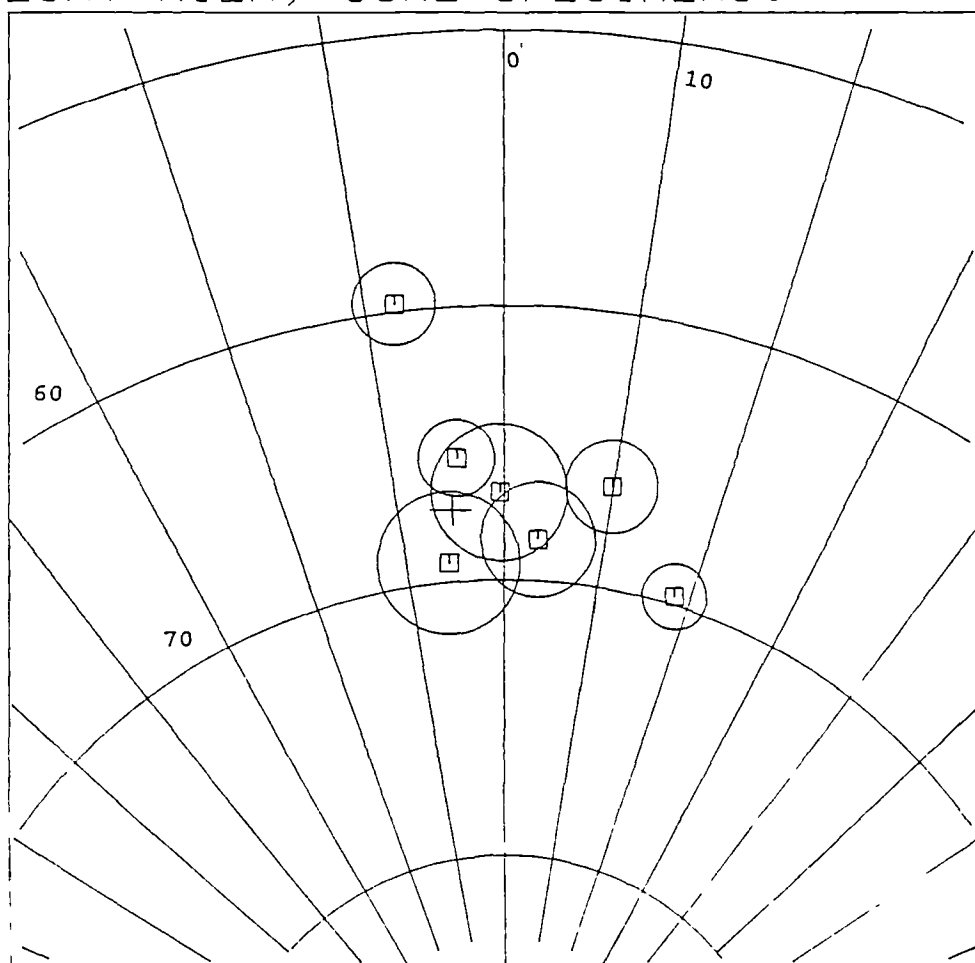


Figure 6.10 Stereoplot of level A specimen magnetic directions.

# LUNT KILN, CORE SPECIMENS.

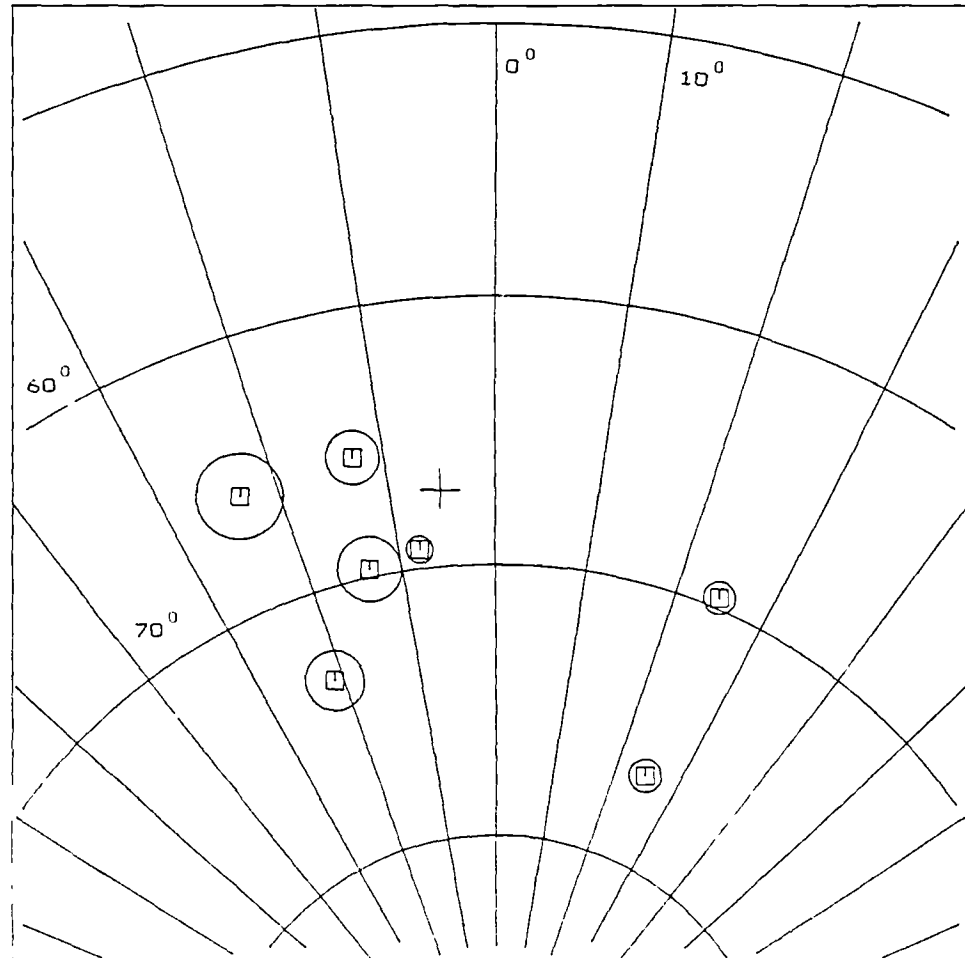


Figure 6.11 Stereoplot of level B specimen  
magnetic directions.

# LUNT KILN, CORE SPECIMENS.

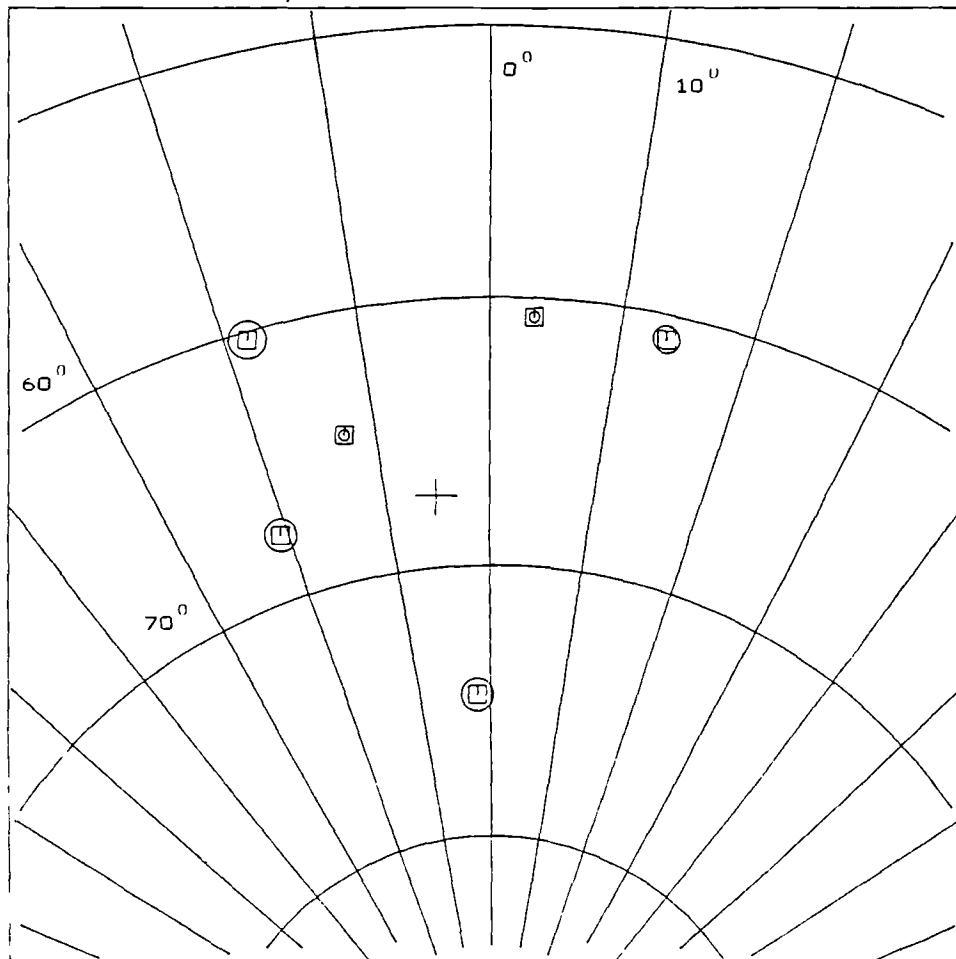


Figure 6.12 Stereoplot of level C specimen  
magnetic directions.

# LUNT KILN, CORE SPECIMENS.

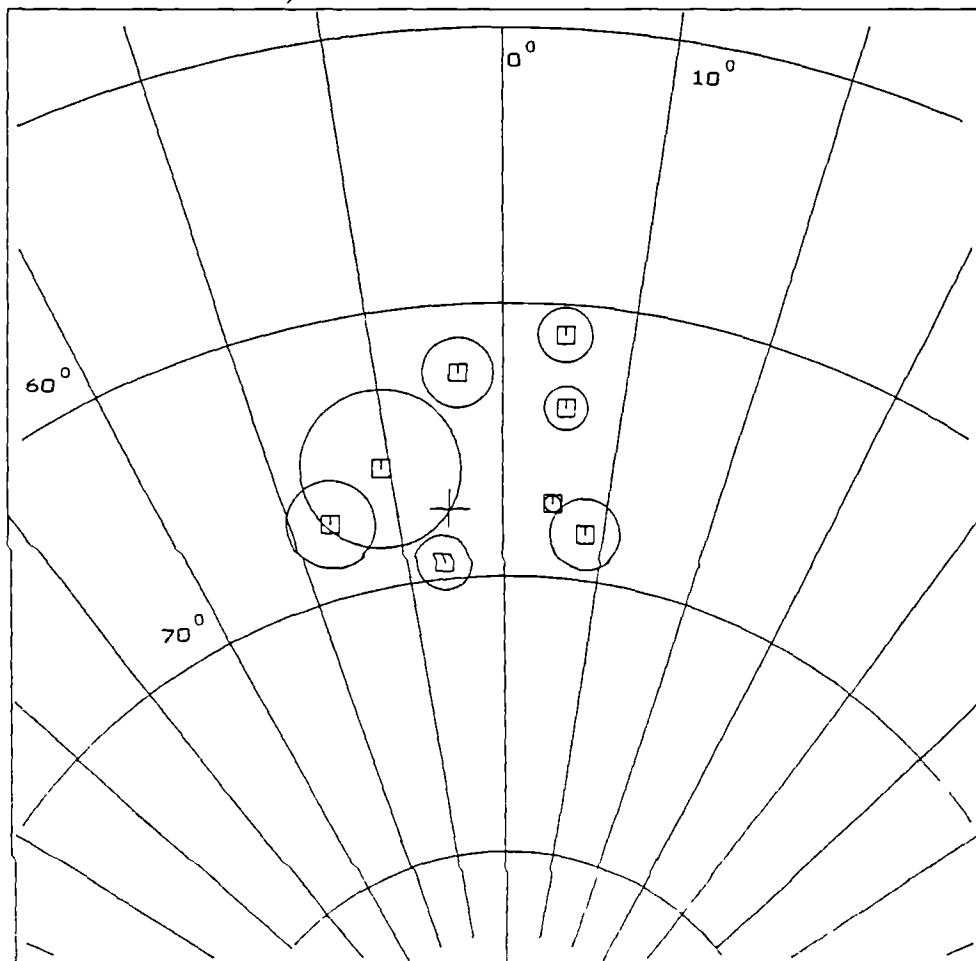


Figure 6.13 Stereoplot of floor core specimens .



MEAN OF ALL LEVEL A CORE SPECIMENS.

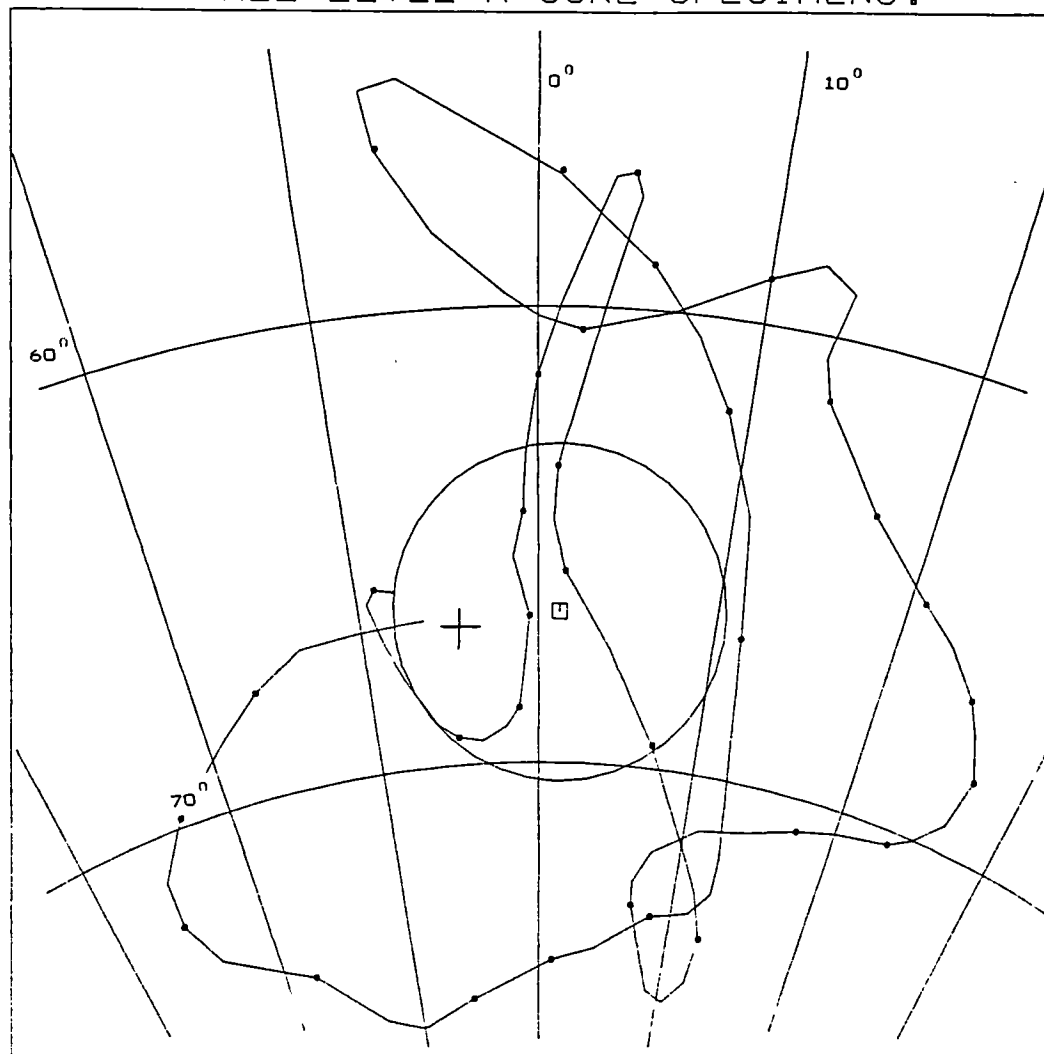


Figure 6.14

MEAN OF ALL LEVEL B CORE SPECIMENS.

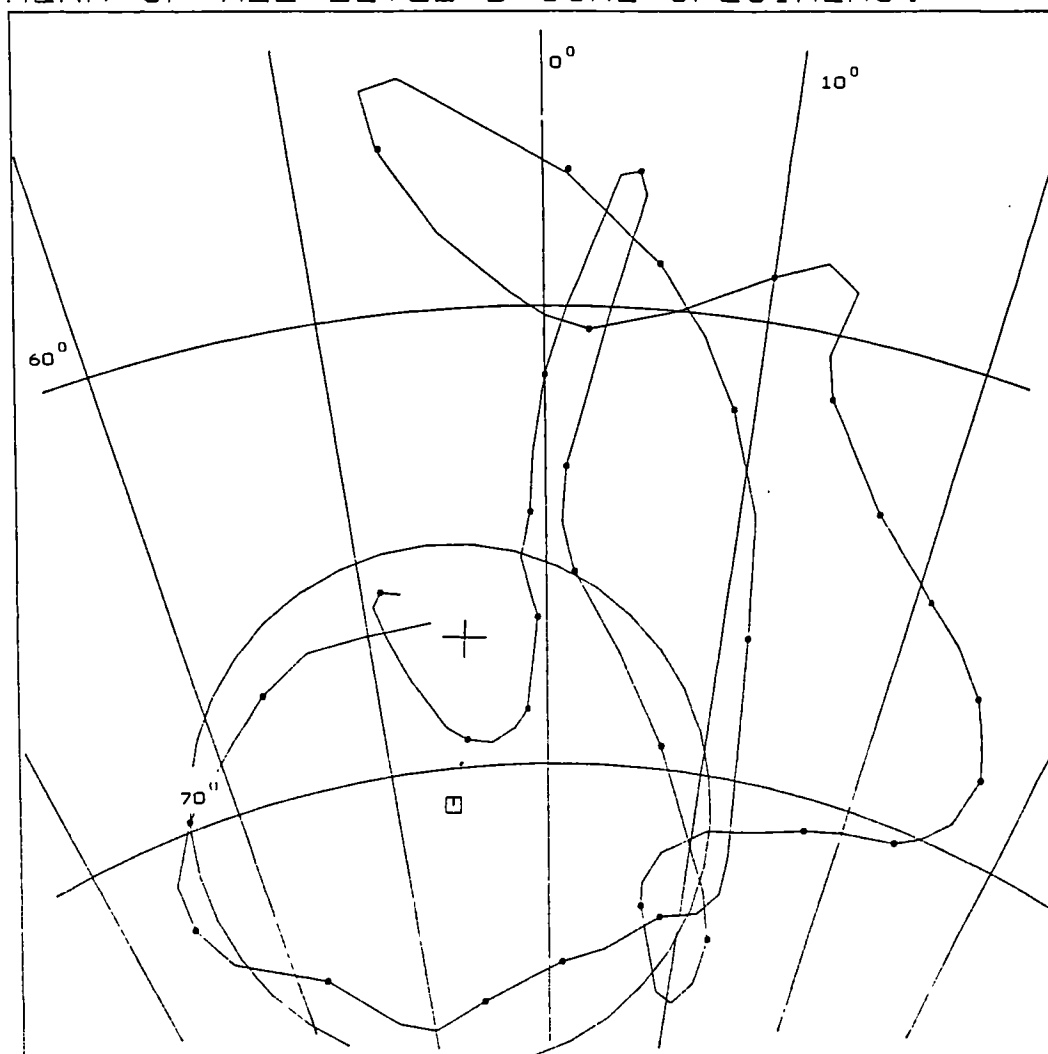


Figure 6.15

MEAN OF ALL LEVEL C CORE SPECIMENS.

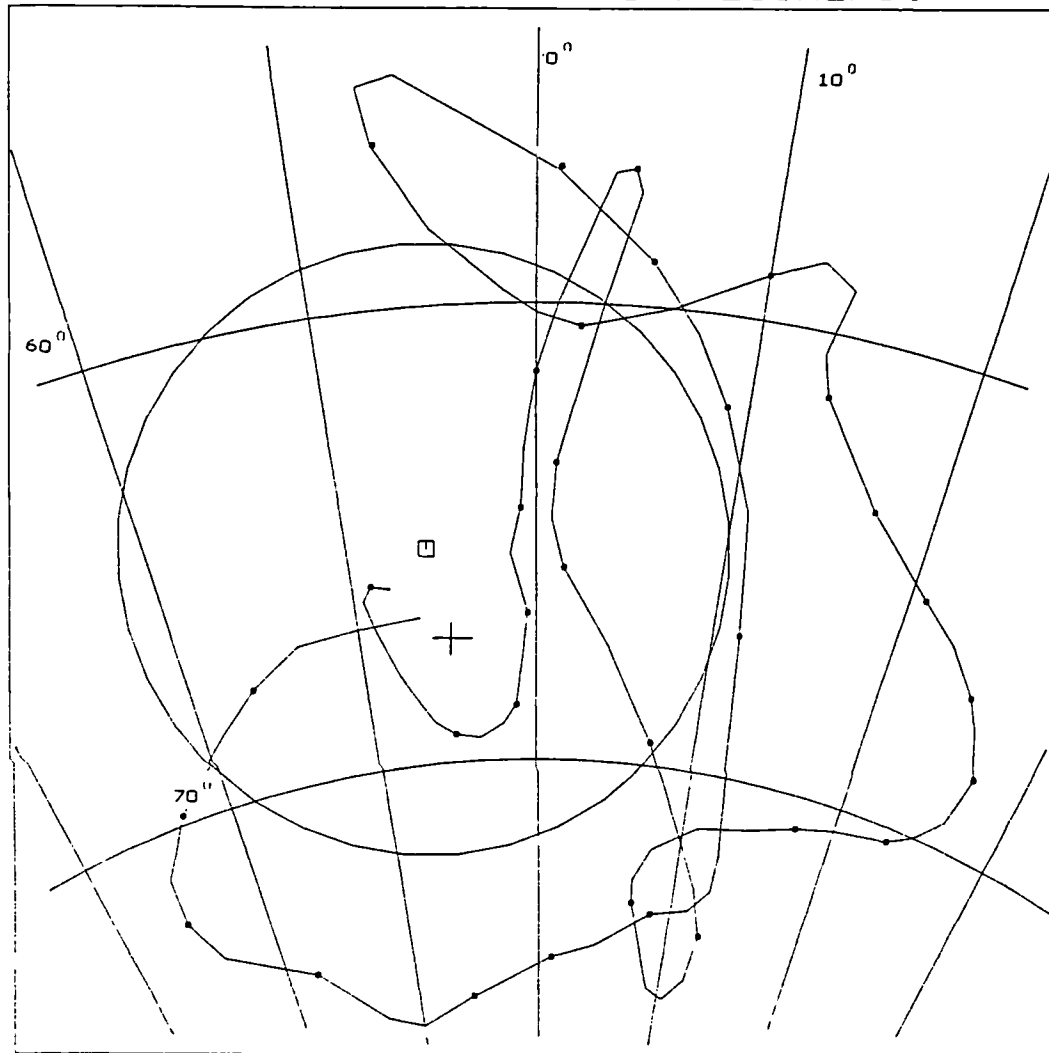


Figure 6.16

OVERALL MEAN OF ALL CORE SPECIMENS.

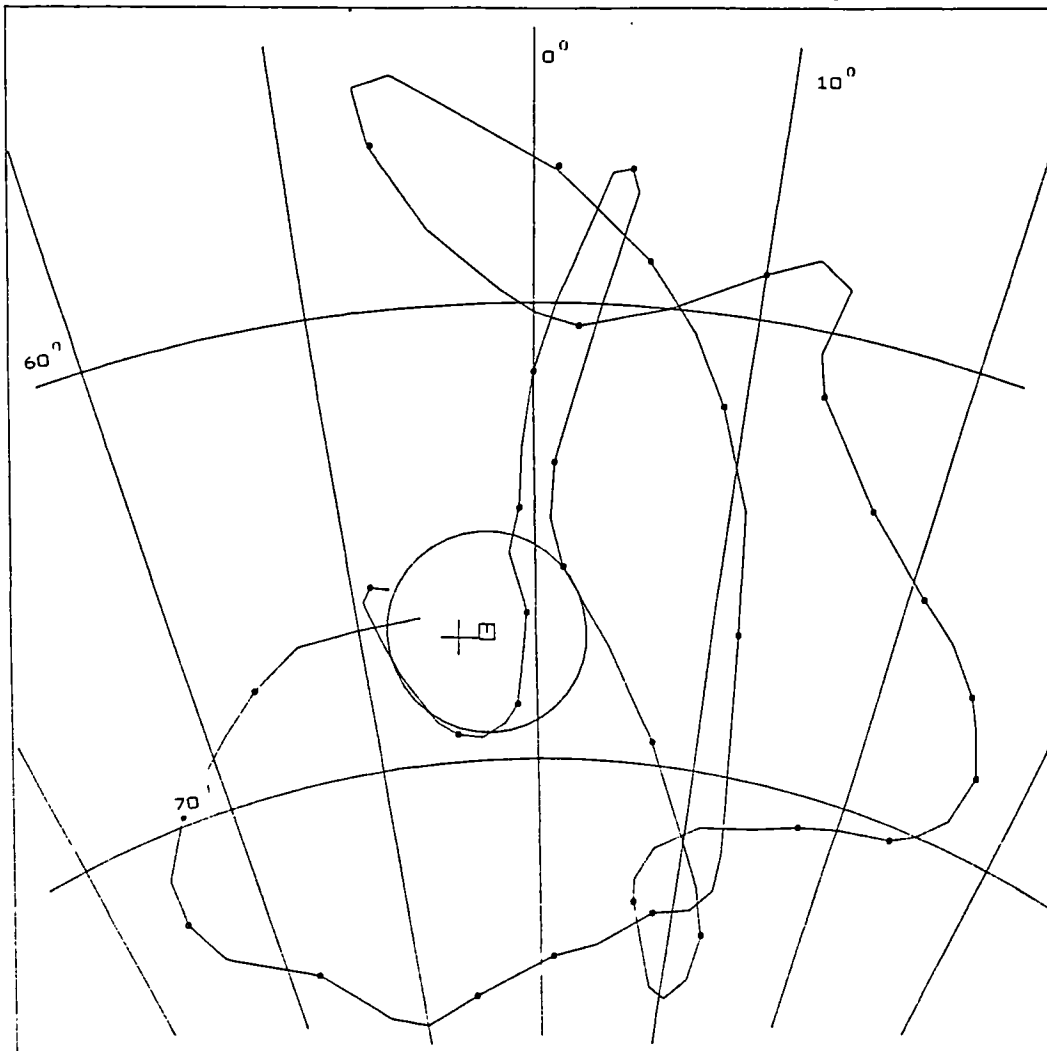


Figure 6.17

MEAN OF ALL CORE FLOOR SPECIMENS.

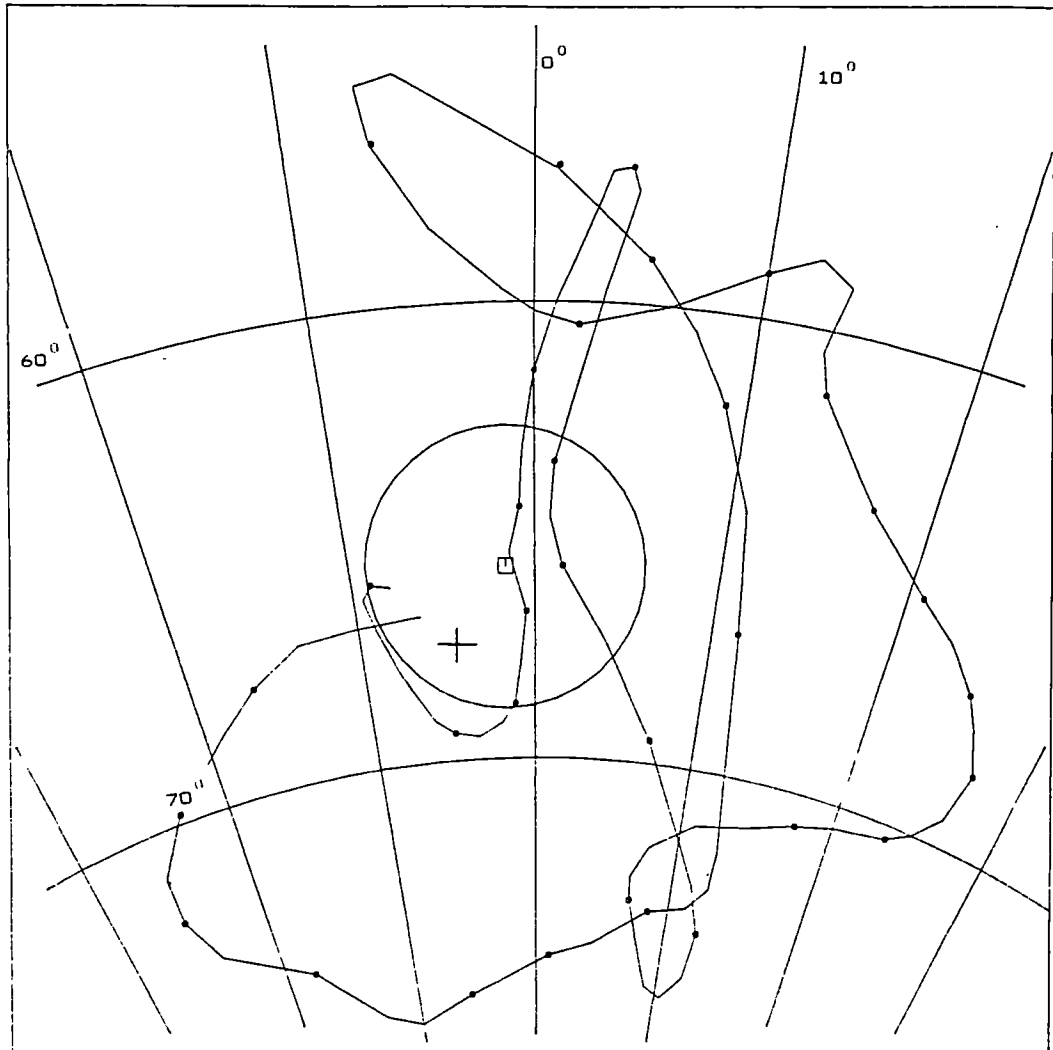


Figure 6.13

magnetic field for the site locality. Levels B and C were less well defined but the observed means were consistent with level A at the 95% confidence level. The circle of confidence of level C specimens showed the greater degree of directional scatter at this depth into the kiln wall. Nevertheless the overall mean of all specimens (Fig. 6.17), the mean of the floor specimens (Fig. 6.18), the mean of the kiln wall specimens (Fig. 6.19), and the level A specimens were similar when plotted.

Magnetic intensities and susceptibilities, showed a tendency to increase through the kiln wall at any one azimuthal location (Fig. 6.20-6.22), although the magnitude of these changes was variable, particularly for those specimens from the inner surface of the wall (Table 6.1). Magnetic directions (dec. and inc.) also showed a variation with depth - declinations on the West trending East and vice versa (6.23, 6.24). Inclinations showed less variation but were least similar to each other at 4cm and 6cm depth into the kiln wall (Fig. 6.25, 6.26). Taking specimen 5A as the reference the angular separation of it from 5B and 5C was calculated. This showed that the outer specimen direction was increasingly dissimilar to those at greater depth (there was a  $12^{\circ}$  separation of 5A and 5C; Fig. 6.27). This confirmed the general, though not

OVERALL MEAN OF ALL KILN WALL CORE SPECIMENS.

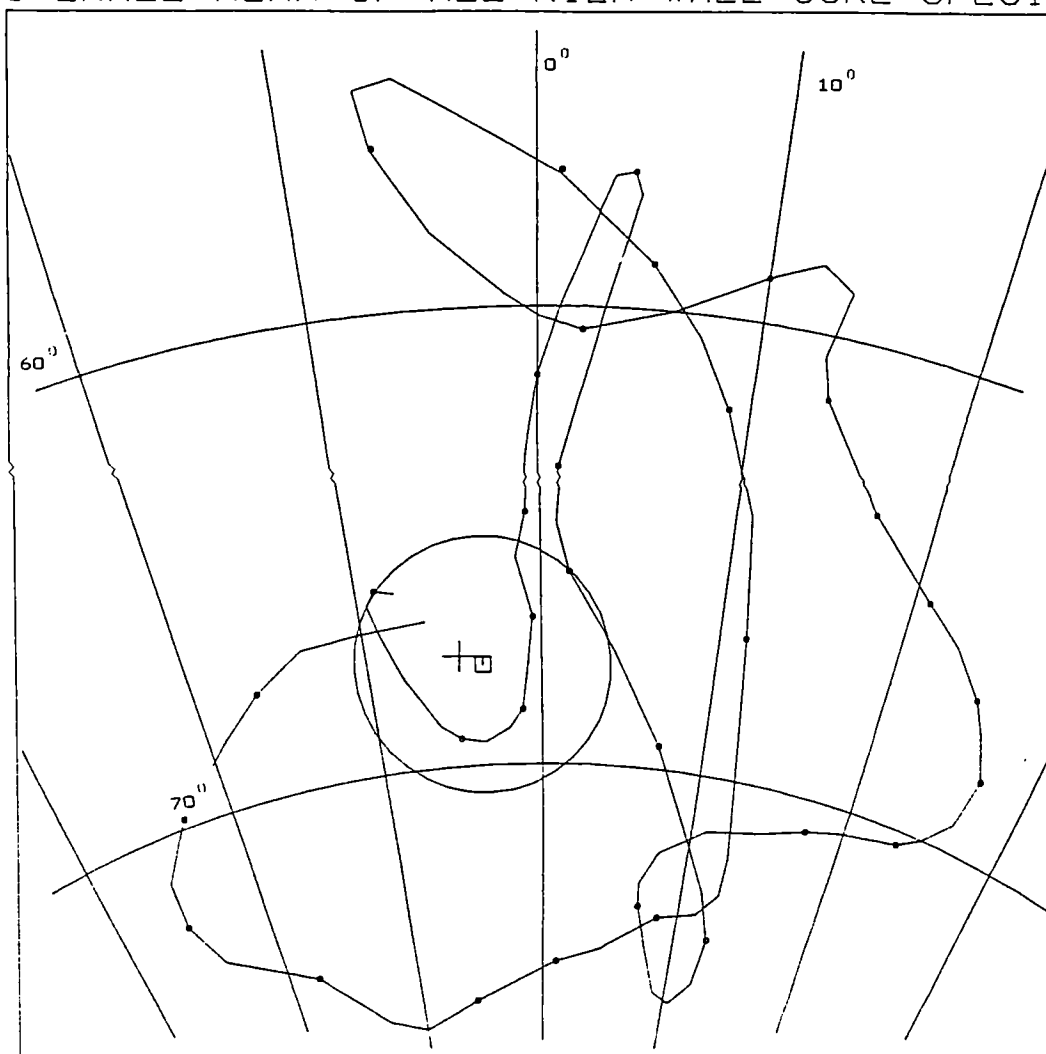


Figure 6.19

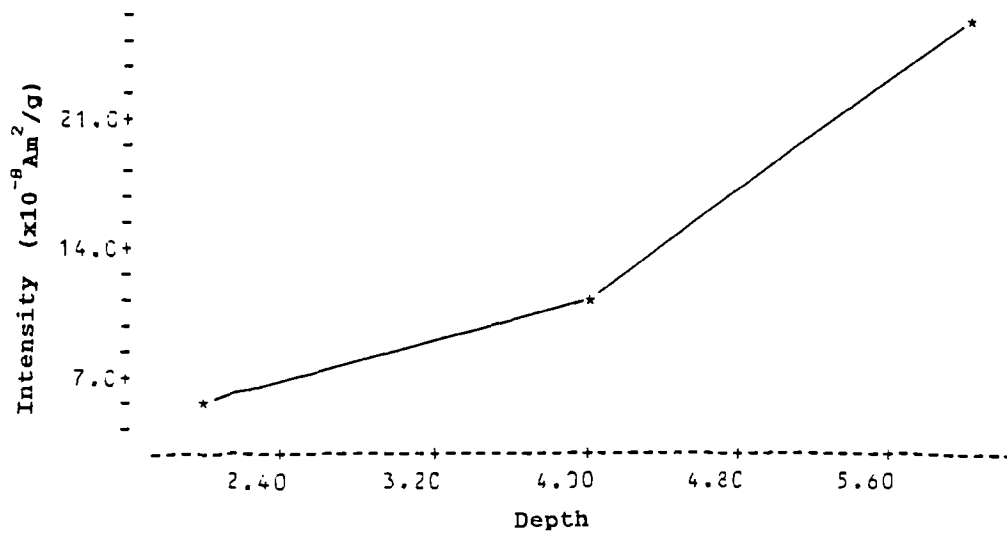


Figure 6.20 Intensity as a function of depth into  
kiln wall (core specimens). Specimen 5

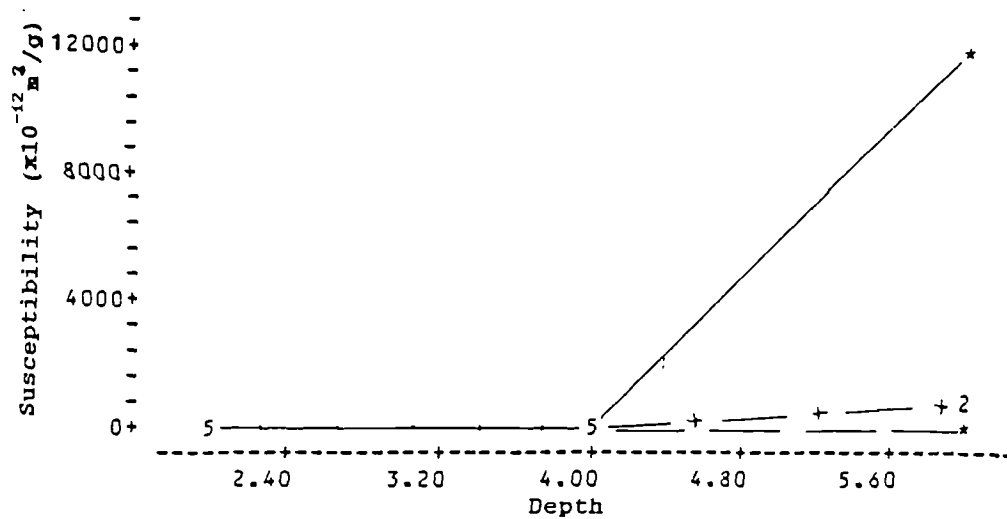


Figure 6.21 Susceptibility as a function of depth into  
kiln wall (core specimens).  
East side.

Key for core specimen magnetic properties as a function of depth  
into kiln wall (East side):

Specimen 1 ( $0^\circ$ ) = \_\_\_\_\_

Specimen 3 ( $45^\circ$ ) = -.-.-.-.-

Specimen 5 ( $90^\circ$ ) = -----

Specimen 7 ( $135^\circ$ ) = -+--+--+--

Specimen 9 ( $180^\circ$ ) = ->->->->-



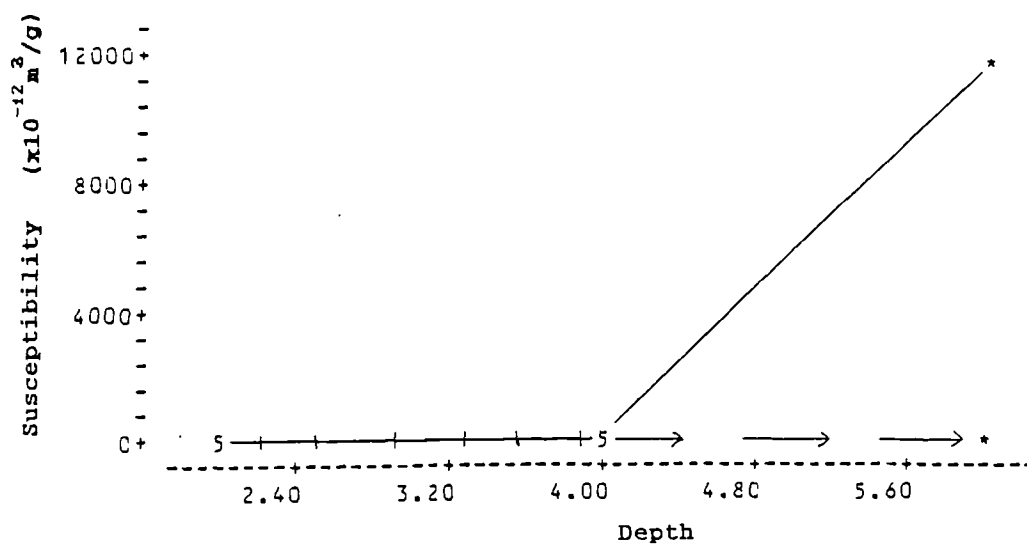


Figure 6.22 Susceptibility as a function of depth into Kiln wall (core specimens).

West side.

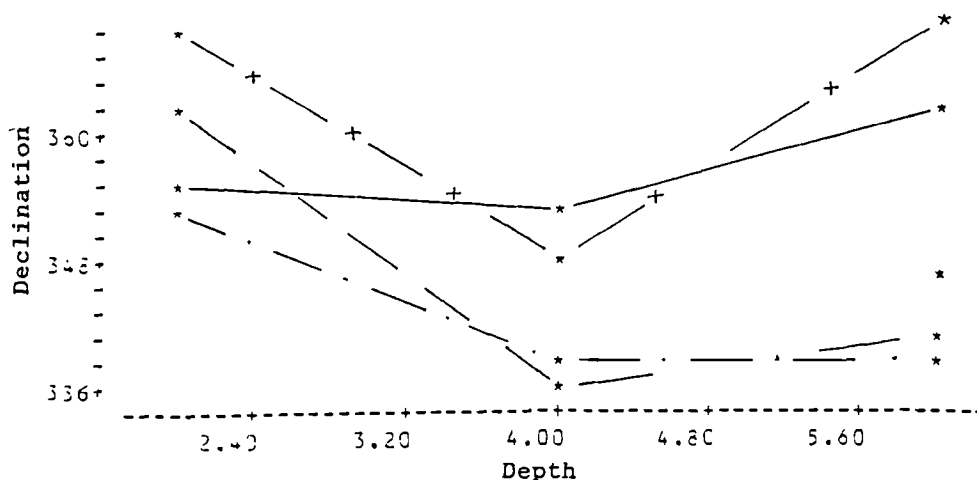


Figure 6.23 Declination as a function of depth into kiln wall (core specimens).

East side.

Key for core specimen magnetic properties as a function of depth into kiln wall (West side):

Specimen 1 ( $0^{\circ}$ ) = \_\_\_\_\_

Specimen 9 ( $180^{\circ}$ ) = ->->->->-

Specimen 10 ( $225^{\circ}$ ) = I—I I—I

Specimen 12 ( $270^{\circ}$ ) = .....

Specimen 16 ( $315^{\circ}$ ) = ---> --->

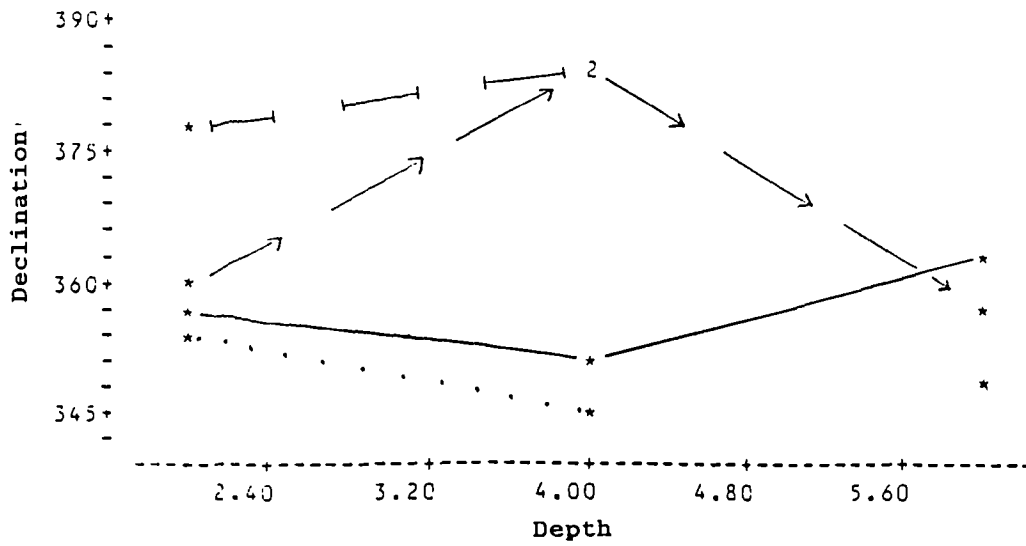


Figure 6.24 Declination as a function of depth into kiln wall (core specimens).

West side.

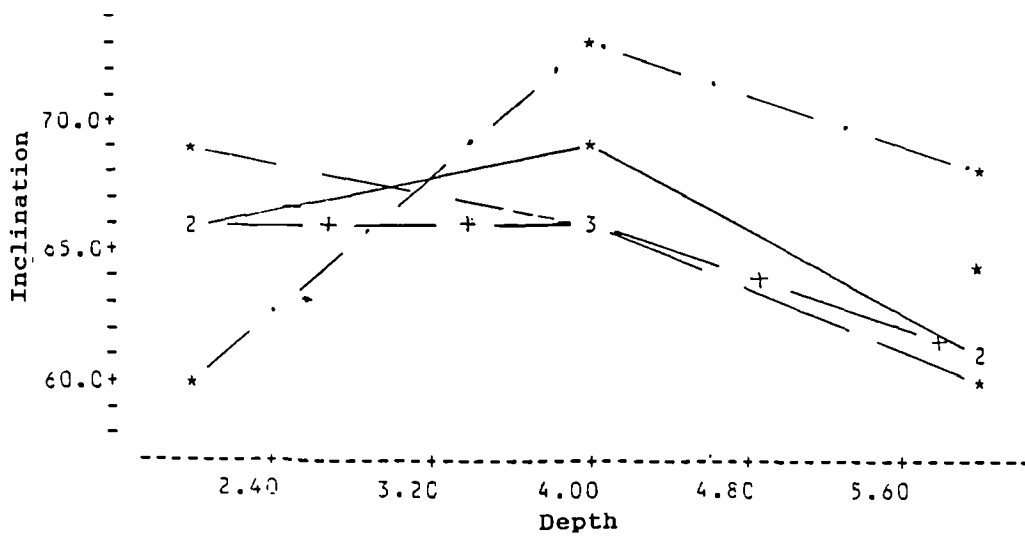


Figure 6.25 Inclination as a function of depth into kiln wall (core specimens).

East side.

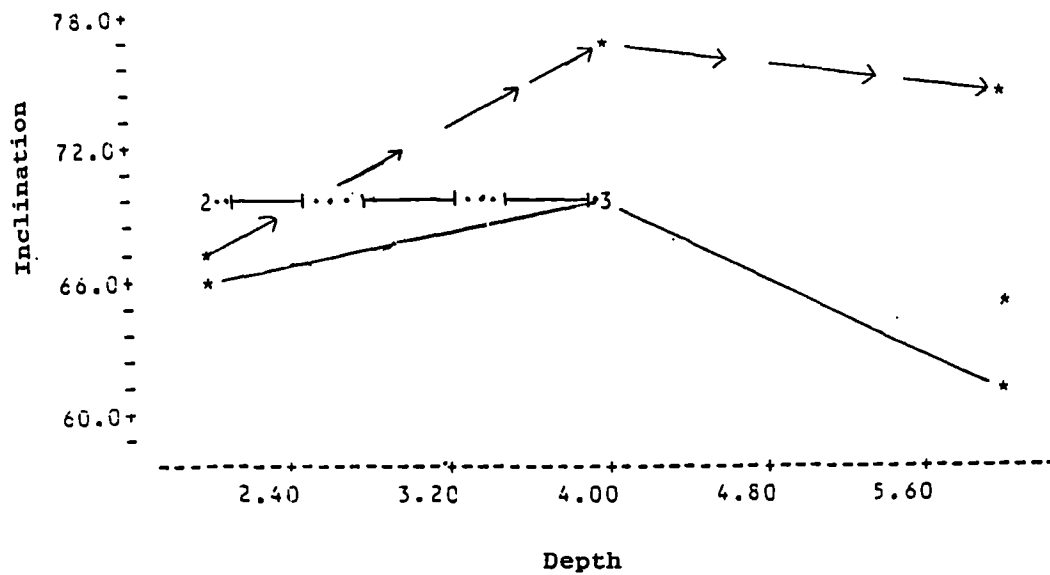


Figure 6.26 Inclination as a function of depth  
into kiln wall (core specimens).  
West side.

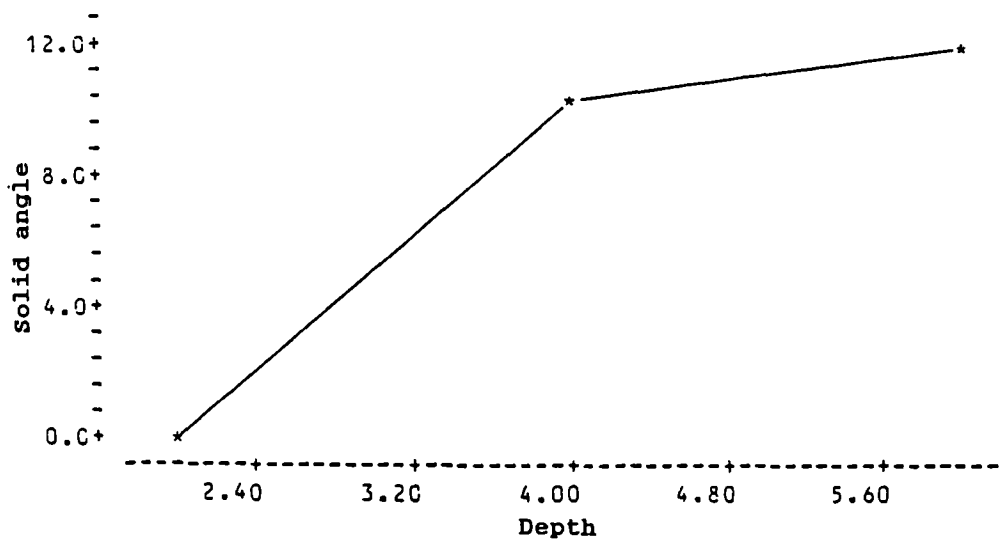


Figure 6.27 Solid angle as a function of depth  
into kiln wall (core specimens).  
Specimen 5

consistent pattern of increased dissimilarity of the outer specimen directions with the inner as seen in declination.

Clearly there is a coincidence between higher intensities, susceptibilities and the magnitude of magnetic directional deviation in many of the specimens at individual azimuthal locations. (Higher magnetic intensities and susceptibilities correlating in some cases with greater directional scatter). However the ratio of intensity to susceptibility for cores 1 and 3 showed no 1:1 relationship. Therefore although there was a coincidence in some cases between greater directional scatter and other magnetic properties, the magnetic dispersion of the inside of the kiln wall must be at least partially due to factors other than the concentration/type of magnetic mineral present and/or the grain size of the magnetic particles. When the inner surface specimen intensities were compared, the greater dispersion of some specimen directions from level C were found to be associated with a range of magnetic intensities, although some directions were similar to the 1985 geomagnetic field direction (Table 6.1). This suggested that the magnetic directional deviations observed were not precisely related to the magnitude of intensity, although the latter may also be related to azimuthal position.

#### 6.4. Magnetic properties of the sub-specimens.

The core specimens previously described were cut again at 1cm intervals using a brass hacksaw in order to define in more detail the pattern observed in the magnetic properties from the kiln. They were then demagnetised again at 50 mT in order to remove any viscous magnetisations and measured ten times. The most repeatable directions were then tabulated and plotted (Table 6.2).

The sub-specimen magnetic properties (Dec., Inc., and mean intensities) were plotted against azimuth and depth through the wall, as previously undertaken on the 2cm cores. Specimen declinations showed a sinusoidal pattern when plotted against azimuth except for the 1cm depth specimens (Fig. 6.28). The latter were consistent with the present geomagnetic field, as were most of the declinations at  $0^{\circ}$  and  $180^{\circ}$  irrespective of depth through the kiln wall. The inclinations were not consistently different between the northern and southern walls either (Table 6.2). Inclinations were generally similar to each other when plotted against azimuth although the 1cm depth specimens showed much greater variation than for other depths (Fig. 6.29). A sample of these magnetic directional differences was plotted as a solid angle according to

Table 6.2

Sub-specimen directions defined by  
repeated measurement (ten times) at 50 mT.

Specimen	Dec	Inc	Int	$\alpha_{95}$	S.I.	Range
			$\times 10^{-8} \text{ Am}^2/\text{g}$			
1.1	352.6	65.8	9.7	3.2	5.6	0-9
1.2	348.7	66.3	13.7	2.3	8.0	1-6
1.5	344.8	71.6	68.7	1.0	18.8	0-9
1.6	1.0	63.9	1647.4	0.2	89.4	3-6
5.1	351.3	51.5	5.7	4.9	3.7	0-9
5.2	337.5	70.2	7.0	4.2	4.5	4-8
5.3	328.5	70.9	9.3	2.8	6.6	2-8
5.4	311.9	67.0	13.7	2.1	10.1	0-2
5.5	320.2	62.1	18.3	1.7	10.4	0-9
5.6	317.3	64.2	46.4	1.0	18.6	1-9
7.1	7.4	41.8	8.6	3.0	6.1	1-8
7.2	322.1	70.4	12.1	3.7	5.2	1-5
7.3	336.1	67.6	23.2	2.4	9.1	1-3*
7.4	331.4	62.5	30.3	0.9	20.6	4-9
7.5	331.3	64.1	69.4	0.5	40.7	2-7
7.6	360.0	63.5	467.8	0.2	103.2	7-9

9.1	0.3	67.7	5.8	0.7	25.1	1-9
9.2	355.8	67.6	7.0	1.3	13.7	3-9
9.3	7.4	67.1	10.0	0.3	52.5	2-9
9.4	343.6	62.6	21.7	1.0	17.8	2-8
10.1	358.9	59.7	3.1	4.1	4.4	1-9
10.2	42.0	67.1	7.0	5.0	3.6	0-8
10.3	50.6	71.0	26.3	1.2	15.1	0-8
10.4	30.4	65.8	70.8	0.4	53.9	0-2
12.1	336.3	67.6	8.6	2.3	7.8	0-8
12.2	33.4	72.1	25.4	1.0	17.5	0-9
12.3	26.8	66.5	49.3	0.5	37.2	4-7
16.1	339.4	66.8	6.3	0.8	27.6	0-2
16.2	315.0	71.5	7.9	1.4	15.2	7-9
16.3	14.3	66.9	11.1	0.6	30.1	0-6
16.4	19.6	74.6	13.1	0.5	38.3	0-5
16.5	342.3	74.4	17.9	0.2	109.5	2-5
16.6	342.7	69.3	58.6	0.2	97.3	4-8

\* = This specimen only measured four times.

Mean of 1cm depth specimens:

Dec = 354.0

Inc = 60.5

N = 7

R = 6.881

$\bar{C}_{95}$  = 8.5

K = 50.5

**Mean of 2cm depth specimens:**

Dec = 353.6	Inc = 71.9
N = 7	R = 6.884
$\sigma_{95} = 8.4$	K = 51.6

**Mean of 3cm depth specimens:**

Dec = 7.3	Inc = 70.5
N = 6	R = 5.912
$\sigma_{95} = 8.9$	K = 56.6

**Mean of 4cm depth specimens:**

Dec = 348.5	Inc = 69.0
N = 5	R = 4.894
$\sigma_{95} = 12.6$	K = 37.6

**Mean of 5cm depth specimens:**

Dec = 332.6	Inc = 68.3
N = 4	R = 3.976
$\sigma_{95} = 8.2$	K = 125.0

**Mean of 6cm depth specimens:**

Dec = 345.7	Inc = 66.3
N = 4	R = 3.963
$\sigma_{95} = 10.2$	K = 80.6



Mean of all sub-specimen magnetic directions:

Dec = 351.7

Inc = 67.9

N = 33

R = 32.364

$\alpha_{95}$  = 3.5

K = 50.3

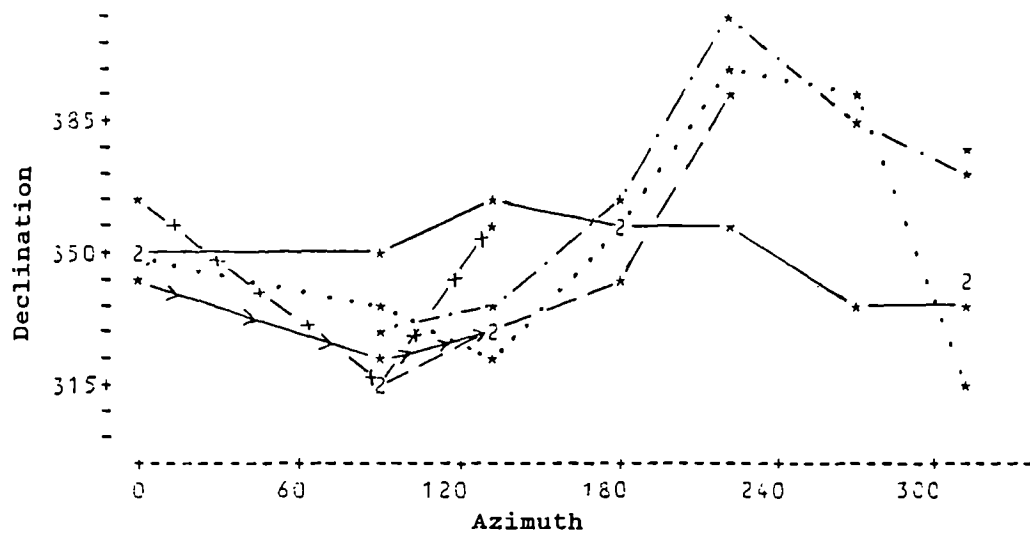


Figure 6.28 Declination as a function of azimuth (sub-specimens).

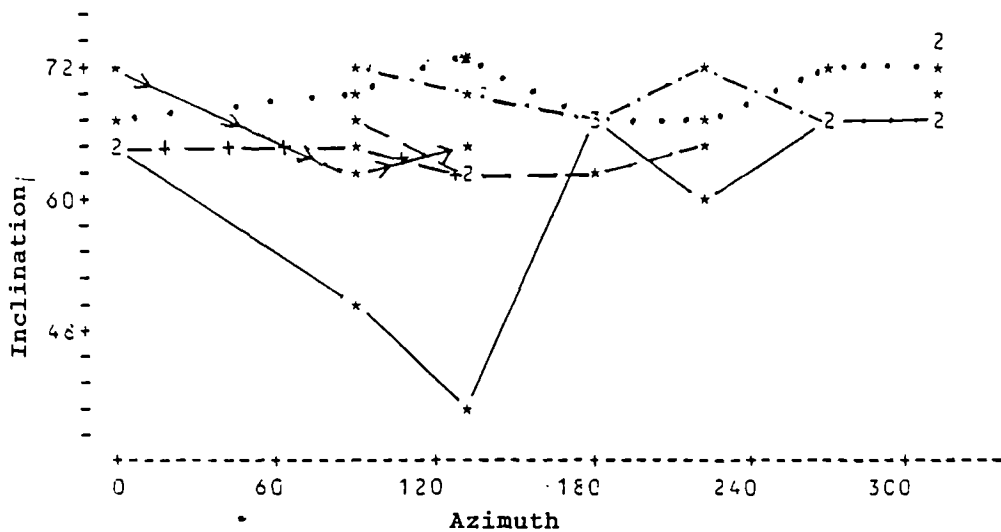


Figure 6.29 Inclination as a function of azimuth (sub-specimens).

Key for sub-specimen magnetic properties as a function of azimuth:

1cm = \_\_\_\_\_

2cm = .....

3cm = -.-.-.-.-

4cm = -----

5cm = ->-->-->-->

6cm = -+-+--+--+

azimuth which showed that there was a variation in the angular separation of specimens around the circumference of the kiln (Fig. 6.30).

Mean intensities of magnetisations at 6cm depth showed higher values for those specimens adjacent to two stoke holes at  $0^{\circ}$  and  $140^{\circ}$ . The greatest variation in intensity was also for the 6cm depth specimens (Fig. 6.31). Smaller differences in intensity for the other levels were present but were best distinguished by reference to Table 6.2.

When specimen magnetic directions were plotted on stereographic projections for different depths into the kiln wall it was observed that the specimen directions showed greater scatter with depth toward the kiln interior (Figs 6.32-6.37). Magnetic directions were most consistent at 1cm depth and at  $0^{\circ}$  and  $180^{\circ}$  positions. The magnitude of scatter was greater for the sub-specimens than the original core specimens. The observed means of each level were variable but were broadly consistent with the present geomagnetic field as most of their circles of 95% confidence overlapped with that direction and with each other (Figs 6.38-6.43). However the confidence circles were large, ( $\sigma_{95} > 8.2^{\circ}$ ) as a result of the directional scatter with depth through the kiln wall. Nevertheless the

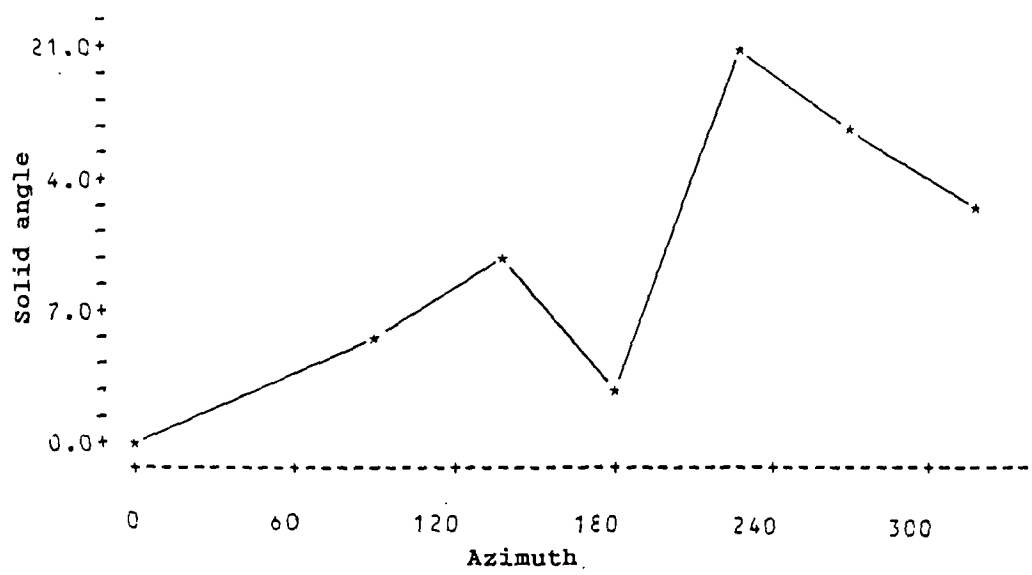


Figure 6.30 Solid angle as a function of azimuth (sub-specimens). 2cm Specimens

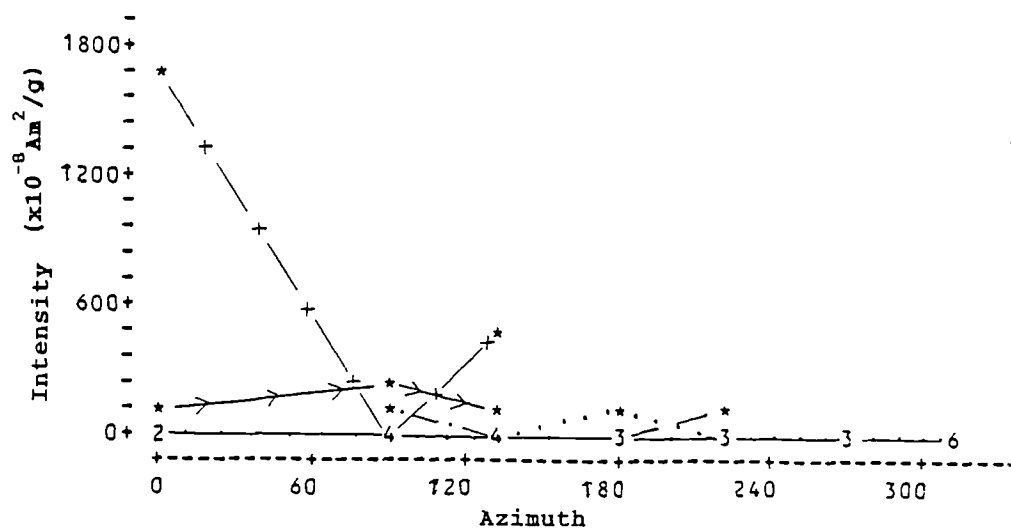


Figure 6.31 Intensity as a function of azimuth (sub-specimens).  
LUNT KILN, SUB SPECIMENS.

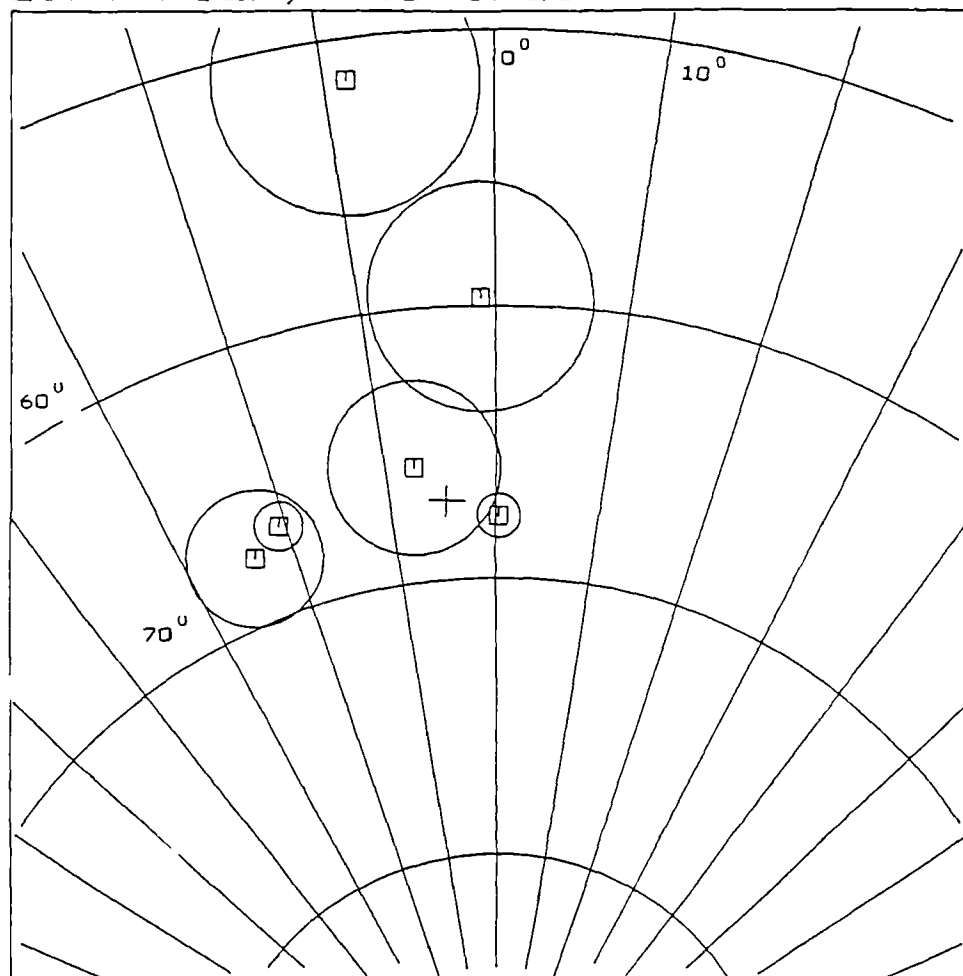


Figure 6.32 Stereoplot of 1cm depth specimen  
magnetic directions.

LUNT KILN, SUB SPECIMENS.

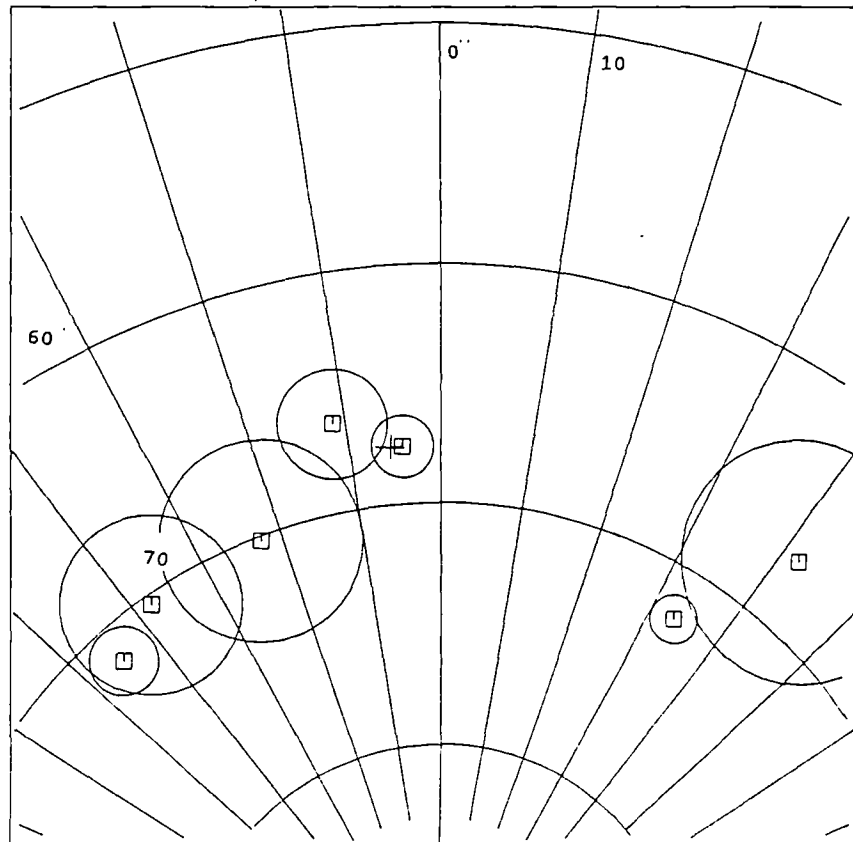


Figure 6.33 Stereoplot of 2cm depth specimen  
magnetic directions.

# LUNT KILN, SUB SPECIMENS.

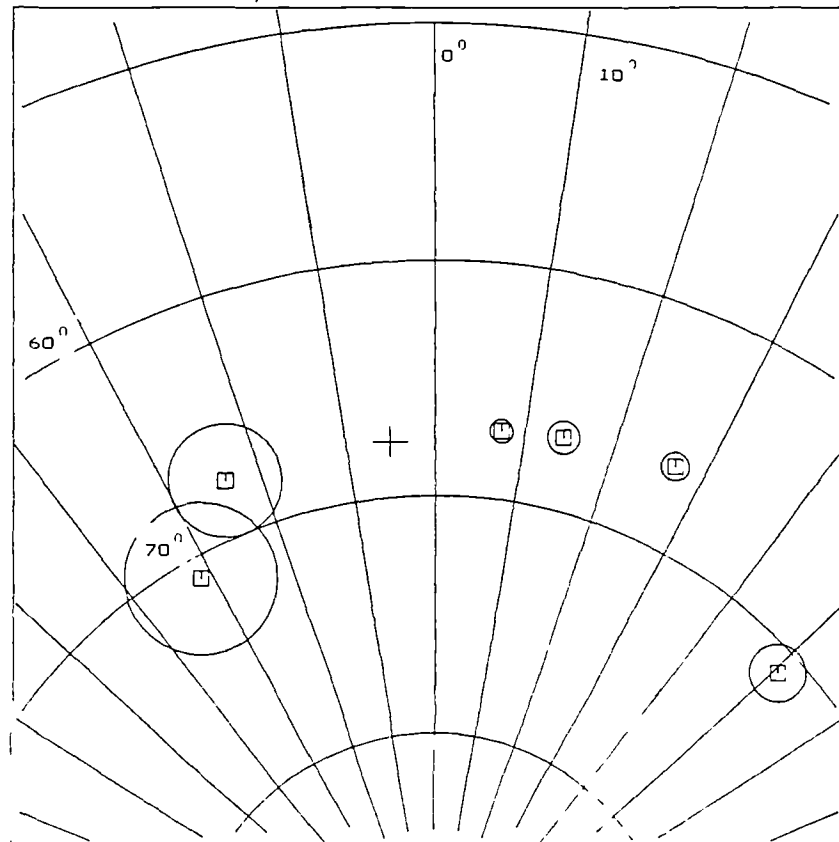


Figure 6.34 Stereoplot of 3cm depth specimen magnetic directions.

LUNT KILN, SUB SPECIMENS.

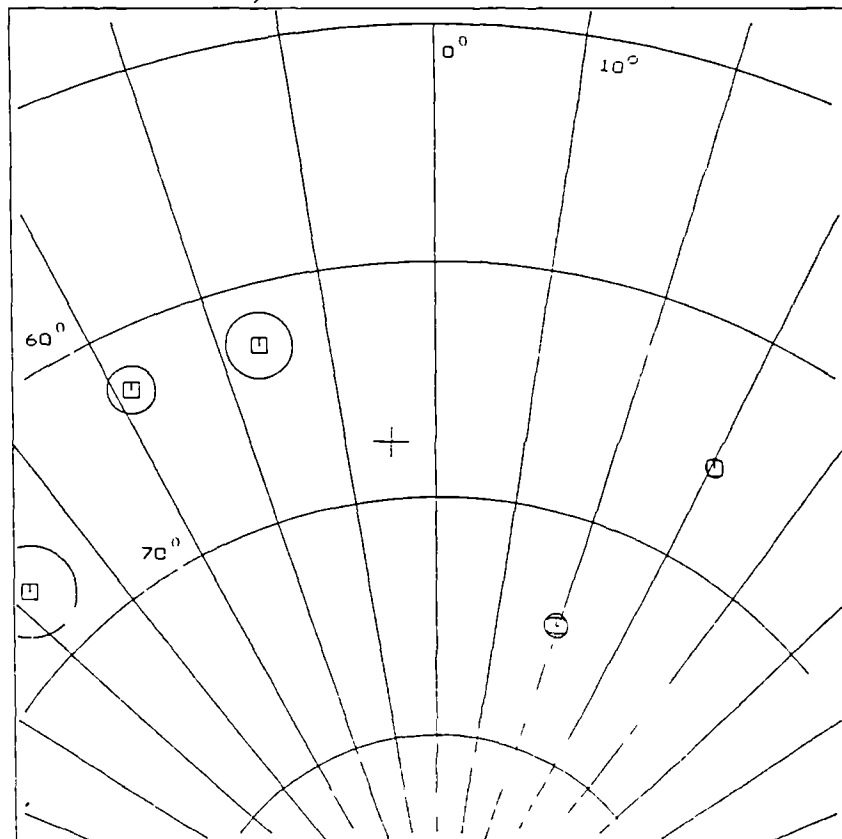


Figure 6.35 Stereoplot of 4cm depth specimen  
magnetic directions.



LUNT KILN, SUB SPECIMENS.

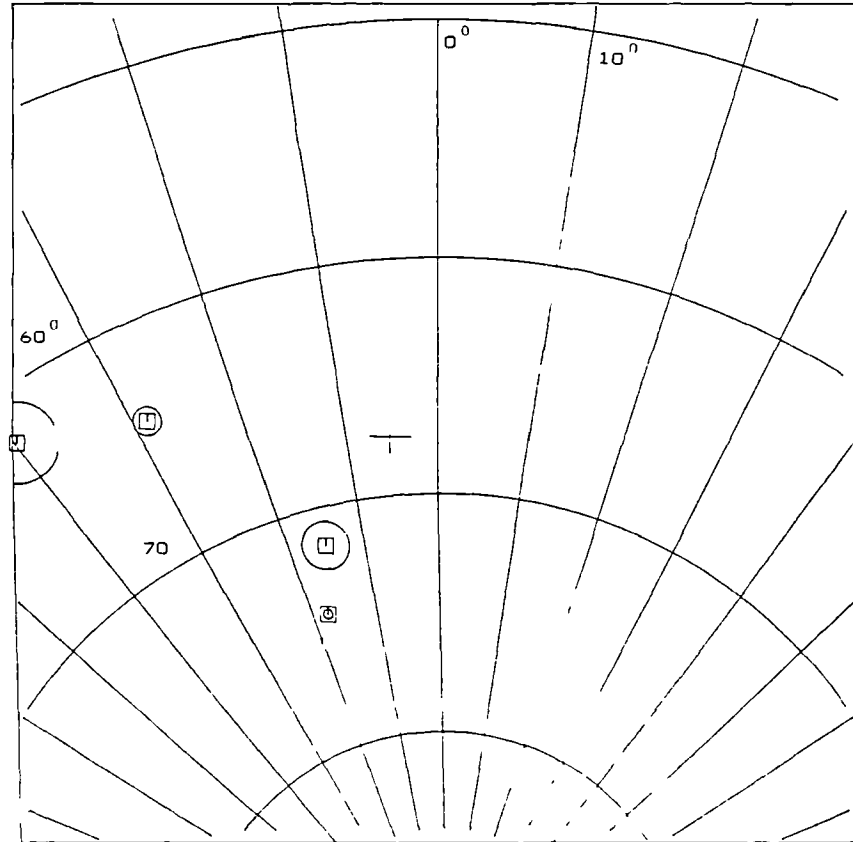


Figure 6.36 Stereonet of 5cm depth specimen  
magnetic directions.

# LUNT KILN, SUB SPECIMENS.

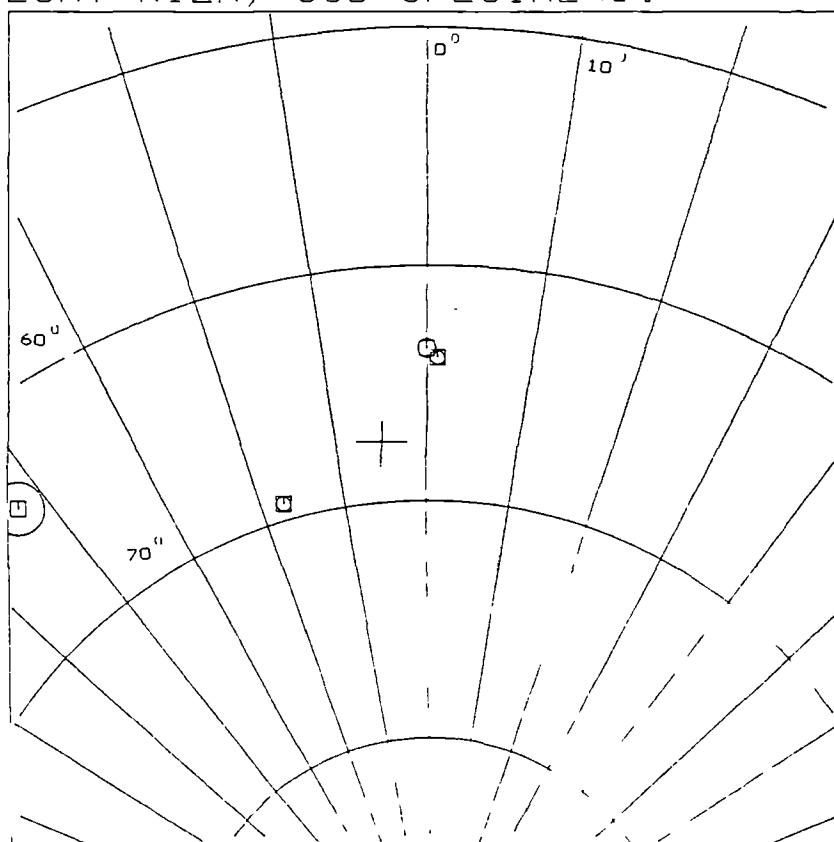


Figure 6.37 Stereoplot of 6cm depth specimen magnetic directions.

MEAN OF ALL LEVEL 1 SUB SPECIMENS.

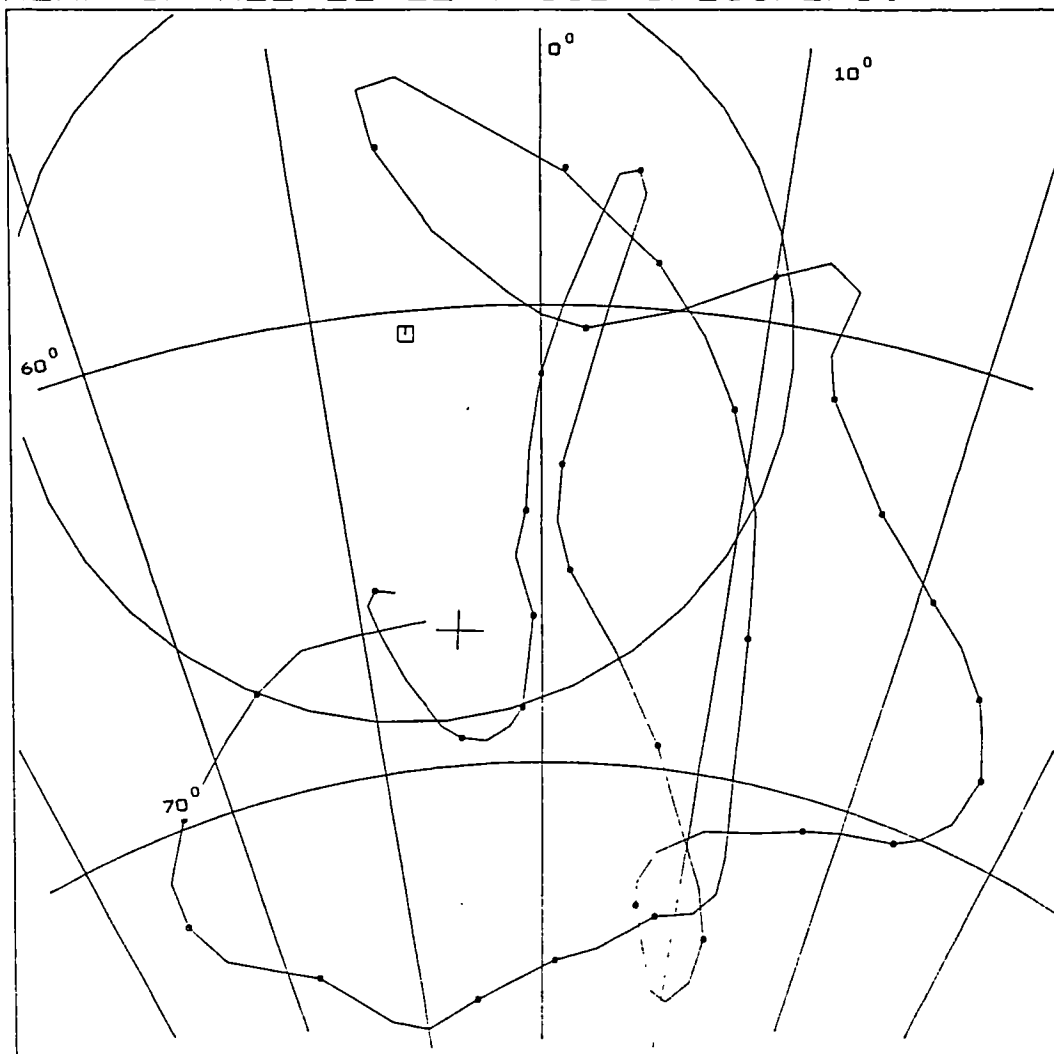


Figure 6.38

MEAN OF ALL LEVEL 2 SUB SPECIMENS.

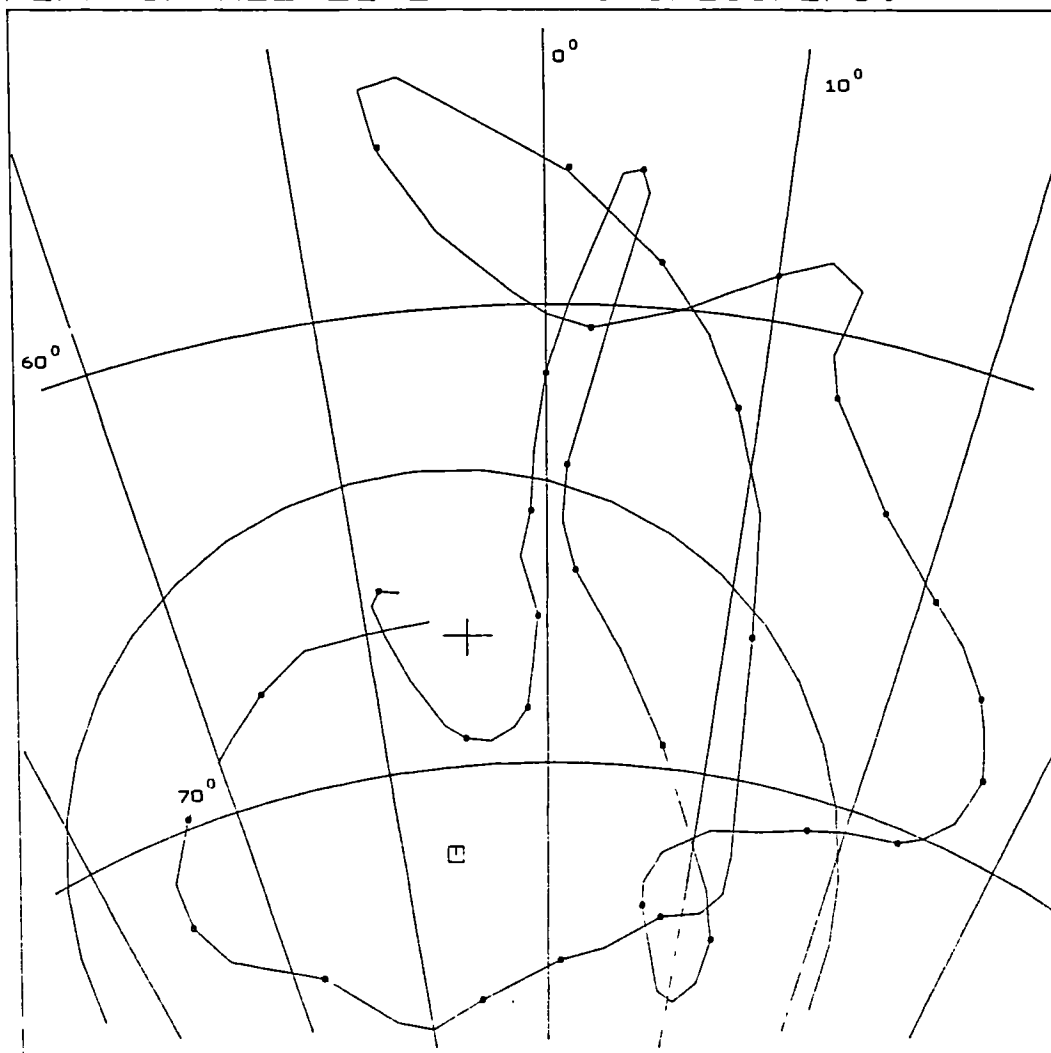


Figure 6.39

MEAN OF ALL LEVEL 3 SUB SPECIMENS.

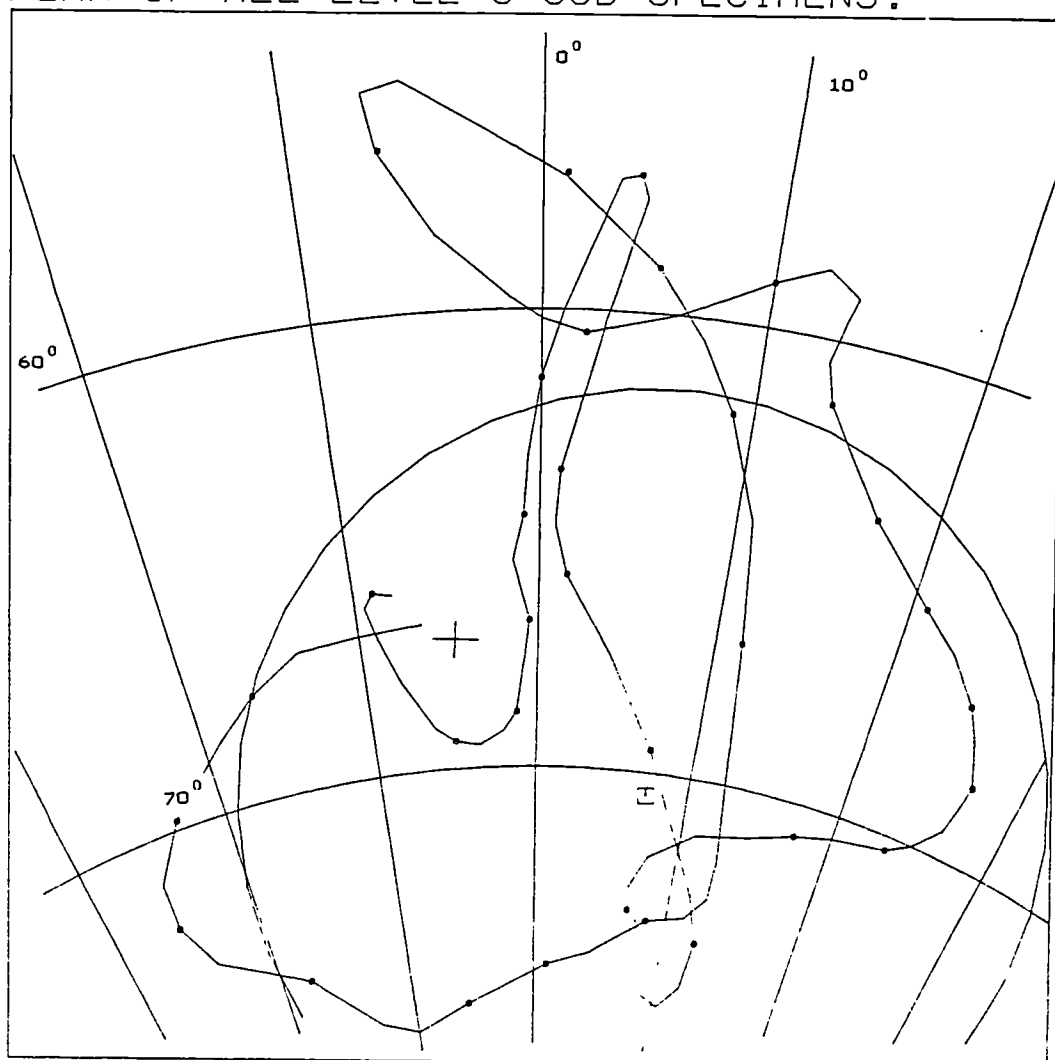


Figure 6.40

MEAN OF ALL LEVEL 4 SUB SPECIMENS.

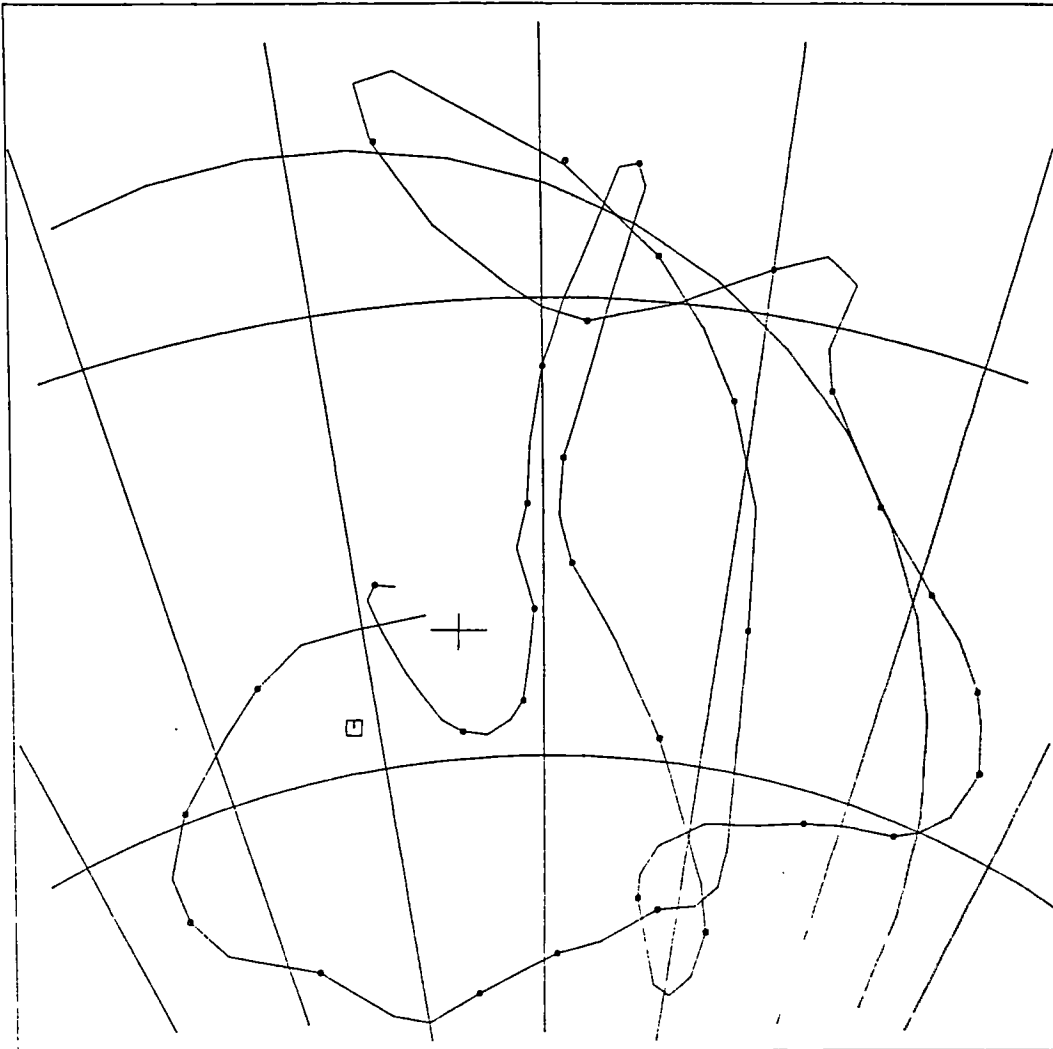


Figure 6.41

MEAN OF ALL LEVEL 5 SUB SPECIMENS.

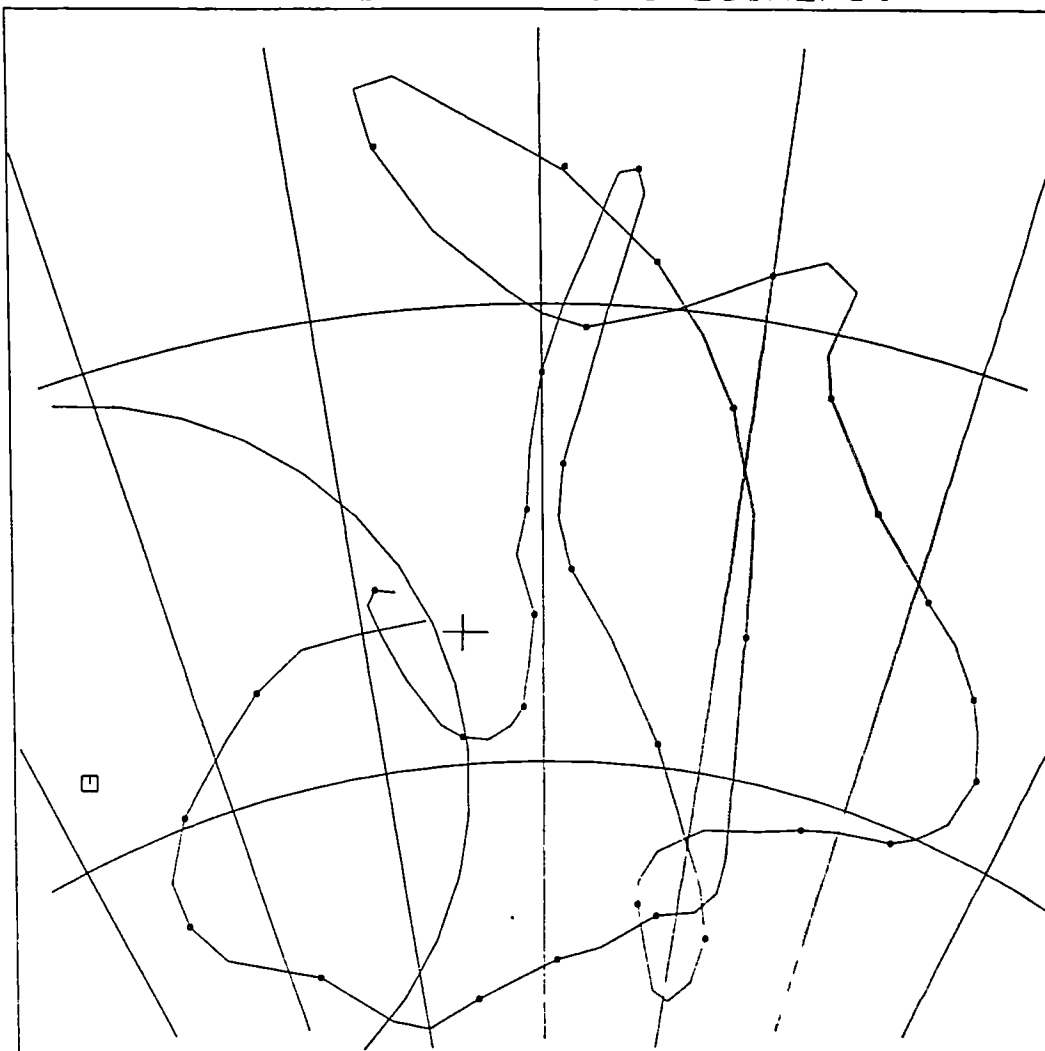


Figure 6.42

MEAN OF ALL LEVEL 6 SUB SPECIMENS.

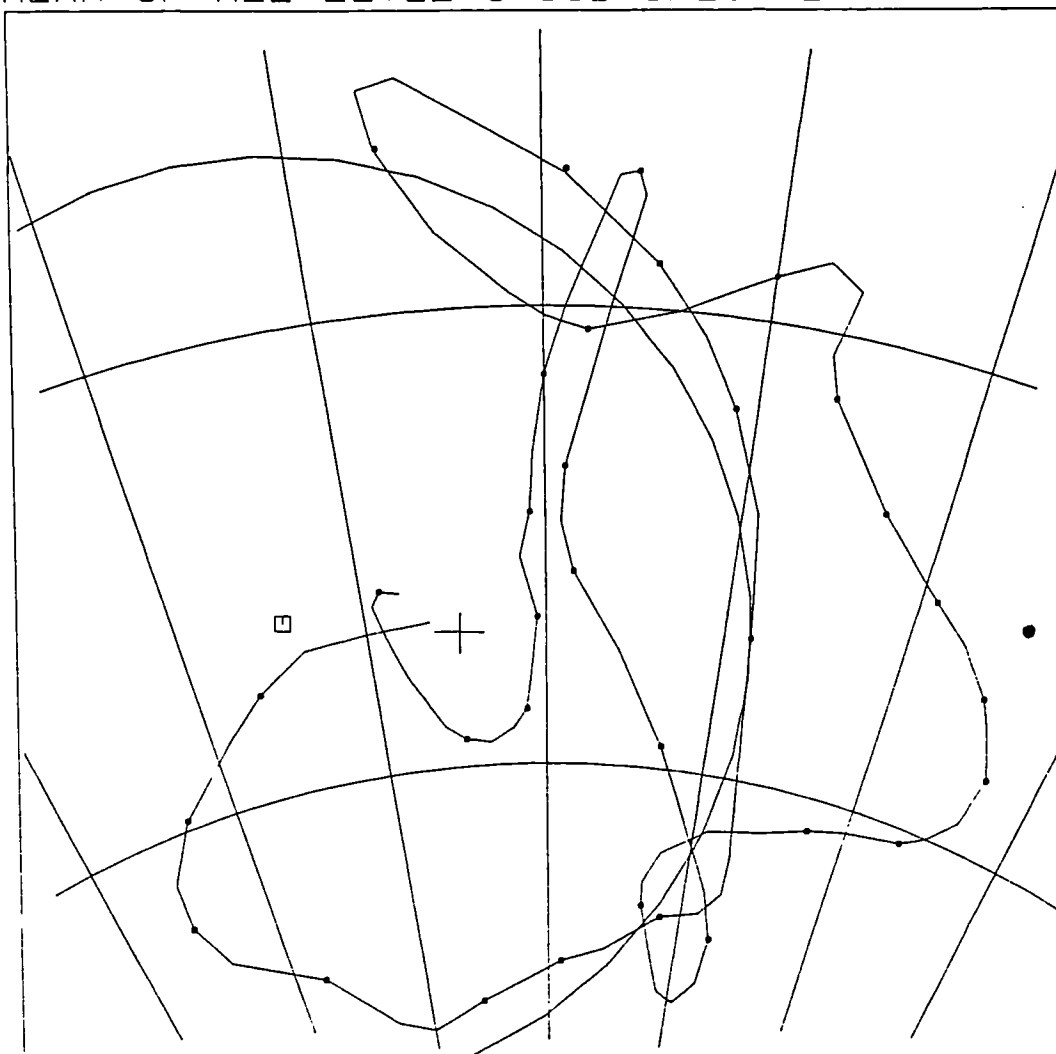


Figure 6.43



overall mean of all wall specimens was consistent with the present geomagnetic field having a declination of  $351.7^{\circ}$  and inclination of  $57.9^{\circ}$  (Fig 6.44).

When plotted against depth magnetic intensities generally increased, (Figs 6.45, 6.46). Declination and inclination also showed considerable variation with depth through the wall (Figs 6.47-6.50), whilst when this was shown as a solid angle for one azimuthal location ( $90^{\circ}$ , core 5), the outer specimen direction was generally dissimilar to specimen directions at greater depth, although this was not consistently the case (Fig 6.51).

The differences in the magnetic properties in both the core and sub-specimens could be due to a number of different factors e.g. differential heating, variations in the concentration of the magnetic mineral or differences in the type of magnetic mineral present. The following is a discussion of the possible causes of the observed pattern in magnetic directions.

#### 6.5. Magnetic distortions on cooling.

With increasing external energy (temperature) more domain walls unroll and energy barriers are exceeded. Thus those secondary cooled grains with blocking temperatures ( $T_c$ ) less than the temperature to which the

OVERALL MEAN OF ALL SUB-SPECIMENS.

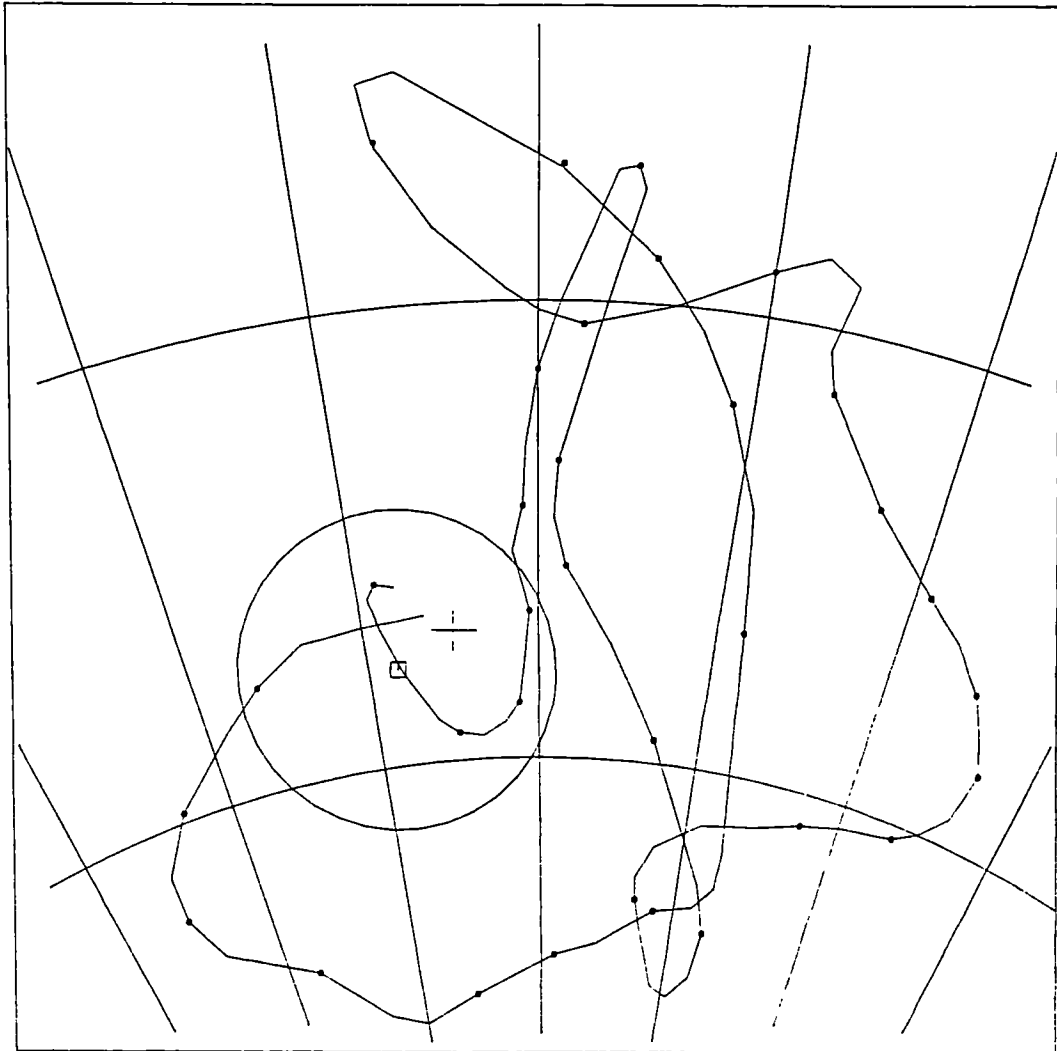


Figure 6.44

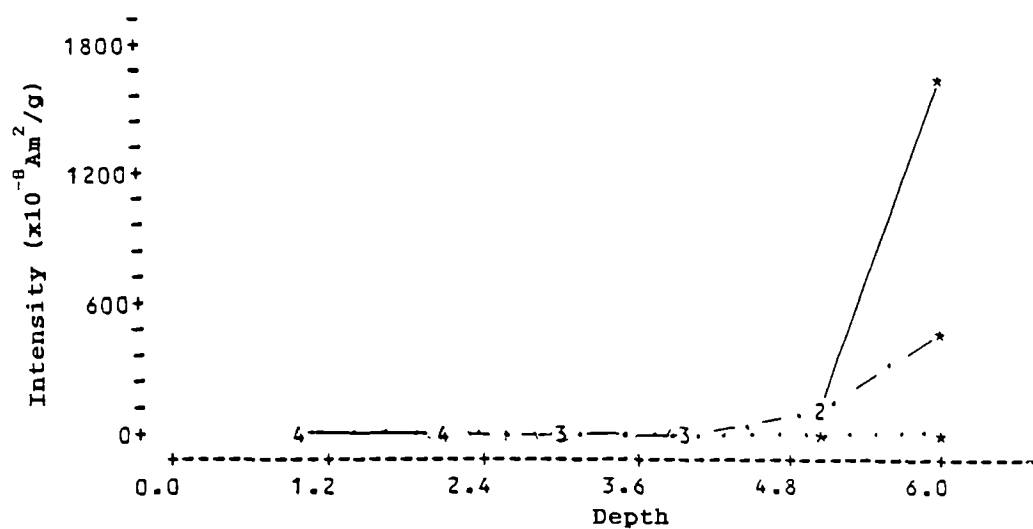


Figure 6.45 Intensity as a function of depth into kiln wall  
(sub specimens).  
East side.

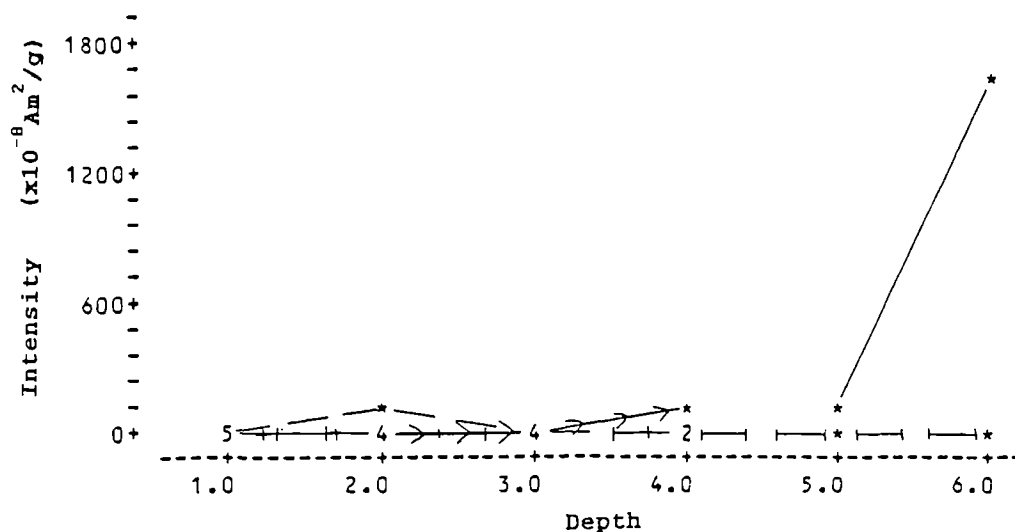


Figure 6.46 Intensity as a function of depth into  
kiln wall (sub-specimens). West side.

Key for sub-specimen magnetic properties as a function of depth  
into kiln wall (East side):

Specimen 1 ( $0^\circ$ ) = \_\_\_\_\_

Specimen 5 ( $90^\circ$ ) = .....

Specimen 7 ( $135^\circ$ ) = .-.-.-.-. .

Specimen 9 ( $180^\circ$ ) = -----

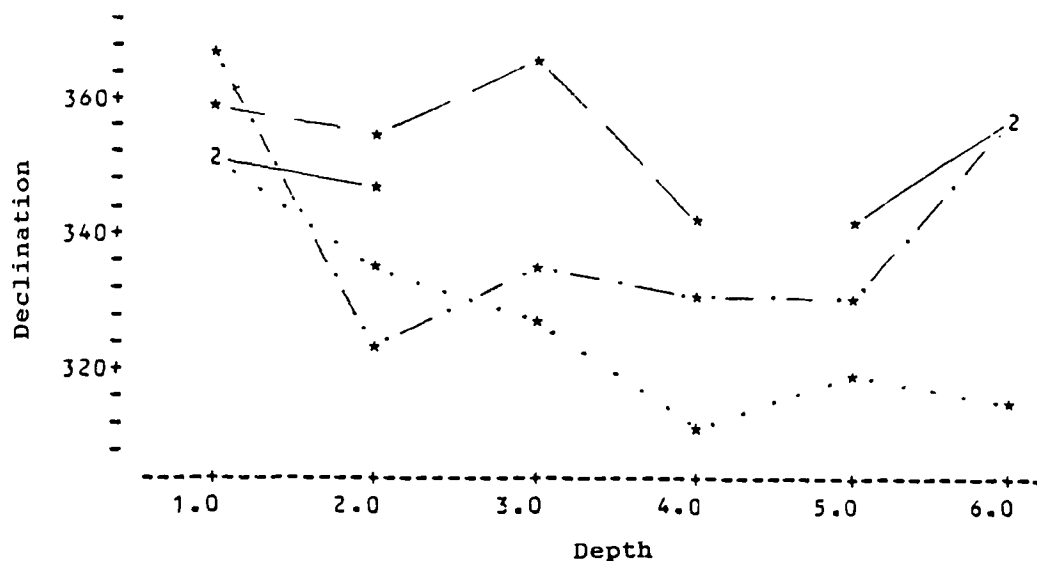


Figure 6.47 Declination as a function of depth  
into kiln wall (sub- specimens).  
East side.

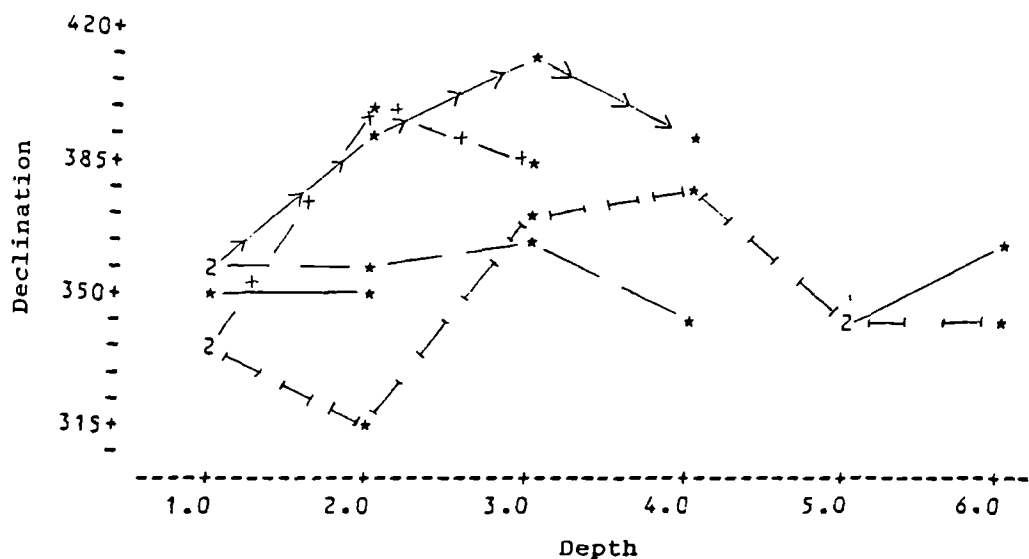


Figure 6.48 Declination as a function of depth  
into kiln wall (sub-specimens).  
West side.

Key for sub-specimen magnetic properties as a function of depth  
into kiln wall (West side):

Specimen 1 ( $0^\circ$ ) = \_\_\_\_\_  
Specimen 9 ( $180^\circ$ ) = - - - - -  
Specimen 10 ( $225^\circ$ ) = ->->->->-  
Specimen 12 ( $270^\circ$ ) = -+-+--+--  
Specimen 16 ( $315^\circ$ ) = I—I I—I

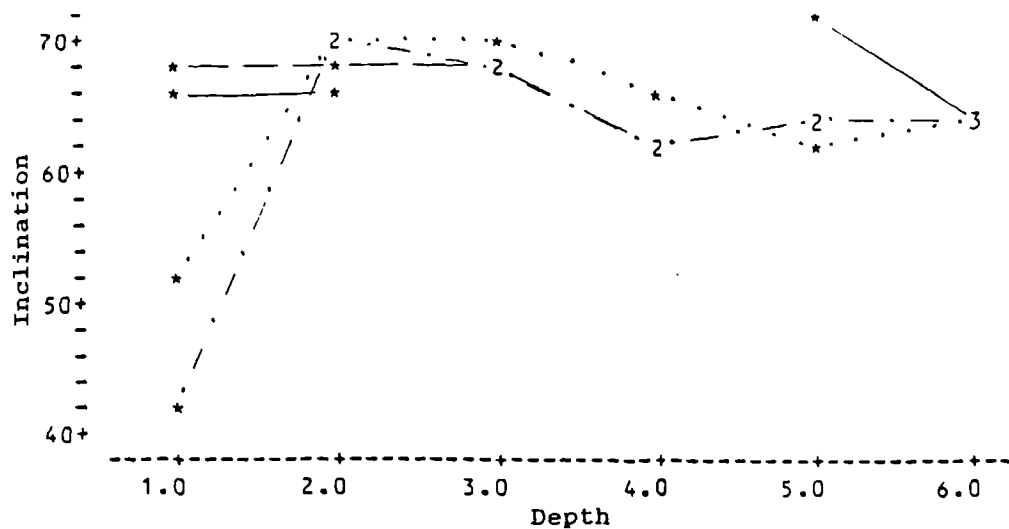


Figure 6.49 Inclination as a function of depth into  
kiln wall (sub-specimens).  
East side.

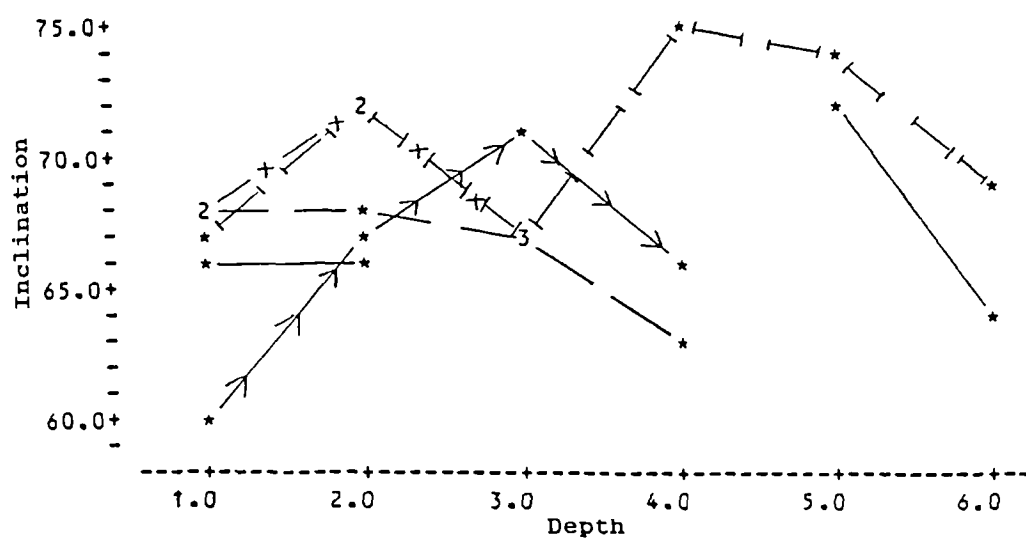


Figure 6.50 Inclination as a function of depth into  
kiln wall (sub-specimens).  
West side.

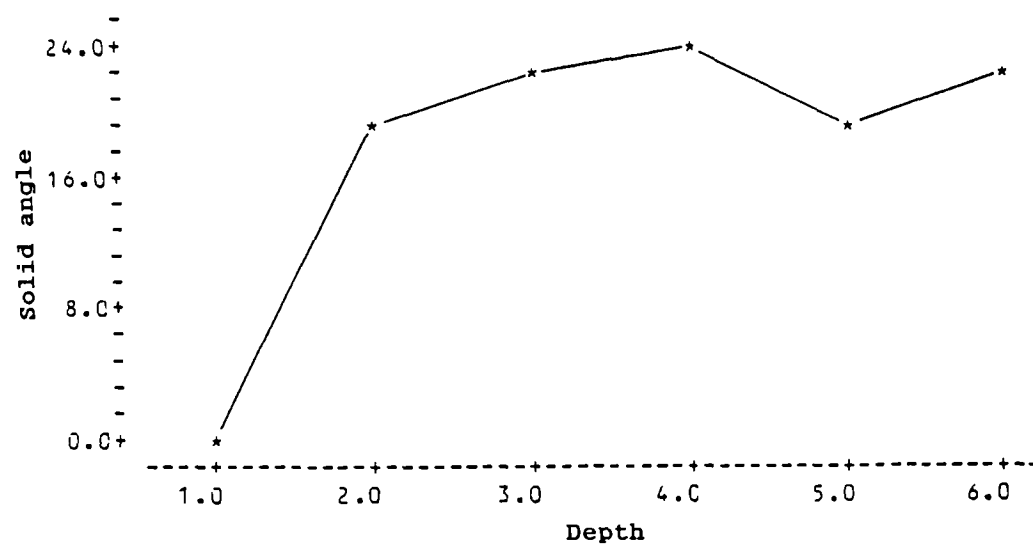


Figure 6.51 Solid angle as a function of depth  
into kiln wall (sub-specimens).  
Specimen 5

primary cooled material has been heated will become magnetised by the ambient geomagnetic field and the magnetic field acquired in the primary cooled area. Therefore it is conceivable that directional scatter could arise as a result of grains with lower blocking temperatures acquiring magnetisations in addition to those from the Earth's magnetic field alone. The problem arises when one tries to determine which part of the structure cooled first and/or fastest as no direct temperature measurements were made through the wall. It is likely however that the outside of the kiln wall cooled first as this was exposed to the outside air and it was the least heated. It is interesting to note the directional consistency of this layer. It is also reasonable to assume that the inner wall should cool last as this part would be exposed to heat the longest. The middle of the wall would also receive heat from the interior although it was adjacent to the outer shell of the wall which should cool first. For this layer it is envisaged that its cooling pattern was intermediate between layers A and C. If this cooling pattern is correct then the magnetisation in the kiln lining will be influenced by the cumulative effect of magnetisations acquired in levels A and B. Thus the differences in magnetic intensity and

direction through the wall could be explained in terms of primary and secondary cooled areas. However another effect could be the rate at which levels A, B and C respectively cooled.

If the pottery stack cooled first then it would behave like a magnet with lines of force. In that case the magnetisation associated with the pottery stack could cause magnetic deviations in toward the centre of the kiln. This effect would be dependent strongly on distance from the kiln wall to the pottery stack and the magnetic intensity of the pots.

Air temperatures were monitored in two places during heating and cooling (Fig 6.2). It was found that both temperature curves were similar irrespective of location of thermocouples, particularly during the cooling phase. This suggested a uniform cooling of the sampled inner part of the kiln structure which implies a uniform cooling of the inner wall of the kiln although no direct measurements of the wall temperature were undertaken.

If it is accepted that the inner part of the wall uniformly cooled then the directional scatter observed, if due to differential cooling could be due to the pattern of cooling through the wall. In support of this is the fact that the same pattern of magnetic directions is observed



in other single flued kiln structures, sampled internally. Thus the pattern of magnetic directions seems to be unrelated to the number of flues.

#### 6.6. Spatial distribution/concentration of magnetic materials in the building materials.

The fact that there are clear differences in magnetic susceptibilities as well as other magnetic properties suggests variations in the magnetic content of the specimens. Thus the differences in magnetic intensity could be due to e.g. variations in magnetic grain concentrations. However given the fact that the clay used to build the structure was mixed thoroughly before firing, it is unlikely that the spatial distribution of magnetic materials arising from the construction of the kiln before firing would result in the systematic pattern observed in the kiln after heating. This therefore suggested that the variations in magnetic susceptibilities was more likely to be due to different degrees of heating.

#### 6.7. Spatial variation in the type of magnetic mineral

The kiln was fired in oxidising conditions with an updraught created in all three flue systems. The fuel used was coal which was dry before firing encouraging

complete combustion. Magnetic analyses of the magnetic mineral(s) present were not undertaken but the kiln wall lacked the grey to black colour often associated with the presence of magnetite, normally indicative of limited oxidation. Also the core of the wall, although darker in colour, did not have a magnetic intensity higher than the inside which was presumably oxidised. This suggested that the higher magnetic intensities of level C, for any one azimuthal location, were primarily thermo-remanent whilst the lower magnetic intensities of levels B and A were the result of lower temperature heating. However the presence of more than one magnetic mineral cannot be ruled out without direct laboratory measurements.

#### 6.8. Demagnetisation methods.

Najid (1986) found that demagnetisation using A.F. and thermal methods obtained different results in terms of the precision of the magnetic direction. It is therefore conceivable that the use of A.F. on materials well and less well heated may have dissected the remanence more effectively for level A (materials less well heated and therefore grains of lower coercivity), than for the other levels with grains with

longer relaxation times. However results from the vitrified dun at Langwell (Chapter Three) suggest a close correlation between magnetic directions defined in materials demagnetised using thermal and A.F. methods. Further it is difficult to explain how the A.F. method alone could give rise to the systematic directional differences observed in this kiln.

#### 6.9. Movement during cooling.

It was noted during firing that parts of the outer casing of the kiln wall exfoliated away from parts better fired. On cooling the walls contracted leaving a gap of c.1cm between the core of the wall and the outer casing. A gap of c.3cm was left around the whole kiln circumference suggesting movement on heating and cooling. However the amount of movement noted would be insufficient to cause the magnitude of directional scatter observed. Also the sinusoidal declinations attributed in some kilns (e.g. Harold 1960), to kiln wall fall out, were not noted in many other archaeological examples (Tarling *et al* 1986). A possible explanation of this is the number of firings of the walls or the type of wall structure itself. With greater numbers of firings the elasticity of the clay is likely to reduce with water loss from

within the kiln fabric, whilst repairs, re-lining etc. would further contribute toward greater rigidity in the kiln structure making wall movements on cooling less likely.

#### 6.10. Magnetic anisotropy.

During construction the walls were systematically pinched and smoothed prior to firing so that it was likely that a fabric anisotropy would result. However examination of the magnetic directions isolated from specimens removed from the outside of the kiln showed the most directional similarity. This suggested that fabric anisotropy was not the cause of magnetic deviations in this kiln. However at different temperatures different magnetic grains would become "actively" anisotropic, depending on their blocking temperatures, whilst the degree of magnetic deflection would be dependent on grain shape/size, the grains orientation relative to the direction of the geomagnetic field, and the relative magnitudes of the principal axes (Stephenson *et al* 1986). The fact that magnetic directions were most similar at  $0^{\circ}$  and  $180^{\circ}$  suggests there was some relationship between the angle of the applied field and the remanence acquired.

### 6.11. Summary.

It seems most likely that the directional differences observed are dominated by the pattern of cooling through the wall, given that the kiln chamber cooled fast and uniformly in the region of the specimens. The pottery stack, being at a greater distance from the inner wall should be less relevant. Fabric anisotropy appears from the directional consistency of the outer casing to be insignificant although the anisotropy of the thermal remanence may be important, and measurements of this are advocated. Movement, although present, does not appear to be significant whilst the material was magnetically homogeneous before firing.

Magnetic directions consistent with the present Earth's magnetic field are obtainable by systematic sampling of the whole kiln and the overall mean. Floor mean directions are statistically the same as those from the wall and agree with the present geomagnetic field direction. Preferential sampling of azimuths  $0^\circ$  and  $180^\circ$  can result in the isolation of magnetic directions consistent with the present geomagnetic field, although level C and 6cm depth specimens still show the greatest scatter (Fig. 6.12, 6.37). Sampling of the outer casing can also result in similar specimen magnetic directions

being isolated (e.g. level A core specimens). The overall mean magnetic direction for any one level of the Lunt kiln would be consistent at the 95% confidence level with the ambient Earths magnetic field. However due to the directional scatter of levels B and C (4-6cm), the mean direction would not be statistically well defined. This is also applicable to the 1cm-3cm sub-specimens. However the sub-specimen observed means were variable, and in some cases (e.g. 1cm, 3cm, 5cm specimen means), could only be related to the present geomagnetic field direction because of the large 95% confidence circles.

The inside of clay built structures are likely to suffer from exfoliation affects (flaking of inner c.1cm of kiln lining), which may happen during the last firing. Given the differences in magnetic direction between the inside and outside of the kiln wall this could be significant in terms of the recording of the true geomagnetic field direction.

An experiment carried out on site showed that samples of the low fired clay of the outside of the kiln when slaked with water disintegrated easily. When this kiln was left for only one winter it had disintegrated. Thus the part of the kiln most highly fired is more likely to survive post burial processes than that less well

heated bar exceptional circumstances (e.g. arid climate). Therefore extreme caution is advised where sampling, for one reason or another, is restricted to a limited area of a structure as this could result in the definition of a different mean direction from that of the true geomagnetic field direction.

## CHAPTER SEVEN

---

### Other ancient structures sampled

7.1. Archaeomagnetic report on two clay hearths from the Neolithic site at Buxton, Lismore Fields, 53.2° N, 1.9° W.

In July 1985 three burnt clay hollows (contexts 0009, 0057, 0059) found in association with lithic industries dated to the Neolithic period, were sampled at Lismore Fields, Buxton. Eighteen specimens were oriented using a magnetic compass (which did not appear to be affected by the magnetism of the burnt clay), and inclinometer. It was necessary to exclude 8 specimens from the analysis due to the friability of some of the specimens or their weak magnetisations after subjection to A.F. (0009/5, 0057/1, 0057/2, 0057/5, 0059/1, 0059/2, 0059/4, 0059/5). All specimens had moderate to low intensities of magnetisations whilst they varied from unstable to stable to demagnetisation using A.F.

Most specimen vectors showed erratic changes during



demagnetisation (Fig. 7.1). The Stability Index (Symons and Tarling, 1967) was used to define each most stable direction giving equal weight to each stable component (Table 7.1).

The majority of specimens were metastable (S.I. 1-2) whilst four had stable magnetisations (S.I. 2-5). Only one was unstable (S.I. <1). However only four specimens (0059/3, 0059/5, 0057/7, 0009/4) showed archaeologically meaningful directions after demagnetisation. Interestingly the inclinations from these specimens from separate contexts were similar although individual declinations were generally dissimilar.

The degree of directional scatter (Table 7.1) ruled out any age determination by archaeomagnetic methods for any of the contexts sampled (Gentles, forthcoming). As such no overall mean magnetic direction was calculated. Thus although there were measurable magnetisations confirming the clay had been burnt, the scatter of directions suggested considerable physical disturbance of these features subsequent to the acquisition of the last remanence. Nevertheless as the magnetic directions were not random this suggested that the disturbance was not major e.g. ploughing, but was consistent with the effects

HOR. SCALE (\*-\*) = 6.000  
VER. SCALE (X-X) = 7.000

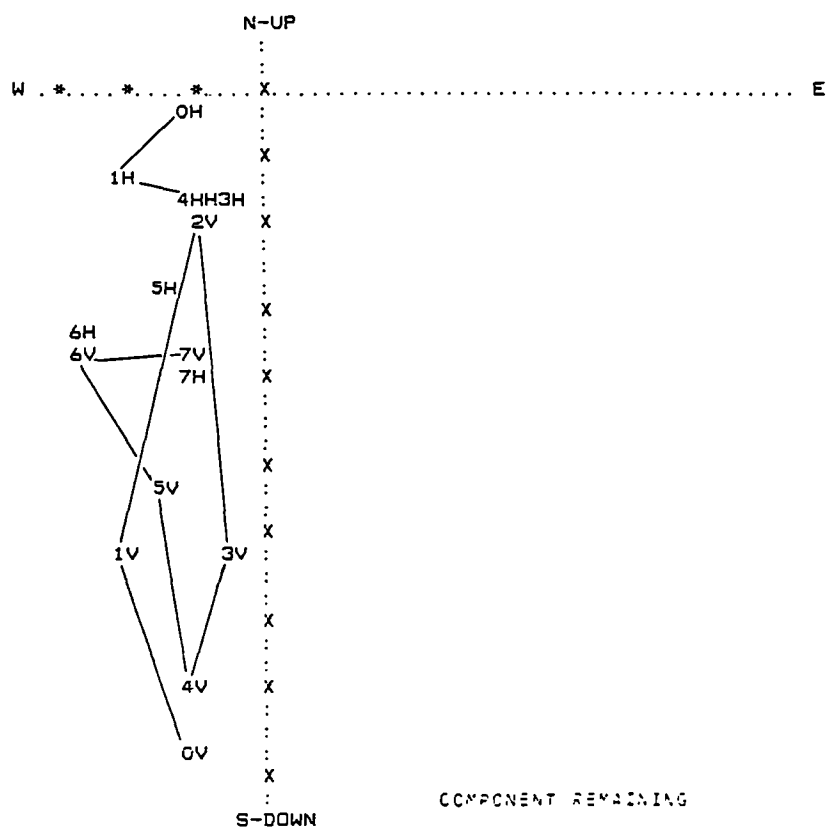


Figure 7.1 As/Zijdeveld plot of  
0057/4.  $\times 10^{-8} \text{ Am}^2/\text{g}$ .

of differential subsidence. As a result of this disturbance no overall mean was calculated for these features.

**Table 7.1**

**Most stable specimen directions.**

Specimen	Dec	Inc	Int	$\alpha_{95}$	S.I.	Range.
			$\times 10^{-8} \text{ Am}^2/\text{g}$			mT
0059/1	95.8	50.5	4.1	8.8	1.5	0-7.5
0059/3	8.1	70.1	8.1	2.1	5.2	5-10
0059/5	346.3	74.0	3.7	7.8	1.4	0-12.5
0057/3	78.4	10.3	32.1	7.1	2.0	5-40
0057/4	211.0	61.9	36.9	12.6	1.0	0-30
0057/6	259.6	28.1	30.3	13.6	1.0	0-7.5
0057/7	47.1	73.3	29.6	6.6	2.0	0-7.5
0057/8	274.2	66.9	12.4	15.5	0.7	7.5-12.5
0009/1	337.2	44.3	8.2	9.6	1.1	0-5
0009/2	169.3	50.7	12.6	8.3	1.3	0-5
0009/3	353.7	83.0	121.0	7.5	1.4	0-5
0009/4	329.9	72.7	147.1	3.0	3.6	0-5

7.2. Archaeomagnetic report on two iron smelting furnaces from Crawcwellt, North Wales, 53.2°N, 4.0°W.

In October 1986 two circular iron smelting furnaces were revealed during excavation at Crawcwellt. Previous magnetic results suggested a Late Iron Age date for these types of structure (Crewe, 1986; Tarling *et al*, 1986). Examination of their walls revealed that they had been vitrified as a result of high temperatures. At the time of sampling the furnaces were exposed to a maximum height of 7cm above present ground surface. Specimens were removed from apparently physically stable parts of the structures prior to further excavation as the latter could cause disturbance of the features.

Orientation of the specimens was by sun compass and inclinometer. Eight specimens were removed from furnace F10 but only five from furnace F41 as this feature was less well preserved. All specimens had strong magnetisations, and were subjected to incremental alternating magnetic field partial demagnetisation. All intensities of magnetisation were high to very high before demagnetisation, ( $> 3512 \times 10^{-8} \text{ Am}^2/\text{g}$ ). Only one component was isolated in each of the specimens suggesting that only

the final firing was recorded. The vector paths showed an initial change as a viscous component was removed whilst subsequent vectors were linear (Fig. 7.2a). The most stable directions were defined using the Stability Index (Tarling and Symons, 1967). However for feature 10 it was necessary to exclude specimen directions (1a, 2a) taken from parts of the furnace which, on closer study were clearly deviant in inclination from the closely agreeing majority. This is considered to be due to post firing disturbances (Table 7.2). Although 3a had a declination which was deviant from the rest this was difficult to explain in terms of movement for this structure.

The observed mean of the most consistent specimens from feature 10 plotted adjacent to that part of the archaeomagnetic secular variation curve consistent with a Late First Century B.C. date whilst the 95% confidence circle incorporated that part of the curve consistent with the Late Iron Age to Early second century A.D. (Fig. 7.2b).

The individual specimen directions from feature 41 were consistent with individual specimen directions from feature 10. Both furnaces appear to be most consistent with a Late Iron Age date, although the overall mean from

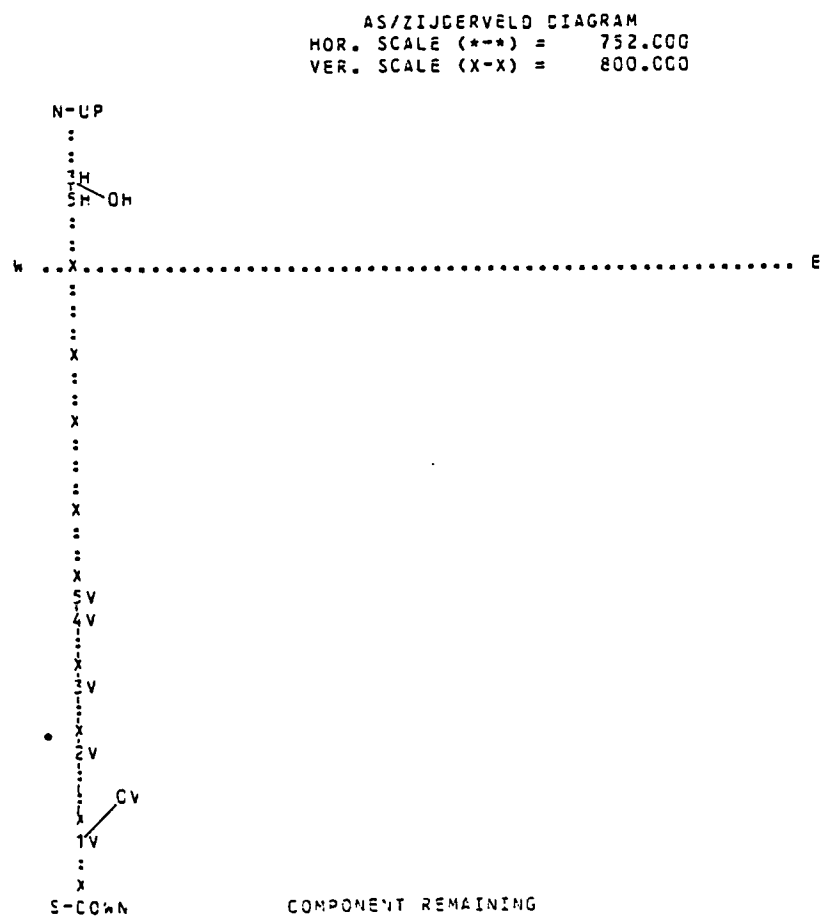


Figure 7.2a(i) As/Zijderveld plot of F41/2  
 $\times 10^{-8} \text{ Am}^2/\text{g}$ .

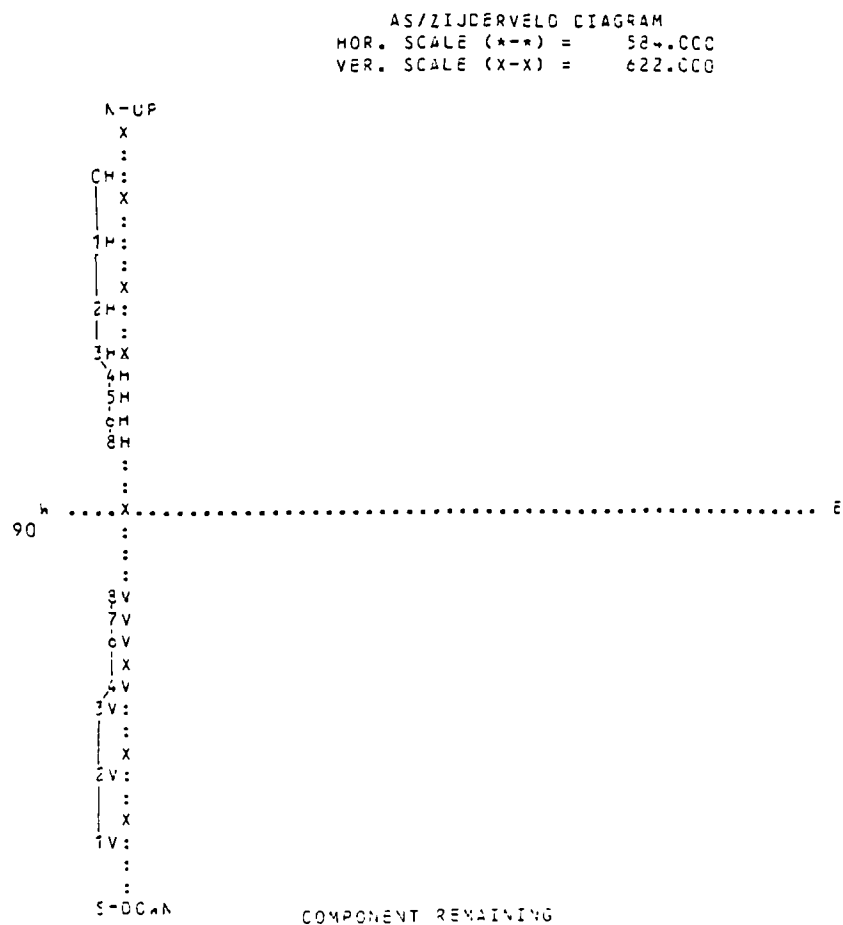


Figure 7.2a(1) As/Zijderveld plot of F10 2a  
 $\times 10^{-8} \text{ Am}^2/\text{g}$ .

CRAWCWELLT IRON SMELTING FURNACE, F 10.

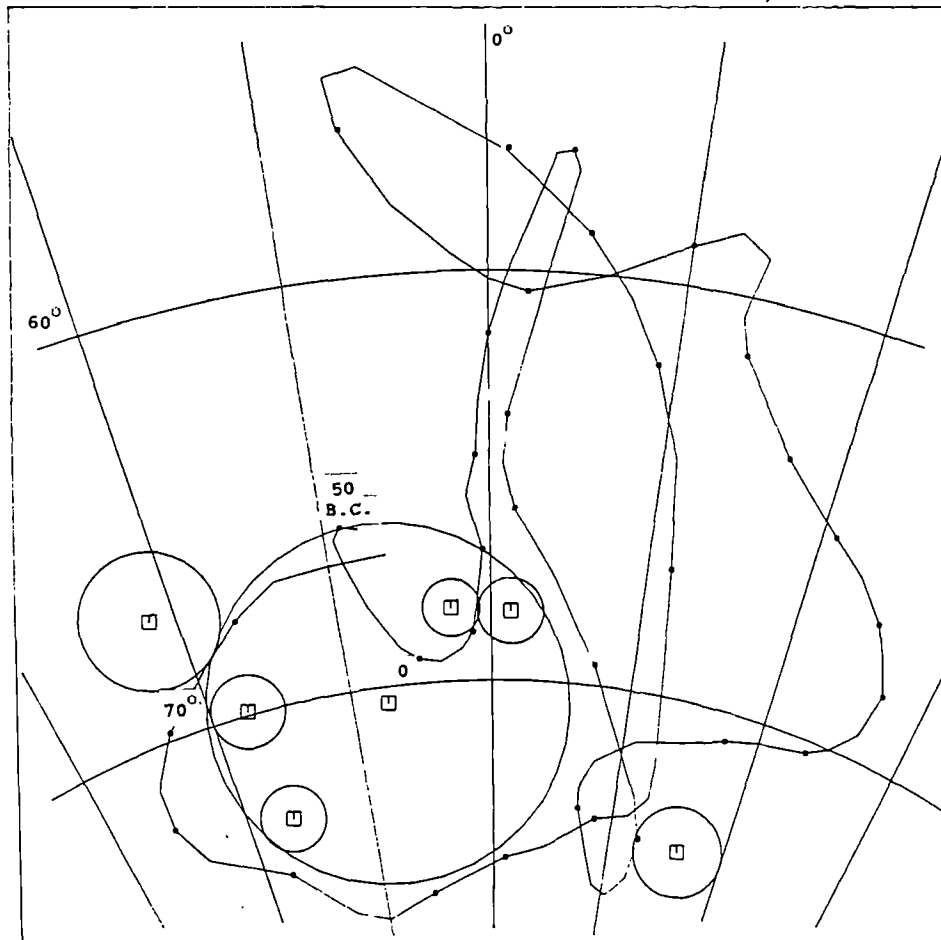


Figure 7.2b Mean magnetic direction of Crawcwellt  
Iron Smelting Furnace



feature 41 should be treated as tenuous in the absence of greater numbers of specimens.

Table 7.2.

Most stable specimen directions.

Specimen	Dec	Inc	Int $\times 10^{-8} \text{ Am}^2/\text{g}$	$\alpha_{95}$	S.I.	Range. mT
*F 10/1	325.7	35.9	1261.7	0.4	24.2	20-27.5
*F 10/2a	353.8	52.0	1265.4	0.4	34.7	10-30
F 10/2b	338.4	67.1	6323.2	1.7	10.7	10-25
F 10/3a	16.1	73.6	8450.8	1.1	14.0	20-30
F 10/3b	357.4	68.2	11740.7	0.7	20.3	25-40
F 10/4	343.6	72.7	8165.9	0.8	17.3	10-25
F 10/5	342.6	69.9	3593.2	0.9	16.9	10-20
F 10/6	1.3	68.3	4151.6	0.8	17.6	5-25
F 41/1	339.8	73.0	10627.8	0.3	44.0	10-20
F 41/2	352.4	78.8	3789.6	0.8	19.7	10-20
F 41/3	17.5	81.6	1140.7	1.1	13.5	15-25

Anomalous directions\*

Mean Meriden corrected direction for F10:

Dec = 352.5

Inc = 70.4

$\alpha_{95}$  = 4.4

K = 225.6

N = 6

R = 5.978

Mean Meriden corrected direction for F41:

Dec = 352.2

Inc = 78.1

$\alpha_{95}$  = 8.8

K = 196.2

N = 3

R = 2.990

7.3. Archaeomagnetic report on a brick kiln from the Quayside, Newcastle upon Tyne, 54.9°N, 1.5°W.

In May 1986 the most westerly of two kilns, assigned 17th century A.D. dates based on contextual evidence was sampled from the Quayside, Newcastle upon Tyne. It was composed mainly of fired brick which appeared oxidised, presumably as a result of firing. The North West portion of the brick structure was missing due to wall collapse although the lowest course of bricks remained at this point. The structure was roughly oval in shape, with interstitial friable white powder in some areas. Externally the kiln was faced with the same friable material and burnt clay. The South Eastern portion (mouth of the kiln) was flanked by sub-rectangular sandstone blocks which continued South East as a continuation of the brick wall on the West side of the kiln. Underlying the mouth of the kiln and extending South Eastward for 1m were burnt flags of irregular shape and size. These were curtained to the West by the sub-rectangular blocks, but the flags did not appear to underly them. The burnt flags therefore appeared to have been built at approximately the same time or later than the block wall. As such they may

be contemporary with the kiln as a whole. Removal of the kiln during excavation revealed that it had been sited on compacted sand and rock which was physically stable.

Twelve specimens were oriented using an inclinometer and a magnetic compass (which did not appear to be affected by the magnetism of the structure). These were measured and subjected to incremental thermal demagnetisation steps. (Although susceptibility measurements were made, these were lost during the move from Newcastle Upon Tyne to Plymouth). Initial intensities of magnetisation were low to very high ( $1-4807 \times 10^{-8} \text{ Am}^2/\text{g}$ ). A notable common characteristic was a rise in magnetic intensity at c.  $200^{\circ}\text{C}$  in some of the specimens, and the vector often showed a marked non-linearity (Fig. 7.3a). Nevertheless the magnetic directions were stable with stability indices of 2.0-15.2, although the most consistent directions were mostly defined at temperatures between  $0-250^{\circ}\text{C}$ . Half of those defined at higher temperatures ( $200-450^{\circ}\text{C}$ ) plotted too far East of the curve to be related to it. An overall mean was calculated without the directionally deviant specimens (10F1/2 and 10f/2), which were considered to have either moved significantly subsequent to the last firing, or to

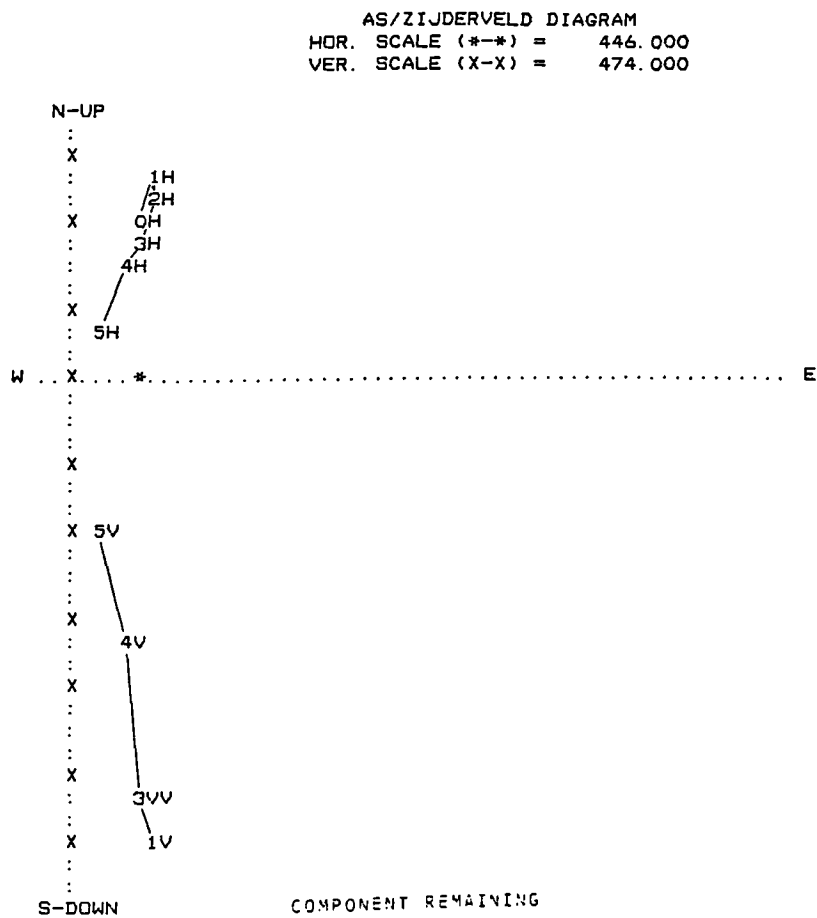


Figure 7.3a As/Zijdeveld plot of  $10F1/1 \times 10^{-8} \text{ Am}^2/\text{g}$ .

have been chemically changed. Interestingly however specimens 10f3/1 and 10f1/1 showed archaeomagnetic directions consistent with the secular variation curve at higher temperatures, and were also broadly consistent with those defined at temperatures  $<250^{\circ}\text{C}$ .

The observed mean of all most stable Meriden corrected directions plotted adjacent to that part of the secular variation curve with an early 13th century A.D. date whilst the 95% circle of confidence incorporated parts of the curve with a late 12th to late 15th century date (Fig 7.3b). Therefore the remanence directions isolated in this kiln defined a chronological span older than that proposed based on contextual evidence. However as there were no susceptibility measurements available caution is advised, although the correlation, in some instances, of magnetic directions at low and high temperatures may indicate the absence of effective chemical change for some specimens.

# QUAYSIDE, NEWCASTLE.

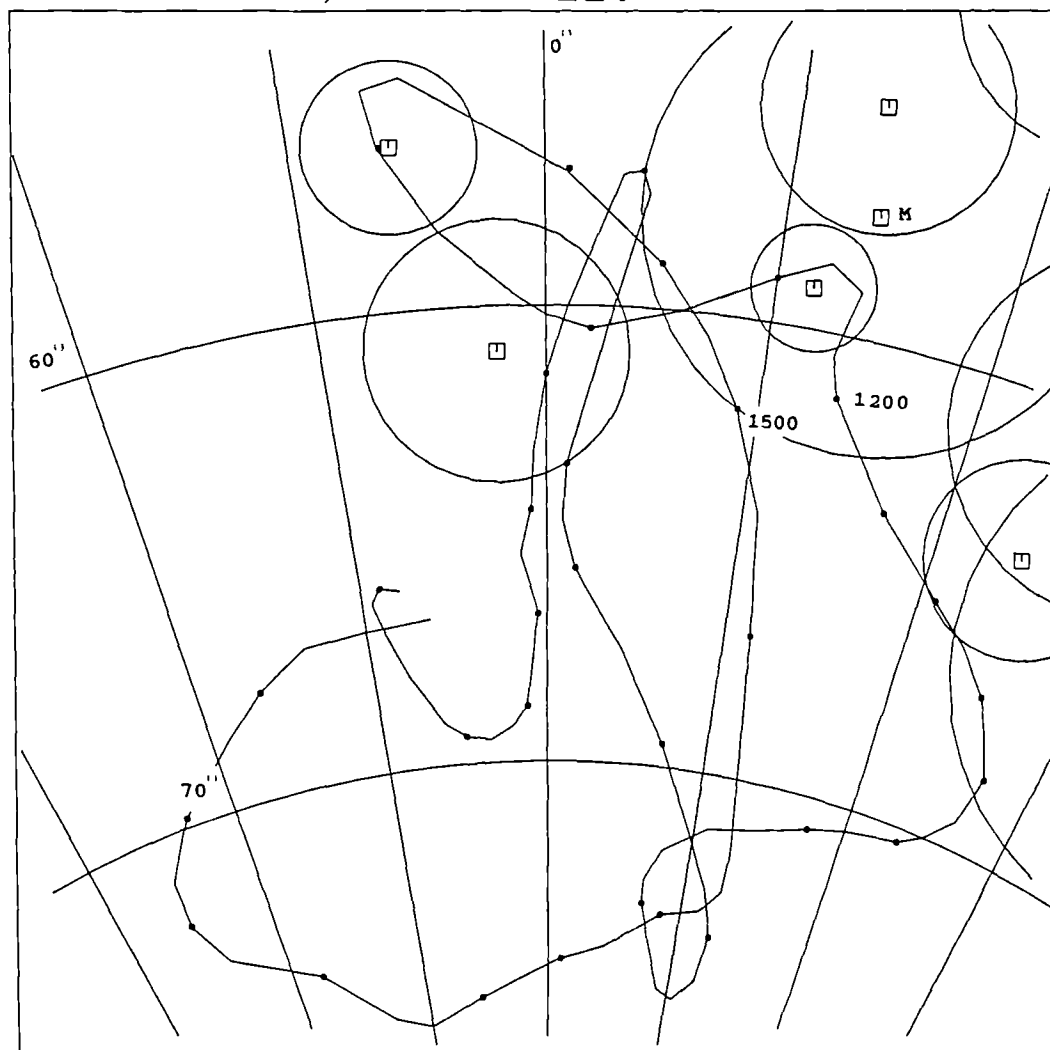


Figure 7.3b Mean magnetic direction of Quayside Brick Kiln

**Table 7.3**

**Most stable specimen directions:**

Specimen.	Dec.	Inc.	Int.	$\alpha_{95}$	S.I.	Range.
			$\times 10^{-8} \text{ Am}^2/\text{g}$			$^{\circ}\text{C}$
SP1f	7.0	50.0	3.0	3.7	6.5	0-250
SP2f	357.7	63.1	12.0	2.9	6.3	0-500
SP3f	353.7	58.7	350.0	1.9	12.6	0-250
SP6f	20.7	54.1	566.0	3.2	7.5	0-250
SP7f1	16.1	52.6	3677.0	2.0	11.8	0-250
SP7f2	13.7	57.3	132.0	2.8	8.7	0-250
10f1/1	25.5	65.4	1007.1	2.2	8.6	0-500
*10f1/2	63.4	55.4	1522.0	3.4	4.7	200-310
*10f/2	85.3	33.6	487.7	10.6	2.0	250-450
10f3/1	12.1	61.3	3599.7	1.4	15.2	250-450
10f3/2	27.9	62.0	2227.5	4.1	5.9	0-250
20f1/1	36.9	65.7	1281.8	5.7	4.2	0-250

\*excluded directions.

**Mean Meriden corrected direction:**

Dec = 13.8	Inc = 57.3
$\alpha_{95} = 5.3$	K = 83.7
N = 10	R = 9.893



7.4. Archaeomagnetic report on a tile kiln from the Roman Fort, (Arbeia), South Shields, 54.9° N, 1.5° W.

In September 1985, the most complete of two kilns lying within the Hadrianic Granary of the Roman Fort at South Shields was partially re-excavated for archaeomagnetic analyses. This kiln, which lay on a North West to South East axis, had been assigned a fourth century A.D. date based on contextual evidence, (Miket, 1981). It was roughly oblong in shape and constructed of tiles, sub-rectangular stone blocks and fired clay. Specimens were taken from the inner and outer faces whilst orientation was by magnetic compass and inclinometer. (The magnetism of the structure had no detectable effects on magnetic compass readings).

Six specimens were taken from the inner face of two fired arches which provided support for the front and most South Easterly parts of the kiln nearest to the stoke hole. Four specimens were taken from the baked clay exterior on the North East and North West flanks of the tile kiln.

All specimens were subjected to A.F. partial demagnetisation to a maximum field of 50 mT although in

some instances a stable component was defined by 30 mT. All intensities of magnetisation were high 536-15917 x  $10^{-8}$  Am<sup>2</sup>/g before demagnetisation whilst all specimens had an intensity > 176 x  $10^{-8}$  Am<sup>2</sup>/g after demagnetisation to 30 mT, well above the noise level of the magnetometer. Vector paths showed an initial change as a low coercivity viscous component was removed, usually below 10 mT, after which only one component of magnetisation was distinguished in each of the specimens. (Fig. 7.4a).

Subsequent vectors were mostly linear although the vector path of specimen 1 showed a slight curvature, with small erratic changes. In all cases the Stability Index, (Symons and Tarling, 1967) was used to define the most stable direction per specimen (Table 7.4) but it was necessary to exclude specimens taken from parts of the kiln structure which were considered, on closer study, to have moved, subsequent to the last firing and the overall mean has been calculated without these specimens.

The high magnetic stability and well defined specimen directions were in contrast to the large scatter between the individual specimen directions. Some specimen directions showed a greater departure than others from the

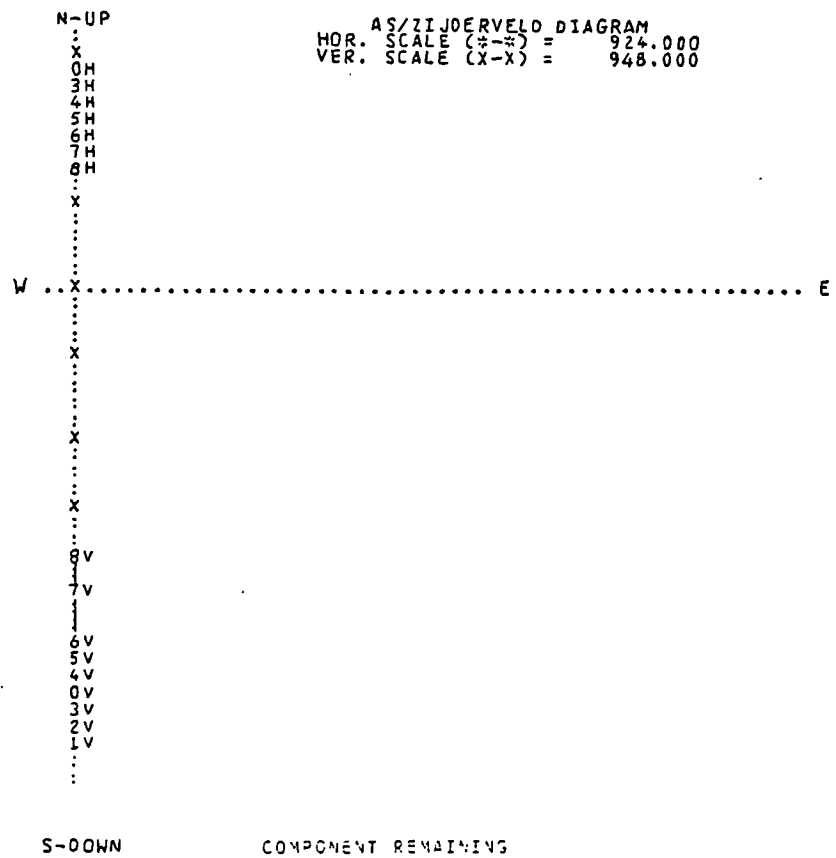


Figure 7.4a As/Zijderveld plot of SH6  
 $\times 10^{-8} \text{ Am}^2/\text{g}$ .

archaeomagnetic curve for the fourth century A.D., (Fig. 7.4b). Differential cooling, anisotropy and inhomogeneity may have contributed to this, but none of these adequately account for both the high magnetic stability and the large magnitude of the directional scatter.

Internal specimens, 1, 2, and 3 plotted South West of the relevant part of the curve (Table 7.4). These specimens were derived from the most South Western of the kiln arches and show the greatest deviation from a fourth century direction. It is possible that this arch has moved independently of the other sampled arch. However the structure of the arches needs to be taken into account. Each is composed of individual flat, rectangular fired tiles superimposed upon each other with a thinner layer of mortar acting as a fill between each one. Thus each tile could be disturbed to a different extent in the same arch. Specimens 1 to 3 show considerable difference (Table 7.4) in both inclination and declination although from the same arch (specimen 3 plots off the diagram). The magnitude of directional scatter between all the specimens appears to be most consistent with large scale differential movement subsequent to the last firing.

# SOUTH SHIELDS TILE KILN.

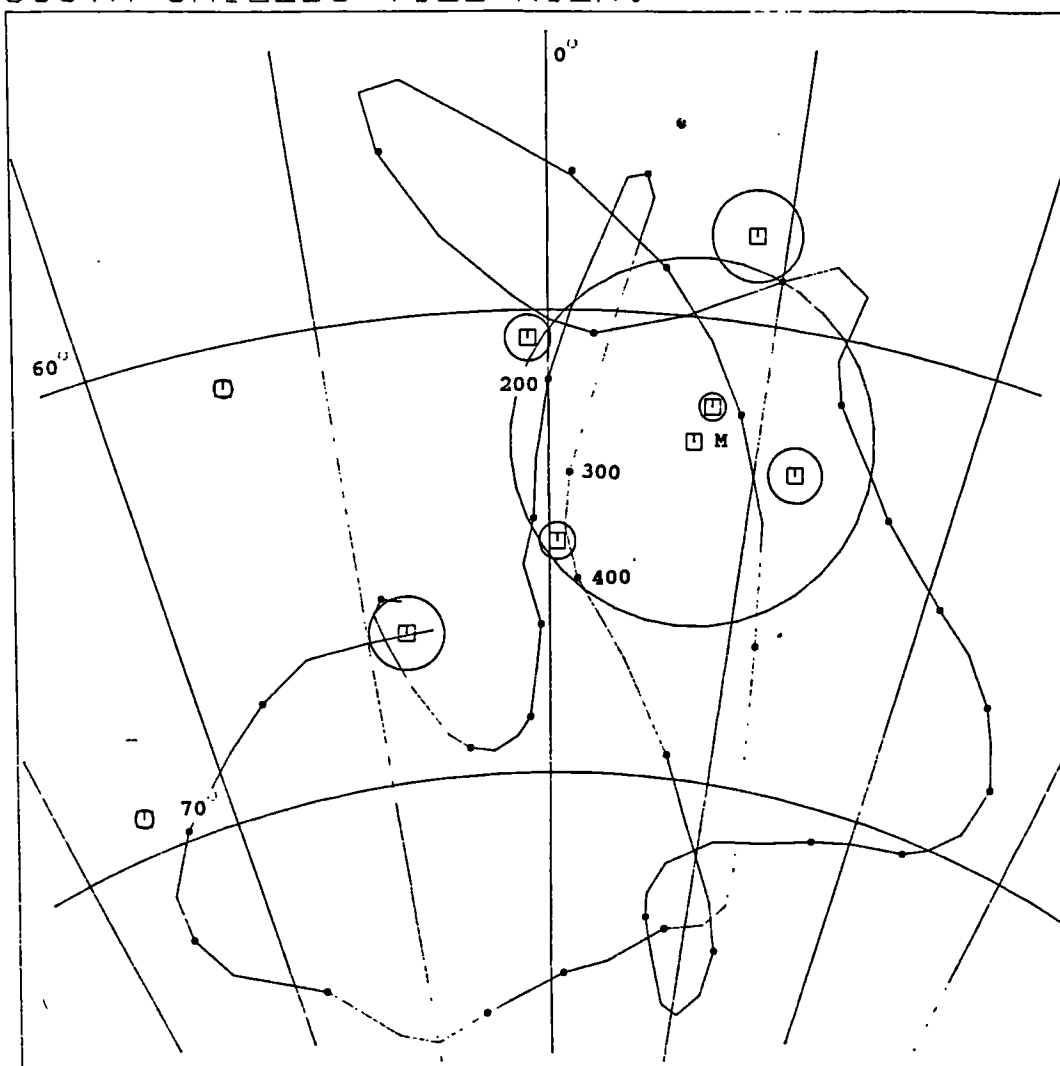


Figure 7.4b Mean magnetic direction of South Shields  
Tile Kiln

External specimen, (1W), plotted West of the fourth century part of the curve. This specimen showed a large deviation from specimens 2W, 3E, and 4E, (Table 7.4). This too may reflect differential movement as, unlike the other specimens, this one was taken at a greater vertical height on the kiln and the upper parts of this structure were severely disturbed.

The directional trend of most specimens is to show a greater westerly scatter in declination away from the fourth century A.D., with a smaller number showing a slight easterly dispersion. Even if specimens 1, 2, and 3 are excluded there is still a maximum c.28° variation in declination values between specimens whilst only a maximum c.10° variation in inclination (before correction to Meriden).

The observed mean of the most consistent Meriden corrected specimens plotted c.4° East of the relevant part of the curve. the circle of 95% confidence reflected the large scatter of directions incorporating mid-Late Roman, (150-410 A.D.) dated directions of the curve (Fig. 7.4b). However the scatter is so large that any age assessment is uncertain.

Given the magnetic stability and well defined

specimen directions it seems likely that different parts of this kiln have moved to different extents since the last firing. The nature of this disturbance cannot be defined in detail from the number of specimens taken, which were intended for dating purposes only. The overall scatter of magnetic directions from these specimens prevents any chronological assessment by archaeomagnetic methods.

**Table 7.4**

**Internal specimen directions:**

Specimen	Dec	Inc	Int	$\alpha_{95}$	S.I.	Range
			$\times 10^{-8} \text{ Am}^2/\text{g}$			mT
*1	330.7	63.5	4595.4	0.3	38.8	0-40
*2	333.3	70.7	5207.9	0.2	60.0	10-25
*3	346.1	81.6	2181.9	0.5	36.0	15-30
4	8.0	63.9	2972.3	0.3	49.9	7-20
6	0.5	66.9	3747.0	0.4	39.0	15-25
9	351.6	68.6	4376.2	0.8	17.5	12.5-20

### External specimen directions:

*1W	345.0	62.9	5924.5	0.2	55.6	0-20
2W	359.0	62.7	1141.3	0.5	58.5	20-50
3E	9.1	60.3	5565.2	1.0	20.8	15-50
4E	12.6	65.1	5731.1	0.6	26.7	10-20

\*Excluded specimens.

### Mean Meriden corrected magnetic direction:

Dec = 6.9	Inc = 62.7
$\alpha = 4.0$	K = 275.3
N = 6	R = 5.982

### 7.5. Summary.

Although in most instances specimens in this chapter had stable magnetisations, there was in some cases an unacceptable scatter of magnetic directions. At South Shields the deviant directions could be explained in terms of the type of movement likely in this tile kiln, whilst at Buxton the directional scatter could also be related to possible post firing disturbances of the clay hearths. Although chemical changes were possible during heating for the Quayside brick kiln specimens, (thus precluding a



definite explanation of the directional scatter of some specimens), nevertheless spurious declinations were thought unlikely to have arisen from this structure as each brick abutted neighbouring bricks, whilst there was no evidence for skewing. Thus the anomalous specimens noted as a result of their easterly declinations, are puzzling. However magnetic directional variation can in some instances be compared to likely patterns of movement as deduced by an examination of the structure to be sampled.

## CHAPTER EIGHT

---

### Conclusions

#### 8.1. Physical movement

##### 8.1a. Large scale

The magnitude of directional scatter resulting from physical movement, e.g. Dunnideer, makes this factor the biggest potential source of error in archaeomagnetic directional studies. However providing the movement is non-uniform it can be detected by comparing specimen magnetic directions from different parts of the same structure, assuming all parts relate to the same firing. (Even if this is not the case, if the magnetic direction lies off the secular variation curve it is likely that this has resulted from movement). Subsidence can be detected by archaeological excavation prior to sampling (e.g. Craig Phadrig) but most vitrified sites in this study were not excavated because of lack of time, manpower and permissions and because excavation could have had the effect of destabilising the walls. In most cases the exposures available were sufficient to determine at least

local physical stability which was confirmed, on the whole, by the statistically identical mean directions from each sampling locality for most of the vitrified forts. Although the possibility of uniform movement exists it is unlikely that parts of the same structure  $\pm 12$  m and often c.30m apart are going to move in the same way. The detailed study at Langwell also suggested there had been no significant movement during or since cooling below 600°C.

In fact in some instances there is a correlation between the pattern of directions and likely pattern of movement as seen in the South Shields kiln (Chapter Seven). Clay hearths are also likely to show magnetic directional scatter due to compaction, whilst hearths composed of physically independent stone blocks are also likely to show differential movement. However in some instances directionally consistent results are obtainable from brick structures e.g. the Quayside oven, (Chapter Seven). Another significant factor is the superposition of settlement on individual sites.

#### 8.1b. Small scale.

Results from the Lunt experimental kiln suggested that movement on cooling was insignificant with respect to the dispersion of the thermoremanent directions observed. This agrees with results obtained by Weaver (1962) who also thought movement was insignificant. However the possibility of wall and /or floor movements in kilns does exist and therefore the conclusions of some earlier workers as to the importance of this factor cannot be ignored (Harold, 1960; Hoyer, 1982).

The exfoliation effect noted on the inner c.1cm of the Lunt kiln lining, plus the erosion effects on this kiln after only one winter, emphasise, along with the marked changes in direction according to wall position, that preferential weathering could result in the definition of aberrant magnetic directions. This also implied that those archaeological kilns sampled must have been fired successively to survive in a British archaeological context.

It is nevertheless surprising that so many sites which have a history of disturbance possess apparently *in situ* remanences. For example Finavon had a trackway built through the walls whilst at Dun Skeig vitrified blocks

were used in the construction of the later dry stone dun. This points to local physical stability of the vitrified walls.

## 8.2. Magnetic anisotropy

Results from Langwell suggested that there was no systematic correlation between the specimen field orientations and the remanence acquired. Thus although the specimens were visually anisotropic this did not result in consistent magnetic deviations. The absence of anisotropic effects was further supported by the statistically identical mean magnetic directions from vesicular and non-vesicular materials. Hoyer (1982) and Dunlop and Zinn (1980) also concluded that the variations in direction found in an Italian lime kiln and a 19th century pottery kiln, could not be fully explained in terms of fabric anisotropy, even though this was >10% in the case of the lime kiln. However the anisotropy of the thermal remanence is complex (Stephenson *et al* 1986) and may contribute towards vector changes at different temperatures, as observed in thermally demagnetised specimens from Langwell. Different grains possessing different anisotropies and orientations are likely to magnetically

interact as they acquire their magnetisations on cooling. Heterogeneous concentrations and/or distribution of anisotropic grains would further serve to complicate the process. Results from level A of the Lunt kiln suggested that any anisotropic effects due to pinching and smoothing of the walls prior to firing did not cause significant deviations in specimen magnetic directions. However the greater scatter of those specimen directions from the inside of the kiln could be at least partially explained in terms of the anisotropy of the thermal remanence. Measurements of this are therefore advocated.

### 8.3. Weathering

I.R.M. acquisition curves and the thermal demagnetisation curves for Langwell suggest that magnetite was the dominant remanence carrier in most specimens analysed. This suggests that little significant weathering had taken place since firing as at least some of the magnetite would otherwise have oxidised to haematite. Generally speaking the weathering observed on many of the vitrified sites was restricted to visibly oxidised outer wall casings which could be avoided during sampling.

#### 8.4. Inhomogeneity and magnetic interactions on cooling

Results from Langwell and the Lunt kiln partially support the conclusions of Tarling *et al* (1986) and Tarling (1988) that consistent systematic magnetic deviations (conforming to a sine  $2\phi$  curve in declination and steeper inclinations in the northern parts of circular kilns (shallower in the South)), were not observed in many of the structures examined. Although in the Lunt kiln the distribution of magnetic directions was similar to that found in the Boston kiln (Weaver, 1962), not all the magnetic deviations followed a consistent pattern with azimuth. For example core specimen declinations on the West side of the Lunt kiln deviated westward, i.e. opposite to that expected from some previous studies. Such inconsistencies suggest that magnetic distortions through an already cooled or cooling magnetically permeable material, do not necessarily lead to systematic magnetic deviations in a secondary cooled area in the way normally attributed to magnetic "refraction". In particular inhomogeneous magnetisation can lead to an inhomogeneous internal magnetic field (Dunlop and Zinn, 1980), resulting

in non-systematic magnetic deviations. This may occur, for example, as a result of differential heating.

The "refraction correction" as proposed by Aitken and Hawley, (1971), involves the supposition that there is a correlation between higher intensities and directional deviations. The fact that the dun at Langwell and, arguably, the Lunt kiln do not show a consistent relationship of these two magnetic properties, shows that if this correction was applied automatically it could lead to incorrect results. As magnetic distortions seem to occur as a result of differential cooling, the distortion process involves magnetic interactions through a material in the process of acquiring a full magnetisation. The degree of deviance in magnetic direction therefore is also related to the rate at which the remanence is acquired in the distorting medium, and not completely due to magnetic distortions through an already magnetised material. Indeed Aitken and Hawley (1971) also point out that the "refraction" phenomenon is dependent on complex interactions of a variety of properties in the material, so that: "there will not necessarily be a strong correlation between deviation and the strength of magnetization of a structure."



The rate of cooling seems most likely to account for the vector pattern observed during thermal demagnetisation at Langwell. The fact that at Langwell there was no obvious consistent systematic correlation between specimen magnetic directions and other magnetic properties through a vitrified wall, coupled with the lack of a consistent 1:1 correlation between susceptibilities and intensities for the Lunt kiln further suggests that systematic magnetic distortion, (as predicted by the "refraction" model), does not fully explain the observations. In fact the Langwell results suggest that magnetic heterogeneity was dominant. However there was a correlation in most Langwell specimens of anomalous low coercivity directions and higher intensities. This seemed best explained by magnetic interactions during a slow localised cooling.

Nevertheless for the Lunt kiln the greatest directional scatter does correlate, in many instances, with higher intensities, whilst the lower intensities often correlated with the least directional scatter. This was not related to differential rates of cooling in the kiln chamber as this was uniform at the height at which the specimens were removed. It could be related to the pattern of heating as the most consistent directions were

least well heated whilst those most scattered were strongly heated. As the inner wall was heated for some time at a high temperature, a high temperature viscous component (Tarling, 1983) could result, contributing towards higher magnetic intensities. Also the fact that the magnetic grains from the inner wall are likely to have been heated to above the Curie point of haematite ( $675^{\circ}\text{C}$ ; see Chapter Six), localised magnetic interactions were more likely to occur here on cooling than the least heated outer surface of the wall. However as the kiln chamber cooled fast and uniformly, at least in the region of the specimens, local magnetic interactions as a result of slow cooling were unlikely to occur. Nevertheless inner surface specimen directions generally (though not consistently) deviated more than those from other parts of the kiln wall, whilst in some cases there was little directional variation for individual specimens between incremental steps. Thus the pattern of inter-specimen directional variation and the repeatability of individual directional components on demagnetisation (the latter reflected in the different statistical parameters of the outside/inside of the kiln) suggested that, in some cases, the directional deviancy of specimens from the inside of the kiln was due

to magnetic distortions as a result of already cooled outer parts of the kiln wall and not local magnetic interactions on cooling.

This was reinforced by the fact that many of the high coercivity remanence directions from the inner surface of the kiln were statistically different from the specimen directions from the outer surface. As it is likely that the high coercivity grains will acquire their magnetisations first on cooling (Gentles and Tarling, 1988), this suggested that these grains were cooling in an already distorted magnetic field. However it has been shown that A.F. and thermal methods define different vector paths during demagnetisation for the Volubilis kiln, depending whether the specimens are from slowly cooled or fast cooled areas (Najid, 1986). (The use of A.F. on slowly cooled materials defines a single highly stable component, whilst thermal methods define a curving vector path and a high temperature component of greater similarity to the mean magnetic direction than A.F.). Nevertheless there is directional agreement between low coercivity/low temperature magnetic directions, and high coercivity/high temperature magnetic directions from Langwell, which, like the Volubilis kiln, had magnetite as

the dominant remanence carrier. Thus there is evidence to suggest that the observed differences in magnetic direction from the outside and inside of the Lunt kiln were not related to the type of demagnetisation employed. Notable though was the fact that the vector paths of thermally demagnetised specimens from Langwell revealed greater numbers of erratic changes in direction between the high temperature and low temperature components. Thus thermal demagnetisation is recommended to resolve whether greater numbers of magnetic interactions can be observed by this method for the Lunt kiln.

Interestingly the clay was well mixed before firing whilst all foreign objects were removed from it. Thus although it is possible that there was an inhomogeneous distribution of magnetic grains in the clay, nevertheless there was no large scale heterogeneity. Comparison with magnetic deviations present in heterogeneously built structures (Tarling *et al*, 1986), suggested that the relatively greater systematic pattern observed in some of the specimens from the Lunt kiln after firing, may be related to the absence of large scale magnetic inhomogeneity in the building materials. This also suggests that the different magnetisations through the

wall, where they are systematic were more likely to be related to the firing conditions than systematic differences in the concentration of magnetic grains.

Therefore although in many archaeological structures the greatest scatter was associated with the greatest large scale inhomogeneity (Tarling et al 1986), it is still possible to observe large variations in specimen magnetic directions from homogeneously built structures. Also the results from the iron smelting furnace from Crawcwellt (Chapter Seven), further show that high intensities of magnetisations do not necessarily result in an unacceptable directional scatter. All of the results together suggest that there are a number of likely magnetic interactions occurring on cooling for any one structure, new or old. Each of these is likely to partially mask the effect of the other resulting in a variety of different magnetic patterns in structures of different cooling histories. In this respect these conclusions agree with those of Weaver (1962) who could not isolate any one factor as the predominant cause of dispersion, which was observed to be both systematic and random.

Nevertheless preferential sampling of rapidly cooled

areas should, in most cases, give the true geomagnetic field direction as in the outer surface of the Lunt kiln. However sampling of this kind is dependent on knowing the pattern of cooling of any one structure. This is often not obvious. In many of the vitrified structures the outer wall casing had fallen away, preventing the sampling of the most likely primarily cooled area. In kiln structures the pattern of cooling is integrally related to the product being fired, the weather, the number of flues, the type of fuel, the provision of kiln furniture and the kiln superstructure (Leach, 1959). All or some of these may not be known or preserved. The primarily cooled high coercivity remanence should be reliable but it remains possible that even these grains will cool in the magnetic field of a first cooled area. Detailed excavation, where practicable, is therefore advised to aid the location of areas of primary cooling. A combination of meticulous recording, and careful archaeomagnetic sampling would go some way to providing tighter controls on the cooling patterns of different types of fired structure. (See section on future work).

### 8.5. Demagnetisation methods

Comparison of those specimens thermally and A.F. demagnetised from Langwell showed that both methods defined a similar component although the vector paths of thermally treated specimens showed a distinct curvature. The primary remanence was statistically better defined in those specimens from Langwell subjected to A.F., but the end point thermal directions conformed with the most stable A.F. directions. Nevertheless the thermal method revealed changes in the magnetic vector which were not shown after A.F. treatment. The thermal method therefore appears to dissect the remanence more effectively but the problem of thermally induced chemical changes remains.

### 8.6. Accuracy of archaeomagnetic dating

Where possible detailed archaeological excavation, demagnetisation by thermal methods, preferential sampling of fast cooled areas and systematic sampling to detect differential movement and/or magnetic deviations should help to reduce the directional scatter from any sampled structure. Large numbers of specimens (>10) will also serve to average out the effects of inhomogeneity. Measurement and orientation of the remanence should be

accurate to within  $\pm 2^\circ$  (Tarling 1983), so that the remanence of any one specimen can be closely defined. The latter, coupled with preferential sampling should increase the precision in the definition of a mean magnetic direction.

Results from Langwell suggest that the large scale inhomogeneity, erratic differential cooling, plus the variably oriented fabrics of the wall serve to randomise magnetic distortion effects resulting in reasonable directional consistency and thus a statistically well defined mean magnetic direction. The Lunt kiln core specimen directions, when averaged for any depth into the kiln wall, all show observed means similar to the present geomagnetic field direction. Also the mean of outer surface specimen directions, the mean of all wall specimens, and the mean of the floor specimens all had circles of 95% confidence which were well defined and consistent with the geomagnetic direction in 1985. As such it is possible, by systematic sampling and/or sampling of primary cooled areas, to locate and obtain archaeologically sensible and statistically well defined mean magnetic directions from structures showing large scale magnetic inhomogeneity in their building materials



or showing large variations in direction.

However the fact that there is in some cases poor correlation of A.M. dates with those of other methods remains disturbing e.g. Finavon. Even where there is agreement there remains the problem that each age assignment by different methods have their own statistical errors so that the mean magnetic direction from the Langwell vitrification could be assigned to a  $\sim$  200 year time span if the overall T.L. error alone is taken into account (see Chapter Five). It is therefore essential that a combination of archaeological and absolute dating methods are used to obtain a best-fit curve although broad trends in the magnetic curve can be defined on smaller numbers of absolute or relative dates. As each observed mean has different statistical precision it is difficult to put error bars on the secular variation curve although the statistics associated with each mean are available within the literature. Also the rate of change makes it difficult to assign a  $\pm$  error to the observed mean. Hence age assignments are presented as age ranges in Chapter Five. Thus the accuracy of the age assignment is also dependent on where the observed mean lies on the curve, its statistical precision, and also the degree of

directional ambiguity between different ages. Nevertheless with increasing numbers of reliable archaeologically/absolutely and relatively dated magnetic directions the precision and accuracy of the curve will increase, enabling relative, and potentially absolute dating of archaeological materials.

In some cases already dated curve directions are consistent with dates obtained by other methods e.g. the A.M. dates based on already dated Late Iron Age magnetic directions from Langwell agree with those of T.L. This appears to indicate broad chronological accuracy but there remain the cases where absolute dates do not correlate with A.M. (e.g. Finavon), although this may be due to problems with the other dating methods. As insufficient detail is published on individual dating errors this problem cannot be properly evaluated at this time.

#### 8.7. Archaeological implications of the A.M. age assignments

Archaeomagnetism can be used to date the final firing of the vitrification on the basis of present magnetic information, by reference to a dated secular variation curve (Turner and Thompson 1982; Clark et al 1988; Tarling

1988). This should provide a *terminus ante quem* for the primary phases of the fort.

The archaeomagnetic age assignments do not appear to support the idea of a single vitrification phase in all the forts sampled although there is broad agreement between the mean magnetic directions from Finavon, Craig Phadrig, and Knockfarril.

Tap o'Noth appears to have been fired slightly later in date but, interestingly, all of the rectilinear forts sampled on the eastern seaboard are burnt earlier than those further inland. This is not inconsistent with a widespread destruction of rectilinear timber laced forts between the late third century B.C. and early first century A.D., possibly as a result of population incursion. Notable however is the general lack of military hardware discovered on these vitrified sites (Ralston, 1985), although this may be due to the soil conditions. The overall distribution of locally manufactured swords and spearheads show similar distributions to those of many of the forts, with which they were contemporary in the Early Iron Age (Ritchie and Ritchie, 1985). Nevertheless there are few examples where these objects occur actually on the sites, whilst they are not contemporary with the

A.M. dates for the vitrification of the walls. Although there is evidence of continuing continental contact during the 6th and 5th centuries B.C., generally speaking, (with the exception of the Atlantic seaboard), much of the pottery is insensitive as a chronological indicator (Megaw and Simpson, 1984). Further it is often difficult to isolate archaeological evidence for "invasions" which may be recorded in reliable histories or otherwise known to have occurred. Even the Roman conquest for example of South East Britain is hardly detectable at Colchester or Owslebury (Hawkes and Hull, 1947 in Collis 1977; Collis, 1977).

The magnetic results are also consistent with the evolution of the form of the fort as proposed by Mackie (1976). (It is of course possible to argue that the occupation of dun and rectilinear fort overlapped in time but were vitrified at different times). The vitrification is also likely to mark the end of use of many of the sites sampled (Mackie, 1976; Ralston, 1986), although re-occupation may occur after a significant time lapse e.g. Craig Phadrig, whilst rarely vitrification may be followed by "immediate" occupation, e.g. Langwell (Nisbet, 1974).

On the other hand during the first quarter of the first millenium B.C. there was climatic deterioration (Evans, 1975). The Sub- Atlantic period saw a wetter climate with waterlogged lowland peat bogs and leaching of nutrients from the soil. The use of timber for building may have hastened this process as well as stock grazing, leading to podsolisation (Megaw and Simpson, 1984). Thus there may be a link between environmental deterioration and fort wall vitrification which may not involve population incursion but possibly indigenous competition for scarce resources.

These points serve as examples of the problem of assigning meaning to structures of this type, and therefore the reason for the vitrification, in the absence of widespread large scale modern excavations.

#### 8.8. The vitrification process

It is possible to suggest from evidence excavated, the geochemical results, and the magnetic analyses that:

1). The vitrification occurred on sites with associated combustible organic materials (often timber lacing or internal wooden structures). 2). That the vitrification occurred mostly under oxygen starved conditions (Nisbet,

1975; Youngblood et al 1978; Fredrikkson et al 1983; Gentles and Tarling, 1988). 3). That temperatures were in excess of  $600^{\circ}\text{C}$ , and most likely in the region of  $1000^{\circ}\text{C}$ . (Nisbet, 1975; Youngblood et al 1978; Fredrikkson et al 1983; Gentles and Tarling, 1988). 4). That melting occurred of some of the constituents of the wall, thereby fusing together other materials either less well heated or with higher melting points. 5). That cooling rates of different parts of the vitrification were variable, but that most of the core of the wall at Langwell, and by implication elsewhere, cooled slowly (in archaeological terms; Chapter Three). 6). That although there is some evidence of movement during cooling, that this did not occur to a significant degree at temperatures below  $600^{\circ}\text{C}$  or after the last firing at Langwell or at most of the other vitrified structures sampled. 7). That it remains possible that fluxing agents may have played a part in the vitrification process, (Chapter Two; Ralston, 1986).

#### 8.9. Future work

Further sampling of archaeological structures should involve detailed excavation and recording in order to reconstruct as far as possible the conditions under which

the last remanence was acquired. Unfortunately most features which have been magnetically sampled are already excavated. The information therefore obtained by the excavators is dominated by the priorities of the site supervisor. If excavation is completed or supervised by the person to sample the feature on initial discovery of it, the presence and/or position of possibly significant magnetic materials e.g. kiln furniture, (Swan 1984), can be meticulously recorded and its likely effect on the remanence assessed. Similarly the problem of physical movement can be assessed in more detail, although it is often necessary to see the feature in section to determine if the structure has slumped or skewed as a whole.

Coupled with this further work in experimental archaeology, based on known and excavated fired archaeological structures (Hartley 1961; Mayes 1961; Bryant 1970, 1971), would also help to reconstruct the patterns of magnetic remanence acquired in different firing conditions. Laboratory firings of magnetic particles in non-magnetic and magnetic building materials with controlled magnetic fields and rates of cooling etc. would help further resolve the problems of differential cooling, the anisotropy of the thermal remanence, and the

effects of inhomogeneity. These results, compared with those found in full size archaeological and archaeologically analogous kilns should place tighter controls on how the magnetic remanence patterns were acquired in ancient structures. This type of study would be equally relevant to magnetic intensity work as those factors leading to magnetic directional variation also lead to different magnetic intensities.

Further comparisons of demagnetisation patterns from specimens A.F. and thermally treated would help resolve in more detail how effective each technique is in demagnetising fast cooled and slow cooled magnetic remanences. In particular thermal demagnetisation of further specimens from the Lunt kiln wall would enable the ~~coercivity~~<sup>blocking temperature</sup> spectra of magnetic grains at different distances through the wall to be defined. Comparison of the most stable directions defined at different depths (as already done for A.F.), and the demagnetisation patterns should show if the greater directional scatter at 6cm depth into the kiln wall is related to local (4-6cm depth), magnetic interactions on cooling and/or a cumulative effect of cooling rate through the wall. Monitoring of magnetic intensities during heating would



also give an approximation of the maximum temperature to which the material was heated.

Sampling of greater numbers of independently dated Late Bronze Age/Early Iron Age fired structures would help further resolve the pattern of directional change during these times and the degree of correlation between the magnetic sediment curve and that based on thermoremanences (Turner and Thompson, 1982; Tarling, 1988). Also there is a need to up-date the archaeological/absolute dating of previously sampled structures in the light of completed excavations, whilst continuing to sample structures most likely to give independent dating evidence as well as those requiring A.M. dates.

## References

- Abrahamsen, N. (1986)  
On shape anisotropy.  
Geoskrifter, 24, 11-21.
- Aitken, M.J. (1974)  
Physics and Archaeology.  
Second edition, Clarendon press, Oxford. 1-287.
- Aitken, M.J. and Weaver, G.H. (1962)  
Magnetic dating: some archaeomagnetic measurements in  
Britain.  
Archaeometry, 5, 4-22.
- Aitken, M.J. and Hawley, H.N., (1971)  
Archaeomagnetism: Evidence for magnetic refraction in kiln  
structures.  
Archaeometry, 13, 83-85.
- Alcock, L. (1971)  
Arthurs Britain.  
Penguin press. 1-387.
- Alcock, L. (1985)  
Early historic fortifications in Scotland.  
In Guilbert (ed) Hillfort Studies,  
Leicester.
- Anderson, James (1779)  
An account of ancient monuments and fortifications in the  
highlands of Scotland.  
Arch., 5, 241-66. (Letter of 1777).
- Anderson, Joseph (1883)  
Scotland in pagan times: The Iron Age.  
David Douglas, Edinburgh, 276-9.
- As, J.A. and Zijderveld, J.D.A. (1958).  
Magnetic cleaning of rocks in palaeomagnetic research.  
Geophys. J. R. Astr. Soc., 1, 308-319.

- Benton, S. (1931)  
The excavation of the Sculptors Cave, Covesea, Morayshire.  
Proc. Soc. Ant. Scot., Jan. 12th
- Briden, J.C. (1972)  
A stability index of remanent magnetisation.  
J. Geophys. Res. 77, 1401-1405.
- Brothwell, D.R., Bishop, A.C., and Woolley, A.R. (1974)  
Vitrified forts in Scotland; a problem in interpretation  
and primitive technology.  
J. Arch. Sci. 1, 101-107.
- Bryant, G.F. (1970)  
Two experimental Romano-British kiln firings at Barton-on-  
Humber, Lincs.  
Workers Educational Association 3, (1).
- Bryant, G.F. (1971)  
Experimental Romano-British kiln firings at Barton on Humber  
Lincs.  
Workers Educational Association, occ. paper no. 1.
- Buscenschutz, O.E. et Ralston, I.B.M. (1981)  
Les Fortifications des Ages des Metaux.  
Archeologia, (Dijon), 154, 24-36.
- Champion, (1980)  
A Dictionary of Terms and Techniques in Archaeology.  
Morrison and Gibb, London and Edinburgh. 3-144.
- Childe, V.G. (1934)  
Excavation of the vitrified fort at Finavon, Angus.  
Proc. Soc. Ant. Scot. 69, 49-80.
- Childe, V.G. (1935)  
The Prehistory of Scotland
- Childe, V.G., and Thorneycroft, W. (1937a)  
The experimental production of the phenomena distinctive of  
vitrified forts.  
Proc. Soc. Ant. Scot., 72, 44-55.
- Childe, V.G. (1946)  
Scotland before the Scots

Christison, D. (1898).  
Early fortifications in Scotland.  
Blackwood, Edinburgh and London.

Christison, D. (1899-1900).  
The forts, camps and other field works of Perth, Forfar and  
Kincardine.  
Proc. Soc. Ant. Scot., xxxiv, 43-120.

Clark, A.J., Tarling D.H. and Noel, M. (1988)  
Developments in archaeomagnetic directional dating in Great  
Britain.  
J. Arch. Sci., (in press).

Collinson, D.W. (1983).  
Methods in Rock magnetism and Palaeomagnetism.  
Chapman and Hall, London.

Collinson, D.W. and Molyneux, L (1967).  
An instrument for the measurement of isotropic initial  
susceptibility of rock samples.  
In Collinson, D.W., Creer, K.M. and Runcorn, S.K. (eds)  
Methods in Palaeomagnetism.  
Elsevier, Amsterdam 368-371.

Collis, J. (1977).  
An approach to the Iron Age in  
Collis, J. (ed)  
The Iron Age - a review.  
University of Sheffield, 1-8.

Cotton, M.A. (1954)  
British camps with timber-laced ramparts.  
Arch. J., 3, 26-105.

Cox, A. (1961).  
Anomalous remanent magnetisation of basalt.  
U.S. Geol. Survey Bulletin 1083 E, 131-160.

Crewe, P. (1986)  
Bryn y Castell hillfort, a late prehistoric iron-working  
settlement in North West Wales, in Scott, B.G. and Cleere,  
H. (eds), The Crafts of the Blacksmith.  
Proc. vii symposium de la consite pour la siderugne Ancienne  
de L' uispp, Belfast, (1984).

- Dunlop, D.J., (1979)  
On the use of Zijderveld vector diagrams in multi-component palaeomagnetic studies.  
Physics of the Earth and Planetary interiors, 20, 12-24.
- Dunlop, D.J. and Zinn, M.B. (1980)  
Archaeomagnetism of a 19th century pottery kiln near Jordan, Ontario, Canada.  
Can. Jl. Earth Sci. 17, 1275-1285.
- Evans, (1975).  
The Environment of Early Man in the British Isles.  
Unwin, London. 1-210.
- Evans, M.E. and Mareschal, M. (1986)  
An archaeomagnetic example of polyphase magnetization.  
Jl. Geomag. Geoelect., 38, 923-929.
- Feachem, (1983)  
Guide to Prehistoric Scotland.  
Batsford, London. 7-215.
- Fisher, R.A. (1953)  
Dispersion on a sphere.  
Proc. Roy. Soc., A217, 295-305.
- Fleming, (1976)  
Dating in Archaeology.  
Dent and Sons, London. 5-272.
- Fox, J.M.W. and Aitken, M.J. (1980)  
Cooling rate dependance of thermoremanent magnetization.  
Nature, 283, 462-463.
- Fredriksson, K., Youngblood, F., Fredriksson, B. (1983)  
The Celtic vitrified forts.  
In: Kempe, D.R.C. and Harvey, A.P., (eds.) (1983)  
The Petrology of Archaeological Artefacts.  
Clarendon Press, Oxford.
- Gentles, D.S.  
Archaeomagnetic report on the Neolithic site at Buxton, Lismore Fields, Derbyshire.  
(Submitted).

- Gentles, D.S. and Smithson, P.A. (1986)  
 Fires in Caves: Effects on temperature and airflow.  
 Proc. Univ. Bristol Spelaeol. Soc., 17 (3), 205-217.
- Gentles, D.S. and Tarling, D.H. (1988)  
 Archaeomagnetic directional dating and magnetic analyses  
 with special reference to a Scottish vitrified dun.  
 In: Slater, E.A. and Tate, J.O. (eds.)  
 Science in Archaeology, Glasgow, 1987.  
 B.A.R. British series, Oxford, 647-667.
- Goodyear, F.H. (1971),  
 Archaeological Site Science  
 Heineman, London. 5-275.
- Greene, K. (1983)  
 Archaeology, An Introduction.  
 Batsford, London. 7-185.
- Greig, J.C., (1970)  
 Excavations at Castle Point, Troup. Banffshire.  
 Aberdeen University Review, 43, 274-283.
- Greig, J.C. (1972)  
 Cullykhan.  
 Curr. Arch. 3, 227-231.
- Harold, M.R. (1960)  
 Magnetic dating: kiln wall fallout.  
 Archaeometry, 3, 45-47.
- Hartley, B.R. (1961).  
 The firing of kilns of Romano-British type.  
 Archaeological notes  
 Archaeometry 4, 1-3.
- Hedges, J. (1975)  
 Excavation of two Orcadian burnt mounds at Liddle and  
 Beaquoy.  
 Proc. Soc. Ant. Scot. (1974-5) 39-98.
- Hibbert, S. (1831; 1833)  
 Observations on the theories which have been proposed to  
 explain the vitrified forts of Scotland. Collections  
 relative to vitrified forts.  
 Arch. Scot. 4, (1), 160-201; Ibid. 4, (2), (1833) 280-297.

- Hoye, G.S. (1982)  
A magnetic investigation of kiln wall distortion.  
*Archaeometry*, 24, 80-84.
- Hunt, J. (1970)  
The Rosedale glass furnace and the Elizabethan glass workers.  
Ryedale Folk Museum.
- Hutchings, A. (1967). Computation of the behaviour of two and three axis rotating systems. In Collinson, D.W., Creer, K.M., and Runcorn, S.K. (eds) *Methods in Palaeomagnetism*, Elsevier, Amsterdam.
- Kirschvink, J.L. (1980)  
The least squares line and plane and the analysis of palaeomagnetic data.  
*Geophys. J. R. Astr. Soc.* 62, 699-718.
- Laing, L. (1979)  
Celtic Britain.  
Granada pub. London, Toronto, Sydney, New York. 1-254.
- Leach, B. (1959)  
A Potters Book.  
London. 1-294.
- Macculloch, J. (1824)  
History of the Highlands.
- Mackie, E.W. (1965c)  
The Origin and Development of the Broch and Wheelhouse Building Cultures of the Scottish Iron Age.  
*Proc. Preh. Soc.*, 31, 93-146.
- Mackie, E.W. (1969)  
Radiocarbon dates of the Scottish Iron Age.  
*Antiquity*, 42, 15-26.
- Mackie, G.W. (1976)  
The Vitrified forts of Scotland.  
In: Harding, D.W. (ed.)  
Hillforts, later prehistoric earthworks in Britain and Ireland.

London. 205-235.

Macksween, A. (1985)  
in Burgess, C., Maddison, M. and Sellers, P. (eds)  
The Brochs, Duns, and Enclosures of Skye.  
Northern Archaeology, Vols 5 and 6, (1984-5), 1-40.

Mayes, P. (1961).  
The firing of a pottery kiln of Romano-British type at  
Boston, Lincs.  
Archaeometry 4, 4-30.

McLelland Brown, E. (1984)  
Experiments on TRM intensity dependence on cooling rate.  
Geophys. Res. Lett. 11, (3), 205-208.

Megaw, J.V.S. and Simpson, D.D.A. (eds), (1984)  
Introduction to British Prehistory  
Leicester University Press. 1-560.

M'Hardy, A.B. (1906)  
On vitrified forts , with results of experiments as to the  
probable manner in which their vitrification may have been  
produced.  
Proc. Soc. Ant. Scot. xl, 136-50.

Miket, R. (1981)  
The Roman Fort at South Shields. Excavation of the defences  
1977-1981.

Molyneux, L. (1971). A complete result magnetometer for  
measuring the remanent magnetisation of rocks.  
Geophys. J. R, Astr. Soc., 24, 429-433.

Nagata, T. (1961).  
Rock magnetism.  
Second edition, Maruzen, Tokyo.

Najid, D. (1986)  
Palaeomagnetic studies of Morrocco.  
Ph.D thesis, University of Newcastle upon Tyne.

Neel, L. (1949)  
Theory of magnetic viscosity of fine-grained ferromagnetics  
with application to baked clays.  
Ann. Geophys., 5, 99-136.



- Nisbet, H.C. (1974)  
Excavations at Tor a' Chorcain, Langwell, Ross and Cromarty.  
Unpublished excavation report.
- Nisbet, H.C. (1975)  
A geological approach to vitrified forts. Part II. Bedrock  
and building stone.  
Sci. Arch., 15, 3-16.
- Pearson, and Stuiver (1986)  
High precision calibration of the radiocarbon timescale  
500-2500 B.C.  
Radiocarbon 28, (2b) 839-862.
- Potter, D.K. and Stephenson, A. (1988).  
Single domain particles in rocks and magnetic fabric  
analysis.  
Geophys. Res. Letters. 15, 10, 1097-1100.
- Ralston, I.B.M., (1978)  
Green Castle, Portknockie and the promontory forts of N.E.  
Scotland.  
Scottish Arch Forum, 10, 27-40.
- Ralston, I.B.M., (1980)  
Yorkshire Television vitrified wall experiment.  
Unpublished report.
- Ralston, I.B.M. (1983)  
Settlement in North Britain, 1000 B.C. to A.D. 1000  
in Hands, A.R. and Walker, D.R. (eds)  
Papers presented to George Jobey, Newcastle upon Tyne.  
B.A.R. British series 118, Oxford. 149-173.
- Ralston, I.B.M., (1985)  
Notes compiled on forts in Aberdeenshire.  
Unpubl. site reports.
- Ralston, I.B.M., (1986)  
The Yorkshire Television vitrified wall experiment at East  
Tullos, City of Aberdeen District.  
Proc. Soc. Ant. Scot. 116, 17-40.
- Ritchie, A. and Ritchie, D. (1985)  
Scotland: Archaeology and Early History.

Thames and Hudson, London. 7-189.

Sanderson, D.C.W., Placido, F., and Tate, J.O. (1985)  
Vitrified Forts, background and potential for T.L. dating.  
Nucl. Tracks. 10, 799-809.

Simpson, W.D. (1935)  
The castles of Dunnideer and Woodhouse in the Garioch,  
Aberdeenshire.  
Proc. Soc. Ant. Scot., May 13, 460-470.

Shepherd, I.A.G. and Ralston, I.B.M., (1979)  
Early Grampian, a guide to the archaeology.  
Grampian Regional Council, Aberdeen.

Small, and Cottam, (1972)  
Craig Phadrig: Interim report on 1971 excavation, Dundee.  
(=occ. paper dept. Geography, university of Aberdeen, 1).

Smith, R.A., (1872)  
Descriptive list of antiquities near Loch Etive, Argyllshire.  
Proc. soc. Ant. Scot. (4), 81-106.

Stephenson, A. Saddikun, S. and Potter, D.K. (1986)  
A theoretical and experimental comparison of the  
anisotropies of magnetic susceptibility and remanance in  
rocks and minerals.  
Geophys. J. R. Astr. Soc. 62, 113-132.

Strickertsson, K., Sanderson, D.C.W., Placido, F. and Tate,  
J.O. (1988)  
Thermoluminescence dating of Scottish Vitrified Forts. New  
results and a review in Slater E.A. and Tate J.O. (eds)  
Science in Archaeology. B.A.R. British series, Oxford. (Pre-print)  
625-633.

Stuart, J. (1869)  
On some of the vitrified forts of Scotland, with reference  
to the description of similar remains in Bohemia in a  
communication from Dr. Ferdinand Keller of Zurich.  
Proc. Soc. Ant. Scot., 8, 145-64.

Stuiver, and Pearson, (1986)  
High precision calibration of the radiocarbon timescale,

- A.D. 1950-500 B.C.  
Radiocarbon 28, (2b) 805-838.
- Swan, V.G. (1984).  
The Pottery Kilns of Roman Britain.  
Crown copyright. 1-177.
- Tarling, D.H. (1983)  
Palaeomagnetism.  
Chapman and Hall, London. 1-369.
- Tarling, D.H. (1988)  
Secular variations of the geomagnetic field in the  
archaeomagnetic record. In Stephenson F.R. and  
Wolfendale (eds) Secular, solar and  
geomagnetic variations in the last 10,000 years.  
Kluwer acad. publ., 349-365.
- Tarling, D.H. and Symons, D.T.A. (1967). A Stability index of  
remanence in palaeomagnetism.  
Geophys. J. R. Astr. Soc., 12, 443-448.
- Tarling, D.H., Hammo, N.B. and Downey, W.S. (1986)  
The scatter of magnetic directions in archaeomagnetic  
studies.  
Geophys, 51, 634-639.
- Thomas, R.C., (1981)  
Archaeomagnetism of Greek pottery and Cretan kilns.  
Ph.D thesis, University of Edinburgh.
- Tytler, A.F. (1783)  
An account of some extraordinary structures on the top of  
hills in the Highlands, with remarks on the progress of the  
Arts among the ancient inhabitants of Scotland.  
Trans. Roy. Soc. Edinb.
- Turner, G.M. and Thomson, R. (1982)  
Detransformation of the British geomagnetic secular  
variation record for Holocene times.  
Geophys. J. Roy. Astr. Soc., 70, 789-793.
- Wallace, T. (1912-1918)  
Archaeological notes.  
Trans. Inv. S. Soc., 8, 87-136.

- Walton, D. (1980)  
Time-temperature relations in magnetisation of single  
domain grains .  
Nature, 286, 245-247.
- Weaver, G.H, (1961)  
Magnetic dating measurements.  
Archaeometry, 4, 23-28.
- Weaver, G.H. (1962)  
Archaeomagnetic measurements on the second Boston  
experimental kiln.  
Archaeometry, 4, 93-107.
- Williams, J. (1777)  
An account of some remarkable ancient ruins lately  
discovered in the Highlands and northern parts of Scotland.  
Edinburgh
- Wilson, R.L. and Lomax, (1972)  
Magnetic remanence related to slow rotation of  
ferromagnetic material in alternating magnetic fields.  
Geophys. J.R. Astr. Soc., 30, 295-303.
- Youngblood, E., Fredriksson, B.J., Kraut, F. and  
Fredriksson, K. (1978)  
Celtic vitrified forts: implications of a chemical  
petrological study of glass and source rocks.  
J. Arch. Sci., 5, 99-121.